antioxidants

Special Issue Reprint

Oxidative Stress Induced by Air Pollution, 2nd Edition

Edited by
Yasuhiro Yoshida

mdpi.com/journal/antioxidants

MDPI

Oxidative Stress Induced by Air Pollution, 2nd Edition

Oxidative Stress Induced by Air Pollution, 2nd Edition

Guest Editor

Yasuhiro Yoshida

MDPI

Basel • Beijing • Wuhan • Barcelona • Belgrade • Novi Sad • Cluj • Manchester

Guest Editor
Yasuhiro Yoshida
Department of Immunology
and Parasitology
University of Occupational
and Environmental Health
Kitakyushu
Japan

Editorial Office
MDPI AG
Grosspeteranlage 5
4052 Basel, Switzerland

This is a reprint of the Special Issue, published open access by the journal *Antioxidants* (ISSN 2076-3921), freely accessible at: https://www.mdpi.com/journal/antioxidants/special_issues/air_pollution_2.

For citation purposes, cite each article independently as indicated on the article page online and as indicated below:

Lastname, A.A.; Lastname, B.B. Article Title. *Journal Name* **Year**, *Volume Number*, Page Range.

ISBN 978-3-7258-7150-6 (Hbk)
ISBN 978-3-7258-7151-3 (PDF)
https://doi.org/10.3390/books978-3-7258-7151-3

Contents

Preface . . . . . **vii**

Yasuhiro Yoshida
Beyond Exposure Levels: Oxidative Stress as a Unifying Axis Linking Particulate Matter, Light, and Protective Interventions
Reprinted from: *Antioxidants* **2026**, *15*, 236, https://doi.org/10.3390/antiox15020236 . . . . . **1**

Daniele Grifoni, Elisa Bustaffa, Laura Sabatino, Francesca Calastrini, Fabrizio Minichilli, Melania Gaggini, et al.
The Dark Triad of Particulate Matter, Oxidative Stress and Coronary Artery Disease: What About the Antioxidant Therapeutic Potential
Reprinted from: *Antioxidants* **2025**, *14*, 572, https://doi.org/10.3390/antiox14050572 . . . . . **4**

Chiang-Wen Lee, Yao-Chang Chiang, Thi Thuy Tien Vo, Zih-Chan Lin, Miao-Ching Chi, Mei-Ling Fang, et al.
Deciphering the Liaison Between Fine Particulate Matter Pollution, Oxidative Stress, and Prostate Cancer: Where Are We Now?
Reprinted from: *Antioxidants* **2024**, *13*, 1505, https://doi.org/10.3390/antiox13121505 . . . . . **41**

Duo Wang, Zirui Zeng, Aya Nawata, Ryoko Baba, Ryuji Okazaki, Tomoaki Okuda and Yasuhiro Yoshida
Seasonal Variation in $PM_{2.5}$ Composition Modulates Oxidative Stress and Neutrophilic Inflammation with Involvement of TLR4 Signaling
Reprinted from: *Antioxidants* **2026**, *15*, 89, https://doi.org/10.3390/antiox15010089 . . . . . **56**

Jae-Kyoung Lee, Khawaja Muhammad Imran Bashir, Hye-Rim Park, Jin-Gwan Kwon, Beom-Rak Choi, Jae-Suk Choi and Sae-Kwang Ku
Protective Effects of Thyme Leaf Extract Against Particulate Matter-Induced Pulmonary Injury in Mice
Reprinted from: *Antioxidants* **2025**, *14*, 1343, https://doi.org/10.3390/antiox14111343 . . . . . **76**

Alfredo Miranda-Martínez, Erika Rodríguez-Martínez, Marlen Valdés-Fuentes and Selva Rivas-Arancibia
Alterations of the Intestinal Barrier and Inflammatory Response, Caused by Chronic Ozone Exposure in a Rat Model
Reprinted from: *Antioxidants* **2025**, *14*, 1000, https://doi.org/10.3390/antiox14081000 . . . . . **96**

In Young Kim, Hyo Lim Lee, Hye Ji Choi, Yeong Hyeon Ju, Yu Mi Heo, Hwa Rang Na, et al.
A Combined Extract from *Dioscorea bulbifera* and *Zingiber officinale* Mitigates $PM_{2.5}$-Induced Respiratory Damage by NF-κB/TGF-β1 Pathway
Reprinted from: *Antioxidants* **2024**, *13*, 1572, https://doi.org/10.3390/antiox13121572 . . . . . **123**

Miguel Santibáñez, Juan José Ruiz-Cubillán, Andrea Expósito, Juan Agüero, Juan Luis García-Rivero, Beatriz Abascal, et al.
Association Between Oxidative Potential of Particulate Matter Collected by Personal Samplers and Systemic Inflammation Among Asthmatic and Non-Asthmatic Adults
Reprinted from: *Antioxidants* **2024**, *13*, 1464, https://doi.org/10.3390/antiox13121464 . . . . . **144**

Jisu Park, Bo-Young Kim, Eun Jung Park, Yong-Il Shin and Ji Hyeon Ryu
Photobiomodulation Mitigates $PM_{2.5}$-Exacerbated Pathologies in a Mouse Model of Allergic Asthma
Reprinted from: *Antioxidants* **2024**, *13*, 1003, https://doi.org/10.3390/antiox13081003 . . . . . **157**

Preface

This reprint examines oxidative stress as a unifying molecular axis through which environmental exposure reshapes biological systems. Focusing on particulate matter and related atmospheric factors, it highlights how chemical composition and oxidative potential govern cellular injury, immune activation, barrier dysfunction, and systemic inflammatory propagation. Rather than treating exposure as a purely toxicological event, the volume positions oxidative stress as a central organizing principle linking environmental chemistry with molecular and systemic pathophysiology.

The aim of this collection is to integrate mechanistic redox biology with organism-level consequences, providing a coherent framework that connects epithelial damage, immune signaling, and chronic disease susceptibility. By assembling contributions that span molecular mechanisms, tissue responses, and host-directed interventions, this reprint advances a systems-oriented perspective on how environmental information is biologically encoded.

This volume is intended for researchers in redox biology, molecular and cellular biology, environmental health sciences, and immunology who seek integrative approaches to understanding how oxidative imbalance translates environmental exposure into adaptive or maladaptive outcomes.

Yasuhiro Yoshida
Guest Editor

antioxidants

MDPI

Editorial

Beyond Exposure Levels: Oxidative Stress as a Unifying Axis Linking Particulate Matter, Light, and Protective Interventions

Yasuhiro Yoshida

Department of Immunology and Parasitology, School of Medicine, University of Occupational and Environmental Health, Japan, 1-1 Iseigaoka, Yahatanishi-ku, Kitakyushu 807-8555, Japan; freude@med.uoeh-u.ac.jp

Air pollution remains one of the most pervasive environmental health threats worldwide, contributing substantially to the global burden of respiratory, cardiovascular, and metabolic diseases. Among various pollutants, fine particulate matter ($PM_{2.5}$) has attracted particular attention because of its ability to penetrate deep into the respiratory tract and induce oxidative stress and inflammation. Importantly, accumulating evidence indicates that the health effects of $PM_{2.5}$ cannot be explained solely by particle mass or exposure concentration. Instead, the quality of exposure—including chemical composition, oxidative potential, and host susceptibility—critically determines biological outcomes [1].

This Special Issue "Oxidative Stress Induced by Air Pollution, 2nd Edition" brings together six original research articles and two comprehensive reviews, all converging on oxidative stress as a central biological axis linking environmental exposure to inflammation, tissue injury, and disease modification across multiple organs.

A central contribution of this Issue is the demonstration that $PM_{2.5}$ is not a uniform toxicant, but rather a complex and dynamic mixture whose biological effects are dictated by its chemical composition. In this Issue, Wang et al. show that seasonal variation in $PM_{2.5}$ composition profoundly shapes pulmonary immune responses using a two-year continuous sampling approach combined with in vivo exposure models [Contribution 1]. Their study demonstrates that PAH-rich $PM_{2.5}$ preferentially induces robust ROS generation and neutrophilic inflammation, whereas mineral-enriched winter $PM_{2.5}$ strongly correlates with IL-1α production, an epithelial- and macrophage-derived alarmin that initiates innate immune activation.

These findings extend prior observations that particle-bound organic compounds drive oxidative stress and mitochondrial dysfunction [2], while mineral and crystalline components can induce cell death-associated alarmin and inflammasome activation [3]. Importantly, the partial attenuation of inflammatory responses in TLR4-deficient mice reported by Wang et al. highlights the limitations of single-receptor models and supports a broader framework in which oxidative stress, cellular injury, and danger signal release jointly orchestrate $PM_{2.5}$-induced inflammation [Contribution 1].

While the lung is the primary portal of entry for inhaled pollutants, several studies in this Issue emphasize that oxidative stress propagates beyond the respiratory system. Miranda-Martínez et al. demonstrate that chronic low-dose ozone exposure disrupts intestinal barrier integrity and induces sustained inflammatory responses along the gastrointestinal tract, supporting the emerging concept of a lung–gut axis in environmental disease [Contribution 2].

Complementing these experimental findings, Santibáñez et al. report that the oxidative potential of personally collected particulate matter is strongly associated with systemic inflammatory markers, including IL-6 and the IL-6/IL-10 ratio, with particularly

pronounced effects observed in individuals with asthma [Contribution 3]. These data are consistent with previous epidemiological and mechanistic studies linking particulate oxidative potential to systemic inflammation and cardiovascular risk [4].

The two review articles in this Issue further extend the systemic perspective. Grifoni et al. summarize evidence connecting PM-induced oxidative stress and inflammation to coronary artery disease [Contribution 4], framing particulate matter, oxidative stress, and cardiovascular pathology as a "dark triad." Lee et al. review emerging data linking $PM_{2.5}$ exposure to prostate cancer risk, highlighting oxidative stress and endocrine-disrupting chemicals as potential mechanistic mediators. Together, these contributions underscore that air pollution should be regarded as a systemic risk factor rather than a lung-restricted hazard [Contribution 5].

Several studies in this Issue explore strategies to mitigate pollution-induced oxidative stress and inflammation [Contribution 6]. Lee et al. demonstrate that thyme leaf extract dose-dependently attenuates $PM_{2.5}$-induced pulmonary injury by reducing ROS generation, inflammatory cytokine production, and mucus hypersecretion while preserving antioxidant defenses. Similarly, Kim et al. report that a combined extract of Dioscorea bulbifera and Zingiber officinale mitigates $PM_{2.5}$-induced respiratory dysfunction through modulation of NF-κB, MAPK, and TGF-β/Smad signaling pathways, ultimately suppressing inflammation and fibrosis [Contribution 7].

Beyond pharmacological and nutritional approaches, Park et al. introduce photobiomodulation as a non-invasive physical intervention capable of attenuating $PM_{2.5}$-exacerbated allergic asthma [Contribution 8]. Their findings demonstrate that light-based therapy suppresses oxidative stress, immune cell infiltration, airway remodeling, and multiple forms of regulated cell death, including ferroptosis. These results align with emerging concepts that host-directed interventions may complement exposure reduction strategies [5].

Collectively, the studies in this Issue converge on a critical insight: oxidative stress represents a shared biological currency through which diverse environmental exposures interact with host immunity and tissue homeostasis. However, the downstream consequences of oxidative stress are highly context dependent, shaped by particle composition, exposure duration, genetic background, and the availability of protective modifiers.

Future research should prioritize integrative approaches that combine detailed exposure characterization with molecular, immunological, and clinical profiling. Such strategies will be essential for advancing precision environmental health, identifying susceptible populations, and developing tailored interventions that enhance resilience against pollution-related diseases.

Conflicts of Interest: The author declares no conflicts of interest.

List of Contributions:

1. Wang, D.; Zeng, Z.; Nawata, A.; Baba, R.; Okazaki, R.; Okuda, T.; Yoshida, Y. Seasonal Variation in $PM_{2.5}$ Composition Modulates Oxidative Stress and Neutrophilic Inflammation with Involvement of TLR4 Signaling. *Antioxidants* **2026**, *15*, 89. https://doi.org/10.3390/antiox15010089.
2. Miranda-Martinez, A.; Rodriguez-Martinez, E.; Valdés-Fuentes, M.; Rivas-Arancibia, S. Alterations of the Intestinal Barrier and Inflammatory Response, Caused by Chronic Ozone Exposure in a Rat Model. *Antioxidants* **2025**, *14*, 1000. https://doi.org/10.3390/antiox14081000.
3. Santibanez, M.; Ruiz-Cubillan, J.J.; Expósito, A.; Agüero, J.; García-Rivero, J.L.; Abascal, B.; Amado, C.A.; Ruiz-Azcona, L.; Lopez-Hoyos, M.; Irure, J.; et al. Association Between Oxidative Potential of Particulate Matter Collected by Personal Samplers and Systemic Inflammation Among Asthmatic and Non-Asthmatic Adults. *Antioxidants* **2024**, *13*, 1464. https://doi.org/10.3390/antiox13121464.

4. Grifoni, D.; Bustaffa, E.; Sabatino, L.; Calastrini, F.; Minichilli, F.; Gaggini, M.; Berti, S.; Vassalle, C. The Dark Triad of Particulate Matter, Oxidative Stress and Coronary Artery Disease: What About the Antioxidant Therapeutic Potential. *Antioxidants* **2025**, *14*, 572. https://doi.org/10.3390/antiox14050572.
5. Lee, C.W.; Chiang, Y.C.; Vo, T.T.T.; Lin, Z.-C.; Chi, M.-C.; Fang, M.-L.; Peng, K.-T.; Tsai, M.-H.; Lee, I.-T. Deciphering the Liaison Between Fine Particulate Matter Pollution, Oxidative Stress, and Prostate Cancer: Where Are We Now? *Antioxidants* **2024**, *13*, 1505. https://doi.org/10.3390/antiox13121505.
6. Lee, J.K.; Bashir, K.M.I.; Park, H.-R.; Kwon, J.-G.; Choi, B.-R.; Choi, J.-S.; Ku, S.-K. Protective Effects of Thyme Leaf Extract Against Particulate Matter-Induced Pulmonary Injury in Mice. *Antioxidants* **2025**, *14*, 1343. https://doi.org/10.3390/antiox14111343.
7. Kim, I.Y.; Lee, H.L.; Choi, H.J.; Ju, Y.H.; Heo, Y.M.; Na, H.R.; Lee, D.Y.; Jeong, W.M.; Heo, H.J. A Combined Extract from Dioscorea bulbifera and Zingiber officinale Mitigates $PM_{2.5}$-Induced Respiratory Damage by NF-kappaB/TGF-beta1 Pathway. *Antioxidants* **2024**, *13*, 1572. https://doi.org/10.3390/antiox13121572.
8. Park, J.; Kim, B.Y.; Park, E.J.; Shin, Y.-I.; Ryu, J.H. Photobiomodulation Mitigates $PM_{2.5}$-Exacerbated Pathologies in a Mouse Model of Allergic Asthma. *Antioxidants* **2024**, *13*, 1003. https://doi.org/10.3390/antiox13081003.

References

1. Kelly, F.J.; Fussell, J.C. Air pollution and public health: Emerging hazards and improved understanding of risk. *Environ. Geochem. Health* **2015**, *37*, 631–649. [CrossRef] [PubMed]
2. Li, N.; Sioutas, C.; Cho, A.; Schmitz, D.; Misra, C.; Sempf, J.; Wang, M.; Oberley, T.; Froines, J.; Nel, A. Ultrafine particulate pollutants induce oxidative stress and mitochondrial damage. *Environ. Health Perspect.* **2003**, *111*, 455–460. [CrossRef] [PubMed]
3. Hornung, V.; Bauernfeind, F.; Halle, A.; Samstad, E.O.; Kono, H.; Rock, K.L.; Fitzgerald, K.A.; Latz, E. Silica crystals and aluminum salts activate the NALP3 inflammasome through phagosomal destabilization. *Nat. Immunol.* **2008**, *9*, 847–856. [CrossRef] [PubMed]
4. Schraufnagel, D.E.; Balmes, J.R.; Cowl, C.T.; De Matteis, S.; Jung, S.-H.; Mortimer, K.; Perez-Padilla, R.; Rice, M.B.; Riojas-Rodriguez, H.; Sood, A.; et al. Air Pollution and Noncommunicable Diseases: A Review by the Forum of International Respiratory Societies' Environmental Committee, Part 2: Air Pollution and Organ Systems. *Chest* **2019**, *155*, 417–426. [CrossRef] [PubMed]
5. Forman, H.J.; Zhang, H. Targeting oxidative stress in disease: Promise and limitations of antioxidant therapy. *Nat. Rev. Drug Discov.* **2021**, *20*, 689–709. [CrossRef] [PubMed]

antioxidants

Review

The Dark Triad of Particulate Matter, Oxidative Stress and Coronary Artery Disease: What About the Antioxidant Therapeutic Potential

Daniele Grifoni [1,2], Elisa Bustaffa [3], Laura Sabatino [3], Francesca Calastrini [1,2], Fabrizio Minichilli [3], Melania Gaggini [3], Sergio Berti [4] and Cristina Vassalle [5,*]

[1] Institute of Bioeconomy (IBE), National Research Council (CNR), Via Madonna del Piano 10, 50019 Sesto Fiorentino, Italy; grifoni@lamma.toscana.it (D.G.); calastrini@lamma.toscana.it (F.C.)
[2] Laboratory of Monitoring and Environmental Modelling for the Sustainable Development (LaMMA Consortium), Via Madonna del Piano 10, 50019 Sesto Fiorentino, Italy
[3] Institute of Clinical Physiology, National Research Council, Via G. Moruzzi 1, 56124 Pisa, Italy; elisa.bustaffa@cnr.it (E.B.); laura.sabatino@cnr.it (L.S.); fabrizio.minichilli@cnr.it (F.M.); melania.gaggini@cnr.it (M.G.)
[4] Fondazione CNR-Regione Toscana G Monasterio, Ospedale del Cuore "Gaetano Pasquinucci", Via Aurelia Sud, 54100 Massa, Italy; berti@ftgm.it
[5] Fondazione CNR-Regione Toscana G Monasterio, Via G. Moruzzi 1, 56124 Pisa, Italy
* Correspondence: cristina.vassalle@ftgm.it

Abstract: Particulate matter (PM) is a complex mixture of particles with different adverse effects on health, especially on the cardiovascular (CV) risk and disease (e.g., increased risk of total and CV mortality, ischemic heart disease, heart failure, stroke, hypertension, dyslipidemia and type 2 diabetes). Since oxidative stress (OS) and inflammation are the main key mechanisms by which PM exerted its biological effects on health, several oxidative and inflammatory-related biomarkers have been measured and associated with PM; abnormalities in these parameters in relation to PM highlight the key role of this relationship in terms of adverse health effects, including CV conditions. Antioxidant strategies might prevent/reverse, almost partly, CV effects related to PM exposure, by addressing OS and inflammation, although the clinical gain of these interventional tools is not yet clearly demonstrated. This review aims to summarize PM source and composition, discussing OS and inflammatory events associated with environmental PM exposure as key mechanistic determinants of CV risk and acute event precipitation. Moreover, the modifying potential of antioxidants, especially in subjects more susceptible to the adverse effects of air pollution and/or more highly exposed, will be discussed as a promising research area beyond conventional strategies actually available to prevent the harmful effects of PM (e.g., reduction of pollution sources and population exposure, assessment of air quality standards) in order to better face this dark triad composed of PM, OS and CV disease.

Keywords: oxidative stress; particulate matter; cardiovascular disease; acute myocardial infarction; health; antioxidants; $PM_{2.5}$

1. Introduction

Air pollution is a complex combination of gaseous and particulate molecules, which greatly changes according to geographical, urban/rural, meteorological characteristics and many other factors [1,2]. Particulate matter (e.g., PM_{10}, which includes particles < 10 μm in diameter, $PM_{2.5}$ for particles < 2.5 μm) and gases such as nitric oxide (NO), nitrogen dioxide

(NO_2), sulfur dioxide (SO_2) and ozone (O_3), are among the primary environmental threats to human health and well-being, affecting multiple organ systems [2,3]. In particular, an increase in mortality from exposure to PM, especially $PM_{2.5}$, has been evidenced since the 1990s [4]. Accordingly, exposure to air pollution is now considered a significant contributor to global health risks: it is among the top five risk factors, out of eighty-seven, in a global assessment, alongside other major health concerns such as an unhealthy diet and tobacco smoking [5]. The World Health Organization (WHO) estimates that approximately 4 to 9 million deaths annually are related to air pollution [6,7] and the Global Burden of Disease study attributes 4.1 million of these deaths to ambient $PM_{2.5}$ [5]. Thus, the majority of clinical studies have generally focused on acute and chronic exposure to PM (with stronger evidence for $PM_{2.5}$, judged the most dangerous air pollution component among the first cause of mortality in 2015); in this context, the WHO (2021) has set limits, recommending that the annual average $PM_{2.5}$ should not exceed 5 $\mu g/m^3$, whereas daily levels should remain below 15 $\mu g/m^3$ [7–9].

At present, there is a strong case for causality between pollution and a wide range of cardiovascular (CV) endpoints [10]. In agree with its importance in terms of CV effects, air pollution has been recognized as a key determinant for CV disease (CVD), and one of the modifiable factors which can be modulated in the prevention and management of CVD by an expert position paper on air pollution and CVD from the ESC Working Group on Thrombosis, which declared: "There is now abundant evidence that air pollution contributes to the risk of cardiovascular disease and associated mortality, underpinned by credible evidence of multiple mechanisms that may drive this association" and "air pollution should be viewed as one of several major modifiable risk factors in the prevention and management of cardiovascular disease" [11]. This relationship is particularly evident for $PM_{2.5}$, as also summarized by the American Heart Association "evidence is consistent with a causal relationship between $PM_{2.5}$ exposure and cardiovascular morbidity and mortality", which also reported that the majority of deaths (57–76%) attributable to $PM_{2.5}$ are a result of atherosclerotic events, supporting a consistent relationship between both short-term (days to weeks) and chronic (years) air pollution exposure and the occurrence of acute myocardial infarction (AMI) and stroke; nonetheless, increasing evidences are emerging also on the role that the gaseous component might have in terms of CV pathophysiology [12,13]. In fact, the CV system is one of the major health targets of PM, not only due to CVD's high prevalence as the leading cause of morbidity and mortality, but also because the CV system facilitates the systemic distribution of pollutants, exacerbating damage in multiple organs. Accordingly, the risk functions for $PM_{2.5}$ and CVD, showing a relative risk of 1.11, with a 95% confidence interval (CI) ranging from 1.09 to 1.14, were also updated by WHO in 2021 [7].

It is known that $PM_{2.5}$ promotes inflammation, oxidative stress (OS) and a hypercoagulable state, all of which act as key determinants in the relationship between this pollutant and CVD. In this context, growing evidence suggests that antioxidant intake might prevent/reverse, almost partly, CV effects related to PM exposure, counteracting the increase of OS and inflammation, although the clinical gain of these interventional strategies is not yet clearly demonstrated. Thus, this review aims to summarize PM source and composition, with a focus on OS and inflammatory events elicited by environmental PM exposure as key mechanistic culprits of CV risk and acute event precipitation. It also explores the potential for antioxidants in modifying these adverse effects on CV pathophysiology.

2. Search Strategy

We utilized the PubMed search to evaluate the available topic-related studies published in English on the subject of "oxidative stress effects of air pollution on the CV system"

to discuss in this narrative review. Studies specifically focusing on cancer, cerebrovascular or respiratory pathologies were excluded. Instead, special focus was placed on PM effects, because its concentration is generally found closely related to CV morbidity and mortality.

Different combinations of following main search terms were used: "antioxidants", "oxidative stress", "inflammatory disease", "air pollution", "particulate matter" or "PM", "vehicle emission", "cardiovascular", "CVD", "blood pressure", "cardiac", "coronary heart disease", "ischemic heart disease", "short term", "long term" and "mortality". Then, articles relevant to our topic were selected based on the title, abstract and full text of each paper.

3. Particulate Matter

Atmospheric aerosol, or PM, consists of a broad class of solid or liquid particles with different chemical and physical properties. Aerosol is therefore a heterogeneous collection of particles that differ not only in their chemical and physical properties, but also in their formation mechanisms or emission sources, which can be either natural or anthropogenic. The main natural sources are mineral desert dust, sea spray, volcanic ash, forest fires and pollen, while the main anthropogenic sources are linked to the use of fossil fuels for energy production, heating, land, air and sea transport, as well as to industrial, mining and even agricultural activities. Aerosol can be emitted directly from the source as primary PM or produced in the atmosphere as secondary PM through chemical reactions between primary solid, liquid and gaseous pollutants. Studying aerosols is therefore challenging, as they are a collection of heterogeneous particles that can vary during time because of chemical and physical processes, and in space as a result of transport, dilution and deposition processes [14,15].

The effects on the environment, climate and human health are also closely related to the characteristics and transformation processes of PM itself. Since the 1970s, numerous studies in various scientific fields, including climatology, biogeochemistry and medicine, have emphasized the significant impact of atmospheric aerosols, from the global to the urban scale and even the indoor environment [16–20]. These studies have highlighted the need to monitor this pollutant with standardized measurement systems and specific analyses. In this context, various methodologies have been proposed for the classification of PM based on characteristics such as size, chemical composition, formation processes and origin. The purpose of these classifications is to better understand the environmental and health impacts associated with these properties [15,21–23].

3.1. Particle Size Fractions

One of the main classification methodologies is based on particle size, as this influences radiation scattering and absorption, atmospheric visibility and human health [23–25]. The parameter used to express the size of particles is the equivalent aerodynamic diameter (D_a), defined as the diameter of a spherical particle with a density of 1 g/cm^3 and a settling velocity as that of the particle in question under the same conditions of temperature, relative humidity and pressure [15]. This definition is necessary because, unlike liquid particles that tend to assume spherical shape, solid particles generally have irregular shapes. The D_a can vary significantly from the physical diameter, with variations influenced by factors such as density and aerodynamic properties, which depend on the particle's surface area and volume.

In the classification of particles by size, three different methods are used: modal, based on the observed size distributions and formation mechanisms; sampler cut point, which refers to the particle diameter at which a sampling device collects a certain percentage

(commonly 50%) of particles of that size; dosimetry, based on the particle penetration into different compartments of the human respiratory system [15,23].

3.1.1. Modal Classification

Particle size and formation processes are closely linked: the modal classification, by considering the aerosol distribution as a function of particle diameter, allows the identification of classes of particles formed through different chemical and physical processes [14,15,23]. The idealized aerosol modal distribution shown in Figure 1 highlights four modal peaks: coarse, accumulation, Aitken and nucleation mode.

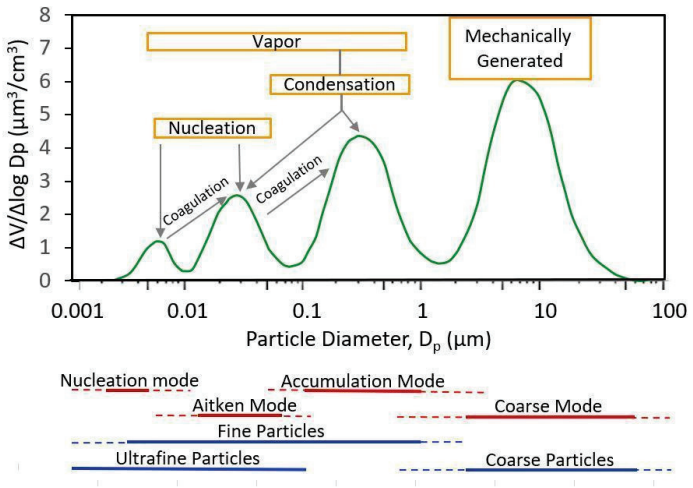

Figure 1. An idealized size distribution, which might be observed in traffic, showing fine and coarse particles, as well as the nucleation, Aitken and accumulation modes (adapted from [15]).

Coarse Mode—The coarse mode consists of particles with diameters that exceed the minimum in the particle mass distribution (the point in the size range of particles where the mass of the aerosol particles is at its lowest), which typically occurs between 1 and 3 μm. The formation of such particles is predominantly due to mechanical processes (e.g., soil erosion, industrial activities such as mining and construction), resuspension (e.g., by wind or human activity such as vehicle traffic) or biogenic sources (such as pollen or spores). This fraction includes dust from desert or arid regions, sea salt from the ocean, and also nitrate and sulfate formed from chemical reactions of nitric acid with sodium chloride and SO_2 with basic particles, respectively. The coarse mode and the accumulation mode overlap in the region between 1 and 3 μm. The sedimentation rate of the particles is faster compared to other modes, such that they can be deposited within hours or days.

Accumulation Mode—The particles with diameters from about 0.1 μm to 1–3 μm are mainly derived by coagulation (smaller particles collide and combine to form larger ones), by condensation (low-equilibrium vapor pressure gas molecules condense onto existing particles or nucleate to form new particles). Additionally, these particles may result from the fragmentation of larger particles. The mechanisms for removing this fraction are less effective, so the residence time in the atmosphere is in the order of days or longer.

Aitken Mode—This mode is constituted by particles with diameters ranging from 0.01 to 0.1 μm. This mode is also referred to as the *transient nucleation mode*. It is the result of particles formed by nucleation (a process by which gaseous substances condense or react to form new solid particles or liquid droplets), as well as by condensation and coagulation.

Nucleation Mode—Freshly formed particles observed during active nucleation events with diameters below about 0.01 μm. The nucleation mode can be observed as a separate mode in clean or remote areas or near sources. The residence time in the atmosphere for this fraction, as for the Aitken mode, is short, on the order of hours.

The term "Fine particles Mode" refers to the fraction of particles with diameters smaller than the minimum in the particle mass distribution, between 1 and 3 μm. The fine mode includes the accumulation, the Aitken and the nucleation modes. Fine particles are formed primarily by combustion or chemical reactions of gases (e.g., industrial emissions, vehicle exhaust emissions). They are composed of sulfate, nitrate, ammonium and hydrogen ions, metals and metal oxides, black carbon or elemental carbon and organic compounds (OCs). Elemental carbon is directly emitted into the atmosphere mainly from combustion processes, whereas OCs can have both primary and secondary origins through the condensation of products in the process of hydrocarbon photooxidation. The secondary component of OCs is a considerable fraction of the total OC [14].

The ultrafine particles (UFPs) are generally defined by size, as particles with diameters of 0.1 μm or less. While UFP includes the nucleation mode and much of the Aitken mode, they are not considered a mode in themselves. The effects of UFP on light scattering and absorption are relevant, producing visibility alterations. Furthermore, these particles act as cloud condensation nuclei. Their ability to penetrate deep into the lungs, enter the bloodstream and induce OS makes them a significant concern for air quality regulations and public health [15].

3.1.2. Sampler Cut Point Classification

To measure size fractions of particles relevant to health, environment, etc., size-selective sampling has been developed, i.e., the collection of particles below or within a specified aerodynamic size range. For example, dichotomous samplers split the particles into two distinct size fractions: smaller and larger, while cascade impactors separate airborne particles into multiple size fractions. A variety of upper-size cut samplers with a single filter are also used. The term cut point is used to describe the performance of particle-size selective devices. Typically, the maximum size of particles that the device will collect with 50% efficiency is defined by the upper 50% cut point size [23].

The use of PM_{10}, the aerosol fraction with a D_a less than 10 μm [26], and $PM_{2.5}$, the fraction with a D_a less than 2.5 μm [27], as indicators is an example of size-selective sampling based on a legally defined, regulatory size for air quality standards. It is important to note that PM_{10} and $PM_{2.5}$ are formally recognized as regulated pollutants in international and European legislation [28]. The threshold choice of PM_{10} is based on health considerations, as particles of this size are able to enter the thoracic compartment (see Figure 2). Conversely, the threshold choice of $PM_{2.5}$ is driven by its distinct sources, rather than its respirable fraction. Numerous studies have demonstrated that the two fractions differ in chemical and physical characteristics, toxicity, emission sources, etc. [14,15,17,22,23].

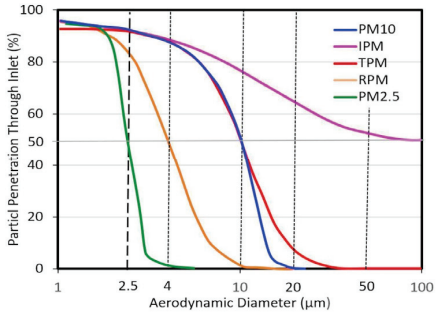

Figure 2. Specified particle penetration (size-cut curves) through an ideal inlet for five different size-selective sampling criteria. Regulatory size cuts are defined in the Code of Federal Regulations: $PM_{2.5}$ [27], PM_{10} [26]. Size-cut curves for inhalable particulate matter (IPM), thoracic particulate matter (TPM) and respirable particulate matter (RPM) size cuts are defined by the ACGIH [29] (adapted from [15]).

3.1.3. Dosimetry Classification

Since 1993, standardized classification of airborne particles based on their ability to penetrate the human respiratory system has been adopted by the American Conference of Governmental Industrial Hygienists [29], the International Standards Organization and the European Committee for Standardization. These organizations established three key fractions of PM: inhalable, thoracic and respirable particles, according to their upper size cut-offs [15,23,29].

Inhalable fraction: these particles enter the respiratory tract through the nose and mouth. Thoracic fraction: these particles pass beyond the larynx and reach the tracheobronchial region. Respirable fraction: this fraction represents a subset of the thoracic particles that are small enough to penetrate even further, reaching the alveolar region of the lungs. In addition, UFP can pass through the alveolar barrier and enter the bloodstream.

Based on dosimetry classification, the curves defining inhalable particulate matter, thoracic particulate matter and respirable particulate matter are shown in Figure 2. This classification ensures accurate evaluation of how different particle sizes affect respiratory health, providing a framework for air quality limits and occupational exposure regulations [29].

3.2. Main Sources and Composition of Particulate Matter

The sources of atmospheric aerosols can be either anthropogenic or natural. Anthropogenic PM originates in urban or industrial areas, primarily from traffic emissions (both exhaust and non-exhaust), domestic heating, construction activities and various industrial activities (such as power plants, oil refineries, mining, etc.). In rural areas, major sources are represented by agricultural activities, including biomass burning. Natural aerosols mainly consist of soil and desert dust, sea spray, volcanic ash, emissions from vegetation and wildfires. These different sources, through a range of chemical and physical processes, generate particles with different chemical compositions and varying environmental and health impacts [14,17,22].

3.2.1. Traffic

Vehicular traffic, especially in urban areas, is an important source of both primary and secondary aerosols. Particle sizes vary depending on the formation processes: vehicles emit a mixture of ultrafine primary carbon particles [30] and gases, including NO_2, a precursor of nitrogen compounds, as part of exhaust emissions [31], while non-exhaust emissions result from abrasion due to tyre wear, brake wear, road wear and the resuspension of road dust [32]). Brake and tyre wear releases metals in small concentrations such as copper, zinc and cadmium [33], while traces of other elements, including potassium, bromine and chlorine, originate from the engine. PM emissions from diesel vehicles are typically higher than those from gasoline vehicles and contain toxic chemicals such as polycyclic aromatic hydrocarbons (PAHs), which are linked to adverse health effects [34].

Maritime transport is a major contributor to air pollution in terms of SO_2 emissions and sulfate aerosols. It is also responsible for NO_2 emissions and carbonaceous PM, with a considerable contribution on a global scale [35,36].

Similarly, aviation plays a role in aerosol and precursor gas emissions. Aircraft engines release metals such as aluminum, titanium, chromium, iron, nickel and barium [37,38].

3.2.2. Industrial Activities

Emissions from the industrial sector are heterogeneous as they derive from a variety of industries, including those of petrochemical, metallurgical, ceramic and pharmaceutical sectors. Consequently, these emissions are influenced by different production cycles and

raw materials used. The activities with the most significant impact are power plants, oil refineries and mining. Energy production from fossil fuels is a major contributor to the emission of secondary aerosol precursor gases. Additionally, coal combustion generates primary PM as well as sulfur, carbonates, chlorides and metals such as mercury [39], while oil combustion releases sulfates and metals such as vanadium and nickel, which can be used as tracers specific for these sources [40].

Industrial activities related to the production of ceramics, bricks and cement, as well as foundries and mining, are significant contributors to primary PM emissions. These activities also release production-specific heavy metals. For instance, the metallurgical industry emits metals such as copper, iron, manganese and zinc, which are used as markers for source identification [41,42].

3.2.3. Biomass Burning

Biomass burning is also an important source of aerosols and gases that contribute to increased air pollution and climate-changing emissions, at both regional and global scales. This source includes forest fires, which can be natural or, more often, human-induced for purposes such as pastoral or agricultural land use. The burning of agricultural biomass residues in fields to prepare the land for the next planting season also has a relevant impact on air quality worldwide [43–45].

Wood burning for domestic heating is a significant source of atmospheric pollution due to biomass combustion. In winter, domestic biomass burning has been identified as a relevant source of pollution not only in rural areas, but also in residential areas of Europe [46–48] and the USA [49]. In Europe, more than 40% of fine PM emissions are attributed to domestic combustion [50]. Many studies have shown that stable atmospheric conditions together with low temperatures, which encourage the use of domestic heating, can lead to critical air quality conditions in the Po Valley (Northern Italy) [51] and Tuscany (Central Italy), where domestic heating is a major contributor to PM_{10} concentrations during the cold season [52–55].

Emissions from wood burning depend on combustion conditions and the characteristics of the biomass, such as the species of wood used [56]. The main components of the aerosol emitted from biomass burning are carbonaceous compounds, including OC and elemental carbon [57]. Elements that are produced during the decomposition of cellulose, such as levoglucosan, can be used as markers of this source [55]. The inorganic component of the emitted aerosol contains mainly potassium, ammonium, sulfate and nitrate [57]. Interestingly, recent data indicate the importance of wood burning, which significantly increases fibrinogen in cardiac patients and contributes to an increased risk of AMI in elderly subjects [58,59].

3.2.4. Mineral Desert Dust

Mineral desert dust is a major component of atmospheric aerosols on a global scale [20,60,61]. They play a crucial role in cloud formation and radiative transfer [62–64], influence both terrestrial and oceanic ecosystems, and affect air quality by reducing visibility and impacting human health [65–68].

The sources are mainly dried or ephemeral lakes or rivers, located within the desert or semi-arid regions of the subtropics. The most important of these is the Sahara, but other major sources are in Arabia, Central Asia, the southwestern United States and Australia [20,69,70]. Mineral dust is mainly composed of calcite, quartz, dolomite, kaolinite, illite, feldspar and traces of calcium sulfate and iron oxides [71], although the chemical and mineralogical composition differs by region of origin [72]. Europe, and particularly the Mediterranean region, is also frequently affected by desert intrusions, which are more

frequent in spring and summer. In some cases, high desert dust concentration can contribute to the exceedance of legal PM_{10} concentration limits [73].

In recent years, the frequency and intensity of desert intrusions in the Mediterranean area have increased [74,75]. These intense episodes, characterized by very high PM_{10} concentrations, have been associated with adverse effects on human health. Recent studies also indicate an increase in mortality from CVD associated with these events [65].

3.2.5. Sea Spray

Sea spray, or marine aerosol, is one of the largest contributors to atmospheric aerosol worldwide [76]. While most prevalent in coastal areas, sea spray can also be found inland [77]. This type of aerosol is mostly primary and consists mainly of sodium and chloride, with smaller amounts of other components such as sulfate, potassium, magnesium and calcium. In addition, sea spray has a secondary component mainly consisting of OC produced by phytoplankton. Among these, dimethyl sulfide, one of the main precursors of atmospheric sulfates in oceanic regions [78].

3.2.6. Biogenic Emissions

Biogenic emissions, produced by vegetation and microorganisms, contribute to the formation of primary and secondary atmospheric aerosols. Primary particles include pollen, spores, but also bacteria, viruses, proteins and carbohydrates [79]. Biogenic volatile OC, e.g., isoprene and terpenes, can act as precursors of secondary aerosol [14,80]. In addition, by interacting with anthropogenic emissions (volatile organic compounds and nitrogen oxides-NOx), biogenic volatile organic compounds contribute to the formation of tropospheric O_3 [81].

4. Particulate Matter and Cardiovascular Diseases

Many studies have shown that long-term exposure to $PM_{2.5}$ is correlated to subclinical atherosclerosis (AS; increase in coronary artery calcium (CAC) or carotid intima-media thickness (IMT)), heart failure (HF) and CV mortality [82]. Recently, de Bont and colleagues performed an umbrella review summarizing the current epidemiological evidence from systematic reviews and meta-analyses linking ambient air pollution (PM and NOx) to multiple CVD manifestations [83]. Specifically, sufficient evidence was observed for the following: (i) both short- and long-term exposure to PM and increased risk of CVD mortality, ischemic heart disease and AMI, (ii) short-term PM exposure and increased risk of stroke, blood pressure, HF and arrhythmias, (iii) short-term NOx exposure and increased risk of stroke and arrhythmias and (iv) long-term NOx exposure and an increased risk of ischemic heart disease and AMI [83]. These associations may be affected by different factors, such as by AMI subtypes (e.g., ST-elevation myocardial infarction-STEMI and non-ST-elevation myocardial infarction-NSTEMI, according to different characteristics of electrocardiogram-ECG), lag times and individual specificities and susceptibility (e.g., elderly subjects or presence of comorbidities as type 2 diabetes-T2D). Moreover, the effects of pollutants are evident not only in more vulnerable groups (e.g., those with comorbidities but also those with asthma, and children) but even in healthy subjects [84,85]. Accordingly, $PM_{2.5}$ short-term exposure is able to induce ECG changes also in healthy subjects [86].

Long-term joint exposure to air pollutants, including $PM_{2.5}$, PM_{10}, NO_2 and NOx, has been repeatedly found to be associated with increased risk of subclinical AS. An association between IMT and PM_{10} mass concentration was observed in 2348 subjects living in London [87]. A meta-analysis including eight cohorts (n = 18,349) for the assessment of cross-sectional association between IMT and PM exposure and three cohorts (n = 7268) for the longitudinal analysis on carotid IMT and PM, confirmed this relationship [88]. A

systematic review including eighteen studies (five cohorts and thirteen cross-sectional), also supported the existence of a positive association between PM exposure and subclinical AS (CAC and IMT) [89]. In a prospective Chinese study (n = 8867 aged 25–92 years with suspected coronary artery disease—CAD), a significant association between long-term exposures to $PM_{2.5}$ and NO_2 with an increase in CAC scores was observed [90]. Accordingly, in a German cohort (4814 middle-aged adults, 5 years follow-up) long-term exposure to $PM_{2.5}$ was found associated to development and progression of subclinical AS (1.5 $\mu g/m^3$ higher exposure to $PM_{2.5}$) with an odds ratio of 1.19 (95% CI: 1.03, 1.39) for progression of CAC, with an increased annual growth rate of 2% (95% CI: 1%, 4%) [91].

Moreover, in the Swedish CArdioPulmonary bioImage Study Gothenburg study (2013–2017, n = 5070, age 50–64 years), although no consistent relation between long-term total $PM_{2.5}$ exposure and CAC score or presence of carotid artery plaques was observed, an association between total $PM_{2.5}$ and larger plaque area in participants with carotid plaques was found; positive correlation with traffic-related air pollutants were found for both a high CAC score and bilateral carotid artery plaques [92]. These associations were stronger among men and those with CV risk factors [92]. In fact, PM may act as an endocrine disruptor and, as such, interfere with hormones (e.g., insulin), contributing to the onset and progression of metabolic diseases (e.g., obesity and T2D) [93]. Moreover, $PM_{2.5}$ and PM_{10} have been associated with an increased risk of developing hypertension and impairment of high-density lipoprotein (HDL) function [94,95].

However, in the Malmö Diet and Cancer study between 1991 and 1994 (n = 6103), no clear relationship was found between air pollution exposure and carotid plaque prevalence [96], whereas the existence of controversial data reflects the complexity and difficulty of studying the relationship between pollutants and CV pathophysiology, which depends on many determinants. Nonetheless, different meta-analyses support the relation between long-term exposure to air pollutants and HF incidence, and other outcomes (e.g., hospital readmissions) [97–101], while other meta-analyses highlight the association between overall and CV mortality and air pollutants [102,103].

Interestingly, satellite-based estimates of long-term $PM_{2.5}$ exposure were associated with both CAD and AMI incidence in cardiac catheterization patients; in particular, 1 $\mu g/m^3$ increase in annual average $PM_{2.5}$ gave an 11.1% relative increase in the odds of CAD (95% CI: 4.0–18.6%) and a 14.2% increase in the odds of having an AMI within a year prior (95% CI: 3.7–25.8%) [104]. A meta-analysis (27 cohort studies, 6,764,987 participants and 94,540 AMI patients) reported that higher levels of $PM_{2.5}$ and PM_{10} exposure were significantly associated with AMI risk (relative risk for each 10 $\mu g/m^3$ increment in $PM_{2.5}$ and PM_{10} corresponding 1.18 (95% CI: 1.11–1.26) and 1.03 (95% CI: 1.00–1.05), respectively) [105].

Different studies also confirmed a significant link between short-term exposure to pollutants (e.g., PM_{10} and $PM_{2.5}$) and the rate of hospitalizations for CV events (especially the occurrence of HF and AMI) [84,85], finding a 2% increased risk of AMI with each 10 $\mu g/m^3$ exposure to $PM_{2.5}$ (relative risk of 1.02; 95% CI, 1.01–1.03; p-value ≤ 0.0001) [85]. In agreement with this observation, short-term exposure to $PM_{2.5}$ and PM_{10} was associated with increased triggering of both mortality and hospital admissions for AMI. Additionally, an increase in long-term exposure to $PM_{2.5}$ was linked to a higher risk of AMI mortality/incidence [83].

A case-crossover study design (n = 12,865, USA) evidenced the relationship between $PM_{2.5}$ and acute ischemic coronary events (unstable angina and AMI; 10 $\mu g/m^3$ elevation associated with increased risk of 4.5%, 95% CI, 1.1–8.0) [106]. Recent data showed that, in areas with a long-term moderate or high severity of air pollution, short-term exposure to

high concentrations of $PM_{2.5}$ and PM_{10} (10 μg/m^3 increase) is positively correlated with both AMI and acute HF [107].

An Italian study performed in winter, when $PM_{2.5}$ are characterized by the presence of nitrate, organic carbon fraction, with high amount of PAHs and elements such as lead, aluminum, zinc, vanadium, iron, chromium and others, evidenced the potential of $PM_{2.5}$ to alter global gene expression in heart tissue (181 upregulated and 178 downregulated genes; e.g., increase in collagen and laminin related genes as well as in genes involved in calcium signaling), highlighting the question of individual susceptibility, and the need to protect more vulnerable subjects [108].

The heterogeneous composition of PM—differing by source, region and season—impacts its toxicity. In this context, the disparate effects of traffic-related PM (enriched in metals and PAHs) have been more studied compared to desert dust (rich in silicates) effects, which remain little investigated.

Experimental and in vitro studies suggested that desert dust is correlated with OS and inflammation, mitochondrial dysfunction, an increase in mean blood pressure and heart rate, as well as being associated with increased blood pressure in humans [109–112].

A systematic review with meta-analysis (20 cohort studies), investigating the effects of occupational silica exposure on the risk of heart disease, evidenced that silica-exposed workers are at a higher risk for overall heart disease, with stronger evidence supporting an association with pulmonary heart disease [113]. Moreover, a Japanese study on 3068 consecutive AMI patients showed that exposure to desert dust a few days before symptom onset is associated with the incidence of AMI [114]. Interestingly, more recent data provide evidence that short-term exposure to desert dust is associated with a higher risk of a particular type of myocardial infarction with nonobstructive coronary arteries (MINOCA), compared to myocardial infarction with CAD [115].

These results open new opportunities for future studies; if there is still much to understand, a better knowledge of how the heterogeneous composition of PM has differential effects of toxicity may be helpful to guide targeted public health strategies informed by PM source characteristics and in accordance with the relevance to various exposure scenarios.

5. Oxidative Stress and Other Mechanisms Mediating Particulate Matter Effects on the Cardiovascular System

Main pathways involved in eliciting the adverse CV outcomes due to pollutant exposure may be broadly categorized into the following:

(1) Primary initiating responses in the lung—these occur following pollutant inhalation and include (a) either exogenous (pollutant-induced) or endogenous OS, (b) pulmonary inflammation and (c) ion channel/receptor activation;
(2) Transmission pathways—these facilitate the systemic impact of initial pulmonary responses and include (a) generation of biologic intermediates (e.g., oxidized lipids, cytokines, activated immune cells, microparticles, microRNA, vasoconstrictors) (b) autonomic imbalance/afferent neurological circuits leading to the central nervous system (sympathetic or hypothalamic pituitary adrenal axis activation);
(3) End-organ effector mechanisms—the previous pathways, in turn, lead to end-organ effector mechanisms responsible for atherosclerotic events [116].

Several biomarkers have been identified in the association between PM and CAD, whereas many others are probably not discovered or fully elucidated, mainly involving endothelial function, OS and inflammation, but also dyslipidemia, increased thrombogenicity and blood pressure. In this context, endogenous antioxidants could act as defense mechanisms that can reduce the stimulation of these particles, modifying the relationship between OS and air pollutants. Main endogenous antioxidants include glutathione (an-

tioxidant and xenobiotic detoxifier), uric acid (a major blood antioxidant), bilirubin (with antioxidant and anti-inflammatory activity), catalase (one key antioxidant enzyme) and superoxide dismutase (SOD) (detoxification enzyme and powerful antioxidant).

Different interindividual capacities to modulate the antioxidant response may be a reason for different susceptibility to pollutant damage. Consequently, air pollution induces erythrocyte enzyme inactivation (Glutathione peroxidase 1 (GPx-1) and Cu, Zn-SOD), although some subjects showed positive GPx-1 and Cu, Zn-SOD correlation with air pollutants. This response could be related to a greater capacity to counteract air pollution effects by increasing the antioxidant enzyme activity (e.g., through a more rapid bone marrow response to PM) [117].

The null genotype for glutathione-S transferase M1 (GSTM1) had a modifying effect in the relationship between PM and AS, resulting in a more marked endothelial dysfunction (flow-mediated dilation) associated with PM exposure in T2D subjects [118]. The adhesion molecules have a role in AS since they are involved in the attraction and tethering of leukocytes to the blood vessels. The same polymorphism also modulates the association between PM and inflammation and endothelial dysfunction, as adhesion molecules, vascular cell adhesion molecule-1 (VCAM-1) and intercellular adhesion molecule-1 (ICAM-1) were particularly higher in subjects carrying the GSTM1 null gene [119].

Also, abnormalities in uric acid concentration have been found to be associated with PM, especially in people exposed to high pollution levels [120–122]. However, as many other antioxidants, uric acid at elevated levels may exert a pro-oxidizing effect instead of antioxidant actions, thus shifting by protection to potentially harmful [123]. Thus, further research is expected to better understand the role of uric acid increase related to air pollutants [124].

Higher $PM_{2.5}$ has been recently found to induce a reduction of bilirubin (and biliverdin, molecules related to heme metabolism) in males; to note, bilirubin seems to represent a stronger risk factor for endothelial dysfunction and AS in men, thus the significance of these observed gender-related differences in the relationship with pollution merit further deepening [125,126].

Experimental data also showed that the activity of antioxidants enzymes (GPx together with SOD and catalase) is significantly reduced in the rat ischemic heart tissue exposed to PM_{10} [127]. Other experimental data (rats) showed that chronic exposure to O_3 reduced cardiac function increased myocardial OS and inflammation in parallel to a reduction of heart SOD activity [128].

Thus, although more data are needed in this research scenario to better evaluate the complexity of the mechanisms involved and the OS-related effects induced by PM exposure, the overexpression of antioxidant enzymes could represent an effective preventive strategy to counteract damage induced by oxidant pollutants [129]. For example, inhaled glutathione seems to increase pulmonary glutathione, a fact which could represent a potential additive preventive tool to mitigate the adverse effects of pollution [130]. Moreover, recent experimental data (mice) suggest that aerobic exercise may act as a tool to both reduce OS and improve antioxidant capacity against negative effects related to PM exposure, a measure which seems particularly effective in older animals [131].

PM can directly generate reactive oxygen species (ROS), molecules that damage cells, or can indirectly cause ROS production [132]. This process, known as OS, can also be initiated by inhaling other toxic compounds present in air pollution [133]. OS is a state where higher levels of free radicals, ROS, are accumulated in different parts of the body, including the lungs, vascular bed and even at a local cellular/tissue level. Therefore, OS is a pathological condition that occurs whenever there is an imbalance between the production of ROS and the body's ability to eliminate them, neutralize them or repair

the damage caused by them, acting with antioxidant systems. When OS occurs, the disruption of redox signaling and excess ROS are suggested to increase adverse biological effects (lipid/protein/DNA oxidation and initiation of proinflammatory cascades) and consequently may alter cardiac and vascular function through the disruption of important redox-sensitive signaling pathways, the depletion of vasodilators and antioxidants, the perturbation of cellular mechanisms and the oxidation of proteins and lipids [134,135].

Exposure to $PM_{2.5}$ has been associated to a variety of biomarkers; pro-inflammatory cytokines (e.g., interleukin-6 (IL-6), tumor necrosis factor (TNF)), acute phase proteins (e.g., C-reactive protein), vasoactive parameters (e.g., endothelin 1, NO), OS biomarkers (e.g., malondialdehyde MDA, oxidized low-density lipoprotein (Ox-LDL) and biomarkers of DNA oxidative modification, isoprostanes, protein carbonyls and nitrotyrosine, homocysteine) as well as different antioxidants in healthy subjects or in CV patients. A study including 40 healthy college students measured the plasma levels of Ox-LDL, highlighting that certain $PM_{2.5}$ chemical constituents/pollution sources were more closely associated with changes in biomarkers of OS associated with AS [136]. Results showed that $PM_{2.5}$ iron and nickel, as well as $PM_{2.5}$ from traffic emissions and coal combustion, were positively associated with Ox-LDL, and $PM_{2.5}$ calcium was associated with an increase in soluble CD36 [136]. Accordingly, air pollutants ($PM_{2.5}$ and constituents, SO_2, CO, NO_2 and O_3) measured during the 2008 Beijing Olympics resulted associated with acute changes in biomarkers of pulmonary and systemic inflammation, OS, and hemostasis and CV physiology biomarkers (heart rate and systolic blood pressure) in healthy, young adults [137].

The ROS can oxidize low-density lipoprotein (LDL), a key factor causing the onset and development of the atherosclerotic plaque, until the plaque can become unstable, resulting in the rupture, leading to acute disease manifestations [138,139]. Specifically, Ox-LDL are recognized by scavenger receptors (CD36) on the macrophages, which engulf Ox-LDL, resulting in foam cell formation, in turn enhancing OS and vascular inflammation and AS progression [140,141]. The scavenger receptor CD36 contributes to the inflammation associated with T2D, AS and thrombosis through the promotion of OS and its signaling to stress kinases [142]. Different studies examined the relationship between air pollution exposure and Ox-LDL levels, finding positive associations in occupationally exposed subjects, patients with T2D, and children [143–145]. Occupational exposure to vehicle emissions (PM_{10}, $PM_{2.5}$ and PAHs) revealed greater levels of several OS biomarkers (such as 8-oxo-2′-deoxyguanosine-a marker of DNA oxidative modification, 15-F(2t)-isoprostane in the urine, and blood levels of protein carbonyls and nitrotyrosine and lower levels of blood antioxidants) compared to controls [146,147]. A similar study, performed on taxi drivers, reported a positive correlation between increased urinary 1-hydroxypyrene, a biomarker of PAH exposure, and Ox-LDL and homocysteine [148]. Exposure to $PM_{2.5}$ has been shown to cause oxidative and methylated DNA damage (8-hydroxy-2-deoxyguanosine and N7-methylguanine) in young subjects [149]. Elevated levels of LDL also have been found associated with traffic-related air pollution in Shanghai with consequent increased blood pressure, and homeostatic model assessment for insulin resistance (HOMA-IR, indicator of insulin resistance) and decreased antioxidant capacity (low levels of NO, SOD and total antioxidant capacity) [150]. Moreover, a recent meta-analysis found significant short-term associations of PM with TNF-α and fibrinogen (the percent change of a 10 $\mu g/m^3$ $PM_{2.5}$ increase on TNF-α and fibrinogen was 3.51%, 95% CI: 1.21–5.81%; 0.54%, 95% CI: 0.21–0.86%, respectively, and between PM_{10} and fibrinogen the percent change resulted 0.17%, 95% CI: 0.04–0.29%) [151].

The oxidative potential of $PM_{2.5}$ has been found to be related to the risk of AMI: particles with the highest oxidative potential were associated with approximately an 8% increase in hospital admissions for AMI [152]. OS, measured as increased blood

MDA levels, has been found in patients with acute coronary events associated with black carbon exposure [153]. Another study found that long-term ambient $PM_{2.5}$ exposures were significantly associated with levels of multiple extracellular vesicle-encapsulated microRNAs in human serum [154]. In fact, pathway analysis on these extracellular vesicle-encapsulated microRNAs associated with $PM_{2.5}$ identified several key related pathways promoting OS, inflammation and AS.

Experimental studies have substantially confirmed the effect of PM exposure on CV risk throughout the induction of oxidative/inflammatory responses. Some studies investigated the molecular pathway through which OS acts following exposure to different types of PM. Thickness of coronary arteries, accompanied by angiotensin pathways upregulation and a decrease of heme oxygenase-1 levels, was observed in healthy rats after PM inhalation [155]. A study revealed that the exposure to diesel exhaust (DE) in ApoE-/- mice increased plaque lipid content, foam cell formation and smooth muscle and the expression of plaque OS biomarkers such as inducible NO synthase (iNOS; inflammatory-related enzyme involved in NO production), CD36 and 3-nitrotyrosine [156] and was associated with impaired HDL antioxidant capacity [157]. A DE particle instillation study used a dose representing the upper range a person could be daily exposed to in a highly polluted city. Results showed an increment of plaque size, number, lipid rich area and frequency of buried fibrous caps in ApoE-/- correlating with lung inflammation (plaques per section of artery and buried fibrous layers) and antioxidant gene expression in the liver (NF-E2-related factor-2, NAD(P)H-quinone oxidoreductase 1 and heme oxygenase-1), indicating a response to systemic pro-oxidative effects [158]. Inhalation exposures to environmental air pollutants from vehicular sources (diesel PM and gasoline exhaust) in ApoE-/- mice resulted in vascular OS mediated by LOX-1 (main Ox-LDL receptor of endothelial cells), expression of MMP-9 (a predictor of atherosclerotic plaque instability) and ET-1 (the most potent vasoconstrictor) and monocyte/macrophage infiltration, associated with progression of AS, atherosclerotic plaque rupture and therefore AMI [159,160]. Direct addition of DE particles to cultured cardiomyocytes reduces contractile function, an effect that could be partially prevented by antioxidants [161]. Similarly, $PM_{2.5}$, which is able to reduce antioxidant capacity, also causes a decrease in cardiomyocyte contractility upon direct exposure [162].

In LDLR-/- mice, UFP exposures have been shown to trigger reduced HDL antioxidant capacity, pro-atherogenic lipid metabolism and a greater atherosclerotic lesion [163,164]. Subacute $PM_{2.5}$ exposure caused insulin resistance through OS, inflammation and the inhibition of the Phosphoinositide 3-kinase-Protein Kinase B (PI3K-AKT) signaling pathway, as evidenced by increased glucose levels in cell supernatants, and elevated insulin levels in parallel to impaired intraperitoneal glucose tolerance test in mice; $PM_{2.5}$ increased OS (ROS, cytochrome P450 2E1 and MDA), and reduced SOD 1/2 and silent information regulator 1. Cytokines (IL-6 and TNF-α) were upregulated, while the PI3K-AKT signaling pathway was inhibited (decreased phosphorylation of PI3K/AKT in HepG2 cells) [165].

However, the effect of other pollutants beyond PM must also be considered: for example, CO exacerbated myocardial injury and depletion of antioxidants in the heart of a rat model of AMI [166]. The CO levels used were at the upper ranges of ambient levels in heavily polluted urban cities (30 ppm), spiked with peaks representative of that very close proximity to vehicle exhaust (100 ppm) [166]. Another work highlighted the involvement of the overexpression of iNOS mediating the higher sensitivity of the myocardium to ischemic events during a simulated urban CO air pollution exposure to daily non-toxic levels (30–100 ppm CO for 4 weeks) [167]. After chronic O_3 exposure (0.8 ppm, 8 h/day for 28 and 56 days), cardiac function decreased in O_3-exposed ischemia/reperfusion rats' hearts [168]. The authors associated this enhanced sensitivity to ischemia/reperfusion

injury with increased myocardial TNF-alpha levels and lipid peroxidation and decreased myocardial activities of SOD and interleukin 10 (IL-10) [168].

6. Metabolomics and Lipidomics Study

Metabolomic and lipidomic are promising tools to identify air pollution-related biomarkers by identifying a lot of metabolic and lipidomic features associated with exogenous exposures and endogenous processes [169]. Thus, focusing on changes in air pollution-related metabolites, these techniques could help in preventing air pollution-induced cardiometabolic risk.

Recently, a metabolome-wide association study was conducted by high-resolution metabolomics, an innovative analytical platform, in 1096 women, and annual average individual exposures to PM, NO_2, O_3, SO_2 and CO were registered in the same year of blood draw. Metabolomics profiling showed that ninety-five metabolites were significantly associated with at least one air pollutant or mixture and related to pathways involved in the OS, energy metabolism, systemic inflammation, signal transduction, nucleic acid damage and repair. In particular, several amino acid pathways were significantly associated with exposure to PM_{10} and O_3, including the urea cycle, tryptophan metabolism, methionine, cysteine, S-adenosylmethionine and taurine metabolism. Tryptophan metabolites were positively associated with PM_{10} exposure and negatively associated with CO exposure [170]. Using a global untargeted metabolomic approach in a longitudinal aging study among men (n = 2280), several significant metabolites and metabolic pathways associated with long-term exposure to $PM_{2.5}$, NO_2 and temperature were identified in the blood samples. The results identify eight metabolic pathways perturbed by long-term exposure to $PM_{2.5}$ and temperature: glycerophospholipid, glutathione, sphingolipid, beta-alanine, purine metabolism, biosynthesis of unsaturated fatty acids, propanoate and possibly taurine and hypotaurine metabolism. The perturbed pathways, such as glycerophospholipid metabolism and unsaturated fatty acids biosynthesis, were linked to OS since these molecules are the main components of biological membranes as well as downstream products from oxidation of the membranes, respectively [171]. In a prospective case-control study involving 1621 incident coronary heart disease cases and matched controls, 161 lipid species were evaluated using liquid chromatography-mass spectrometry in baseline fasting plasma. A panel of seven lipids was indicated as the best biomarker for the prediction of incident CVD: phosphatidylcholine 36:0a, sphingomyelin 41:1b, cholesteryl ester 18:2, sphingomyelin 34:0, phosphatidylethanolamine 36:4a, lysophosphatidylcholine 18:0 and 20:3 sphingolipids and phospholipids showed the most extensive associations with CAD risk [172]. Recently, in 244,842 participants from the UK Biobank, the metabolic signatures associated with exposure to ambient air pollution were investigated, to explore the link with metabolic dysfunction-associated steatotic liver disease (MASLD); 87, 65, 76 and 71 metabolites were found as metabolic signatures of $PM_{2.5}$, PM_{10}, NO_2 and NOx, respectively. Metabolites related to metabolic signatures were associated with several metabolic categories, such as lipids, amino acids, lipoproteins, fatty acids and metabolites related to inflammation. The same study demonstrated that higher levels of $PM_{2.5}$, PM_{10}, NO_2 and NOx were associated with an increased incidence of MASLD and that mixed exposure to different air pollutants also increased the risk [173].

7. Particulate Matter, Genomic Instability, Epigenetic Changes and Mitochondrial Dysfunction

Exposure to $PM_{2.5}$ accelerates cellular and molecular detrimental effects, affecting genomic instability, telomere attrition, epigenetic changes and mitochondrial dysfunction. Toxicological mechanisms of $PM_{2.5}$ in cells interfere with correct cell proliferation and

alter metabolic and gene functions, eliciting inflammatory response and ROS production, contributing to the pathogenesis of various diseases, such as CV, neurodegenerative and musculoskeletal disorders [174]. The genome's integrity is ensured by telomeres, repeated DNA sequences that act as a cap to preserve the end of chromosomes from being recognized as double-strand breaks and from undergoing degradation [175]. At each cell division, telomeres shorten, and this process continues until the cell stops dividing and enters senescence and apoptosis. For this property, telomere length (TL) is considered a biological marker of aging. Because of their sequence (TTAGGG repeats), due to the high number of guanines, telomeres are susceptible to ROS attack [176]. Many epidemiological studies have assessed the susceptibility of telomeres to shortening, both after short- or long-term exposure to $PM_{2.5}$, and have highlighted an association of TL erosion with age-associated conditions such as CV and neurological diseases [177,178]. In a meta-analysis assessing the impact of outdoor $PM_{2.5}$ exposure on TL, it was shown that long-term exposure had a greater impact on telomere attrition, principally by OS mechanisms. Oxidative damage at telomeres triggers the activation of DNA repair enzymatic machinery, which further amplifies the accumulation of telomere attrition leading to senescence and apoptotic processes [179].

Abnormal DNA methylation patterns are among the primary causes of alterations induced by $PM_{2.5}$ exposure. DNA methylation is an important epigenetic feature of DNA that plays a critical role in gene regulation since it is a natural process that suppresses gene expression via the addition of methyl groups. There is growing evidence that PM interferes with global [180] and gene-specific methylation [181]. Several studies on prolonged exposure to PM showed a hypomethylation pattern of transposable repeated elements and proinflammatory genes [182,183]. Recently, controlled studies on human exposure to concentrated ambient particles provided the opportunity to experimentally observe the effects on blood pressure of rapid PM-induced DNA hypomethylation of Alu repeated elements and proinflammatory toll-like receptor-4, both linked to blood pressure and hypertension [184].

Many epidemiological and observational studies highlighted that mitochondria are extremely sensitive targets of $PM_{2.5}$, which can severely damage the morphology, function and DNA of these organelles, contributing to adverse outcomes in various pathological conditions [185]. Mitochondria serve as central players of cellular metabolism, bioenergetics and OS [186], and, upon exposure to $PM_{2.5}$, they undergo important structural and functional alterations, impairment of respiratory chain activity and dysregulation of quality control mechanisms. The large amounts of ROS released from damaged mitochondria, in turn, exacerbate the intracellular redox imbalance, further compromising mitochondrial stability, thus acting as both a cause and a consequence of oxidative and inflammatory states [187]. In particular, human vascular endothelial cells are susceptible to PM that induces disturbances in mitochondrial homeostasis: when PM damages mitochondria, adenosine triphosphate (ATP) production is impaired, compromising muscle contractility and causing early cell death [188]. The heart functions properly if it is provided with a constant and appropriate amount of energy in the form of ATP that is generated through β-oxidation during the Krebs cycle, which is therefore an important pathway for energy metabolism and is regulated by glucose and insulin [189]. PM has been observed to influence energy metabolism, reducing ATP production, and may therefore contribute to myocardial damage and consequently induce AMI [190]. Epidemiological studies have suggested that exposure to air pollutants may disturb glucose–insulin homeostasis [191], and short-term exposure in humans confirms that exposure to PM causes disturbances in Krebs cycles and glycolysis [192]. Disturbing the Krebs cycle may therefore lead to

imbalances in cardiac energy metabolism, which we now know contributes to the onset of many CV clinical manifestations, including AMI [193].

8. General Prevention Strategies

Clearly, the strategies useful to directly reduce pollution, especially the sources of $PM_{2.5}$, including traffic emissions, the use of fossil fuels for energy production and the burning of biomass, are critical targets to minimize adverse health effects and exposure of more vulnerable subjects [194]. In this context, different data suggest that targeted measures to prevent pollution and reduce $PM_{2.5}$ can reliably decrease the risk of AS and CVD and reduce blood levels of biomarkers of OS and inflammation [195,196].

Overall, available evidence indicates that there is no "unharmful" level of PM exposure. Moreover, although WHO data show that the majority of the global population lives in areas that exceed WHO guideline air quality limits, both susceptible individuals and healthy subjects are not fully aware of their risk, which renders a great challenge to fully protect public health [197].

Public strategies, the most important are pollution regulations (establish air quality standards), but also urban planning (e.g., green areas and parks) and educational campaigns (to improve public education and awareness) or improve public transports (e.g., decreasing emissions and encouraging physical activity) are simple but essential interventions to reduce exposure risk. General simple not demanding interventions, such as closing windows (when elevated ambient pollution levels)/opening windows (to ventilate indoor environments when outdoor pollution is low), the use of air purifiers and effective dust-proof masks may be effective preventive measures to reduce personal exposure. Moreover, additive tools (e.g., air quality warning systems to notify daily pollution levels, wearable devices, new exposure models, geospatial assessment) are under study.

In the context of CV settings, PM exposure should be considered as a major modifiable risk factor, to be considered in the promotion of a healthy lifestyle and behaviors (together with a healthy diet, physical activity, maintenance of a normal blood pressure/lipid profile/glycemia values and smoking habit cessation), the control of which in turns reduces the susceptibility to CV events attributed to air pollution exposure. The identification of more vulnerable subjects for exposure risk by physicians may be more accurate considering traditional risk factors and pre-existing disease, but also additive key information such as socioeconomic status, lifestyle and work conditions, which can have an important role.

9. Antioxidant Strategies

9.1. Antioxidant Nutrients and Healthy Dietary Habits

Beyond reductions in air pollution, one further option to counteract the adverse effects of PM on health may be to increase the intake of antioxidants and/or exploit some antioxidant drug properties, found to be effective in reducing air-pollution induced OS and inflammation and as such able to counteract air-pollution negative repercussions on health [198]. Thus, in view of the consistent data highlighting the role of OS in the effects of air pollution on health, there is substantial evidence on the potential use of antioxidant supplementation (e.g., vitamins B12, C, D and E or omega-3 polyunsaturated fatty acids—omega-3 PUFAs), to improve the capacity to counteract adverse pollutant consequence, through OS reduction [199]. Accordingly, a relationship has been hypothesized between different micronutrients, including vitamin B12 and folate and heart rate variability (HRV: the variation of time between consecutive heartbeats, biomarker associated with CV pathophysiology); in this context, although number and heterogeneity between studies did not allow a definitive and clear conclusion for majority of these molecules, increasing findings seem to confirm the association between vitamin D and B12 with reduced HRV [200].

In vitro data showed that vitamin E and omega-3 fatty acids significantly reduced $PM_{2.5}$-induced inflammation and OS (MDA, IL-6) and TNF-α decreased in supernatant and ROS decreased in cytoplasm, while SOD activity increased [201]. In rats, the combined treatment with vitamin E and omega-3 PUFA prevents the $PM_{2.5}$-induced CV injury through alleviating inflammation (TNF-α, interleukin 1β (IL-1β), IL-6) and OS (anti-oxidative activity) [202].

Direct cytotoxicity or apoptotic effects of various PM types in cardiomyocytes could be inhibited by compounds with antioxidant properties (e.g., N-acetylcysteine NAC, an antioxidant precursor of cysteine and glutathione, used to treat paracetamol overdose and dietary supplement or dimethylthiourea, a scavenger of hydroxyl radicals and hydrogen peroxide) [203,204]. In H9C2 cardiomyocytes, $PM_{2.5}$ exposure induces different changes (reduction in cell viability, death, ROS, and increased expression of caspase-3, fatty acid binding protein 3 and IL-6, as well as upregulation of lysophosphatidylcholines and dysregulation of amino acids and other acids and derivatives) that can be improved by vitamin C treatment [205].

Interestingly, vitamin B supplementation attenuated the epigenetic changes (methylation changes in genes involved in mitochondrial oxidative energy metabolism) induced by $PM_{2.5}$ exposure in humans [206]. Other experimental data showed that vitamin B may improve $PM_{2.5}$-induced kidney injury by counteracting endoplasmic reticulum stress and OS [207].

Omega-3 PUFA reduces adverse CV effects of short-term exposure to air pollution, in terms of lipid profile and biomarkers of OS, inflammation, coagulation and endothelial function in healthy middle-aged subjects [208,209]. Fish oil also improved $PM_{2.5}$-induced lung toxicity and systemic inflammation in rats (evidenced by increased levels of total proteins, lactate dehydrogenase, 8-epi-Prostaglandin F2α, IL-1β and TNF-α, and increased infiltration of inflammatory cells, decreased SOD in the bronchoalveolar lavage fluids, and elevated blood C reactive protein and IL-6) [210]. Moreover, a relationship between short-term exposure to $PM_{2.5}$, even at concentrations below the regulatory standard, and subclinical CV biomarker changes (total cholesterol, von Willebrand factor, tissue plasminogen activator, D-dimer and HRV) was observed in healthy adults, which was relieved by omega-3 PUFA consumption [211]. In this context, administration of vanillic acid (phenolic acid and an oxidized vanillin form) in an experimental model of ischemia/reperfusion isolated rat heart exposed to PM_{10} resulted in cardioprotection, as evidenced by effects on hemodynamic parameters, OS and antioxidant enzymes, and endothelial NO synthase (eNOS) and iNOS mRNA expression levels [212].

Recently, air pollutant exposure, low vitamin D status and smoking habits were demonstrated to confer a high risk of hypercholesterolemia (n = 28,134 Korean adults) [213]. Experimental data evidenced the protective role of vitamin D receptor against $PM_{2.5}$-induced injury in the kidney, as vitamin D receptor activation restores mitochondrial calcium balance and reduces OS, downregulating mitochondrial calcium uniporter expression and improving renal function [214].

A healthy diet can represent a simple tool to increase antioxidant intake. In particular, the Mediterranean diet (MD: rich in fruits and vegetables, olive oil, oily fish and moderate alcohol consumption, e.g., antioxidant-rich red wine) appears beneficial to prevent and/or reduce air pollution-associated adverse health effects. A recent prospective study (n = 548,845 in the USA, follow-up period of 1995–2011) evidenced that MD reduced the CV mortality risk related to long-term exposure to air pollutants ($PM_{2.5}$ and NO_2) [215]. An inverse association between adherence to MD and exposure to PM_{10} with LINE-1 methylation suggested the possible beneficial role of a healthy diet to counteract the negative effect of PM_{10} exposure [216]. A recent review evaluated the effects of some healthy diets

(MD, Dietary Approaches to Stop Hypertension DASH, and MD-DASH intervention for Neurodegenerative Delay), which promote a favorable OS and inflammation status, and positive changes in the composition of the human gut microbiota (mitigating adverse effects caused by pollutants on Alzheimer's disease) [217].

According to available data, high consumption of flavonoids (polyphenolic metabolites contained in fruits, vegetables, tea, cocoa, wine, nuts, seeds, spices and other plant-based foods) with their antioxidant and anti-inflammatory properties, consistently resulted in counteracting the CV damage caused by different pollutants (e.g., $P_{2.5}$, PM_{10}, NO_2, O_3 and SO_2), which are instead linked to increased risks of hypertension, stroke, AMI, atrial fibrillation and HF [218]. Hydroxytyrosol (a polyphenol contained in extra virgin olive oil) reduces hepatic insulin resistance (through inhibition of nuclear factor kappa-light-chain-enhancer of activated B cell (NF-κB) activation derived from OS induced by $PM_{2.5}$) [219]. Curcumin, resveratrol and gallic acid prevented $PM_{2.5}$-induced migration and cytokine secretion via blocking the ROS-dependent NF-κB signaling pathway in vascular smooth muscle cells [220]. Moreover, different results evidenced how resveratrol can reduce the effects of $PM_{2.5}$ exposure in different districts by antagonizing OS and inflammatory responses [221–223].

9.2. Probiotics

Recently, probiotic intervention has been the object of interest in view of the capacity to decrease inflammation processes induced by pollutants, especially regarding pulmonary effects. In fact, there is evidence of beneficial effects of the probiotic *Lactiplantibacillus plantarum* in PM-associated pulmonary inflammation [224]. Moreover, experimental data showed that probiotic administration improves lung function, reducing proinflammatory cytokines expression (TNF-α, IL-6, IL-1β, interleukin 17A) while increasing anti-inflammatory mediators (IL-10, transforming growth factor-β) [225]. Gut microbial abundance, which can be modulated by diet and probiotics supplementation, has been negatively associated with asthma incidence derived from $PM_{2.5}$ exposure [226].

In addition, there are data on the beneficial effects of probiotic administration on ischemic CV damage, where probiotic administration was cardioprotective on myocardial ischemic injury through reduction of inflammation and OS [227–229]. Experimental data suggest that probiotics reduce the AMI size and post-infarction cardiac hypertrophy and HF, whereas very recent data confirmed that gut microbiome modulation (L. johnsonii) improves the cardiac function post-AMI [230–232].

9.3. Cardiovascular Drugs

9.3.1. Beta-Blockers

There is a complex relationship between OS, the autonomic system (on which beta-blockers act) and air pollution, targeting the CV system. When the daily variations in ambient particulate air pollution have been investigated in association with increased risk of ST-segment depression during the exercise test in CAD patients, the associations of $PM_{2.5}$ and gaseous pollutants (NO_2 and CO) were stronger among patients who did not use β-blockers, likely in view of the protective effect of β-blockers on ischemia, which may reflect autonomic regulation (likely through OS, but that unfortunately was not specifically evaluated in this study) [233].

Afterwards, experimental data indicated the changes in HRV of rats, exposed to intratracheal instillation of urban air particles (UAP, 750 μg) or to inhalation of concentrated ambient particles (mass concentration 700 ± 180 $\mu g/m^3$) for 5 h, can be inhibited by NAC (50 mg/kg 1 h prior to UAP), while the cardiac OS induced by pollution can be prevented by beta-blocker (5 mg/kg atenolol immediately before concentrated ambient

particles exposure) [234]. Moreover, pulmonary rat exposure to DE particulate increases blood pressure, arrhythmia and reperfusion injury with adverse effect on the myocardium (increased myocardial oxidant radical production, tissue apoptosis and necrosis), whereas metoprolol (10 mg/kg) prevents myocardial OS and reperfusion injury [235]. Instead, propranolol inhibits PM-induced IL-6 release from murine alveolar macrophages, while β2-adrenergic receptor (β2AR-albuterol) increases IL-6 release, mitochondrial ROS and adenylyl cyclase activity, finally modulating the coagulable status and risk of thrombotic CV events [236].

9.3.2. Statins

In a large case-control study (1.2 million adults aged ≥66 years in Canada, 2000–2018) the associations of chronic exposure to $PM_{2.5}$ with CV mortality were stronger among non-statin users compared to users, suggesting that these drugs may act as significant modifiers in the relationship between pollution and CV death [237].

The anti-inflammatory and antioxidant properties of statins seem one of the main mechanisms involved in the pollution defense, because among GSTM1-null subjects (GST are enzymes involved in the metabolism of ROS and xenobiotics), enrolled in the Normative Aging Study (n = 497 individuals), the use of statins eliminated the adverse effect of $PM_{2.5}$ on high-frequency component of HRV [238].

Accordingly, in $PM_{2.5}$ rat exposure models, atorvastatin significantly improved lipid profile, OS and inflammatory-related biomarkers (MDA, SOD, Ox-LDL, high sensitivity C reactive protein), cytokines (IL-6, TNF-α) and blood pressure, reversing the effects caused by pollutant exposure [239,240]. The modulatory effect of statins in the relationship between pollution and inflammatory and endothelial function biomarkers was also observed in humans [241,242]. Nonetheless, the association of $PM_{2.5}$ with incident AMI seems not attenuated by statin therapy in another study; however, as authors declare, this information was available only at baseline, with possible changes in therapy during the follow-up period that could have affected the role of statins on the association between $PM_{2.5}$ and incident AMI [243]. In this context, recent data reported that statin use was associated with a significantly lower risk of stroke among the elderly with high and low or moderate levels of exposure to PM_{10} and $PM_{2.5}$ [244].

9.3.3. Angiotensin Converting Enzyme Inhibitors and Angiotensin Receptor Blockers

Experimental data focused on rats treated with benazepril (ACE inhibitor) or valsartan (an angiotensin receptor blocker ARB) before exposure to fine PM aerosols (5 h, fine PM mass concentration: 440 +/− 80 $\mu g/m^3$) or filtered air; benazepril reduced, while ARB increased angiotensin levels; both drugs improved heart OS (thiobarbituric acid reactive substances) and ECG alterations (shortening of the T-end to T-peak interval), suggesting that PM-related acute cardiac events involved the renin–angiotensin system and can be modulated by ACE inhibitors and ARB [245].

Moreover, fine dust particles induced premature senescence-associated endothelial dysfunction in endothelial cells isolated from porcine coronary arteries. Specifically, fine dust increased senescence-associated beta-galactosidase activity, causing cell cycle arrest and OS, whereas eNOS expression was downregulated and platelet aggregation increased. Angiotensin II receptor type 1 (AT1) antagonist prevented fine dust-induced senescence-associated beta-galactosidase activity, increased cell proliferation and eNOS expression, and improved endothelial function, suggesting the involvement of the local angiotensin system in these events [246].

10. Final Remarks: Points to Solve and Future Directions

There are many key points in the assessment of the relationship between PM and health still to solve (Table 1).

Table 1. Main critical points in the assessment of the relationship between PM, OS and health.

PM-Related Factors		
PM characteristics	different chemical and physical properties	-mass, -number -size, shape -surface area -reactivity -acidity -solubility -internal or surface positioning of chemicals on the particles
	heterogeneity in composition	-metals -salts -organic chemicals -biological materials
	varying mechanisms of formation	-nucleation process -condensation process -coagulation process -mechanical process
	anthropogenic and natural emission sources	-traffic, industrial activities, biomass burning, mineral desert dust, sea spray, biogenic emissions
		-geographical area asset
PM transport and deposition processes	diffusion, dilution and deposition patterns over time and space	-meteorological variables, as air temperature, humidity, wind and other parameters
Interaction with other pollutants	gaseous pollutants	NO_2, SO_2, O_3
		no interaction vs. potential additivity, synergism or antagonism
Sampling methodology	differences between fixed monitoring points and mobile or individual monitoring assessment	-wearable device -sensors mounted on vehicles -geospatial assessment -fixed monitoring stations
	different monitoring instrumentation	different spatial and temporal resolution
Individual Characteristics		
Individual factors	anthropometric, genetic and social characteristics	-age -sex -genetic profile -socioeconomic status
	comorbidities and pre-existing diseases	-cardiovascular disease -respiratory diseases -presence of diabetes, dyslipidemia, hypertension
	behaviors	-diet -outdoor activity -occupation -exercise -smoking -mobility
Modifying or Mitigating Factors		
Antioxidant intake	choice of antioxidant	single compound vs. combination/cocktail
	mechanism of action	direct vs. indirect
	administration	-timing -appropriate dosage -duration of use
	use in the general population vs. targeted application in vulnerable groups	-children, -elderly, -smokers, -individuals with chronic conditions
Individual protectors	wearable or stationary technological devices	-face masks, -indoor air purifiers and filtration systems -air quality warning systems
	general measures	-air exchange
	health interventions	-regular medical screening in subjects at high-risk -lifestyle changes
Community interventions	environmental and policy strategies	-reducing source of pollution: policies to limit emissions -improvement of air quality assessment -urban planning -public health campaigns and education -improvement of public transports

10.1. Individual Issues and Biomarkers

Although no one questions the adverse health consequences of PM in view of the number of findings confirming this relationship, it remains challenging to establish an unambiguous causal relationship between PM and its components with health effects. There are people who live in the same environment but are differentially affected by the PM, due to the fact that many modifiers of an individual's response to PM effects exist. These factors surely include subject movements that influence individual exposure, socioeconomic parameters, the nutritional status, antioxidant supplementation, lifestyle habits adopted and outdoor activities, presence and severity of preexisting chronic diseases and risk factors as well as genetic background (especially candidate genes having specific role in antioxidant activities; e.g., the presence of polymorphisms that change the activity of the detoxification enzymes GST and quinone oxido-reductase-NQO1 may contribute to heart disease as well as to pollution adverse effects and potentially modulate their relationship and the final effects on health) [247,248]. Additional difficulties exist in the demonstration of the connection between PM and health, including difficulties in estimating emissions under all possible conditions and the individual exposure time. Variations in research populations and presence of confounding factors in observational studies that assess air pollution effects on health, such as lifestyle habits (e.g., diet, smoking habit, outdoor activities), socio-economic status, or preexisting risk factors (e.g., dyslipidemia, hypertension, diabetes) or diseases (e.g., CAD), can affect the final results. All these characteristics, which can vary greatly between subjects, affect individual susceptibility to pollution and the biological effects and health repercussions on each individual.

Several oxidative and inflammatory-related biomarkers have been measured and associated with PM; abnormalities in some key parameters related to PM evidence the importance of this relationship in terms of health effects. Nonetheless, further research is needed to identify the role of new biomarkers with innovative techniques (e.g., omics) which may reveal additive mechanistic links between air pollution and health, to fight even more effectively adverse pollution effects with reliable preventive and interventional tools.

10.2. Exposure Misclassification

Exposure assessment is a key determinant in all studies of environmental pollution effects, but several sources of exposure misclassification exist. Exposures are often estimated using a fixed monitoring point or the home locations of individual subjects, without considering residence-based and mobility-based exposures and their impact on health (e.g., which can occur due to residential changes among a study population over follow-up, i.e., residential mobility). Case-control studies often use questionnaires to collect information on exposure, but errors due to the use of questionnaires may be significant in terms of exposure misclassification.

Other methodological aspects may affect exposure assessment, which may often be characterized by using only one or a few blood samples, resulting also in this case in significant exposure misclassification. Moreover, variations of air pollution levels over time can impact exposure levels, and the use of national-scale models may not reflect local changes in air pollution exposure.

10.3. Sampling Methodology and Variability in Particulate Matter Measurement

Sampling and analysis instrumentation in the context of PM samplers may greatly differ depending on the specific application. The sampling methods employed by national environmental protection agencies are aligned with their respective National Ambient Air Quality Standards (NAAQS), but they may differ across countries in aspects such as aspiration efficiency, cutoff calibration, flow rate and flow measurement and control

systems [249]. Beyond the stationary samplers used by national monitoring networks, a range of specialized instruments is also utilized, including indoor air quality monitors, mobile sampling units and personal dosimeters.

While ground-based measurements remain essential for accurately assessing PM concentrations at specific locations, they are inherently limited in spatial coverage. To overcome this limitation, satellite observations offer a valuable complementary tool for monitoring PM on a broader scale. Remote sensing platforms can provide near-global coverage and high temporal frequency, enabling the detection and tracking of large-scale aerosol events such as desert dust outbreaks, volcanic ash plumes and smoke from forest fires. By integrating satellite data with ground-based networks through data assimilation or statistical modeling approaches, it becomes possible to improve spatial estimates of PM concentrations, enhance early warning systems and support air quality forecasting and mitigation strategies at regional and global scales [250].

PM represents a complex and challenging system to study, being heterogeneous in composition. In fact, PM differs greatly in its chemical and physical characteristics, including size and distribution, composition and concentration, toxicity, emission sources, formation and transformation mechanisms, and diffusion patterns, which are influenced by geographical location and meteorological conditions (e.g., transportation and removal rate of atmospheric PM) until extreme events such as volcanic eruptions and dust storms. In particular, several weather-related factors influence the variability of PM measurements. These include temperature (low temperatures are associated with higher PM levels), solar radiation (higher radiation is typically associated with lower PM_{10} concentrations), wind (e.g., low wind speeds tend to correlate with higher PM levels), relative humidity (high humidity is linked to increased PM concentrations), precipitation (which reduces PM levels through atmospheric cleansing) and atmospheric pressure (high pressure is generally associated with higher PM concentrations). The nature and intensity of emission sources also play a significant role in PM measurements. Moreover, studies are usually limited to a few main pollutants without considering global mixture effects, or gaseous components (NO_2, SO_2, O_3), which can have their role on their own.

10.4. Antioxidant-Related Strategies

Antioxidant supplementation is generally harmless (at modest doses at least) and largely available at low cost. This strategy may be effective (seeing the importance of both inflammatory and OS pathways affected by a number of air pollutants) and widely applicable as a general intervention targeting all populations (overcoming both the great variable pollution composition and individual variability in susceptibility). However, vitamin supplementation has largely disappointed expectations in large-scale trials with CV endpoints. The action mechanisms of each antioxidant (be supplemented or contained in the diet) have to be better defined in terms of cellular and molecular pathways involved in the effects, as well as the type of contribution (e.g., directly targeting pollutant effects or indirect, as a more general advantage independent of pollutant exposure). Thus, at present there is no clear evidence to recommend antioxidant supplementation to counteract the adverse consequences of air pollution, also in subgroups of subjects more vulnerable to pollution (e.g., very young and elderly, smokers, subjects with pre-existing cardiorespiratory conditions, those living in very polluted areas) where these strategies may provide more benefits to health.

Future studies should investigate OS-related mechanistic mechanisms to better understand how PM causes adverse health effects, with particular focus on signaling mediator functioning (e.g., through innovative techniques as metabolomic and lipidomic analyses) and the role of genomic instability, epigenetic changes and mitochondrial dysfunction.

Gut microbiome-targeted nutritional intervention may represent an innovative prophylactic strategy to mitigate damage after acute ischemic cardiac events in general, but also potentially effective in relation to the pathophysiological molecular and cellular events (e.g., OS and inflammation) elicited by pollutant exposure, although their precise role in air pollution remains to be validated.

Some common CV drugs have been found effective as modifiers in the relationship between OS elicited by pollutants and CV pathophysiology and thus worthy of evaluation as potentially profitably exploitable additional pharmacological tools for the prevention and/or treatment of air pollution-associated CVD in vulnerable patient groups.

11. Conclusions

Air pollution is by now a recognized risk for health, directly affecting the CV pathophysiology as well as because pollutants enter the bloodstream as a highway to distribute throughout the body to act on other organs; the sum of these events leads to an annual mortality rate in excess of ~~a~~ million people. OS, with its close relationship with inflammatory responses, represents a key determinant by which the actions of air pollution can be expanded to produce adverse responses in multiple organs, including the CV system (Figure 3). Future efforts will be necessary to address the accuracy and effectiveness of OS biomarkers and their association with pollutant characteristics (e.g., dimension, components and oxidative burden), but, above all, to assess the modulatory role of the antioxidant responses on these relationships.

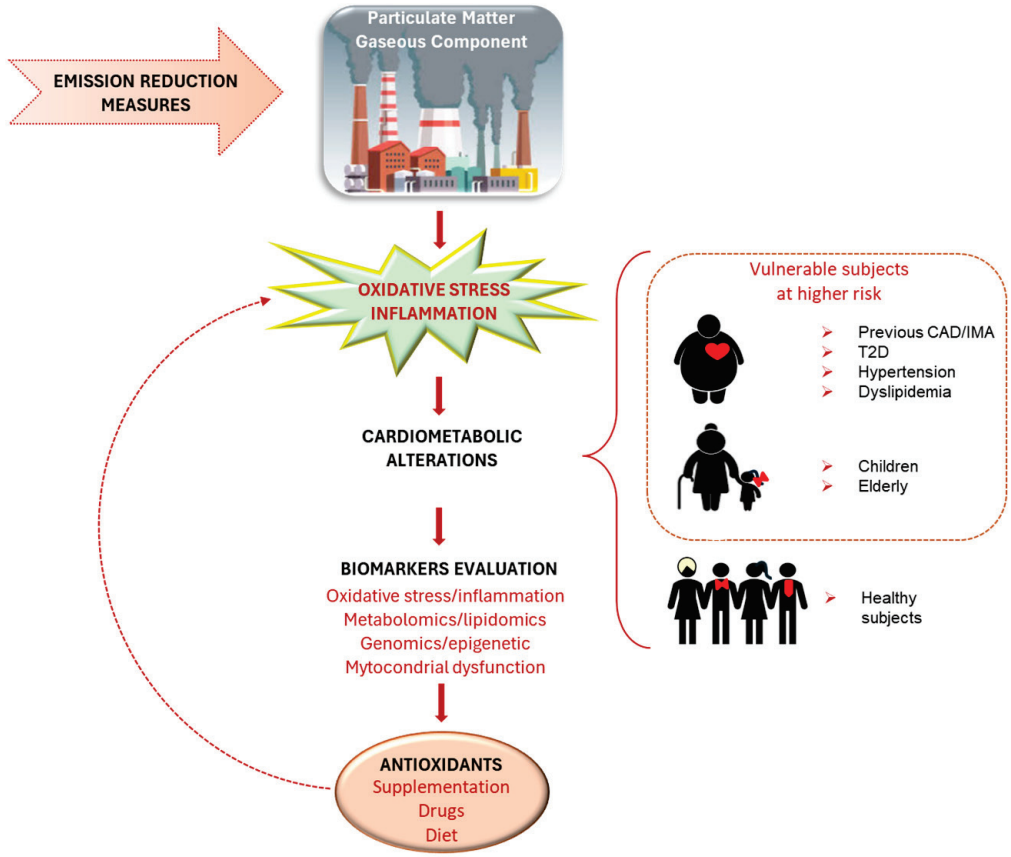

Figure 3. Pollution, oxidative stress/inflammation and related biological effects, which can be modulated by antioxidants, as potential additive tools beyond emission reduction measures, to counteract pollution's detrimental effects on health.

Clearly, reducing the sources remains the main and more effective solution to reduce the burden of air pollution on health, although this strategy is not always easy to implement. In addition to this solution, experimental studies and clinical trials have demonstrated clear effectiveness of antioxidant compounds (dietary or drugs) in the prevention/reversal of pollutant adverse effects, confirming OS as a main determinant in these biological effects (Figure 3). However, whether an improvement of the OS and inflammatory status was associated with vitamin supplementation, a clear clinical benefit of supplementation of these nutrients in the relationship between air pollution and the cardiometabolic risk and disease remains to be definitively proved. Nonetheless, in view of the pivotal role of oxidative pathways in the air pollution consequences on health, if it is reasonable to think of the use of antioxidant compounds to improve adverse effects following exposure to pollutants in future, potentially beneficial also for other conditions driven by pollutant exposure and/or OS elevation, further data are needed to explain in detail the complex relationship between air pollution, OS and CV health.

Author Contributions: Conceptualization, writing—original draft preparation, supervision C.V.; particulate matter section, D.G. and F.C.; epidemiological section, E.B. and F.M.; lipidomic and metabolomic section, M.G.; genomic instability, epigenetic changes and mitochondrial dysfunction section, L.S.; review and editing, D.G., E.B., L.S., F.C., F.M., M.G., S.B. and C.V. All authors have read and agreed to the published version of the manuscript.

Funding: This research received no external funding.

Conflicts of Interest: The authors declare no conflicts of interest.

List of Abbreviations

ACE	Angiotensin-converting enzyme
AMI	Acute myocardial infarction
ARB	Angiotensin receptor blocker
AS	Atherosclerosis
ATP	Adenosine triphosphate
CAC	Coronary artery calcium
CI	Confidence interval
CV	Cardiovascular
CVD	Cardiovascular disease
Da	aerodynamic diameter
DE	Diesel exhaust
ECG	Electrocardiogram
GPx	Glutathione peroxidase
GPx-1	Glutathione peroxidase 1
GST	Glutathione-S transferase
GSTM1	Glutathione-S transferase M1
HDL	High-density lipoprotein
HF	Heart failure
HRV	Heart rate variability
IL-1β	Interleukin-1β
IL-6	Interleukin-6
IL-10	Interleukin-10
IMT	Intima media thickness
ICAM-1	Intercellular adhesion molecule-1

eNOS	Endothelial NO synthase
iNOS	Inducible NO synthase
LDL	Low-density lipoprotein
MASLD	Metabolic dysfunction-associated steatotic liver disease
MD	Mediterranean diet
MDA	Malondialdehyde
NF-κb	Nuclear factor kappa-light-chain-enhancer of activated B cell
NO	Nitric oxide
NO_2	Nitrogen dioxide
OC	Organic compound
Omega-3 PUFA	Omega-3 polyunsaturated fatty acid
OS	Oxidative stress
Ox-LDL	Oxidized low-density lipoprotein
O_3	Ozone
PAH	Polycyclic aromatic hydrocarbon
PI3K-AKT	Phosphoinositide 3-kinase-Protein Kinase B
PM	Particulate matter
$PM_{2.5}$	Particulate matter with a diameter less than 2.5 μm
PM_{10}	Particulate matter with a diameter less than 10 μm
ROS	Reactive oxygen species
SOD	Superoxide dismutase
SO_2	Sulfur dioxide
TL	Telomere length
TNF	Tumor necrosis factor
TNF-α	Tumor necrosis factor α
UFP	Ultrafine particle
VCAM-1	Vascular cell adhesion molecule-1
WHO	World Health Organization

References

1. Yang, M.; Wu, K.; Wu, Q.; Huang, C.; Xu, Z.; Ho, H.C.; Tao, J.; Zheng, H.; Hossain, M.Z.; Zhang, W.; et al. A Systematic Review and Meta-Analysis of Air Pollution and Angina Pectoris Attacks: Identification of Hazardous Pollutant, Short-Term Effect, and Vulnerable Population. *Environ. Sci. Pollut. Res. Int.* **2023**, *30*, 32246–32254. [CrossRef] [PubMed]
2. Yin, Z.; Huang, X.; He, L.; Cao, S.; Zhang, J.J. Trends in Ambient Air Pollution Levels and PM2.5 Chemical Compositions in Four Chinese Cities from 1995 to 2017. *J. Thorac. Dis.* **2020**, *12*, 6396–6410. [CrossRef] [PubMed]
3. Brauer, M.; Davaakhuu, N.; Escamilla Nuñez, M.C.; Hadley, M.; Kass, D.; Miller, M.; Prabhakaran, D.; Sliwa, K.; Su, T.-C.; Vaartjes, I.C.H.; et al. Clean Air, Smart Cities, Healthy Hearts: Action on Air Pollution for Cardiovascular Health. *Glob. Heart* **2021**, *16*, 61. [CrossRef] [PubMed]
4. Dockery, D.W.; Schwartz, J.; Spengler, J.D. Air Pollution and Daily Mortality: Associations with Particulates and Acid Aerosols. *Environ. Res.* **1992**, *59*, 362–373. [CrossRef]
5. GBD 2019 Risk Factors Collaborators. Global Burden of 87 Risk Factors in 204 Countries and Territories, 1990–2019: A Systematic Analysis for the Global Burden of Disease Study 2019. *Lancet* **2020**, *396*, 1223–1249. [CrossRef]
6. WHO. Burden of Disease from Ambient Air Pollution for 2016 Description of Method. Available online: https://cdn.who.int/media/docs/default-source/air-quality-database/aqd-2018/aap_bod_methods_apr2018_final.pdf?sfvrsn=30ac0d62_3 (accessed on 25 March 2025).
7. World Health Organization (WHO). *WHO Global Air Quality Guidelines: Particulate Matter ($PM_{2.5}$ and PM_{10}), Ozone, Nitrogen Dioxide, Sulfur Dioxide and Carbon Monoxide*; World Health Organization: Geneva, Switzerland, 2021; ISBN 978-92-4-003422-8. Available online: https://www.who.int/publications/i/item/9789240034228 (accessed on 7 May 2025).
8. Kumar, V.; S, H.; Huligowda, L.K.D.; Umesh, M.; Chakraborty, P.; Thazeem, B.; Singh, A.P. Environmental Pollutants as Emerging Concerns for Cardiac Diseases: A Review on Their Impacts on Cardiac Health. *Biomedicines* **2025**, *13*, 241. [CrossRef]
9. Cohen, A.J.; Brauer, M.; Burnett, R.; Anderson, H.R.; Frostad, J.; Estep, K.; Balakrishnan, K.; Brunekreef, B.; Dandona, L.; Dandona, R.; et al. Estimates and 25-Year Trends of the Global Burden of Disease Attributable to Ambient Air Pollution: An Analysis of Data from the Global Burden of Diseases Study 2015. *Lancet* **2017**, *389*, 1907–1918. [CrossRef]

10. Kelly, F.J. *The Effects of Long-Term Exposure to Ambient Air Pollution on Cardiovascular Morbidity: Mechanistic Evidence*; Committee on the Medical Effects of Air Pollutants (COMEAP): London, UK, 2018; p. 96. Available online: https://www.gov.uk/government/publications/air-pollution-and-cardiovascular-disease-mechanistic-evidence (accessed on 7 May 2025).
11. Newby, D.E.; Mannucci, P.M.; Tell, G.S.; Baccarelli, A.A.; Brook, R.D.; Donaldson, K.; Forastiere, F.; Franchini, M.; Franco, O.H.; Graham, I.; et al. Expert Position Paper on Air Pollution and Cardiovascular Disease. *Eur. Heart J.* **2015**, *36*, 83–93b. [CrossRef]
12. Brook, R.D.; Franklin, B.; Cascio, W.; Hong, Y.; Howard, G.; Lipsett, M.; Luepker, R.; Mittleman, M.; Samet, J.; Smith, S.C.; et al. Air Pollution and Cardiovascular Disease: A Statement for Healthcare Professionals from the Expert Panel on Population and Prevention Science of the American Heart Association. *Circulation* **2004**, *109*, 2655–2671. [CrossRef]
13. Brook, R.D.; Rajagopalan, S.; Pope, C.A.; Brook, J.R.; Bhatnagar, A.; Diez-Roux, A.V.; Holguin, F.; Hong, Y.; Luepker, R.V.; Mittleman, M.A.; et al. Particulate Matter Air Pollution and Cardiovascular Disease: An Update to the Scientific Statement from the American Heart Association. *Circulation* **2010**, *121*, 2331–2378. [CrossRef]
14. Seinfeld, J.H.; Pandis, S.N. *Atmospheric Chemistry and Physics—From Air Pollution to Climate Change*, 2nd ed.; John Wiley & Sons: Hoboken, NJ, USA, 2006; ISBN 978-0-471-72018-8.
15. US EPA. *Air Quality Criteria for Particulate Matter*; U.S. Environmental Protection Agency: Washington, DC, USA, 2004; ISBN EPA/600/P-99/002aF.
16. Pörtner, H.-O.; Roberts, D.C.; Tignor, M.M.; Poloczanska, E.; Mintenbeck, K.; Alegría, A.; Craig, M.; Langsdorf, S.; Löschke, S.; Möller, V.; et al. *Climate Change 2022: Impacts, Adaptation and Vulnerability. Contribution of Working Group II to the Sixth Assessment Report of the Intergovernmental Panel on Climate Change*; Cambridge University Press: Cambridge, UK; New York, NY, USA, 2022. Available online: https://www.ipcc.ch/report/ar6/wg2/ (accessed on 7 May 2025).
17. Harrison, R.M.; Yin, J. Particulate Matter in the Atmosphere: Which Particle Properties Are Important for Its Effects on Health? *Sci. Total Environ.* **2000**, *249*, 85–101. [CrossRef] [PubMed]
18. Fan, J.; Wang, Y.; Rosenfeld, D.; Liu, X. Review of Aerosol–Cloud Interactions: Mechanisms, Significance, and Challenges. *J. Atmos. Sci.* **2016**, *73*, 4221–4252. [CrossRef]
19. Li, X.; Zhang, Q.; Xue, H. The Role of Initial Cloud Condensation Nuclei Concentration in Hail Using the WRF NSSL 2-Moment Microphysics Scheme. *Adv. Atmos. Sci.* **2017**, *34*, 1106–1120. [CrossRef]
20. Ginoux, P.; Prospero, J.M.; Gill, T.E.; Hsu, N.C.; Zhao, M. Global-Scale Attribution of Anthropogenic and Natural Dust Sources and Their Emission Rates Based on MODIS Deep Blue Aerosol Products. *Rev. Geophys.* **2012**, *50*, RG3005. [CrossRef]
21. Amaral, S.S.; De Carvalho, J.A.; Costa, M.A.M.; Pinheiro, C. An Overview of Particulate Matter Measurement Instruments. *Atmosphere* **2015**, *6*, 1327–1345. [CrossRef]
22. Calvo, A.I.; Alves, C.; Castro, A.; Pont, V.; Vicente, A.M.; Fraile, R. Research on Aerosol Sources and Chemical Composition: Past, Current and Emerging Issues. *Atmos. Res.* **2013**, *120–121*, 1–28. [CrossRef]
23. Wilson, W.E.; Chow, J.C.; Claiborn, C.; Fusheng, W.; Engelbrecht, J.; Watson, J.G. Monitoring of Particulate Matter Outdoors. *Chemosphere* **2002**, *49*, 1009–1043. [CrossRef]
24. Wilson, W.E.; Suh, H.H. Fine Particles and Coarse Particles: Concentration Relationships Relevant to Epidemiologic Studies. *J. Air Waste Manag. Assoc.* **1997**, *47*, 1238–1249. [CrossRef]
25. Willeke, K.; Whitby, K.T. Atmospheric Aerosols: Size Distribution Interpretation. *J. Air Pollut. Control Assoc.* **1975**, *25*, 529–534. [CrossRef]
26. EPA. Revisions to the National Ambient Air Quality Standards for Particulate Matter. *Fed. Regist.* **1987**, *52*, 24634–24669.
27. EPA. National Ambient Air Quality Standards for Particulate Matter. *Fed. Regist.* **1997**, *62*, 38652–38752.
28. Directive 2008/50/EC of the European Parliament and of the Council of 21 May 2008 on Ambient Air Quality and Cleaner Air for Europe. Available online: https://eur-lex.europa.eu/eli/dir/2008/50/oj (accessed on 25 March 2025).
29. American Conference of Governmental Industrial Hygienists (ACGIH). Appendix D: Particle Size-Selective Sampling Criteria for Airborne Particulate Matter. In *1994–1995 Threshold Limit Values for Chemical Substances and Physical Agents and Biological Exposure Indices*; ACGIH: Cincinnati, OH, USA, 1994; pp. 43–46.
30. Jiang, M.; Marr, L.C.; Dunlea, E.J.; Herndon, S.C.; Jayne, J.T.; Kolb, C.E.; Knighton, W.B.; Rogers, T.M.; Zavala, M.; Molina, L.T.; et al. Vehicle Fleet Emissions of Black Carbon, Polycyclic Aromatic Hydrocarbons, and Other Pollutants Measured by a Mobile Laboratory in Mexico City. *Atmos. Chem. Phys.* **2005**, *5*, 3377–3387. [CrossRef]
31. Singh, R.B.; Sloan, J.J. A High-Resolution NO*x* Emission Factor Model for North American Motor Vehicles. *Atmos. Environ.* **2006**, *40*, 5214–5223. [CrossRef]
32. Thorpe, A.; Harrison, R.M. Sources and Properties of Non-Exhaust Particulate Matter from Road Traffic: A Review. *Sci. Total Environ.* **2008**, *400*, 270–282. [CrossRef]
33. Hjortenkrans, D.S.T.; Bergbäck, B.G.; Häggerud, A.V. Metal Emissions from Brake Linings and Tires: Case Studies of Stockholm, Sweden 1995/1998 and 2005. *Environ. Sci. Technol.* **2007**, *41*, 5224–5230. [CrossRef]

34. Chirico, R.; DeCarlo, P.F.; Heringa, M.F.; Tritscher, T.; Richter, R.; Prévôt, A.S.H.; Dommen, J.; Weingartner, E.; Wehrle, G.; Gysel, M.; et al. Impact of Aftertreatment Devices on Primary Emissions and Secondary Organic Aerosol Formation Potential from In-Use Diesel Vehicles: Results from Smog Chamber Experiments. *Atmos. Chem. Phys.* **2010**, *10*, 11545–11563. [CrossRef]
35. Viana, M.; Hammingh, P.; Colette, A.; Querol, X.; Degraeuwe, B.; de Vlieger, I.; van Aardenne, J. Impact of Maritime Transport Emissions on Coastal Air Quality in Europe. *Atmos. Environ.* **2014**, *90*, 96–105. [CrossRef]
36. International Maritime Organization (IMO). *Amendments to the Annex of the Protocol of 1997 to Amend the International Convention for the Prevention of Pollution from Ships, 1973, as Modified by the Protocol of 1978 Relating Thereto (Inclusion of Regulations on Energy Efficiency for Ships in MARPOL Annex VI). Resolution MEPC.203(62)*; IMO: London, UK, 2011. Available online: https://wwwcdn.imo.org/localresources/en/KnowledgeCentre/IndexofIMOResolutions/MEPCDocuments/MEPC.203(62).pdf (accessed on 7 May 2025).
37. Miracolo, M.A.; Hennigan, C.J.; Ranjan, M.; Nguyen, N.T.; Gordon, T.D.; Lipsky, E.M.; Presto, A.A.; Donahue, N.M.; Robinson, A.L. Secondary Aerosol Formation from Photochemical Aging of Aircraft Exhaust in a Smog Chamber. *Atmos. Chem. Phys.* **2011**, *11*, 4135–4147. [CrossRef]
38. Starik, A.M. Gaseous and Particulate Emissions with Jet Engine Exhaust and Atmospheric Pollution. In *Advances on Propulsion Technology for High-Speed Aircraft*; Educational Notes RTO-EN-AVT-150, Paper 15; Research and Technology Organization (RTO), NATO: Neuilly-sur-Seine, France, 2008; pp. 15-1–15-22. Available online: https://www.sto.nato.int/publications/STO%20Educational%20Notes/RTO-EN-AVT-150/EN-AVT-150-15.pdf (accessed on 7 May 2025).
39. Shindell, D.; Faluvegi, G. The Net Climate Impact of Coal-Fired Power Plant Emissions. *Atmos. Chem. Phys.* **2010**, *10*, 3247–3260. [CrossRef]
40. Viana, M.; Kuhlbusch, T.A.J.; Querol, X.; Alastuey, A.; Harrison, R.M.; Hopke, P.K.; Winiwarter, W.; Vallius, M.; Szidat, S.; Prévôt, A.S.H.; et al. Source Apportionment of Particulate Matter in Europe: A Review of Methods and Results. *J. Aerosol Sci.* **2008**, *39*, 827–849. [CrossRef]
41. Sánchez de la Campa, A.M.; de la Rosa, J.D.; González-Castanedo, Y.; Fernández-Camacho, R.; Alastuey, A.; Querol, X.; Pio, C. High Concentrations of Heavy Metals in PM from Ceramic Factories of Southern Spain. *Atmos. Res.* **2010**, *96*, 633–644. [CrossRef]
42. Viana, M.; Querol, X.; Alastuey, A.; Gil, J.I.; Menéndez, M. Identification of PM Sources by Principal Component Analysis (PCA) Coupled with Wind Direction Data. *Chemosphere* **2006**, *65*, 2411–2418. [CrossRef] [PubMed]
43. Calvo, A.I.; Castro, A.; Pont, V.; Cuetos, M.J.; Sánchez, M.E.; Fraile, R. Aerosol Size Distribution and Gaseous Products from the Oven-Controlled Combustion of Straw Materials. *Aerosol Air Qual. Res.* **2011**, *11*, 616–629. [CrossRef]
44. van der Werf, G.R.; Randerson, J.T.; Giglio, L.; Collatz, G.J.; Mu, M.; Kasibhatla, P.S.; Morton, D.C.; DeFries, R.S.; Jin, Y.; van Leeuwen, T.T. Global Fire Emissions and the Contribution of Deforestation, Savanna, Forest, Agricultural, and Peat Fires (1997–2009). *Atmos. Chem. Phys.* **2010**, *10*, 11707–11735. [CrossRef]
45. Ortiz de Zárate, I.; Ezcurra, A.; Lacaux, J.P.; Van Dinh, P.; de Argandoña, J.D. Pollution by Cereal Waste Burning in Spain. *Atmos. Res.* **2005**, *73*, 161–170. [CrossRef]
46. Perrino, C.; Tofful, L.; Torre, S.D.; Sargolini, T.; Canepari, S. Biomass Burning Contribution to PM10 Concentration in Rome (Italy): Seasonal, Daily and Two-Hourly Variations. *Chemosphere* **2019**, *222*, 839–848. [CrossRef]
47. Amato, F.; Alastuey, A.; Karanasiou, A.; Lucarelli, F.; Nava, S.; Calzolai, G.; Severi, M.; Becagli, S.; Gianelle, V.L.; Colombi, C.; et al. AIRUSE-LIFE+: A Harmonized PM Speciation and Source Apportionment in Five Southern European Cities. *Atmos. Chem. Phys.* **2016**, *16*, 3289–3309. [CrossRef]
48. Caserini, S.; Livio, S.; Giugliano, M.; Grosso, M.; Rigamonti, L. LCA of Domestic and Centralized Biomass Combustion: The Case of Lombardy (Italy). *Biomass Bioenergy* **2010**, *34*, 474–482. [CrossRef]
49. McDonald, J.; Zielinska, B.; Fujita, E.M.; Sagebiel, J.C.; Chow, J.C.; Watson, J.G. Fine Particle and Gaseous Emission Rates from Residential Wood Combustion. *Environ. Sci. Technol.* **2000**, *34*, 2080–2091. [CrossRef]
50. EEA. *EU Emission Inventory Report 1990–2011 Under the UNECE Convention on LRTAP*; EEA: Copenhagen, Denmark, 2013.
51. Perrino, C.; Catrambone, M.; Dalla Torre, S.; Rantica, E.; Sargolini, T.; Canepari, S. Seasonal Variations in the Chemical Composition of Particulate Matter: A Case Study in the Po Valley. Part I: Macro-Components and Mass Closure. *Environ. Sci. Pollut. Res. Int.* **2014**, *21*, 3999–4009. [CrossRef]
52. Nava, S.; Calzolai, G.; Chiari, M.; Giannoni, M.; Giardi, F.; Becagli, S.; Severi, M.; Traversi, R.; Lucarelli, F. Source Apportionment of PM2.5 in Florence (Italy) by PMF Analysis of Aerosol Composition Records. *Atmosphere* **2020**, *11*, 484. [CrossRef]
53. Giardi, F.; Nava, S.; Calzolai, G.; Pazzi, G.; Chiari, M.; Faggi, A.; Andreini, B.P.; Collaveri, C.; Franchi, E.; Nincheri, G.; et al. PM_{10} Variation, Composition, and Source Analysis in Tuscany (Italy) Following the COVID-19 Lockdown Restrictions. *Atmos. Chem. Phys.* **2022**, *22*, 9987–10005. [CrossRef]
54. Nava, S.; Lucarelli, F.; Amato, F.; Becagli, S.; Calzolai, G.; Chiari, M.; Giannoni, M.; Traversi, R.; Udisti, R. Biomass Burning Contributions Estimated by Synergistic Coupling of Daily and Hourly Aerosol Composition Records. *Sci. Total Environ.* **2015**, *511*, 11–20. [CrossRef] [PubMed]

55. Giannoni, M.; Martellini, T.; Del Bubba, M.; Gambaro, A.; Zangrando, R.; Chiari, M.; Lepri, L.; Cincinelli, A. The Use of Levoglucosan for Tracing Biomass Burning in $PM_{2.5}$ Samples in Tuscany (Italy). *Environ. Pollut.* **2012**, *167*, 7–15. [CrossRef]
56. Denier van der Gon, H.A.C.; Bergström, R.; Fountoukis, C.; Johansson, C.; Pandis, S.N.; Simpson, D.; Visschedijk, A.J.H. Particulate Emissions from Residential Wood Combustion in Europe—Revised Estimates and an Evaluation. *Atmos. Chem. Phys.* **2015**, *15*, 6503–6519. [CrossRef]
57. Reid, J.S.; Koppmann, R.; Eck, T.F.; Eleuterio, D.P. A Review of Biomass Burning Emissions Part II: Intensive Physical Properties of Biomass Burning Particles. *Atmos. Chem. Phys.* **2005**, *5*, 799–825. [CrossRef]
58. Croft, D.; Cameron, S.; Morrell, C.; Lowenstein, C.; Ling, F.; Zareba, W.; Hopke, P.; Utell, M.; Thurston, S.; Thevenet-Morrison, K.; et al. Associations between Ambient Wood Smoke and Other Particulate Pollutants and Biomarkers of Systemic Inflammation, Coagulation and Thrombosis in Cardiac Patients. *Environ. Res.* **2017**, *154*, 352–361. [CrossRef]
59. Weichenthal, S.; Kulka, R.; Lavigne, E.; van Rijswijk, D.; Brauer, M.; Villeneuve, P.J.; Stieb, D.; Joseph, L.; Burnett, R.T. Biomass Burning as a Source of Ambient Fine Particulate Air Pollution and Acute Myocardial Infarction. *Epidemiology* **2017**, *28*, 329–337. [CrossRef]
60. Wu, M.; Liu, X.; Yu, H.; Wang, H.; Shi, Y.; Yang, K.; Darmenov, A.; Wu, C.; Wang, Z.; Luo, T.; et al. Understanding Processes That Control Dust Spatial Distributions with Global Climate Models and Satellite Observations. *Atmos. Chem. Phys.* **2020**, *20*, 13835–13855. [CrossRef]
61. Kinne, S.; Schulz, M.; Textor, C.; Guibert, S.; Balkanski, Y.; Bauer, S.E.; Berntsen, T.; Berglen, T.F.; Boucher, O.; Chin, M.; et al. An AeroCom Initial Assessment—Optical Properties in Aerosol Component Modules of Global Models. *Atmos. Chem. Phys.* **2006**, *6*, 1815–1834. [CrossRef]
62. Mahowald, N.M.; Li, L.; Albani, S.; Hamilton, D.S.; Kok, J.F. Opinion: The Importance of Historical and Paleoclimate Aerosol Radiative Effects. *Atmos. Chem. Phys.* **2024**, *24*, 533–551. [CrossRef]
63. Skeie, R.B.; Aldrin, M.; Berntsen, T.K.; Holden, M.; Huseby, R.B.; Myhre, G.; Storelvmo, T. The Aerosol Pathway Is Crucial for Observationally Constraining Climate Sensitivity and Anthropogenic Forcing. *Earth Syst. Dyn.* **2024**, *15*, 1435–1458. [CrossRef]
64. Szopa, S.; Naik, V.; Adhikary, B.; Artaxo, P.; Berntsen, T.; Collins, W.; Fuzzi, S.; Gallardo, L.; Kiendler-Scharr, A.; Klimont, Z.; et al. Short-Lived Climate Forcers. In *Climate Change 2021: The Physical Science Basis. Contribution of Working Group I to the Sixth Assessment Report of the Intergovernmental Panel on Climate Change*; Cambridge University Press: Cambridge, UK; New York, NY, USA, 2021; pp. 817–922. ISBN 978-1-00-915788-9.
65. Domínguez-Rodríguez, A.; Báez-Ferrer, N.; Abreu-González, P.; Rodríguez, S.; Díaz, R.; Avanzas, P.; Hernández-Vaquero, D. Impact of Desert Dust Events on the Cardiovascular Disease: A Systematic Review and Meta-Analysis. *J. Clin. Med.* **2021**, *10*, 727. [CrossRef] [PubMed]
66. Kotsyfakis, M.; Zarogiannis, S.G.; Patelarou, E. The Health Impact of Saharan Dust Exposure. *Int. J. Occup. Med. Environ. Health* **2019**, *32*, 749–760. [CrossRef]
67. Stafoggia, M.; Zauli-Sajani, S.; Pey, J.; Samoli, E.; Alessandrini, E.; Basagaña, X.; Cernigliaro, A.; Chiusolo, M.; Demaria, M.; Díaz, J.; et al. Desert Dust Outbreaks in Southern Europe: Contribution to Daily PM_{10} Concentrations and Short-Term Associations with Mortality and Hospital Admissions. *Environ. Health Perspect.* **2016**, *124*, 413–419. [CrossRef]
68. Karanasiou, A.; Moreno, N.; Moreno, T.; Viana, M.; de Leeuw, F.; Querol, X. Health Effects from Sahara Dust Episodes in Europe: Literature Review and Research Gaps. *Environ. Int.* **2012**, *47*, 107–114. [CrossRef]
69. Gavrouzou, M.; Hatzianastassiou, N.; Gkikas, A.; Korras-Carraca, M.-B.; Mihalopoulos, N. A Global Climatology of Dust Aerosols Based on Satellite Data: Spatial, Seasonal and Inter-Annual Patterns over the Period 2005–2019. *Remote Sens.* **2021**, *13*, 359. [CrossRef]
70. Prospero, J.M.; Ginoux, P.; Torres, O.; Nicholson, S.E.; Gill, T.E. Environmental Characterization of Global Sources of Atmospheric Soil Dust Identified with the Nimbus 7 Total Ozone Mapping Spectrometer (Toms) Absorbing Aerosol Product. *Rev. Geophys.* **2002**, *40*, 2-1–2-31. [CrossRef]
71. Klaver, A.; Formenti, P.; Caquineau, S.; Chevaillier, S.; Ausset, P.; Calzolai, G.; Osborne, S.; Johnson, B.; Harrison, M.; Dubovik, O. Physico-Chemical and Optical Properties of Sahelian and Saharan Mineral Dust: In Situ Measurements during the GERBILS Campaign. *Q. J. R. Meteorol. Soc.* **2011**, *137*, 1193–1210. [CrossRef]
72. Rodríguez, S.; Calzolai, G.; Chiari, M.; Nava, S.; García, M.I.; López-Solano, J.; Marrero, C.; López-Darias, J.; Cuevas, E.; Alonso-Pérez, S.; et al. Rapid Changes of Dust Geochemistry in the Saharan Air Layer Linked to Sources and Meteorology. *Atmos. Environ.* **2020**, *223*, 117186. [CrossRef]
73. Barnaba, F.; Bolignano, A.; Di Liberto, L.; Morelli, M.; Lucarelli, F.; Nava, S.; Perrino, C.; Canepari, S.; Basart, S.; Costabile, F.; et al. Desert Dust Contribution to PM10 Loads in Italy: Methods and Recommendations Addressing the Relevant European Commission Guidelines in Support to the Air Quality Directive 2008/50. *Atmos. Environ.* **2017**, *161*, 288–305. [CrossRef]
74. Cuevas-Agulló, E.; Barriopedro, D.; García, R.D.; Alonso-Pérez, S.; González-Alemán, J.J.; Werner, E.; Suárez, D.; Bustos, J.J.; García-Castrillo, G.; García, O.; et al. Sharp Increase in Saharan Dust Intrusions over the Western Euro-Mediterranean in February–March 2020–2022 and Associated Atmospheric Circulation. *Atmos. Chem. Phys.* **2024**, *24*, 4083–4104. [CrossRef]

75. Salvador, P.; Pey, J.; Pérez, N.; Querol, X.; Artíñano, B. Increasing Atmospheric Dust Transport towards the Western Mediterranean over 1948–2020. *Npj Clim. Atmos. Sci.* **2022**, *5*, 34. [CrossRef]
76. White, W.H. Chemical Markers for Sea Salt in IMPROVE Aerosol Data. *Atmos. Environ.* **2008**, *42*, 261–274. [CrossRef]
77. Pósfai, M.; Molnár, Á. Atmospheric Aerosol Particles: A Mineralogical Introduction. In *Environmental Mineralogy II*; Vaughan, D.J., Wogelius, R.A., Eds.; Mineralogical Society of Great Britain and Ireland: Middlesex, UK, 2012; Volume 13, pp. 1–38, ISBN 978-0-903056-32-8.
78. Yang, G.-P.; Zhang, H.-H.; Zhou, L.-M.; Yang, J. Temporal and Spatial Variations of Dimethylsulfide (DMS) and Dimethylsulfoniopropionate (DMSP) in the East China Sea and the Yellow Sea. *Cont. Shelf Res.* **2011**, *31*, 1325–1335. [CrossRef]
79. Winiwarter, W.; Bauer, H.; Caseiro, A.; Puxbaum, H. Quantifying Emissions of Primary Biological Aerosol Particle Mass in Europe. *Atmos. Environ.* **2009**, *43*, 1403–1409. [CrossRef]
80. Guenther, A.; Karl, T.; Harley, P.; Wiedinmyer, C.; Palmer, P.I.; Geron, C. Estimates of Global Terrestrial Isoprene Emissions Using MEGAN (Model of Emissions of Gases and Aerosols from Nature). *Atmos. Chem. Phys.* **2006**, *6*, 3181–3210. [CrossRef]
81. Henze, D.K.; Seinfeld, J.H. Global Secondary Organic Aerosol from Isoprene Oxidation. *Geophys. Res. Lett.* **2006**, *33*, L09812. [CrossRef]
82. Du, Y.; Xu, X.; Chu, M.; Guo, Y.; Wang, J. Air Particulate Matter and Cardiovascular Disease: The Epidemiological, Biomedical and Clinical Evidence. *J. Thorac. Dis.* **2016**, *8*, E8–E19. [CrossRef]
83. de Bont, J.; Jaganathan, S.; Dahlquist, M.; Persson, Å.; Stafoggia, M.; Ljungman, P. Ambient Air Pollution and Cardiovascular Diseases: An Umbrella Review of Systematic Reviews and Meta-Analyses. *J. Intern. Med.* **2022**, *291*, 779–800. [CrossRef]
84. Yang, Y.-S.; Pei, Y.-H.; Gu, Y.-Y.; Zhu, J.-F.; Yu, P.; Chen, X.-H. Association between Short-Term Exposure to Ambient Air Pollution and Heart Failure: An Updated Systematic Review and Meta-Analysis of More than 7 Million Participants. *Front. Public Health* **2022**, *10*, 948765. [CrossRef] [PubMed]
85. Farhadi, Z.; Abulghasem Gorgi, H.; Shabaninejad, H.; Aghajani Delavar, M.; Torani, S. Association between PM2.5 and Risk of Hospitalization for Myocardial Infarction: A Systematic Review and a Meta-Analysis. *BMC Public Health* **2020**, *20*, 314. [CrossRef] [PubMed]
86. Rich, D.Q.; Peters, A.; Schneider, A.; Zareba, W.; Breitner, S.; Oakes, D.; Wiltshire, J.; Kane, C.; Frampton, M.W.; Hampel, R.; et al. Ambient and Controlled Particle Exposures as Triggers for Acute ECG Changes. *Res. Rep. Health Eff. Inst.* **2016**, *186*, 5–75.
87. Tonne, C.; Yanosky, J.D.; Beevers, S.; Wilkinson, P.; Kelly, F.J. PM Mass Concentration and PM Oxidative Potential in Relation to Carotid Intima-Media Thickness. *Epidemiology* **2012**, *23*, 486–494. [CrossRef]
88. Provost, E.B.; Madhloum, N.; Int Panis, L.; De Boever, P.; Nawrot, T.S. Carotid Intima-Media Thickness, a Marker of Subclinical Atherosclerosis, and Particulate Air Pollution Exposure: The Meta-Analytical Evidence. *PLoS ONE* **2015**, *10*, e0127014. [CrossRef]
89. Jilani, M.H.; Simon-Friedt, B.; Yahya, T.; Khan, A.Y.; Hassan, S.Z.; Kash, B.; Blankstein, R.; Blaha, M.J.; Virani, S.S.; Rajagopalan, S.; et al. Associations between Particulate Matter Air Pollution, Presence and Progression of Subclinical Coronary and Carotid Atherosclerosis: A Systematic Review. *Atherosclerosis* **2020**, *306*, 22–32. [CrossRef]
90. Wang, M.; Hou, Z.-H.; Xu, H.; Liu, Y.; Budoff, M.J.; Szpiro, A.A.; Kaufman, J.D.; Vedal, S.; Lu, B. Association of Estimated Long-Term Exposure to Air Pollution and Traffic Proximity with a Marker for Coronary Atherosclerosis in a Nationwide Study in China. *JAMA Netw. Open* **2019**, *2*, e196553. [CrossRef]
91. Hennig, F.; Geisel, M.H.; Kälsch, H.; Lucht, S.; Mahabadi, A.A.; Moebus, S.; Erbel, R.; Lehmann, N.; Jöckel, K.-H.; Scherag, A.; et al. Air Pollution and Progression of Atherosclerosis in Different Vessel Beds-Results from a Prospective Cohort Study in the Ruhr Area, Germany. *Environ. Health Perspect.* **2020**, *128*, 107003. [CrossRef]
92. Kilbo Edlund, K.; Sallsten, G.; Molnár, P.; Andersson, E.M.; Ögren, M.; Segersson, D.; Fagman, E.; Fagerberg, B.; Barregard, L.; Bergström, G.; et al. Long-Term Exposure to Air Pollution, Coronary Artery Calcification, and Carotid Artery Plaques in the Population-Based Swedish SCAPIS Gothenburg Cohort. *Environ. Res.* **2022**, *214*, 113926. [CrossRef]
93. Gorini, F.; Sabatino, L.; Gaggini, M.; Chatzianagnostou, K.; Vassalle, C. Oxidative Stress Biomarkers in the Relationship between Type 2 Diabetes and Air Pollution. *Antioxidants* **2021**, *10*, 1234. [CrossRef]
94. Zhu, X.; Mao, H.; Zeng, H.; Lv, F.; Wang, J. Causal Relationship Between Air Pollutants and Blood Pressure Phenotypes: A Mendelian Randomization Study. *Glob. Heart* **2025**, *20*, 18. [CrossRef] [PubMed]
95. Ossoli, A.; Cetti, F.; Gomaraschi, M. Air Pollution: Another Threat to HDL Function. *Int. J. Mol. Sci.* **2022**, *24*, 317. [CrossRef] [PubMed]
96. Hasslöf, H.; Molnár, P.; Andersson, E.M.; Spanne, M.; Gustafsson, S.; Stroh, E.; Engström, G.; Stockfelt, L. Long-Term Exposure to Air Pollution and Atherosclerosis in the Carotid Arteries in the Malmö Diet and Cancer Cohort. *Environ. Res.* **2020**, *191*, 110095. [CrossRef] [PubMed]
97. Jia, Y.; Lin, Z.; He, Z.; Li, C.; Zhang, Y.; Wang, J.; Liu, F.; Li, J.; Huang, K.; Cao, J.; et al. Effect of Air Pollution on Heart Failure: Systematic Review and Meta-Analysis. *Environ. Health Perspect.* **2023**, *131*, 76001. [CrossRef]
98. Zhang, D.; Chen, W.; Cheng, C.; Huang, H.; Li, X.; Qin, P.; Chen, C.; Luo, X.; Zhang, M.; Li, J.; et al. Air Pollution Exposure and Heart Failure: A Systematic Review and Meta-Analysis. *Sci. Total Environ.* **2023**, *872*, 162191. [CrossRef]

99. Lim, Y.-H.; Jørgensen, J.T.; So, R.; Cole-Hunter, T.; Mehta, A.J.; Amini, H.; Bräuner, E.V.; Westendorp, R.G.J.; Liu, S.; Mortensen, L.H.; et al. Long-Term Exposure to Air Pollution, Road Traffic Noise, and Heart Failure Incidence: The Danish Nurse Cohort. *J. Am. Heart Assoc.* **2021**, *10*, e021436. [CrossRef]
100. Shi, Y.; Zhang, L.; Li, W.; Wang, Q.; Tian, A.; Peng, K.; Li, Y.; Li, J. Association between Long-Term Exposure to Ambient Air Pollution and Clinical Outcomes among Patients with Heart Failure: Findings from the China PEACE Prospective Heart Failure Study. *Ecotoxicol. Environ. Saf.* **2021**, *222*, 112517. [CrossRef]
101. Ward-Caviness, C.K.; Danesh Yazdi, M.; Moyer, J.; Weaver, A.M.; Cascio, W.E.; Di, Q.; Schwartz, J.D.; Diaz-Sanchez, D. Long-Term Exposure to Particulate Air Pollution Is Associated with 30-Day Readmissions and Hospital Visits Among Patients with Heart Failure. *J. Am. Heart Assoc.* **2021**, *10*, e019430. [CrossRef]
102. Orellano, P.; Kasdagli, M.-I.; Pérez Velasco, R.; Samoli, E. Long-Term Exposure to Particulate Matter and Mortality: An Update of the WHO Global Air Quality Guidelines Systematic Review and Meta-Analysis. *Int. J. Public Health* **2024**, *69*, 1607683. [CrossRef]
103. Wang, Y.; Chang, J.; Hu, P.; Deng, C.; Luo, Z.; Zhao, J.; Zhang, Z.; Yi, W.; Zhu, G.; Zheng, G.; et al. Key Factors in Epidemiological Exposure and Insights for Environmental Management: Evidence from Meta-Analysis. *Environ. Pollut.* **2024**, *362*, 124991. [CrossRef]
104. McGuinn, L.A.; Ward-Caviness, C.K.; Neas, L.M.; Schneider, A.; Diaz-Sanchez, D.; Cascio, W.E.; Kraus, W.E.; Hauser, E.; Dowdy, E.; Haynes, C.; et al. Association between Satellite-Based Estimates of Long-Term PM2.5 Exposure and Coronary Artery Disease. *Environ. Res.* **2016**, *145*, 9–17. [CrossRef] [PubMed]
105. Zou, L.; Zong, Q.; Fu, W.; Zhang, Z.; Xu, H.; Yan, S.; Mao, J.; Zhang, Y.; Cao, S.; Lv, C. Long-Term Exposure to Ambient Air Pollution and Myocardial Infarction: A Systematic Review and Meta-Analysis. *Front. Med.* **2021**, *8*, 616355. [CrossRef] [PubMed]
106. Pope, C.A.; Muhlestein, J.B.; May, H.T.; Renlund, D.G.; Anderson, J.L.; Horne, B.D. Ischemic Heart Disease Events Triggered by Short-Term Exposure to Fine Particulate Air Pollution. *Circulation* **2006**, *114*, 2443–2448. [CrossRef] [PubMed]
107. Yen, C.-C.; Chen, P.-L. Effect of Short-Term Exposure to Fine Particulate Matter and Particulate Matter Pollutants on Triggering Acute Myocardial Infarction and Acute Heart Failure. *Am. J. Cardiol.* **2022**, *175*, 158–163. [CrossRef]
108. Sancini, G.; Farina, F.; Battaglia, C.; Cifola, I.; Mangano, E.; Mantecca, P.; Camatini, M.; Palestini, P. Health Risk Assessment for Air Pollutants: Alterations in Lung and Cardiac Gene Expression in Mice Exposed to Milano Winter Fine Particulate Matter (PM2.5). *PLoS ONE* **2014**, *9*, e109685. [CrossRef]
109. Bredeck, G.; Busch, M.; Rossi, A.; Stahlmecke, B.; Fomba, K.W.; Herrmann, H.; Schins, R.P.F. Inhalable Saharan dust induces oxidative stress, NLRP3 inflammasome activation, and inflammatory cytokine release. *Environ. Int.* **2023**, *172*, 107732. [CrossRef]
110. Pardo, M.; Katra, I.; Schaeur, J.J.; Rudich, Y. Mitochondria-mediated oxidative stress induced by desert dust in rat alveolar macrophages. *Geohealth* **2017**, *6*, 4–16. [CrossRef]
111. Chang, C.C.; Hwang, J.S.; Chan, C.C.; Wang, P.Y.; Cheng, T.J. Effects of concentrated ambient particles on heart rate, blood pressure, and cardiac contractility in spontaneously hypertensive rats during a dust storm event. *Inhal. Toxicol.* **2007**, *19*, 973–978. [CrossRef]
112. Ishii, M.; Seki, T.; Sakamoto, K.; Kaikita, K.; Miyamoto, Y.; Tsujita, K.; Masuda, I.; Kawakami, K. Association of short term exposure to Asian dust with increased blood pressure. *Sci. Rep.* **2020**, *19*, 17630. [CrossRef]
113. Liu, K.; Mu, M.; Fang, K.; Qian, Y.; Xue, S.; Hu, W.; Ye, M. Occupational exposure to silica and risk of heart disease: A systematic review with meta-analysis. *BMJ Open* **2020**, *7*, e029653. [CrossRef]
114. Matsukawa, R.; Michikawa, T.; Ueda, K.; Nitta, H.; Kawasaki, T.; Tashiro, H.; Mohri, M.; Yamamoto, Y. Desert dust is a risk factor for the incidence of acute myocardial infarction in Western Japan. *Circ. Cardiovasc. Qual. Outcomes* **2014**, *7*, 743–748. [CrossRef] [PubMed]
115. Ishii, M.; Seki, T.; Kaikita, K.; Sakamoto, K.; Nakai, M.; Sumita, Y.; Nishimura, K.; Miyamoto, Y.; Noguchi, T.; Yasuda, S.; et al. Short-term exposure to desert dust and the risk of acute myocardial infarction in Japan: A time-stratified case-crossover study. *Eur. J. Epidemiol.* **2020**, *35*, 455–464. [CrossRef] [PubMed]
116. Bevan, G.H.; Al-Kindi, S.G.; Brook, R.D.; Münzel, T.; Rajagopalan, S. Ambient Air Pollution and Atherosclerosis: Insights into Dose, Time, and Mechanisms. *Arter. Thromb. Vasc. Biol.* **2021**, *41*, 628–637. [CrossRef] [PubMed]
117. Delfino, R.J.; Staimer, N.; Tjoa, T.; Gillen, D.L.; Polidori, A.; Arhami, M.; Kleinman, M.T.; Vaziri, N.D.; Longhurst, J.; Sioutas, C. Air pollution exposures and circulating biomarkers of effect in a susceptible population: Clues to potential causal component mixtures and mechanisms. *Environ. Health Perspect.* **2009**, *117*, 1232–1238. [CrossRef]
118. Schneider, A.; Neas, L.; Herbst, M.C.; Case, M.; Williams, R.W.; Cascio, W.; Hinderliter, A.; Holguin, F.; Buse, J.B.; Dungan, K.; et al. Endothelial dysfunction: Associations with exposure to ambient fine particles in diabetic individuals. *Environ. Health Perspect.* **2008**, *116*, 1666–1674. [CrossRef]
119. Madrigano, J.; Baccarelli, A.; Wright, R.O.; Suh, H.; Sparrow, D.; Vokonas, P.S.; Schwartz, J. Air Pollution, Obesity, Genes and Cellular Adhesion Molecules. *Occup. Environ. Med.* **2010**, *67*, 312–317. [CrossRef]

120. Kilbo Edlund, K.; Xu, Y.; Andersson, E.M.; Christensson, A.; Dehlin, M.; Forsblad-d'Elia, H.; Harari, F.; Ljunggren, S.; Molnár, P.; Oudin, A.; et al. Long-term ambient air pollution exposure and renal function and biomarkers of renal disease. *Environ. Health* **2024**, *9*, 67. [CrossRef]
121. Tang, Y.X.; Bloom, M.S.; Qian, Z.M.; Liu, E.; Jansson, D.R.; Vaughn, M.G.; Lin, H.L.; Xiao, L.W.; Duan, C.W.; Yang, L.; et al. Association between ambient air pollution and hyperuricemia in traffic police officers in China: A cohort study. *Int. J. Environ. Health Res.* **2021**, *31*, 54–62. [CrossRef]
122. Hu, L.K.; Liu, Y.H.; Yang, K.; Chen, N.; Ma, L.L.; Yan, Y.X. Associations between long-term exposure to ambient fine particulate pollution with the decline of kidney function and hyperuricemia: A longitudinal cohort study. *Environ. Sci. Pollut. Res. Int.* **2023**, *30*, 40507–40518. [CrossRef]
123. Vassalle, C.; Mazzone, A.; Sabatino, L.; Carpeggiani, C. Uric Acid for Cardiovascular Risk: Dr. Jekyll or Mr. Hide? *Diseases* **2016**, *26*, 12. [CrossRef]
124. Guo, L.H.; Zeeshan, M.; Huang, G.F.; Chen, D.H.; Xie, M.; Liu, J.; Dong, G.H. Influence of Air Pollution Exposures on Cardiometabolic Risk Factors: A Review. *Curr. Environ. Health Rep.* **2023**, *10*, 501–507. [CrossRef] [PubMed]
125. Huan, S.; Jin, S.; Liu, H.; Xia, W.; Liang, G.; Xu, S.; Fang, X.; Li, C.; Wang, Q.; Sun, X.; et al. Fine particulate matter exposure and perturbation of serum metabolome: A longitudinal study in Baoding, China. *Chemosphere* **2021**, *276*, 130102. [CrossRef] [PubMed]
126. Dong, Y.; Liu, C.; Wang, J.; Li, H.; Wang, Q.; Feng, A.; Tang, Z. Association between total bilirubin and gender-specific incidence of fundus arteriosclerosis in a Chinese population: A retrospective cohort study. *Sci. Rep.* **2023**, *11*, 11244. [CrossRef] [PubMed]
127. Radmanesh, E.; Dianat, M.; Badavi, M.; Goudarzi, G.; Mard, S.A.; Radan, M. Protective effect of crocin on hemodynamic parameters, electrocardiogram parameters, and oxidative stress in isolated hearts of rats exposed to PM_{10}. *Iran. J. Basic. Med. Sci.* **2022**, *25*, 460–467. [CrossRef]
128. Perepu, R.S.; Dostal, D.E.; Garcia, C.; Kennedy, R.H.; Sethi, R. Cardiac dysfunction subsequent to chronic ozone exposure in rats. *Mol. Cell. Biochem.* **2012**, *360*, 339–345. [CrossRef]
129. Wan, J.; Diaz-Sanchez, D. Antioxidant enzyme induction: A new protective approach against the adverse effects of diesel exhaust particles. *Inhal. Toxicol.* **2007**, *19*, 177–182. [CrossRef]
130. Allen, J. Inhaled glutathione for the prevention of air pollution-related health effects: A brief review. *Altern. Ther. Health Med.* **2008**, *14*, 42–44.
131. Cho, S.Y.; Roh, H.T. Impact of Particulate Matter Exposure and Aerobic Exercise on Circulating Biomarkers of Oxidative Stress, Antioxidant Status, and Inflammation in Young and Aged Mice. *Life* **2023**, *13*, 1952. [CrossRef]
132. Shah, A.S.V.; Langrish, J.P.; Nair, H.; McAllister, D.A.; Hunter, A.L.; Donaldson, K.; Newby, D.E.; Mills, N.L. Global Association of Air Pollution and Heart Failure: A Systematic Review and Meta-Analysis. *Lancet* **2013**, *382*, 1039–1048. [CrossRef]
133. Caldeira, D.; Franco, F.; Bravo Baptista, S.; Cabral, S.; Cachulo, M.d.C.; Dores, H.; Peixeiro, A.; Rodrigues, R.; Santos, M.; Timóteo, A.T.; et al. Air Pollution and Cardiovascular Diseases: A Position Paper. *Rev. Port. Cardiol.* **2022**, *41*, 709–717. [CrossRef]
134. US EPA. *Integrated Science Assessment (ISA) for Particulate Matter*; Final Report; U.S. Environmental Protection Agency: Washington, DC, USA, 2019.
135. Rajagopalan, S.; Al-Kindi, S.G.; Brook, R.D. Air Pollution and Cardiovascular Disease: JACC State-of-the-Art Review. *J. Am. Coll. Cardiol.* **2018**, *72*, 2054–2070. [CrossRef] [PubMed]
136. Wu, S.; Yang, D.; Wei, H.; Wang, B.; Huang, J.; Li, H.; Shima, M.; Deng, F.; Guo, X. Association of Chemical Constituents and Pollution Sources of Ambient Fine Particulate Air Pollution and Biomarkers of Oxidative Stress Associated with Atherosclerosis: A Panel Study among Young Adults in Beijing, China. *Chemosphere* **2015**, *135*, 347–353. [CrossRef] [PubMed]
137. Zhang, J.; Zhu, T.; Kipen, H.; Wang, G.; Huang, W.; Rich, D.; Zhu, P.; Wang, Y.; Lu, S.-E.; Ohman-Strickland, P.; et al. Cardiorespiratory Biomarker Responses in Healthy Young Adults to Drastic Air Quality Changes Surrounding the 2008 Beijing Olympics. *Res. Rep. Health Eff. Inst.* **2013**, *5*, 174.
138. Münzel, T.; Hahad, O.; Sørensen, M.; Lelieveld, J.; Duerr, G.D.; Nieuwenhuijsen, M.; Daiber, A. Environmental Risk Factors and Cardiovascular Diseases: A Comprehensive Expert Review. *Cardiovasc. Res.* **2022**, *118*, 2880–2902. [CrossRef]
139. Kelly, F.J.; Fussell, J.C. Role of Oxidative Stress in Cardiovascular Disease Outcomes Following Exposure to Ambient Air Pollution. *Free Radic. Biol. Med.* **2017**, *110*, 345–367. [CrossRef]
140. Itabe, H. Oxidized Low-Density Lipoprotein as a Biomarker of in Vivo Oxidative Stress: From Atherosclerosis to Periodontitis. *J. Clin. Biochem. Nutr.* **2012**, *51*, 1–8. [CrossRef]
141. Steinberg, D.; Witztum, J.L. Oxidized Low-Density Lipoprotein and Atherosclerosis. *Arter. Thromb. Vasc. Biol.* **2010**, *30*, 2311–2316. [CrossRef]
142. Kuda, O.; Jenkins, C.M.; Skinner, J.R.; Moon, S.H.; Su, X.; Gross, R.W.; Abumrad, N.A. CD36 Protein Is Involved in Store-Operated Calcium Flux, Phospholipase A2 Activation, and Production of Prostaglandin E2. *J. Biol. Chem.* **2011**, *286*, 17785–17795. [CrossRef]
143. Jacobs, L.; Emmerechts, J.; Mathieu, C.; Hoylaerts, M.F.; Fierens, F.; Hoet, P.H.; Nemery, B.; Nawrot, T.S. Air Pollution Related Prothrombotic Changes in Persons with Diabetes. *Environ. Health Perspect.* **2010**, *118*, 191–196. [CrossRef]

144. Kelishadi, R.; Mirghaffari, N.; Poursafa, P.; Gidding, S.S. Lifestyle and Environmental Factors Associated with Inflammation, Oxidative Stress and Insulin Resistance in Children. *Atherosclerosis* **2009**, *203*, 311–319. [CrossRef]
145. Li, R.; Ning, Z.; Cui, J.; Khalsa, B.; Ai, L.; Takabe, W.; Beebe, T.; Majumdar, R.; Sioutas, C.; Hsiai, T. Ultrafine Particles from Diesel Engines Induce Vascular Oxidative Stress via JNK Activation. *Free Radic. Biol. Med.* **2009**, *46*, 775–782. [CrossRef] [PubMed]
146. Bagryantseva, Y.; Novotna, B.; Rossner, P.; Chvatalova, I.; Milcova, A.; Svecova, V.; Lnenickova, Z.; Solansky, I.; Sram, R.J. Oxidative Damage to Biological Macromolecules in Prague Bus Drivers and Garagemen: Impact of Air Pollution and Genetic Polymorphisms. *Toxicol. Lett.* **2010**, *199*, 60–68. [CrossRef] [PubMed]
147. Rossner, P.; Svecova, V.; Milcova, A.; Lnenickova, Z.; Solansky, I.; Santella, R.M.; Sram, R.J. Oxidative and Nitrosative Stress Markers in Bus Drivers. *Mutat. Res.* **2007**, *617*, 23–32. [CrossRef] [PubMed]
148. Brucker, N.; Moro, A.M.; Charão, M.F.; Durgante, J.; Freitas, F.; Baierle, M.; Nascimento, S.; Gauer, B.; Bulcão, R.P.; Bubols, G.B.; et al. Biomarkers of Occupational Exposure to Air Pollution, Inflammation and Oxidative Damage in Taxi Drivers. *Sci. Total Environ.* **2013**, *463–464*, 884–893. [CrossRef]
149. Lai, C.-H.; Huang, H.-B.; Chang, Y.-C.; Su, T.-Y.; Wang, Y.-C.; Wang, G.-C.; Chen, J.-E.; Tang, C.-S.; Wu, T.-N.; Liou, S.-H. Exposure to Fine Particulate Matter Causes Oxidative and Methylated DNA Damage in Young Adults: A Longitudinal Study. *Sci. Total Environ.* **2017**, *598*, 289–296. [CrossRef]
150. Jiang, S.; Bo, L.; Gong, C.; Du, X.; Kan, H.; Xie, Y.; Song, W.; Zhao, J. Traffic-Related Air Pollution Is Associated with Cardio-Metabolic Biomarkers in General Residents. *Int. Arch. Occup. Environ. Health* **2016**, *89*, 911–921. [CrossRef]
151. Tang, H.; Cheng, Z.; Li, N.; Mao, S.; Ma, R.; He, H.; Niu, Z.; Chen, X.; Xiang, H. The Short- and Long-Term Associations of Particulate Matter with Inflammation and Blood Coagulation Markers: A Meta-Analysis. *Environ. Pollut.* **2020**, *267*, 115630. [CrossRef]
152. Weichenthal, S.; Lavigne, E.; Evans, G.; Pollitt, K.; Burnett, R.T. Ambient PM2.5 and Risk of Emergency Room Visits for Myocardial Infarction: Impact of Regional PM2.5 Oxidative Potential: A Case-Crossover Study. *Environ. Health* **2016**, *15*, 46. [CrossRef]
153. Dominguez-Rodriguez, A.; Rodríguez, S.; Abreu-Gonzalez, P.; Avanzas, P.; Juarez-Prera, R.A. Black Carbon Exposure, Oxidative Stress Markers and Major Adverse Cardiovascular Events in Patients with Acute Coronary Syndromes. *Int. J. Cardiol.* **2015**, *188*, 47–49. [CrossRef]
154. Rodosthenous, R.S.; Coull, B.A.; Lu, Q.; Vokonas, P.S.; Schwartz, J.D.; Baccarelli, A.A. Ambient Particulate Matter and microRNAs in Extracellular Vesicles: A Pilot Study of Older Individuals. *Part. Fibre Toxicol.* **2016**, *13*, 13. [CrossRef]
155. Aztatzi-Aguilar, O.G.; Uribe-Ramírez, M.; Arias-Montaño, J.A.; Barbier, O.; De Vizcaya-Ruiz, A. Acute and Subchronic Exposure to Air Particulate Matter Induces Expression of Angiotensin and Bradykinin-Related Genes in the Lungs and Heart: Angiotensin-II Type-I Receptor as a Molecular Target of Particulate Matter Exposure. *Part. Fibre Toxicol.* **2015**, *12*, 17. [CrossRef] [PubMed]
156. Bai, N.; Kido, T.; Suzuki, H.; Yang, G.; Kavanagh, T.J.; Kaufman, J.D.; Rosenfeld, M.E.; van Breemen, C.; Eeden, S.F. van Changes in Atherosclerotic Plaques Induced by Inhalation of Diesel Exhaust. *Atherosclerosis* **2011**, *216*, 299–306. [CrossRef] [PubMed]
157. Yin, F.; Lawal, A.; Ricks, J.; Fox, J.R.; Larson, T.; Navab, M.; Fogelman, A.M.; Rosenfeld, M.E.; Araujo, J.A. Diesel Exhaust Induces Systemic Lipid Peroxidation and Development of Dysfunctional Pro-Oxidant and pro-Inflammatory High-Density Lipoprotein. *Arter. Thromb. Vasc. Biol.* **2013**, *33*, 1153–1161. [CrossRef]
158. Miller, M.R.; McLean, S.G.; Duffin, R.; Lawal, A.O.; Araujo, J.A.; Shaw, C.A.; Mills, N.L.; Donaldson, K.; Newby, D.E.; Hadoke, P.W.F. Diesel Exhaust Particulate Increases the Size and Complexity of Lesions in Atherosclerotic Mice. *Part. Fibre Toxicol.* **2013**, *10*, 61. [CrossRef]
159. Kodavanti, U.P.; Thomas, R.; Ledbetter, A.D.; Schladweiler, M.C.; Shannahan, J.H.; Wallenborn, J.G.; Lund, A.K.; Campen, M.J.; Butler, E.O.; Gottipolu, R.R.; et al. Vascular and Cardiac Impairments in Rats Inhaling Ozone and Diesel Exhaust Particles. *Environ. Health Perspect.* **2011**, *119*, 312–318. [CrossRef]
160. Lund, A.K.; Lucero, J.; Harman, M.; Madden, M.C.; McDonald, J.D.; Seagrave, J.C.; Campen, M.J. The Oxidized Low-Density Lipoprotein Receptor Mediates Vascular Effects of Inhaled Vehicle Emissions. *Am. J. Respir. Crit. Care Med.* **2011**, *184*, 82–91. [CrossRef]
161. Gorr, M.W.; Youtz, D.J.; Eichenseer, C.M.; Smith, K.E.; Nelin, T.D.; Cormet-Boyaka, E.; Wold, L.E. In Vitro Particulate Matter Exposure Causes Direct and Lung-Mediated Indirect Effects on Cardiomyocyte Function. *Am. J. Physiol. Heart Circ. Physiol.* **2015**, *309*, H53-62. [CrossRef]
162. Wold, L.E.; Ying, Z.; Hutchinson, K.R.; Velten, M.; Gorr, M.W.; Velten, C.; Youtz, D.J.; Wang, A.; Lucchesi, P.A.; Sun, Q.; et al. Cardiovascular Remodeling in Response to Long-Term Exposure to Fine Particulate Matter Air Pollution. *Circ. Heart Fail.* **2012**, *5*, 452–461. [CrossRef]
163. Li, R.; Navab, M.; Pakbin, P.; Ning, Z.; Navab, K.; Hough, G.; Morgan, T.E.; Finch, C.E.; Araujo, J.A.; Fogelman, A.M.; et al. Ambient Ultrafine Particles Alter Lipid Metabolism and HDL Anti-Oxidant Capacity in LDLR-Null Mice. *J. Lipid Res.* **2013**, *54*, 1608–1615. [CrossRef]

164. Araujo, J.A.; Barajas, B.; Kleinman, M.; Wang, X.; Bennett, B.J.; Gong, K.W.; Navab, M.; Harkema, J.; Sioutas, C.; Lusis, A.J.; et al. Ambient Particulate Pollutants in the Ultrafine Range Promote Early Atherosclerosis and Systemic Oxidative Stress. *Circ. Res.* **2008**, *102*, 589–596. [CrossRef]
165. Lu, Y.; Qiu, W.; Liao, R.; Cao, W.; Huang, F.; Wang, X.; Li, M.; Li, Y. Subacute PM2.5 Exposure Induces Hepatic Insulin Resistance Through Inflammation and Oxidative Stress. *Int. J. Mol. Sci.* **2025**, *26*, 812. [CrossRef] [PubMed]
166. Meyer, G.; André, L.; Tanguy, S.; Boissiere, J.; Farah, C.; Lopez-Lauri, F.; Gayrard, S.; Richard, S.; Boucher, F.; Cazorla, O.; et al. Simulated Urban Carbon Monoxide Air Pollution Exacerbates Rat Heart Ischemia-Reperfusion Injury. *Am. J. Physiol. Heart Circ. Physiol.* **2010**, *298*, H1445-1453. [CrossRef] [PubMed]
167. Meyer, G.; André, L.; Kleindienst, A.; Singh, F.; Tanguy, S.; Richard, S.; Obert, P.; Boucher, F.; Jover, B.; Cazorla, O.; et al. Carbon Monoxide Increases Inducible NOS Expression That Mediates CO-Induced Myocardial Damage during Ischemia-Reperfusion. *Am. J. Physiol. Heart Circ. Physiol.* **2015**, *308*, H759–H767. [CrossRef] [PubMed]
168. Perepu, R.S.P.; Garcia, C.; Dostal, D.; Sethi, R. Enhanced Death Signaling in Ozone-Exposed Ischemic-Reperfused Hearts. *Mol. Cell. Biochem.* **2010**, *336*, 55–64. [CrossRef]
169. Bundy, J.G.; Davey, M.P.; Viant, M.R. Environmental Metabolomics: A Critical Review and Future Perspectives. *Metabolomics* **2009**, *5*, 3–21. [CrossRef]
170. Liang, D.; Tang, Z.; Diver, W.R.; Sarnat, J.A.; Chow, S.S.; Cheng, H.; Deubler, E.L.; Tan, Y.; Eick, S.M.; Jerrett, M.; et al. Metabolomics Signatures of Exposure to Ambient Air Pollution: A Large-Scale Metabolome-Wide Association Study in the Cancer Prevention Study-II Nutrition Cohort. *Environ. Sci. Technol.* **2025**, *59*, 212–223. [CrossRef]
171. Nassan, F.L.; Kelly, R.S.; Kosheleva, A.; Koutrakis, P.; Vokonas, P.S.; Lasky-Su, J.A.; Schwartz, J.D. Metabolomic Signatures of the Long-Term Exposure to Air Pollution and Temperature. *Environ. Health* **2021**, *20*, 3. [CrossRef]
172. Li, Y.; Wang, H.; Xiao, Y.; Yang, H.; Wang, S.; Liu, L.; Cai, H.; Zhang, X.; Tang, H.; Wu, T.; et al. Lipidomics Identified Novel Cholesterol-Independent Predictors for Risk of Incident Coronary Heart Disease: Mediation of Risk from Diabetes and Aggravation of Risk by Ambient Air Pollution. *J. Adv. Res.* **2024**, *65*, 273–282. [CrossRef]
173. Ran, S.; Zhang, J.; Tian, F.; Qian, Z.M.; Wei, S.; Wang, Y.; Chen, G.; Zhang, J.; Arnold, L.D.; McMillin, S.E.; et al. Association of Metabolic Signatures of Air Pollution with MASLD: Observational and Mendelian Randomization Study. *J. Hepatol.* **2025**, *82*, 560–570. [CrossRef]
174. Arias-Pérez, R.D.; Taborda, N.A.; Gómez, D.M.; Narvaez, J.F.; Porras, J.; Hernandez, J.C. Inflammatory Effects of Particulate Matter Air Pollution. *Environ. Sci. Pollut. Res. Int.* **2020**, *27*, 42390–42404. [CrossRef]
175. Blackburn, E.H. Structure and Function of Telomeres. *Nature* **1991**, *350*, 569–573. [CrossRef] [PubMed]
176. Houben, J.M.J.; Moonen, H.J.J.; van Schooten, F.J.; Hageman, G.J. Telomere Length Assessment: Biomarker of Chronic Oxidative Stress? *Free Radic. Biol. Med.* **2008**, *44*, 235–246. [CrossRef] [PubMed]
177. Wong, J.Y.Y.; De Vivo, I.; Lin, X.; Christiani, D.C. Cumulative PM(2.5) Exposure and Telomere Length in Workers Exposed to Welding Fumes. *J. Toxicol. Environ. Health A* **2014**, *77*, 441–455. [CrossRef] [PubMed]
178. Hou, L.; Wang, S.; Dou, C.; Zhang, X.; Yu, Y.; Zheng, Y.; Avula, U.; Hoxha, M.; Díaz, A.; McCracken, J.; et al. Air Pollution Exposure and Telomere Length in Highly Exposed Subjects in Beijing, China: A Repeated-Measure Study. *Environ. Int.* **2012**, *48*, 71–77. [CrossRef]
179. Wei, B.; Zhou, Y.; Li, Q.; Zhen, S.; Wu, Q.; Xiao, Z.; Liao, J.; Zhu, B.; Duan, J.; Yang, X.; et al. Outdoor Fine Particulate Matter Exposure and Telomere Length in Humans: A Systematic Review and Meta-Analysis. *Ecotoxicol. Environ. Saf.* **2024**, *275*, 116206. [CrossRef]
180. Dai, L.; Mehta, A.; Mordukhovich, I.; Just, A.C.; Shen, J.; Hou, L.; Koutrakis, P.; Sparrow, D.; Vokonas, P.S.; Baccarelli, A.A.; et al. Differential DNA Methylation and PM2.5 Species in a 450K Epigenome-Wide Association Study. *Epigenetics* **2017**, *12*, 139–148. [CrossRef]
181. Bellavia, A.; Urch, B.; Speck, M.; Brook, R.D.; Scott, J.A.; Albetti, B.; Behbod, B.; North, M.; Valeri, L.; Bertazzi, P.A.; et al. DNA Hypomethylation, Ambient Particulate Matter, and Increased Blood Pressure: Findings from Controlled Human Exposure Experiments. *J. Am. Heart Assoc.* **2013**, *2*, e000212. [CrossRef]
182. Madrigano, J.; Baccarelli, A.; Mittleman, M.A.; Wright, R.O.; Sparrow, D.; Vokonas, P.S.; Tarantini, L.; Schwartz, J. Prolonged Exposure to Particulate Pollution, Genes Associated with Glutathione Pathways, and DNA Methylation in a Cohort of Older Men. *Environ. Health Perspect.* **2011**, *119*, 977–982. [CrossRef]
183. Tarantini, L.; Bonzini, M.; Apostoli, P.; Pegoraro, V.; Bollati, V.; Marinelli, B.; Cantone, L.; Rizzo, G.; Hou, L.; Schwartz, J.; et al. Effects of Particulate Matter on Genomic DNA Methylation Content and iNOS Promoter Methylation. *Environ. Health Perspect.* **2009**, *117*, 217–222. [CrossRef]
184. Marketou, M.E.; Kontaraki, J.E.; Zacharis, E.A.; Kochiadakis, G.E.; Giaouzaki, A.; Chlouverakis, G.; Vardas, P.E. TLR2 and TLR4 Gene Expression in Peripheral Monocytes in Nondiabetic Hypertensive Patients: The Effect of Intensive Blood Pressure-Lowering. *J. Clin. Hypertens.* **2012**, *14*, 330–335. [CrossRef]

185. Boovarahan, S.R.; Kurian, G.A. Mitochondrial Dysfunction: A Key Player in the Pathogenesis of Cardiovascular Diseases Linked to Air Pollution. *Rev. Environ. Health* **2018**, *33*, 111–122. [CrossRef] [PubMed]
186. Annesley, S.J.; Fisher, P.R. Mitochondria in Health and Disease. *Cells* **2019**, *8*, 680. [CrossRef] [PubMed]
187. Sotty, J.; Kluza, J.; De Sousa, C.; Tardivel, M.; Anthérieu, S.; Alleman, L.-Y.; Canivet, L.; Perdrix, E.; Loyens, A.; Marchetti, P.; et al. Mitochondrial Alterations Triggered by Repeated Exposure to Fine (PM2.5–0.18) and Quasi-Ultrafine (PM0.18) Fractions of Ambient Particulate Matter. *Environ. Int.* **2020**, *142*, 105830. [CrossRef] [PubMed]
188. Wang, Y.; Kong, L.; Wu, T.; Tang, M. Urban Particulate Matter Disturbs the Equilibrium of Mitochondrial Dynamics and Biogenesis in Human Vascular Endothelial Cells. *Environ. Pollut.* **2020**, *264*, 114639. [CrossRef]
189. Piloquet, H.; Ferchaud-Roucher, V.; Duengler, F.; Zair, Y.; Maugere, P.; Krempf, M. Insulin Effects on Acetate Metabolism. *Am. J. Physiol. Endocrinol. Metab.* **2003**, *285*, E561–E565. [CrossRef]
190. Zhang, Z.; Su, H.; Ahmed, R.Z.; Zheng, Y.; Jin, X. Critical Biomarkers for Myocardial Damage by Fine Particulate Matter: Focused on PPARα-Regulated Energy Metabolism. *Environ. Pollut.* **2020**, *264*, 114659. [CrossRef]
191. Wolf, K.; Popp, A.; Schneider, A.; Breitner, S.; Hampel, R.; Rathmann, W.; Herder, C.; Roden, M.; Koenig, W.; Meisinger, C.; et al. Association Between Long-Term Exposure to Air Pollution and Biomarkers Related to Insulin Resistance, Subclinical Inflammation, and Adipokines. *Diabetes* **2016**, *65*, 3314–3326. [CrossRef]
192. Zhang, Y.; Chu, M.; Zhang, J.; Duan, J.; Hu, D.; Zhang, W.; Yang, X.; Jia, X.; Deng, F.; Sun, Z. Urine Metabolites Associated with Cardiovascular Effects from Exposure of Size-Fractioned Particulate Matter in a Subway Environment: A Randomized Crossover Study. *Environ. Int.* **2019**, *130*, 104920. [CrossRef]
193. Ussher, J.R.; Elmariah, S.; Gerszten, R.E.; Dyck, J.R.B. The Emerging Role of Metabolomics in the Diagnosis and Prognosis of Cardiovascular Disease. *J. Am. Coll. Cardiol.* **2016**, *68*, 2850–2870. [CrossRef]
194. Zarate-Gonzalez, G.; Brown, P.; Cisneros, R. Assessing Public Support for Air Pollution Mitigation and Control Policies: Health, Socioeconomic, and Ideological Predictors in an Overburdened and Vulnerable Region of the U.S. *BMC Public Health* **2025**, *25*, 263. [CrossRef]
195. Huang, W.; Wang, G.; Lu, S.-E.; Kipen, H.; Wang, Y.; Hu, M.; Lin, W.; Rich, D.; Ohman-Strickland, P.; Diehl, S.R.; et al. Inflammatory and Oxidative Stress Responses of Healthy Young Adults to Changes in Air Quality during the Beijing Olympics. *Am. J. Respir. Crit. Care Med.* **2012**, *186*, 1150–1159. [CrossRef] [PubMed]
196. Rich, D.Q.; Kipen, H.M.; Huang, W.; Wang, G.; Wang, Y.; Zhu, P.; Ohman-Strickland, P.; Hu, M.; Philipp, C.; Diehl, S.R.; et al. Association between Changes in Air Pollution Levels during the Beijing Olympics and Biomarkers of Inflammation and Thrombosis in Healthy Young Adults. *JAMA* **2012**, *307*, 2068–2078. [CrossRef] [PubMed]
197. WHO. Air Pollution. Available online: https://www.who.int/health-topics/air-pollution#tab=tab_1 (accessed on 29 April 2025).
198. Barthelemy, J.; Sanchez, K.; Miller, M.R.; Khreis, H. New Opportunities to Mitigate the Burden of Disease Caused by Traffic Related Air Pollution: Antioxidant-Rich Diets and Supplements. *Int. J. Environ. Res. Public Health* **2020**, *17*, 630. [CrossRef] [PubMed]
199. Péter, S.; Holguin, F.; Wood, L.G.; Clougherty, J.E.; Raederstorff, D.; Antal, M.; Weber, P.; Eggersdorfer, M. Nutritional Solutions to Reduce Risks of Negative Health Impacts of Air Pollution. *Nutrients* **2015**, *7*, 10398–10416. [CrossRef]
200. Lopresti, A.L. Association between Micronutrients and Heart Rate Variability: A Review of Human Studies. *Adv. Nutr.* **2020**, *11*, 559–575. [CrossRef]
201. Bo, L.; Jiang, S.; Xie, Y.; Kan, H.; Song, W.; Zhao, J. Effect of Vitamin E and Omega-3 Fatty Acids on Protecting Ambient PM2.5-Induced Inflammatory Response and Oxidative Stress in Vascular Endothelial Cells. *PLoS ONE* **2016**, *11*, e0152216. [CrossRef]
202. Du, X.; Jiang, S.; Bo, L.; Liu, J.; Zeng, X.; Xie, Y.; He, Q.; Ye, X.; Song, W.; Zhao, J. Combined Effects of Vitamin E and Omega-3 Fatty Acids on Protecting Ambient PM2.5-Induced Cardiovascular Injury in Rats. *Chemosphere* **2017**, *173*, 14–21. [CrossRef]
203. Knuckles, T.L.; Jaskot, R.; Richards, J.H.; Miller, C.A.; Ledbetter, A.; McGee, J.; Linak, W.P.; Dreher, K.L. Biokinetically-Based in Vitro Cardiotoxicity of Residual Oil Fly Ash: Hazard Identification and Mechanisms of Injury. *Cardiovasc. Toxicol.* **2013**, *13*, 426–437. [CrossRef]
204. Kim, J.-B.; Kim, C.; Choi, E.; Park, S.; Park, H.; Pak, H.-N.; Lee, M.-H.; Shin, D.C.; Hwang, K.-C.; Joung, B. Particulate Air Pollution Induces Arrhythmia via Oxidative Stress and Calcium Calmodulin Kinase II Activation. *Toxicol. Appl. Pharmacol.* **2012**, *259*, 66–73. [CrossRef]
205. Li, W.; Hou, Z.; Li, Y.; Zhang, X.; Bao, X.; Hou, X.; Zhang, H.; Zhang, S. Amelioration of Metabolic Disorders in H9C2 Cardiomyocytes Induced by PM2.5 Treated with Vitamin C. *Drug Chem. Toxicol.* **2024**, *47*, 347–355. [CrossRef]
206. Zhong, J.; Karlsson, O.; Wang, G.; Li, J.; Guo, Y.; Lin, X.; Zemplenyi, M.; Sanchez-Guerra, M.; Trevisi, L.; Urch, B.; et al. B Vitamins Attenuate the Epigenetic Effects of Ambient Fine Particles in a Pilot Human Intervention Trial. *Proc. Natl. Acad. Sci. USA* **2017**, *114*, 3503–3508. [CrossRef] [PubMed]

207. Xu, C.; Zhang, Q.; Huang, G.; Huang, J.; Fu, X.; Liu, M.; Sun, Y.; Zhang, H. Vitamin B Ameliorates PM2.5-Induced Kidney Damage by Reducing Endoplasmic Reticulum Stress and Oxidative Stress in Pregnant Mice and HK-2. *Toxicology* **2023**, *494*, 153568. [CrossRef] [PubMed]
208. Lin, Z.; Chen, R.; Jiang, Y.; Xia, Y.; Niu, Y.; Wang, C.; Liu, C.; Chen, C.; Ge, Y.; Wang, W.; et al. Cardiovascular Benefits of Fish-Oil Supplementation Against Fine Particulate Air Pollution in China. *J. Am. Coll. Cardiol.* **2019**, *73*, 2076–2085. [CrossRef]
209. Tong, H.; Rappold, A.G.; Diaz-Sanchez, D.; Steck, S.E.; Berntsen, J.; Cascio, W.E.; Devlin, R.B.; Samet, J.M. Omega-3 Fatty Acid Supplementation Appears to Attenuate Particulate Air Pollution-Induced Cardiac Effects and Lipid Changes in Healthy Middle-Aged Adults. *Environ. Health Perspect.* **2012**, *120*, 952–957. [CrossRef]
210. Li, J.; Li, H.; Li, H.; Guo, W.; An, Z.; Zeng, X.; Li, W.; Li, H.; Song, J.; Wu, W. Amelioration of PM2.5-Induced Lung Toxicity in Rats by Nutritional Supplementation with Fish Oil and Vitamin E. *Respir. Res.* **2019**, *20*, 76. [CrossRef]
211. Chen, H.; Zhang, S.; Shen, W.; Salazar, C.; Schneider, A.; Wyatt, L.H.; Rappold, A.G.; Diaz-Sanchez, D.; Devlin, R.B.; Samet, J.M.; et al. Omega-3 Fatty Acids Attenuate Cardiovascular Effects of Short-Term Exposure to Ambient Air Pollution. *Part. Fibre Toxicol.* **2022**, *19*, 12. [CrossRef]
212. Dianat, M.; Radmanesh, E.; Badavi, M.; Mard, S.A.; Goudarzi, G. Disturbance Effects of PM_{10} on iNOS and eNOS mRNA Expression Levels and Antioxidant Activity Induced by Ischemia-Reperfusion Injury in Isolated Rat Heart: Protective Role of Vanillic Acid. *Environ. Sci. Pollut. Res. Int.* **2016**, *23*, 5154–5165. [CrossRef]
213. Kwak, J.H.; Kim, H.J. High Air Pollution Exposure, Vitamin D Deficiency and Ever Smokers Were Associated with Higher Prevalence of Hypercholesterolemia: A Cross-Sectional Study from the 2008–2014 Korea National Health and Nutrition Examination Survey. *Nutr. Res.* **2025**, *134*, 1–12. [CrossRef]
214. Lu, M.; Zhan, Z.; Li, D.; Chen, H.; Li, A.; Hu, J.; Huang, Z.; Yi, B. Protective Role of Vitamin D Receptor against Mitochondrial Calcium Overload from PM2.5-Induced Injury in Renal Tubular Cells. *Redox Biol.* **2025**, *80*, 103518. [CrossRef]
215. Lim, C.C.; Hayes, R.B.; Ahn, J.; Shao, Y.; Silverman, D.T.; Jones, R.R.; Thurston, G.D. Mediterranean Diet and the Association Between Air Pollution and Cardiovascular Disease Mortality Risk. *Circulation* **2019**, *139*, 1766–1775. [CrossRef]
216. Barchitta, M.; Maugeri, A.; Quattrocchi, A.; Barone, G.; Mazzoleni, P.; Catalfo, A.; De Guidi, G.; Iemmolo, M.G.; Crimi, N.; Agodi, A. Mediterranean Diet and Particulate Matter Exposure Are Associated with LINE-1 Methylation: Results From a Cross-Sectional Study in Women. *Front. Genet.* **2018**, *9*, 514. [CrossRef] [PubMed]
217. Khandayataray, P.; Murthy, M.K. Dietary Interventions in Mitigating the Impact of Environmental Pollutants on Alzheimer's Disease—A Review. *Neuroscience* **2024**, *563*, 148–166. [CrossRef] [PubMed]
218. Rocha-Velasco, O.A.; Morales-Suárez-Varela, M.; Llopis-González, A. Dietary Flavonoids: Mitigating Air Pollution's Cardiovascular Risks. *Nutrients* **2024**, *16*, 2647. [CrossRef] [PubMed]
219. Wang, N.; Ma, Y.; Liu, Z.; Liu, L.; Yang, K.; Wei, Y.; Liu, Y.; Chen, X.; Sun, X.; Wen, D. Hydroxytyrosol Prevents PM2.5-Induced Adiposity and Insulin Resistance by Restraining Oxidative Stress Related NF-κB Pathway and Modulation of Gut Microbiota in a Murine Model. *Free Radic. Biol. Med.* **2019**, *141*, 393–407. [CrossRef]
220. Ho, C.-C.; Chen, Y.-C.; Tsai, M.-H.; Tsai, H.-T.; Weng, C.-Y.; Yet, S.-F.; Lin, P. Ambient Particulate Matter Induces Vascular Smooth Muscle Cell Phenotypic Changes via NOX1/ROS/NF-κB Dependent and Independent Pathways: Protective Effects of Polyphenols. *Antioxidants* **2021**, *10*, 782. [CrossRef]
221. Chiang, M.-C.; Nicol, C.J.B.; Yang, Y.-P.; Chiang, T.; Yen, C. Protective Effects of Resveratrol against PM2.5-Induced Damage in hNSCs and Its Mitigation of PM2.5-Induced Mitochondrial Dysfunction in a 3D Scaffold System. *Neuroscience* **2025**, *569*, 67–84. [CrossRef]
222. Shin, J.-W.; Lee, H.-S.; Na, J.-I.; Huh, C.-H.; Park, K.-C.; Choi, H.-R. Resveratrol Inhibits Particulate Matter-Induced Inflammatory Responses in Human Keratinocytes. *Int. J. Mol. Sci.* **2020**, *21*, 3446. [CrossRef]
223. Li, Y.; Qian, W.; Wang, D.; Meng, Y.; Wang, X.; Chen, Y.; Li, X.; Xie, C.; Zhong, C.; Fu, S. Resveratrol Relieves Particulate Matter (Mean Diameter < 2.5 Mm)-Induced Oxidative Injury of Lung Cells through Attenuation of Autophagy Deregulation. *J. Appl. Toxicol.* **2018**, *38*, 1251–1261. [CrossRef]
224. Gupta, N.; Abd El-Gawaad, N.S.; Osman Abdallah, S.A.; Al-Dossari, M. Possible Modulating Functions of Probiotic Lactiplantibacillus Plantarum in Particulate Matter-Associated Pulmonary Inflammation. *Front. Cell. Infect. Microbiol.* **2023**, *13*, 1290914. [CrossRef]
225. Wu, Y.; Pei, C.; Wang, X.; Wang, Y.; Huang, D.; Shi, S.; Shen, Z.; Li, S.; He, Y.; Wang, Z.; et al. Probiotics Ameliorates Pulmonary Inflammation via Modulating Gut Microbiota and Rectifying Th17/Treg Imbalance in a Rat Model of PM2.5 Induced Lung Injury. *Ecotoxicol. Environ. Saf.* **2022**, *244*, 114060. [CrossRef]
226. Zhang, H.; Feng, Y.; Yang, H.; Li, Y.; Ma, Z.; Li, L.; Chen, L.; Zhao, Y.; Shan, L.; Xia, Y. The Interaction between Genetic Predicted Gut Microbiome Abundance and Particulate Matter on the Risk of Incident Asthma in Adults. *Ecotoxicol. Environ. Saf.* **2025**, *291*, 117848. [CrossRef] [PubMed]

227. Wang, J.; Zhang, H.; Yuan, H.; Chen, S.; Yu, Y.; Zhang, X.; Gao, Z.; Du, H.; Li, W.; Wang, Y.; et al. Prophylactic Supplementation with Lactobacillus Reuteri or Its Metabolite GABA Protects Against Acute Ischemic Cardiac Injury. *Adv. Sci.* **2024**, *11*, e2307233. [CrossRef] [PubMed]
228. Borshchev, Y.Y.; Sonin, D.L.; Burovenko, I.Y.; Borshchev, V.Y.; Cheburkin, Y.V.; Borshcheva, O.V.; Galagudza, M.M. The Effect of Probiotic Strains on Myocardial Infarction Size, Biochemical and Immunological Parameters in Rats with Systemic Inflammatory Response Syndrome and Polymorbidity. *J. Evol. Biochem. Physiol.* **2022**, *58*, 2058–2069. [CrossRef] [PubMed]
229. Sadeghzadeh, J.; Vakili, A.; Sameni, H.R.; Shadnoush, M.; Bandegi, A.-R.; Zahedi Khorasani, M. The Effect of Oral Consumption of Probiotics in Prevention of Heart Injury in a Rat Myocardial Infarction Model: A Histopathological, Hemodynamic and Biochemical Evaluation. *Iran. Biomed. J.* **2017**, *21*, 174–181. [CrossRef]
230. Zhong, X.; Zhao, Y.; Huang, L.; Liu, J.; Wang, K.; Gao, X.; Zhao, X.; Wang, X. Remodeling of the Gut Microbiome by Lactobacillus Johnsonii Alleviates the Development of Acute Myocardial Infarction. *Front. Microbiol.* **2023**, *14*, 1140498. [CrossRef]
231. Gan, X.T.; Ettinger, G.; Huang, C.X.; Burton, J.P.; Haist, J.V.; Rajapurohitam, V.; Sidaway, J.E.; Martin, G.; Gloor, G.B.; Swann, J.R.; et al. Probiotic Administration Attenuates Myocardial Hypertrophy and Heart Failure after Myocardial Infarction in the Rat. *Circ. Heart Fail.* **2014**, *7*, 491–499. [CrossRef]
232. Lam, V.; Su, J.; Koprowski, S.; Hsu, A.; Tweddell, J.S.; Rafiee, P.; Gross, G.J.; Salzman, N.H.; Baker, J.E. Intestinal Microbiota Determine Severity of Myocardial Infarction in Rats. *FASEB J.* **2012**, *26*, 1727–1735. [CrossRef]
233. Pekkanen, J.; Peters, A.; Hoek, G.; Tiittanen, P.; Brunekreef, B.; de Hartog, J.; Heinrich, J.; Ibald-Mulli, A.; Kreyling, W.G.; Lanki, T.; et al. Particulate Air Pollution and Risk of ST-Segment Depression during Repeated Submaximal Exercise Tests among Subjects with Coronary Heart Disease: The Exposure and Risk Assessment for Fine and Ultrafine Particles in Ambient Air (ULTRA) Study. *Circulation* **2002**, *106*, 933–938. [CrossRef]
234. Rhoden, C.R.; Wellenius, G.A.; Ghelfi, E.; Lawrence, J.; González-Flecha, B. PM-Induced Cardiac Oxidative Stress and Dysfunction Are Mediated by Autonomic Stimulation. *Biochim. Biophys. Acta* **2005**, *1725*, 305–313. [CrossRef]
235. Robertson, S.; Thomson, A.L.; Carter, R.; Stott, H.R.; Shaw, C.A.; Hadoke, P.W.F.; Newby, D.E.; Miller, M.R.; Gray, G.A. Pulmonary Diesel Particulate Increases Susceptibility to Myocardial Ischemia/Reperfusion Injury via Activation of Sensory TRPV1 and B1 Adrenoreceptors. *Part. Fibre Toxicol.* **2014**, *11*, 12. [CrossRef]
236. Chiarella, S.E.; Soberanes, S.; Urich, D.; Morales-Nebreda, L.; Nigdelioglu, R.; Green, D.; Young, J.B.; Gonzalez, A.; Rosario, C.; Misharin, A.V.; et al. B_2-Adrenergic Agonists Augment Air Pollution-Induced IL-6 Release and Thrombosis. *J. Clin. Investig.* **2014**, *124*, 2935–2946. [CrossRef] [PubMed]
237. Bai, L.; Kwong, J.C.; Kaufman, J.S.; Benmarhnia, T.; Chen, C.; van Donkelaar, A.; Martin, R.V.; Kim, J.; Lu, H.; Burnett, R.T.; et al. Effect Modification by Statin Use Status on the Association between Fine Particulate Matter (PM2.5) and Cardiovascular Mortality. *Int. J. Epidemiol.* **2024**, *53*, dyae084. [CrossRef] [PubMed]
238. Schwartz, J.; Park, S.K.; O'Neill, M.S.; Vokonas, P.S.; Sparrow, D.; Weiss, S.; Kelsey, K. Glutathione-S-Transferase M1, Obesity, Statins, and Autonomic Effects of Particles: Gene-by-Drug-by-Environment Interaction. *Am. J. Respir. Crit. Care Med.* **2005**, *172*, 1529–1533. [CrossRef] [PubMed]
239. Yao, H.; Zhao, X.; Wang, L.; Ren, Y. Atorvastatin Ameliorated PM2.5-Induced Atherosclerosis in Rats. *Arch. Environ. Occup. Health* **2023**, *78*, 267–272. [CrossRef]
240. Yao, H.; Lv, J. Statin Attenuated Myocardial Inflammation Induced by PM2.5 in Rats. *Acta Cardiol. Sin.* **2017**, *33*, 637–645. [CrossRef]
241. Ostro, B.; Malig, B.; Broadwin, R.; Basu, R.; Gold, E.B.; Bromberger, J.T.; Derby, C.; Feinstein, S.; Greendale, G.A.; Jackson, E.A.; et al. Chronic PM2.5 Exposure and Inflammation: Determining Sensitive Subgroups in Mid-Life Women. *Environ. Res.* **2014**, *132*, 168–175. [CrossRef]
242. Alexeeff, S.E.; Coull, B.A.; Gryparis, A.; Suh, H.; Sparrow, D.; Vokonas, P.S.; Schwartz, J. Medium-Term Exposure to Traffic-Related Air Pollution and Markers of Inflammation and Endothelial Function. *Environ. Health Perspect.* **2011**, *119*, 481–486. [CrossRef]
243. Hartiala, J.; Breton, C.V.; Tang, W.H.W.; Lurmann, F.; Hazen, S.L.; Gilliland, F.D.; Allayee, H. Ambient Air Pollution Is Associated with the Severity of Coronary Atherosclerosis and Incident Myocardial Infarction in Patients Undergoing Elective Cardiac Evaluation. *J. Am. Heart Assoc.* **2016**, *5*, e003947. [CrossRef]
244. Kim, K.; Jeong, S.; Choi, S.; Chang, J.; Choi, D.; Lee, G.; Kim, S.R.; Park, S.M. Cardiovascular Benefit of Statin Use Against Air Pollutant Exposure in Older Adults. *Eur. J. Prev. Cardiol.* **2024**, *32*, 288–298. [CrossRef]
245. Ghelfi, E.; Wellenius, G.A.; Lawrence, J.; Millet, E.; Gonzalez-Flecha, B. Cardiac Oxidative Stress and Dysfunction by Fine Concentrated Ambient Particles (CAPs) Are Mediated by Angiotensin-II. *Inhal. Toxicol.* **2010**, *22*, 963–972. [CrossRef]
246. Sharma, K.; Lee, H.-H.; Gong, D.-S.; Park, S.-H.; Yi, E.; Schini-Kerth, V.; Oak, M.-H. Fine Air Pollution Particles Induce Endothelial Senescence via Redox-Sensitive Activation of Local Angiotensin System. *Environ. Pollut.* **2019**, *252*, 317–329. [CrossRef] [PubMed]
247. David, G.L.; Romieu, I.; Sienra-Monge, J.J.; Collins, W.J.; Ramirez-Aguilar, M.; del Rio-Navarro, B.E.; Reyes-Ruiz, N.I.; Morris, R.W.; Marzec, J.M.; London, S.J. Nicotinamide adenine dinucleotide (phosphate) reduced:quinone oxidoreductase and glutathione S-transferase M1 polymorphisms and childhood asthma. *Am. J. Respir. Crit. Care Med.* **2003**, *168*, 1199–1204. [CrossRef] [PubMed]

248. Martin, N.J.; Collier, A.C.; Bowen, L.D.; Pritsos, K.L.; Goodrich, G.G.; Arger, K.; Cutter, G.; Pritsos, C.A. Polymorphisms in the NQO1, GSTT and GSTM genes are associated with coronary heart disease and biomarkers of oxidative stress. *Mutat. Res.* **2009**, *674*, 93–100. [CrossRef] [PubMed]
249. Patel, P.; Aggarwal, S.G. On the techniques and standards of particulate matter sampling. *J. Air Waste Manag. Assoc.* **2022**, *72*, 791–814. [CrossRef]
250. Van Donkelaar, A.; Martin, R.V.; Brauer, M.; Hsu, N.C.; Kahn, R.A.; Levy, R.C.; Lyapustin, A.; Sayer, A.M.; Winker, D.M. Global Estimates of Fine Particulate Matter Using a Combined Geophysical-Statistical Method with Information from Satellites, Models, and Monitors. *Environ. Sci. Technol.* **2016**, *50*, 3762–3772. [CrossRef]

antioxidants

Review

Deciphering the Liaison Between Fine Particulate Matter Pollution, Oxidative Stress, and Prostate Cancer: Where Are We Now?

Chiang-Wen Lee [1,2,3,4,†], Yao-Chang Chiang [2,5,†], Thi Thuy Tien Vo [6], Zih-Chan Lin [2], Miao-Ching Chi [1,2,4,7], Mei-Ling Fang [8,9], Kuo-Ti Peng [3,10], Ming-Horng Tsai [10,11,*] and I-Ta Lee [12,*]

1 Department of Respiratory Care, Chang Gung University of Science and Technology, Chiayi 613, Taiwan; cwlee@gw.cgust.edu.tw (C.-W.L.); mcchi@mail.cgust.edu.tw (M.-C.C.)
2 Chronic Diseases and Health Promotion Research Center, Chang Gung University of Science and Technology, Chiayi 613, Taiwan; ycchiang01@mail.cgust.edu.tw (Y.-C.C.); zclin@mail.cgust.edu.tw (Z.-C.L.)
3 Department of Orthopedic Surgery, Chang Gung Memorial Hospital, Chiayi 613, Taiwan; mr3497@cgmh.org.tw
4 Department of Safety Health and Environmental Engineering, Ming Chi University of Technology, New Taipei City 243, Taiwan
5 Department of Nursing, Division of Basic Medical Sciences, Chang Gung University of Science and Technology, Chiayi 613, Taiwan
6 Faculty of Dentistry, Nguyen Tat Thanh University, Ho Chi Minh 70000, Vietnam; vtttien@ntt.edu.vn
7 Division of Pulmonary and Critical Care Medicine, Chiayi Chang Gung Memorial Hospital, Chiayi 613, Taiwan
8 Center for Environmental Toxin and Emerging-Contaminant Research, Cheng Shiu University, Kaohsiung 833, Taiwan; k6764@gcloud.csu.edu.tw
9 Super Micro Research and Technology Center, Cheng Shiu University, Kaohsiung 833, Taiwan
10 College of Medicine, Chang Gung University, Taoyuan 333, Taiwan
11 Division of Neonatology and Pediatric Hematology/Oncology, Department of Pediatrics, Chang Gung Memorial Hospital, Yunlin 638, Taiwan
12 School of Dentistry, College of Oral Medicine, Taipei Medical University, Taipei 110, Taiwan
* Correspondence: ming5448@cgmh.org.tw (M.-H.T.); itlee0128@tmu.edu.tw (I.-T.L.); Tel.: +886-5-691-5151 (ext. 2878) (M.-H.T.); +886-2-27361661 (ext. 5162) (I.-T.L.); Fax: +886-5-691-3222 (M.-H.T.); +886-2-27362295 (I.-T.L.)
† These authors contributed equally to this work.

Abstract: Prostate cancer (PCa), a highly prevalent cancer in men worldwide, is projected to rise in the coming years. As emerging data indicate the carcinogenic effects of fine particulate matter (PM2.5) in lung cancer and other site-specific cancers, there is an urgent need to evaluate the relationship between this environmental risk factor and PCa as a potential target for intervention. The present review provides up-to-date evidence about the impact of airborne PM2.5 pollution on the initiation and progression of PCa. Examining the composition and characteristics of PM2.5 reveals its ability to induce toxic effects, inflammatory injuries, and oxidative damages. Additionally, PM2.5 can attach to endocrine-disrupting chemicals implicated in prostatic carcinogenesis. Considering the potential significance of oxidative stress in the risk of the disease, our review underlines the protective strategies, such as antioxidant-based approaches, for individuals exposed to increased PM2.5 levels. Moreover, the findings call for further research to understand the associations and mechanisms linking PM2.5 exposure to PCa risk as well as to suggest appropriate measures by policymakers, scientific researchers, and healthcare professionals in order to address this global health issue.

Keywords: endocrine disruptors; fine particulate matter; oxidative stress; prostate cancer; reactive oxygen species

1. Introduction

Prostate cancer (PCa) ranks second by incidence only to lung cancer among men worldwide, leading to significant morbidity and mortality [1]. By 2024, the number of new cases is estimated to double to 2.9 million, whereas the number of deaths is projected to increase by 85% to nearly 700,000 [2]. The development of PCa is linked to complex interactions between inherited germline susceptibility, acquired somatic changes, and environmental variables [3]. The well-established risk factors for the disease include age, ethnicity, and family history, none of which are modifiable [4]. The findings underscore the necessity for further research to better understand the drivers for the upcoming surge in PCa cases and deaths.

Considering the unprecedented urbanization and industrialization globally, air pollution has emerged as one of the greatest scourges in our era. Air pollution, defined as the introduction into the atmosphere of harmful solids, liquids, or gases produced in higher-than-usual concentrations, is linked to many serious health problems, particularly respiratory, cardiovascular, and neurological diseases, cancers, and premature deaths [5,6]. The World Health Organization (WHO) reports that air pollutants of major public health concern include particulate matter (PM), carbon monoxide, ozone, nitrogen dioxide, and sulfur dioxide [7]. PM, a complex mixture of particles with diverse physical and chemical characteristics, is categorized by aerodynamic diameter into coarse (PM10), fine (PM2.5), submicron (PM1) and ultrafine (PM0.1) fractions [8]. A recent review suggests that chronic exposure to PM can compromise every organ in the body, exacerbating existing conditions through toxic, inflammatory, and oxidative mechanisms [9]. In 2013, the specialized cancer agency of the WHO, called the International Agency for Research on Cancer (IARC), classified PM as carcinogenic to humans [10]. Due to the particulate size, PM can easily penetrate deep into the respiratory system and enter the bloodstream, inducing DNA damage, disrupting cellular processes, and promoting the acquisition of biological capabilities required for carcinogenesis at different sites [9]. PM can induce reactive oxygen species (ROS) overproduction that surpasses antioxidant capacity to cause oxidative stress, leading to the damage of mitochondria, endoplasmic reticulum, and DNA; inflammation; the activation of cell death pathways; and even the evasion of immune responses [11–13]. As not all PMs are equally toxic, the pathophysiological mechanisms vary between PM species [14]. Given its significant association with a wide range of health issues that led the WHO to designate PM2.5 as a key air particle pollution indicator in 2006, the focus in recent decades has been on this fraction [15]. The WHO estimated that in 2019, up to 99% of the global population was exposed to air pollution levels exceeding its guidelines. This resulted in 4.2 million premature deaths annually worldwide, primarily due to respiratory, cardiovascular, and cancer-related diseases caused by PM2.5 [16]. Recently, the Global Burden of Diseases, Injuries, and Risk Factors Study (GBD) 2021, which provided comprehensive estimates of exposure levels, relative health risks, and the attributable burden of disease for 88 risk factors in 204 countries and territories and 811 subnational locations from 1990 to 2021, further reported that PM air pollution was the leading cause of the global disease burden in 2021, accounting for 80% of total disability-adjusted life years. Ambient PM air pollution also showed the highest increase in the risk-attributable burden among risk factors associated with the leading Level 3 risks [17]. In order to better measure and manage the health risks related to particulate air pollution exposure, PM2.5 air pollution should be investigated as a complex source-driven mixture. Major sources of PM2.5 include vehicle emissions, industrial manufacturing, fuel oil combustion, and biomass burning. PM2.5 constituents mainly consist of black carbon; polycyclic aromatic hydrocarbons (PAHs); heavy metals; and other organic, inorganic, and biological species [18]. It has been found that varying sources and compositions are crucial factors determining particle behavior in the human body. An observational and modelling study, for example, estimated that among the 8.34 million excess deaths per year worldwide due to PM2.5 and ozone air pollution, 5.13 million (61%) were linked to emissions related to fossil fuels [19]. It is well documented that ambient particles from burning fossil fuels have a higher content of harmful metals per unit mass

than those from other sources, such as crustal-derived windblown soil [20]. Consistently, a recent review concluded that fossil fuel combustion PM2.5 may have greater potential to cause negative health impacts than other ambient particles [21]. This might be due to the fact that transition metals, such as As, Co, Pb, V, Ni, and Zn, are known to be highly capable of participating in redox processes that result in oxidative stress, contributing to metal toxicity [22]. Moreover, fossil fuel combustion PM2.5 contains varying amounts of sulfur, and the acidic nature of the resulting sulfur compounds can further enhance the bioavailability of constituent transition metals. This pronouncedly raises the capacity of particles to induce oxidative stress and systemic health effects [21]. Aside from heavy metals, the carcinogenic effects of PM2.5 also include the adherence of various organic components such as PAHs, PAH-quinones, and bacterial endotoxins [23]. Despite being reported to be between 20% and 30% on average, the concentrations of organic chemicals may reach as high as 90%. The carcinogenicity of PAHs is mainly attributable to their metabolism and genotoxicity through the formation of reactive electrophilic metabolites to cause DNA adducts, resulting in mutations in both oncogenes and tumor suppressor genes [24]. Therefore, elucidating the impact of ambient PM2.5 pollution may give a deeper understanding of detrimental sources and harmful components as well as provide tools for developing more efficient measures to reduce environmental exposure to PM2.5 pollution, which can help to mitigate health adversity, particularly for individuals at higher risk.

While there is robust evidence linking PM2.5 exposure to lung cancer, it has failed to provide a conclusive association for other cancer sites [25]. The possibility that PM2.5 increases the risk of PCa was proposed with findings of the impact of air pollution on urological diseases [26–29]. Since PM2.5 is an essential part of air pollutants, the hypothesis that airborne carcinogenesis is involved in PCa development would make sense. In fact, a retrospective population-based study conducted in China from 1982 to 2010 demonstrated significantly positive correlations between industrial waste gas emissions, including PM2.5, and incidence rates of various cancers, among which was PCa ($r_s = 0.980$, $p < 0.001$). However, this research investigated the overall impact of industrial waste gas emissions as a whole mixture rather than a specific pollutant, and PCa was not the cancer of a priori interest [30]. As more epidemiological studies on the association between PM2.5 and PCa have been documented in the past years, it is crucial to recapitulate the evidence. Although the mechanisms are yet to be fully understood, several studies have proposed potential pathways for related cancers. The large surface area and small size of PM2.5 enable the particles to bind to toxic substances and to translocate into the circulatory system, compromising various tissues in the body [14]. It is known that PM2.5 can induce inflammatory responses and produce excess ROS, establishing a synergistical mechanism through which the particles trigger biologically negative effects at the exposed sites [31]. Moreover, PM2.5 can carry endocrine-disrupting chemicals associated with the development of hormone-sensitive cancers [32], such as testicular cancer [33]. The management of PCa continues to evolve rapidly due to substantial progress in understanding the underlying mechanisms. Integration of the knowledge gained so far about PCa carcinogenesis with those pertaining to redox states in the prostatic pathophysiology is demanded [34,35]. Therefore, this review aims to provide up-to-date evidence on the PCa risk that PM2.5 pollution may pose with a focus on epidemiological studies. In addition, our work seeks to elucidate possible mechanisms that may lead from the inhalation of PM2.5 to adverse outcomes, emphasizing the oxidative paradigm. The paper also highlights research gaps that exist in the field and potential directions that research might take in the future.

2. PM2.5 Exposure and Prostate Cancer: The Current Epidemiological Evidence

A growing body of epidemiological studies has proven a role for PM2.5 exposure in the initiation and progression of PCa. An association between airborne particulate pollution and PCa was first observed in the United States in 1969, where higher levels of suspended particulate pollution were linked to the increased mortality rates of the disease in older white males [36]. However, this ecological study was unable to control for individual-level

risk factors. Moreover, the use of mortality follow-ups may be insufficient to estimate the impact of air pollution on the burden of cancer due to the problem of latency and the possible confounding from mortality of other causes [37]. Therefore, further evidence using cancer incidence rather than mortality has contributed to exploring the health effects associated with PM2.5 exposure. Over the past decade, the relationship between PM2.5 pollution and PCa risk has grown. A large Canadian population-based case-control study (1420 cases and 1424 controls) found a substantial correlation between exposure to ambient PM2.5 over a 20-year period and incident PCa. An interquartile range (IQR) increase in PM2.5 resulted in a 20% to 28% relative increase in PCa risk [38]. Considering a percentage of PCa latent cases, a positive association may indicate higher detection rates as a result of an increased prevalence of PCa screening. In other words, there might be two causes for the positive relationship between PM2.5 exposure and cancer incidence. One is that PM2.5 raises the risk of the disease, and another is that more cancer screening measures do. Consistently, a Chinese study using the time series data of annual incidence and mortality of the ten most common cancers as well as mean PM2.5 concentrations over a 10-year period concluded that PCa was one of the cancers significantly associated with PM2.5 exposure in terms of both incidence and mortality. An analysis of spatiotemporal series data further demonstrated that with every 10 $\mu g/m^3$ increment of annual mean PM2.5 concentrations, the relative risk (RR) of PCa incidence increased by 17% in urban areas but showed no substantial change in rural areas [39].

In order to obtain a more precise exposure–response relationship between PM2.5 and PCa, large-scale prospective cohort studies are required. A nationwide longitudinal cohort study among 87,608 South Korean participants suggested that every 10 $\mu g/m^3$ increase in individual-level PM2.5 concentrations over the previous five years may promote the mortality risk of PCa (hazard ratio (HR) = 1.80, 95% confidence interval (CI): 0.21–15.76) [40]. Similarly, a recent cohort study conducted in the United States also indicated that long-term exposure to PM2.5 increased the risk of PCa within a 10-year period leading up to diagnosis, even at low exposure levels. Importantly, a single-unit decrease in long-term PM2.5 may potentially prevent at least 460 cases per year in the cohort [41].

Recent short- and long-term studies on the relationship between PM2.5 and PCa are summarized in Table 1, the majority of which supports a significantly positive association. While PM2.5 has been the subject of most research, ultrafine particles have not received as much attention. A Canadian population-based case-control study between 2005 and 2009 showed that ambient PM0.1 concentrations were associated with an elevated risk of PCa (odds ratio (OR) = 1.10, 95% CI: 1.01–1.19) [42]. Nonetheless, no long-term studies investigating PM0.1 and PCa can be found to date.

Table 1. Summary of recent epidemiological research on the association between PM2.5 and PCa.

Study				PM2.5 Exposure ($\mu g/m^3$)			Results		Ref
Authors (Year)	Location	Design	Time Period	Number of Participants	Average (S.D)	Range	Outcome	Results	
Felici et al. (2024)	UK	Case-control	2006–2010	Cases: 12,838 Controls: 141,596	N/A	N/A	Incidence	No significant association: OR = 0.982, 95% CI = 0.962–1.002, $p = 0.072$ per 1 $\mu g/m^3$ increase	[43]
Kayyal-Tarabeia et al. (2024)	N/A	Ecological	2007–2015	30,979	N/A	N/A	Incidence	HR per an IQR increase in PM2.5 (2.11 $\mu g/m^3$): 1.41 (95% CI: 1.31–1.52)	[44]
Thomas et al. (2024)	N/A	Cohort	1994–2017	43,184	N/A	N/A	Incidence	No significant association: HR = 1.02, 95% CI = 0.95–1.08 per every 5 $\mu g/m^3$ increase	[45]
Fan et al. (2023)	China	Ecological	2015–2020	N/A	60.3	40.2–81.6	Mortality	RR for the association with a 1 $\mu g/m^3$ increase in long-term exposure to PM2.5: 1.089 (95% CI: 1.034–1.148)	[46]
Wei et al. (2023)	US	Cohort	2000–2016	2,161,156	9.8	0.0–30.9	Incidence	Absolute increase in the risk of cancer diagnosis per unit increase in PM2.5: 0.0112% (95% CI: 0.0094%–0.0131%)	[41]
Huang et al. (2022)	Taiwan	Cohort	2000–2015	407,415	20.89	N/A	Incidence	HR per every 10 $\mu g/m^3$ increase in the 2-year-average PM2.5 concentration: 0.96 (95% CI: 0.84–1.08)	[47]
Shin et al. (2022)	Korea	Cohort	2007–2015	87,608	N/A	N/A	Mortality	HR per every 10 $\mu g/m^3$ increase in individual-level PM2.5 concentrations for the previous 5 years: 1.80 (95% CI: 0.21–15.76)	[40]
Youogo et al. (2022)	Canada	Case-control	1994–1997	Cases: 1420 Controls: 1424	N/A	N/A	Incidence	An IQR increase in PM2.5 (3.56 $\mu g/m^3$ for satellite and 4.48 $\mu g/m^3$ for scaled satellite observations) yielded ORs of 1.28 (95% CI: 1.07–1.52) and 1.20 (95% CI: 1.03–1.40), respectively	[38]
Yu et al. (2022)	Brazil	Ecological	2010–2018	127,449	7.63	3.37–21.02	Mortality	RR for the association with a 10 $\mu g/m^3$ increase in 3-year-average PM2.5: 1.18 (95% CI: 1.05–1.32)	[48]
Yu et al. (2022)	Brazil	Ecological	2010–2016	96,501	2.38	0.60–12.49	Mortality	RR for the association with a 1 $\mu g/m^3$ increase in 2-year-average wildfire-related PM2.5: 1.03 (95% CI: 1.01–1.06)	[49]
Coleman et al. (2020)	US	Cohort	1987–2014	635,539	N/A	N/A	Mortality	HR per every 10 $\mu g/m^3$ increase in PM2.5: 0.91 (95% CI: 0.68–1.22)	[50]
Coleman et al. (2020)	US	Ecological	1992–2016	1,151,454	11.50	N/A	Incidence	Incidence rate ratio for the association with a 10 $\mu g/m^3$ increase in PM2.5: 0.96 (95% CI: 0.87–1.06)	[37]
Wang et al. (2019)	China	Ecological	2006–2009	136	N/A	N/A	Incidence Mortality	RR of PCa incidence in urban area increased by 17% with a 10 $\mu g/m^3$ increase in annual mean PM2.5 concentration	[39]
Turner et al. (2017)	US	Cohort	1982–2004	623,048	12.6	1.4–27.9	Mortality	HR per every 4.4 $\mu g/m^3$ increase in PM2.5: 0.96 (95% CI: 0.86–1.06)	[51]

CI: confidence interval; HR: hazard ratio; IQR: interquartile range; OR: odds ratio; RR: relative risk; S.D.: standard deviation. N/A: Not Applicable.

3. Fine Particulate Matter, Oxidative Stress, and Prostate Cancer: How Are They Linked?

Since its introduction in 1985 [52], oxidative stress is widely defined as "an imbalance between oxidants and antioxidants in favor of the oxidants, leading to a disruption of redox signaling and control and/or molecular damage". Chemically reactive molecules of low molecular mass, also known as reactive species, have been extensively studied in their role in redox regulation, among which ROS is one of the key players [53]. It is known that excessive ROS production, or a deficient antioxidant defense system, or both can push the cell to undergo oxidative stress, triggering various cellular processes linked to the initiation and progression of many cancers, including PCa [54]. Apart from damaging DNA, proteins, and lipids, oxidative stress can modulate gene expression, induce epigenetic alterations, and even modify posttranslational indicators, resulting in signaling disruption, cellular dysfunction, and malignant predisposition [55]. Although the association between PM2.5 and PCa may imply a causal relationship, the mechanisms through which the particles may contribute to prostatic carcinogenesis have yet to be fully understood. A growing body of evidence has demonstrated the significance of ROS in the development of PCa. Higher levels of intracellular ROS, including superoxide and hydrogen peroxide, were found in human PCa cell lines rather than in prostate epithelial cell lines. In addition, the inhibition of ROS production from the NAPDH oxidase system by using a pharmacological inhibitor dramatically attenuated the cell migration ability, anchorage-independent colony formation, and cell proliferation of PCa cells, suggesting an essential role of ROS in malignant cell behaviors [56]. Consistently, increased levels of hydrogen peroxide and NADPH oxidase 1 expression were observed in human PCa tissue samples [57]. Moreover, oxidative stress has been well recognized as one of the primary mechanisms underlying PM2.5 health effects, including carcinogenicity [11,18]. It is known that PM2.5 can reach the systemic circulation for further translocation to other parts in the body upon inhalation through the airway, resulting in adverse effects at both cellular and molecular levels [14]. Although there is currently no evidence that PM2.5 is directly detected in the male prostate, recent studies have shown that the particles can accumulate in the reproductive organs through the blood–testis barrier, –placental barrier, –epithelial barrier, and other barriers protecting reproductive tissues [58]. Therefore, PM2.5-induced oxidative stress may be a critical paradigm. Figure 1 depicts the possible mechanisms through which the exposure to PM2.5 pollution can increase the risk of PCa, focusing on redox biology, as discussed in more detail below.

It is known that PM2.5 can directly generate ROS, such as hydroxyl radicals, through the redox cycling of environmentally persistent free radicals presenting in the particles [59]. Moreover, PM2.5 contains a variety of carcinogens and toxic components, such as heavy metals and PAHs, which may enable the induction and progression of PCa [60,61]. Toxicological research has investigated the inflammatory and oxidative effects of such substances in the context of prostate health. An animal study found that cadmium (Cd), a trace metal content in PM2.5, can cause reproductive toxicity and induce prostatic deficiency. The mechanisms included the induction of prostatic inflammation, oxidative stress, and an epithelial–mesenchymal transition; activation of the TGF-β1/Smad pathway; a reduction in the Bcl-2/Bax ratio; and inhibition of the Nrf-2/HO-1 pathway [62]. Similarly, chronic cigarette smoke exposure was reported to cause prostate deficits by inducing local inflammation, oxidative stress, and epithelial–mesenchymal transitions [63]. In addition, PAHs are known as redox-active species presenting in PM2.5, which lead to ROS production through the quinone redox cycle [55,64]. An in vitro study using prostate-derived cell lines from localized adenocarcinoma and bone metastasis as well as non-neoplastic prostate epithelium cells reported that PAHs can stimulate cell growth, particularly in localized cancer cells, and can increase VEGF and HIF expression as well as ROS production. In addition, the data demonstrated that toxic concentrations of PAHs were associated with GSH depletion, indicative of oxidative stress [65]. These findings suggest that PAH exposure may contribute to PCa progression, in part due to ROS overproduction. Therefore, cumulative biological changes triggered by long-term exposure to PM2.5 and its active

constituents may contribute to a multistage prostatic carcinogenesis process. Additional studies, however, should be conducted to determine PM2.5 concentrations that reach the carcinogenic effects. Considering currently available measures for evaluating the oxidative potential of particulate air pollution, future studies should also investigate whether particle oxidative potential measurements are more markedly related to cancer risk than traditional mass- or number-based exposure metrics [66].

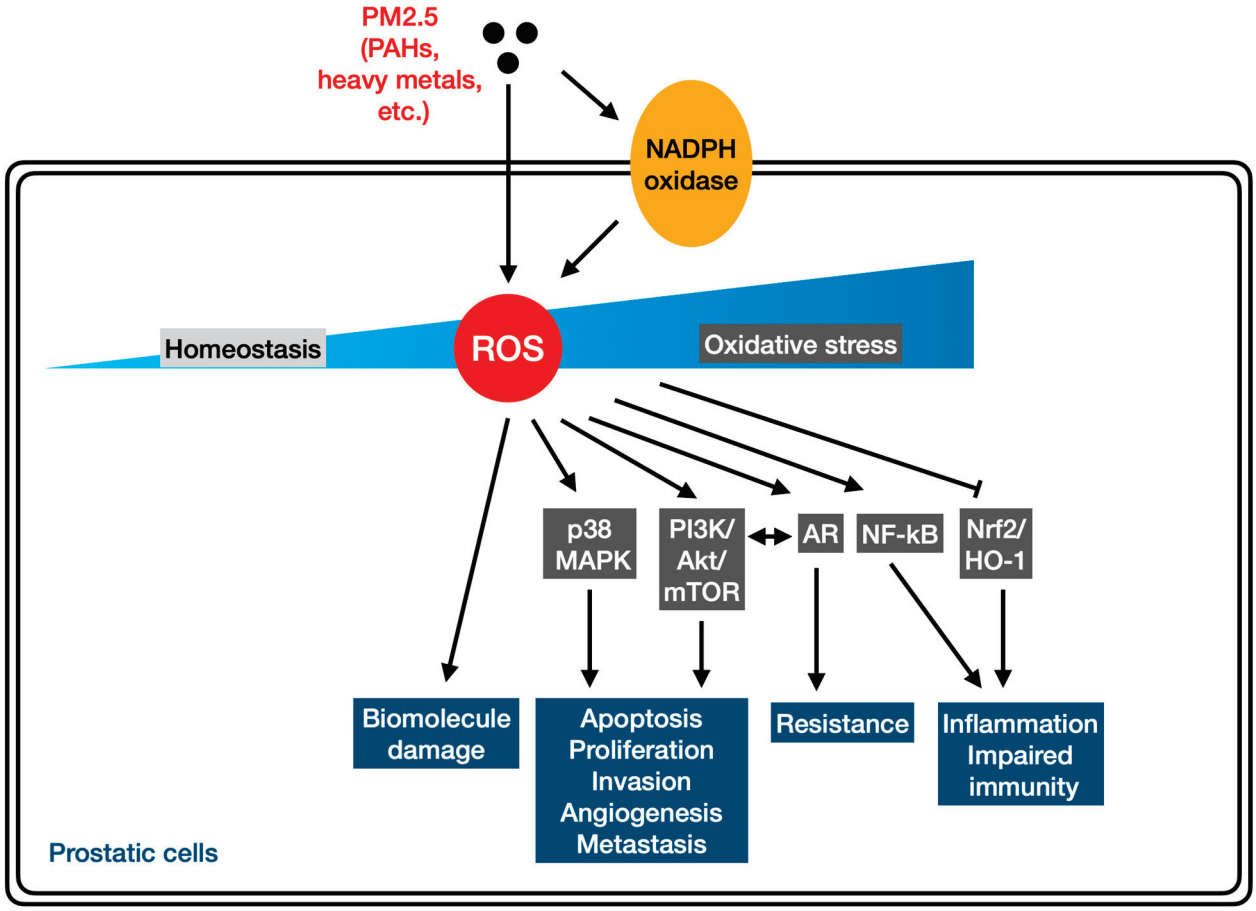

Figure 1. The potential mechanisms through which PM2.5 increases PCa risk with an emphasis on redox biology. PM2.5 can generate ROS both directly and indirectly, which, if not properly counteracted by antioxidant capacity, can lead to oxidative stress. As second messengers, ROS can dysregulate varying redox-sensitive signaling transduction pathways, including the mitogen-activated protein kinases (MAPKs) and phosphoinositide 3-kinase/protein kinase B (PI3K/Akt), that are involved in multistage carcinogenesis. Redox states also play an important role in immunity and T-cell activity, in which ROS levels determine immune responses. ROS overproduction may enhance the release of proinflammatory cytokines orchestrated and regulated by many redox-sensitive transcription factors, such as the NF-κB and Nrf-2. In addition, some genetic alterations during PCa progression may contribute to the activity of the androgen receptor (AR), whose regulation exhibits a reciprocal negative feedback mechanism with PI3K/Akt signaling. Interestingly, PM2.5 may have an endocrine-disrupting potential, presenting another exposure source to endocrine disruptors implicated in prostatic carcinogenesis.

Since ROS act as second messengers in various signal transduction pathways, exposure to PM2.5 can dysregulate multiple redox-sensitive signaling pathways associated with carcinogenesis, among which the mitogen-activated protein kinases (MAPKs) and phosphoinositide 3-kinase/protein kinase B pathways stand out [11]. The MAPK pathway, consisting of ERK1/2, JNK, and p38 MAPK, plays a role in cell proliferation, differentiation, and apoptosis. Several studies have shown a potential connection between p38 MAPK

and PCa [67,68]. In addition, the PI3K/AKT/mammalian target of the rapamycin (mTOR) pathway is considered a pivotal intracellular signaling pathway, whose hyperactivity is also linked to carcinogenesis. The de-regulation of the PI3K/AKT/mTOR pathway was found in 42% of localized and 100% of advanced PCa cases, suggesting that any factor that may disrupt this pathway is predictive of disease progression [69].

Recently, the alarming health impacts induced by endocrine disruptors (EDs) have drawn attention from all around the world. Although ingestion is known as the primary exposure route, inhalation has been proposed as an important route [70]. A recent systematic review about the in vitro endocrine activity of ambient PM has reported that the particles can induce estrogenic, antiestrogenic, androgenic, and antiandrogenic effects. The findings suggest that PM may have an endocrine-disrupting potential, posing an additional exposure source to EDs [71]. Although it is difficult to estimate the amount that inhalation can contribute to the total burden of EDs, the endocrine activity of PM may worsen health issues. Bioassay-based assessments may be a useful tool to measure the health risk caused by airborne EDs. In fact, PAHs can promote the growth of the breast cancer cell line MCF-7, which is mediated by the estrogen receptor [72]. Such receptors may also be expressed in benign and malignant prostate epithelial cells [73]. Furthermore, PAHs may function as agonists to interact with the androgen receptor (AR) [74]. It is well recognized that the majority of PCa cases are dependent on androgen stimulation mediated by AR for cell growth and survival. Additionally, androgens may enhance ROS levels [75]. Interestingly, AR and PI3K/Akt signaling regulation show a reciprocal negative feedback mechanism, in which the inhibition of one inactivates the other, resulting in cancer cell survival and progression [76]. Thus, bypassing the AR pathway associated with androgen independence may be employed as an alternative for PCa survival [77]. However, other genetic alterations during PCa progression may contribute to AR activity, which accounts for high androgen-receptor sensitivity in response to androgens, antiandrogens, or nonandrogenic hormones, providing a selective growth advantage to PCa cells [78].

There is increasing evidence indicating that PM2.5 exposure can impair the immune system, contributing to the development of cancers [79]. Although PCa is not classified as an immunologically responsive tumor, the interaction between prostatic epithelial cells with both immune and non-immune cells that make up the tumor microenvironment (TME) still plays an important role in the disease progression and overall resistance to treatment [80]. The mechanisms through which PCa cells can evade the immune system, maintain the "cold" TME, and mediate immunosuppressions are yet to be elucidated. So far, the literature has reported that redox states have important roles in immunity and T-cell activity, whereby the ROS levels may determine immune responses [81,82]. A mild increase in ROS levels in the immune system may facilitate normal immune function, whereas moderate ROS levels can act as the biochemical mediators in immunity involved in multiple cellular functions and signaling pathways. In contrast, high ROS levels may result in a rise in the release of proinflammatory cytokines orchestrated and regulated by various redox-sensitive signaling pathways [83,84]. The NF-κB family of transcription factors that plays a role in inflammation and immunity can be regulated by ROS [85]. It has been reported that PCa cells may exhibit constitutive NF-κB activity due to the increased activity of the IκB kinase complex, which is inversely associated with AR activity [86,87]. In addition, the function of immune cells is regulated under redox control through the activity of Nrf-2 and cellular antioxidants [88,89]. An in vivo study demonstrated that the progression of prostate tumors was associated with methylation silencing of the Nrf2 promoter as well as decreased transcription of Nrf2 and Nrf2 target genes [90]. The incentive for gaining a better understanding of the TME and immune resistance mechanisms is necessary to further explore the adverse effects of PM2.5-induced oxidative stress.

4. Practical Implications: Mitigation of PM2.5 Oxidative Effects on Prostate Cancer

The fact that oxidative stress is higher in PCa patients than healthy men suggests that antioxidants may play a crucial role in preventing disease progression [91,92]. Antioxidants

are substances able to counteract the free radical generation and oxidation process, which can be classified by their source into endogenous sources, such as enzymes, and exogenous sources, such as beta-carotene; lycopene; and vitamins A, C, and E (tocopherols) [93]. An in vitro study indicated that ROS production rather than accumulation affected PCa phenotypic behavior, implying that antioxidant-based approaches may not be beneficial, since antioxidants can only neutralize the accumulated ROS within the cells [56]. A number of observational studies have examined the effects of dietary antioxidants on the initiation and progression of PCa [94–99]. Some clinical trials concluded that supplemental dietary antioxidants had no substantial impact on the overall risk for PCa [96–98], whereas smokers who took 50 mg of vitamin E daily had a statistically significant 32% lower PCa incidence and 41% lower PCa mortality than those who received a placebo [95]. A recent review reports that most studies have focused on carotenoids, particularly beta-carotene and lycopene, vitamins E and C, phenolic dietary sources such as coffee and tea, and flavonoids. Overall, many of these studies were elusive and equivocal about the actual benefits, since different antioxidants show varying effects on PCa risk [100]. Interestingly, consuming a diet rich in fish, legumes, fresh fruits, and vegetables, along with vitamin D3 supplements, is recommended in areas with high air pollution levels [101]. Although existing data do not provide sufficient support for a population-wide implementation of antioxidant supplementation against PCa, intervention approaches aimed at reducing ROS production still might offer an effective strategy for the prevention of PCa from PM2.5 exposure. Therefore, subjects exposed to high concentrations of ambient PM2.5 should consider mitigating oxidative stress by increasing antioxidant intake through their diet and/or supplements. Antioxidant administration via inhalation is being studied as a promising strategy to protect against oxidative damage caused by air pollution [102].

Androgen deprivation therapy (ADT), which involves either surgical or pharmacological castration to reduce the production and/or action of androgens, remains the first-line treatment for metastatic PCa. While the AR signaling axis is considered to be primarily responsible for castration-resistant PCa, another avenue of research has focused on oxidative stress [103]. A recent study shows that castration can result in dramatic increases in the activity of ROS-generating NADPH oxidases [104]. As increased NADPH oxidase-driven ROS generation can lead to the generation of a malignant phenotype in PCa by modulating various signaling cascades [105], this emerging candidate may prove to be an effective target for therapeutic intervention.

On a broader scale, initiatives to avoid increased exposure to PM2.5 may include enacting and enforcing air pollution regulations, switching to renewable energy sources and encouraging public transit. The utility of cancer screening programs and routine examinations should not be overlooked for individuals residing in areas with high concentrations of ambient PM2.5. Moreover, in our rapidly urbanizing world, green space has shown potentially beneficial effects on human health through a reduction in noise, heat, and air pollution; motivation for physical activity; and improvements in psychophysiological health [106]. A large Taiwanese population-based cohort study on the association between greenness and cancer incidence demonstrated the protective effect of greenness against incident PCa [47]. In line with these findings, a previous Canadian population-based case-control study also suggested that men living in greener areas had a lower risk of PCa [107]. Although the exact impact of green space on PCa remains vague, it is thought that the burden of genetic and epigenetic responses leading to carcinogenesis can be attenuated as less inhaled toxicants reach the tissues.

5. Challenges and Future Research

Although current epidemiological studies have provided evidence on the potential relationship between PM2.5 exposure and the PCa course, several gaps and directions for future research exist. Addressing these challenges would help to gain a deeper understanding of the PCa risk associated with PM2.5 pollution and to develop effective strategies to protect prostate health.

First, it is difficult to demonstrate causality between the exposure to PM2.5 and the development of PCa because of the long latency. Moreover, most of the epidemiological evidence to support this association derives from observational studies, in which the results might be biased by many confounding factors. There were probably measurement errors across studies due to the lack of personal-level exposure information. Compared to ecological and case-control studies, longitudinal cohorts would yield the most reliable findings due to the prospective collection of individual-level data. The existing proofs also did not consider the location of participants (outdoors, at home, or at work) and their movement/migration throughout the study period. As previously stated, varying PM2.5 sources and components are significant determinants for the particle impact on our health. To pave the way for a better understanding of the relationship between PM2.5 exposure and PCa risk, further research that captures individual-level exposure, long-term follow-up, different groups of susceptible populations, varying source-specific PM2.5 effects, and covariate variables is warranted. This may provide tools for developing more effective ways to attenuate the health effects related to PM2.5 exposure in humans, particularly for those who are more vulnerable.

Second, the discrepancy in the magnitude of PM2.5 effects can be due to varying exposure ranges. Nearly half of the studies included in the present review were conducted in regions with relatively low PM2.5 levels, including Europe and North America. Additional studies should be prioritized in developing countries, such as Asian and South American countries, where PM2.5 concentrations are higher.

Third, the global prevalence of PCa differs among various geographical regions and ethnic groups. Although black men have the highest incidence rates of PCa in the world [1,2], little is known about the impact of PM2.5 pollution on PCa risk in African nations. More studies should consider the genetic background, socioeconomic status, and climate to determine possible responses leading to geographical and racial changes in PCa rates associated with PM2.5 exposure.

Last but not least, the single-pollutant model might not be able to reveal potential interactions between air pollutants. Future studies should implement mixture models to investigate the concurrent exposure to multiple air pollutants and the time–microenvironment–activity paradigm. Above all, the underlying mechanisms and potential factors mediating PCa risk require further research to tailor intervention strategies to the specific context of PM2.5 pollution.

6. Conclusions

The ubiquity of airborne PM2.5 pollution poses a serious public health concern worldwide, since it has numerous adverse effects on human health, including a potentially increased risk of PCa. As research continues, it is imperative to implement additional studies from basic science to population-level investigations to uncover the intricate mechanisms linking PM2.5 exposure to PCa development. The collaboration between policymakers, scientific communities, and healthcare professionals is crucial to formulating comprehensive strategies that protect prostate health from the impact of PM2.5 pollution.

Author Contributions: C.-W.L., Y.-C.C., T.T.T.V. and I.-T.L. designed and conceived of this review. C.-W.L., T.T.T.V. and I.-T.L. drafted the manuscript and prepared the figures. T.T.T.V., Z.-C.L., M.-C.C., M.-L.F., K.-T.P. and M.-H.T. edited the manuscript. All authors have read and agreed to the published version of the manuscript.

Funding: This work was supported by the Chang Gung University of Science and Technology Foundation, grant numbers ZRRPF6N0011 and ZRRPF6P0011, and the Chang Gung Medical Research Program Foundation, grant numbers CORPF6P0041, CORPF6P0042, and CORPF6P0043.

Institutional Review Board Statement: Not applicable.

Informed Consent Statement: Not applicable.

Data Availability Statement: The manuscript contains all relevant data.

Acknowledgments: We thank You-Syun Jheng for her suggestions on the manuscript's layout.

Conflicts of Interest: The authors declare no conflicts of interest.

References

1. Bray, F.; Laversanne, M.; Sung, H.; Ferlay, J.; Siegel, R.L.; Soerjomataram, I.; Jemal, A. Global cancer statistics 2022: GLOBOCAN estimates of incidence and mortality worldwide for 36 cancers in 185 countries. *CA Cancer J. Clin.* **2024**, *74*, 229–263. [CrossRef] [PubMed]
2. James, N.D.; Tannock, I.; N'Dow, J.; Feng, F.; Gillessen, S.; Ali, S.A.; Trujillo, B.; Al-Lazikani, B.; Attard, G.; Bray, F.; et al. The Lancet Commission on prostate cancer: Planning for the surge in cases. *Lancet* **2024**, *403*, 1683–1722. [CrossRef] [PubMed]
3. Sandhu, S.; Moore, C.M.; Chiong, E.; Beltran, H.; Bristow, R.G.; Williams, S.G. Prostate cancer. *Lancet* **2021**, *398*, 1075–1090. [CrossRef] [PubMed]
4. Graham, N.J.; Souter, L.H.; Salami, S.S. A Systematic Review of Family History, Race/Ethnicity, and Genetic Risk on Prostate Cancer Detection and Outcomes: Considerations in PSA-based Screening. *Urol. Oncol.* **2024**, *43*, 29–40. [CrossRef]
5. Manisalidis, I.; Stavropoulou, E.; Stavropoulos, A.; Bezirtzoglou, E. Environmental and Health Impacts of Air Pollution: A Review. *Front. Public Health* **2020**, *8*, 14. [CrossRef]
6. Fuller, R.; Landrigan, P.J.; Balakrishnan, K.; Bathan, G.; Bose-O'Reilly, S.; Brauer, M.; Caravanos, J.; Chiles, T.; Cohen, A.; Corra, L.; et al. Pollution and health: A progress update. *Lancet Planet. Health* **2022**, *6*, e535–e547. [CrossRef]
7. World Health Organization. Air Pollution. Available online: https://www.who.int/health-topics/air-pollution#tab=tab_1 (accessed on 29 October 2024).
8. Tang, H.; Chen, S.; Wei, J.; Guo, T.; Zhang, Y.; Wu, W.; Wang, Y.; Chen, S.; Chen, D.; Cai, H.; et al. How long-term PM exposure may affect all-site cancer mortality: Evidence from a large cohort in southern China. *Ecotoxicol. Environ. Saf.* **2024**, *280*, 116478. [CrossRef]
9. Santibanez-Andrade, M.; Chirino, Y.I.; Gonzalez-Ramirez, I.; Sanchez-Perez, Y.; Garcia-Cuellar, C.M. Deciphering the code between air pollution and disease: The effect of particulate matter on cancer hallmarks. *Int. J. Mol. Sci.* **2019**, *21*, 136. [CrossRef] [PubMed]
10. Straif, K.; Cohen, A.; Samet, J. *Air Pollution and Cancer*; IARC Scientific Publication No. 161; International Agency for Research on Cancer: Lyon, France, 2013.
11. Lee, C.W.; Vo, T.T.T.; Wu, C.Z.; Chi, M.C.; Lin, C.M.; Fang, M.L.; Lee, I.T. The Inducible Role of Ambient Particulate Matter in Cancer Progression via Oxidative Stress-Mediated Reactive Oxygen Species Pathways: A Recent Perception. *Cancers* **2020**, *12*, 2505. [CrossRef]
12. Valavanidis, A.; Vlachogianni, T.; Fiotakis, K.; Loridas, S. Pulmonary oxidative stress, inflammation and cancer: Respirable particulate matter, fibrous dusts and ozone as major causes of lung carcinogenesis through reactive oxygen species mechanisms. *Int. J. Environ. Res. Public Health* **2013**, *10*, 3886–3907. [CrossRef]
13. Wang, Y.; Tang, M. PM2.5 induces ferroptosis in human endothelial cells through iron overload and redox imbalance. *Environ. Pollut.* **2019**, *254*, 112937. [CrossRef]
14. Valavanidis, A.; Fiotakis, K.; Vlachogianni, T. Airborne particulate matter and human health: Toxicological assessment and importance of size and composition of particles for oxidative damage and carcinogenic mechanisms. *J. Environ. Sci. Health C Environ. Carcinog. Ecotoxicol. Rev.* **2008**, *26*, 339–362. [CrossRef]
15. World Health Organization. WHO Air Quality Guidelines for Particulate Matter, Ozone, Nitrogen Dioxide and Sulfur Dioxide. 2006. Available online: https://iris.who.int/bitstream/handle/10665/69477/WHO_SDE_PHE_OEH_06.02_eng.pdf;sequence=1 (accessed on 29 October 2024).
16. World Health Organization. Ambient (Outdoor) Air Pollution. Available online: https://www.who.int/news-room/fact-sheets/detail/ambient-(outdoor)-air-quality-and-health (accessed on 29 October 2024).
17. GBD 2021 Risk Factors Collaborators. Global burden and strength of evidence for 88 risk factors in 204 countries and 811 subnational locations, 1990–2021: A systematic analysis for the Global Burden of Disease Study 2021. *Lancet* **2024**, *403*, 2162–2203. [CrossRef]
18. Thangavel, P.; Park, D.; Lee, Y.C. Recent insights into particulate matter (PM(2.5))-mediated toxicity in humans: An overview. *Int. J. Environ. Res. Public Health* **2022**, *19*, 7511. [CrossRef]
19. Lelieveld, J.; Haines, A.; Burnett, R.; Tonne, C.; Klingmüller, K.; Münzel, T.; Pozzer, A. Air pollution deaths attributable to fossil fuels: Observational and modelling study. *BMJ* **2023**, *383*, e077784. [CrossRef]
20. National Research Council. *Airborne Particles/Subcommittee on Airborne Particles, Committee on Medical and Biologic Effects of Environmental Pollutants, Division of Medical Sciences, Assembly of Life Sciences, National Research Council*; University Park Press: Baltimore, MD, USA, 1979.
21. Maciejczyk, P.; Chen, L.C.; Thurston, G. The Role of Fossil Fuel Combustion Metals in $PM_{2.5}$ Air Pollution Health Associations. *Atmosphere* **2021**, *12*, 1086. [CrossRef]
22. Samet, J.M.; Chen, H.; Pennington, E.R.; Bromberg, P.A. Non-redox cycling mechanisms of oxidative stress induced by PM metals. *Free Radic. Biol. Med.* **2020**, *151*, 26–37. [CrossRef]

23. Øvrevik, J.; Refsnes, M.; Låg, M.; Holme, J.A.; Schwarze, P.E. Activation of proinflammatory responses in cells of the airway mucosa by particulate matter: Oxidant- and non-oxidant-mediated triggering mechanisms. *Biomolecules* **2015**, *5*, 1399–1440. [CrossRef]
24. Holme, J.A.; Vondráček, J.; Machala, M.; Lagadic-Gossmann, D.; Vogel, C.F.A.; Le Ferrec, E.; Sparfel, L.; Øvrevik, J. Lung cancer associated with combustion particles and fine particulate matter (PM2.5)—The roles of polycyclic aromatic hydrocarbons (PAHs) and the aryl hydrocarbon receptor (AhR). *Biochem. Pharmacol.* **2023**, *216*, 115801. [CrossRef]
25. Turner, M.C.; Andersen, Z.J.; Baccarelli, A.; Diver, W.R.; Gapstur, S.M.; Pope, C.A., 3rd; Prada, D.; Samet, J.; Thurston, G.; Cohen, A. Outdoor air pollution and cancer: An overview of the current evidence and public health recommendations. *CA Cancer J. Clin.* **2020**, *70*, 460–479. [CrossRef]
26. Kim, H.B.; Shim, J.Y.; Park, B.; Lee, Y.J. Long-term exposure to air pollution and the risk of non-lung cancer: A meta-analysis of observational studies. *Perspect. Public Health* **2020**, *140*, 222–231. [CrossRef]
27. Kim, H.B.; Shim, J.Y.; Park, B.; Lee, Y.J. Long-term exposure to air pollutants and cancer mortality: A meta-analysis of cohort studies. *Int. J. Environ. Res. Public Health* **2018**, *15*, 2608. [CrossRef]
28. Zare Sakhvidi, M.J.; Lequy, E.; Goldberg, M.; Jacquemin, B. Air pollution exposure and bladder, kidney and urinary tract cancer risk: A systematic review. *Environ. Pollut.* **2020**, *267*, 115328. [CrossRef]
29. Kim, E.A. Particulate matter (fine particle) and urologic diseases. *Int. Neurourol. J.* **2017**, *21*, 155–162. [CrossRef]
30. Cong, X. Air pollution from industrial waste gas emissions is associated with cancer incidences in Shanghai, China. *Environ. Sci. Pollut. Res. Int.* **2018**, *25*, 13067–13078. [CrossRef]
31. Feng, S.; Gao, D.; Liao, F.; Zhou, F.; Wang, X. The health effects of ambient PM2.5 and potential mechanisms. *Ecotoxicol. Environ. Saf.* **2016**, *128*, 67–74. [CrossRef]
32. Salgueiro-González, N.; López de Alda, M.J.; Muniategui-Lorenzo, S.; Prada-Rodríguez, D.; Barceló, D. Analysis and occurrence of endocrine-disrupting chemicals in airborne particles. *TrAC Trends Anal. Chem.* **2015**, *66*, 45–52. [CrossRef]
33. De Toni, L.; Sabovic, I.; Cosci, I.; Ghezzi, M.; Foresta, C.; Garolla, A. Testicular cancer: Genes, environment, hormones. *Front. Endocrinol.* **2019**, *10*, 408. [CrossRef]
34. Khandrika, L.; Kumar, B.; Koul, S.; Maroni, P.; Koul, H.K. Oxidative stress in prostate cancer. *Cancer Lett.* **2009**, *282*, 125–136. [CrossRef]
35. Li, S.; Cai, T.; Cui, S.; Liu, F.; Hu, R.; Li, W. Prostate Cancer, Oxidative Stress, and Antioxidant Phytochemicals: A Brief Review. *Curr. Pharmacol. Rep.* **2023**, *9*, 391–396. [CrossRef]
36. Winkelstein, W., Jr.; Kantor, S. Prostatic cancer: Relationship to suspended particulate air pollution. *Am. J. Public Health Nations Health* **1969**, *59*, 1134–1138. [CrossRef]
37. Coleman, N.C.; Burnett, R.T.; Ezzati, M.; Marshall, J.D.; Robinson, A.L.; Pope, C.A., 3rd. Fine Particulate Matter Exposure and Cancer Incidence: Analysis of SEER Cancer Registry Data from 1992–2016. *Environ. Health Perspect.* **2020**, *128*, 107004. [CrossRef]
38. Youogo, L.M.K.; Parent, M.E.; Hystad, P.; Villeneuve, P.J. Ambient air pollution and prostate cancer risk in a population-based Canadian case-control study. *Environ. Epidemiol.* **2022**, *6*, e219. [CrossRef]
39. Wang, H.; Gao, Z.; Ren, J.; Liu, Y.; Chang, L.T.; Cheung, K.; Feng, Y.; Li, Y. An urban-rural and sex differences in cancer incidence and mortality and the relationship with $PM_{2.5}$ exposure: An ecological study in the southeastern side of Hu line. *Chemosphere* **2019**, *216*, 766–773. [CrossRef]
40. Shin, M.; Kim, O.J.; Yang, S.; Choe, S.A.; Kim, S.Y. Different Mortality Risks of Long-Term Exposure to Particulate Matter across Different Cancer Sites. *Int. J. Environ. Res. Public Health* **2022**, *19*, 3180. [CrossRef]
41. Wei, Y.; Danesh Yazdi, M.; Ma, T.; Castro, E.; Liu, C.S.; Qiu, X.; Healy, J.; Vu, B.N.; Wang, C.; Shi, L.; et al. Additive effects of 10-year exposures to PM(2.5) and NO(2) and primary cancer incidence in American older adults. *Environ. Epidemiol.* **2023**, *7*, e265. [CrossRef]
42. Weichenthal, S.; Lavigne, E.; Valois, M.F.; Hatzopoulou, M.; Van Ryswyk, K.; Shekarrizfard, M.; Villeneuve, P.J.; Goldberg, M.S.; Parent, M.E. Spatial variations in ambient ultrafine particle concentrations and the risk of incident prostate cancer: A case-control study. *Environ. Res.* **2017**, *156*, 374–380. [CrossRef]
43. Felici, A.; Peduzzi, G.; Giorgolo, F.; Spinelli, A.; Calderisi, M.; Monreale, A.; Farinella, R.; Pellungrini, R.; Canzian, F.; Campa, D. The local environment and germline genetic variation predict cancer risk in the UK Biobank prospective cohort. *Environ. Res.* **2024**, *241*, 117562. [CrossRef]
44. Kayyal-Tarabeia, I.; Zick, A.; Kloog, I.; Levy, I.; Blank, M.; Agay-Shay, K. Beyond lung cancer: Air pollution and bladder, breast and prostate cancer incidence. *Int. J. Epidemiol.* **2024**, *53*, dyae093. [CrossRef]
45. Thomas, A.L.; Rhee, J.; Fisher, J.A.; Horner, M.J.; Jones, R.R. Fine Particulate Matter, Noise Pollution, and Greenspace and Prostate Cancer Risk in the Prostate, Lung, Colorectal, and Ovarian Cancer Screening Trial Cohort. *Cancer Epidemiol. Biomark. Prev.* **2024**, *33*, 857–860. [CrossRef]
46. Fan, Z.; Li, Y.; Wei, J.; Chen, G.; Wang, R.; Xu, R.; Liu, T.; Lv, Z.; Huang, S.; Sun, H.; et al. Long-term exposure to fine particulate matter and site-specific cancer mortality: A difference-in-differences analysis in Jiangsu province, China. *Environ. Res.* **2023**, *222*, 115405. [CrossRef]
47. Huang, Y.J.; Lee, P.H.; Chen, L.C.; Lin, B.C.; Lin, C.; Chan, T.C. Relationships among green space, ambient fine particulate matter, and cancer incidence in Taiwan: A 16-year retrospective cohort study. *Environ. Res.* **2022**, *212*, 113416. [CrossRef]

48. Yu, P.; Xu, R.; Li, S.; Coelho, M.S.Z.S.; Saldiva, P.H.N.; Sim, M.R.; Abramson, M.J.; Guo, Y. Associations between long-term exposure to $PM_{2.5}$ and site-specific cancer mortality: A nationwide study in Brazil between 2010 and 2018. *Environ. Pollut.* **2022**, *302*, 119070. [CrossRef]
49. Yu, P.; Xu, R.; Li, S.; Yue, X.; Chen, G.; Ye, T.; Coêlho, M.S.Z.S.; Saldiva, P.H.N.; Sim, M.R.; Abramson, M.J.; et al. Exposure to wildfire-related PM2.5 and site-specific cancer mortality in Brazil from 2010 to 2016: A retrospective study. *PLoS Med.* **2022**, *19*, e1004103. [CrossRef]
50. Coleman, N.C.; Burnett, R.T.; Higbee, J.D.; Lefler, J.S.; Merrill, R.M.; Ezzati, M.; Marshall, J.D.; Kim, S.Y.; Bechle, M.; Robinson, A.L.; et al. Cancer mortality risk, fine particulate air pollution, and smoking in a large, representative cohort of US adults. *Cancer Causes Control* **2020**, *31*, 767–776. [CrossRef]
51. Turner, M.C.; Krewski, D.; Diver, W.R.; Pope, C.A., 3rd; Burnett, R.T.; Jerrett, M.; Marshall, J.D.; Gapstur, S.M. Ambient Air Pollution and Cancer Mortality in the Cancer Prevention Study II. *Environ. Health Perspect.* **2017**, *125*, 087013. [CrossRef]
52. Sies, H. *Oxidative Stress*; Academic Press: London, UK, 1985; pp. 1–507.
53. Sies, H. Oxidative Stress: Concept and Some Practical Aspects. *Antioxidants* **2020**, *9*, 852. [CrossRef]
54. Iqbal, M.J.; Kabeer, A.; Abbas, Z.; Siddiqui, H.A.; Calina, D.; Sharifi-Rad, J.; Cho, W.C. Interplay of oxidative stress, cellular communication and signaling pathways in cancer. *Cell Commun. Signal.* **2024**, *22*, 7. [CrossRef]
55. Santibáñez-Andrade, M.; Quezada-Maldonado, E.M.; Rivera-Pineda, A.; Chirino, Y.I.; García-Cuellar, C.M.; Sánchez-Pérez, Y. The Road to Malignant Cell Transformation after Particulate Matter Exposure: From Oxidative Stress to Genotoxicity. *Int. J. Mol. Sci.* **2023**, *24*, 1782. [CrossRef]
56. Kumar, B.; Koul, S.; Khandrika, L.; Meacham, R.B.; Koul, H.K. Oxidative stress is inherent in prostate cancer cells and is required for aggressive phenotype. *Cancer Res.* **2008**, *68*, 1777–1785. [CrossRef]
57. Lim, S.D.; Sun, C.; Lambeth, J.D.; Marshall, F.; Amin, M.; Chung, L.; Petros, J.A.; Arnold, R.S. Increased Nox1 and hydrogen peroxide in prostate cancer. *Prostate* **2005**, *62*, 200–207. [CrossRef] [PubMed]
58. Wang, L.; Luo, D.; Liu, X.; Zhu, J.; Wang, F.; Li, B.; Li, L. Effects of $PM_{2.5}$ exposure on reproductive system and its mechanisms. *Chemosphere* **2021**, *264*, 128436. [CrossRef] [PubMed]
59. Xu, M.; Wu, T.; Tang, Y.T.; Chen, T.; Khachatryan, L.; Iyer, P.R.; Guo, D.; Chen, A.; Lyu, M.; Li, J.; et al. Environmentally persistent free radicals in $PM_{2.5}$: A review. *Waste Dispos. Sustain. Energy* **2019**, *1*, 177–197. [CrossRef] [PubMed]
60. Tshoni, U.A.; Mbonane, T.P.; Rathebe, P.C. The Role of Trace Metals in the Development and Progression of Prostate Cancer. *Int. J. Mol. Sci.* **2024**, *25*, 10725. [CrossRef]
61. Stec, A.A.; Dickens, K.E.; Salden, M.; Hewitt, F.E.; Watts, D.P.; Houldsworth, P.E.; Martin, F.L. Occupational Exposure to Polycyclic Aromatic Hydrocarbons and Elevated Cancer Incidence in Firefighters. *Sci. Rep.* **2018**, *8*, 2476. [CrossRef]
62. Du, L.; Lei, Y.; Chen, J.; Song, H.; Wu, X. Potential Ameliorative Effects of Qing Ye Dan Against Cadmium Induced Prostatic Deficits via Regulating Nrf-2/HO-1 and TGF-β1/Smad Pathways. *Cell. Physiol. Biochem.* **2017**, *43*, 1359–1368. [CrossRef]
63. Chen, J.; Liu, J.; Lei, Y.; Liu, M. The anti-inflammation, anti-oxidative and anti-fibrosis properties of swertiamarin in cigarette smoke exposure-induced prostate dysfunction in rats. *Aging* **2019**, *11*, 10409–10421. [CrossRef]
64. Baumann, K.; Wietzoreck, M.; Shahpoury, P.; Filippi, A.; Hildmann, S.; Lelieveld, S.; Berkemeier, T.; Tong, H.; Pöschl, U.; Lammel, G. Is the oxidative potential of components of fine particulate matter surface-mediated? *Environ. Sci. Pollut. Res.* **2023**, *30*, 16749–16755. [CrossRef]
65. Freitas, M.; Alves, V.; Sarmento-Ribeiro, A.; Mota-Pinto, A. Polycyclic Aromatic Hydrocarbons May Contribute for Prostate Cancer Progression. *J. Cancer Ther.* **2013**, *4*, 37–46. [CrossRef]
66. Ayres, J.G.; Borm, P.; Cassee, F.R.; Castranova, V.; Donaldson, K.; Ghio, A.; Harrison, R.M.; Hider, R.; Kelly, F.; Kooter, I.M.; et al. Evaluating the toxicity of airborne particulate matter and nanoparticles by measuring oxidative stress potential—A workshop report and consensus statement. *Inhal. Toxicol.* **2008**, *20*, 75–99. [CrossRef]
67. Che, J.P.; Li, W.; Yan, Y.; Liu, M.; Wang, G.C.; Li, Q.Y.; Yang, B.; Yao, X.D.; Zheng, J.H. Expression and clinical significance of the nin one binding protein and p38 MAPK in prostate carcinoma. *Int. J. Clin. Exp. Pathol.* **2013**, *6*, 2300–2311. [PubMed]
68. Park, S.; Kwon, W.; Park, J.K.; Baek, S.M.; Lee, S.W.; Cho, G.J.; Ha, Y.S.; Lee, J.N.; Kwon, T.G.; Kim, M.O.; et al. Suppression of cathepsin a inhibits growth, migration, and invasion by inhibiting the p38 MAPK signaling pathway in prostate cancer. *Arch. Biochem. Biophys.* **2020**, *688*, 108407. [CrossRef] [PubMed]
69. Pungsrinont, T.; Kallenbach, J.; Baniahmad, A. Role of pi3k-akt-mtor pathway as a pro-survival signaling and resistance-mediating mechanism to therapy of prostate cancer. *Int. J. Mol. Sci.* **2021**, *22*, 11088. [CrossRef]
70. Vieira, W.T.; de Farias, M.B.; Spaolonzi, M.P.; da Silva, M.G.C.; Vieira, M.G.A. Endocrine-disrupting compounds: Occurrence, detection methods, effects and promising treatment pathways—A critical review. *J. Environ. Chem. Eng.* **2021**, *9*, 104558. [CrossRef]
71. Gea, M.; Fea, E.; Racca, L.; Gilli, G.; Gardois, P.; Schilirò, T. Atmospheric endocrine disruptors: A systematic review on oestrogenic and androgenic activity of particulate matter. *Chemosphere* **2024**, *349*, 140887. [CrossRef]
72. Plísková, M.; Vondrácek, J.; Vojtesek, B.; Kozubík, A.; Machala, M. Deregulation of Cell Proliferation by Polycyclic Aromatic Hydrocarbons in Human Breast Carcinoma MCF-7 Cells Reflects Both Genotoxic and Nongenotoxic Events. *Toxicol. Sci.* **2005**, *83*, 246–256. [CrossRef]

73. Lau, K.M.; La Spina, M.; Long, J.; Ho, S.M. Expression of Estrogen Receptor-Alpha and Estrogen Receptor-Beta in Normal and Malignant Prostatic Epithelial Cells: Regulation by Methylation and Involvement in Growth Regulation. *Cancer Res.* **2000**, *60*, 3175–3182.
74. Vingaard, A.M.; Hnida, C.; Larsen, J.C. Environmental Polycyclic Hydrocarbons affect Androgen Receptor Activation In Vitro. *Toxicology* **2000**, *145*, 173–183. [CrossRef] [PubMed]
75. Mehraein-Ghomi, F.; Lee, E.; Church, D.R.; Thompson, T.A.; Basu, H.S.; Wilding, G. JunD Mediates Androgen-Induced Oxidative Stress in Androgen Dependent LNCaP Human Prostate Cancer Cells. *Prostate* **2008**, *68*, 924–934. [CrossRef]
76. Chandarlapaty, S. Negative Feedback and Adaptive Resistance to the Targeted Therapy of Cancer. *Cancer Discov.* **2012**, *2*, 311–319. [CrossRef]
77. Marques, R.B.; Dit, N.F.; Erkens-Schulze, S.; van Weerden, W.M.; Jenster, G. Bypass Mechanisms of the Androgen Receptor Pathway in Therapy-Resistant Prostate Cancer Cell Models. *PLoS ONE* **2010**, *19*, e135002010. [CrossRef] [PubMed]
78. Koochekpour, S. Androgen Receptor Signaling and Mutations in Prostate Cancer. *Asian J. Androl.* **2010**, *12*, 639–657. [CrossRef] [PubMed]
79. Glencross, D.A.; Ho, T.R.; Camiña, N.; Hawrylowicz, C.M.; Pfeffer, P.E. Air pollution and its effects on the immune system. *Free Radic. Biol. Med.* **2020**, *151*, 56–68. [CrossRef] [PubMed]
80. Movassaghi, M.; Chung, R.; Anderson, C.B.; Stein, M.; Saenger, Y.; Faiena, I. Overcoming Immune Resistance in Prostate Cancer: Challenges and Advances. *Cancers* **2021**, *13*, 4757. [CrossRef] [PubMed]
81. Tavassolifar, M.J.; Vodjgani, M.; Salehi, Z.; Izad, M. The Influence of Reactive Oxygen Species in the Immune System and Pathogenesis of Multiple Sclerosis. *Autoimmune Dis.* **2020**, *2020*, 5793817. [CrossRef]
82. Morris, G.; Gevezova, M.; Sarafian, V.; Maes, M. Redox regulation of the immune response. *Cell. Mol. Immunol.* **2022**, *19*, 1079–1101. [CrossRef]
83. Hultqvist, M.; Bäcklund, J.; Bauer, K.; Gelderman, K.A.; Holmdahl, R. Lack of reactive oxygen species breaks T cell tolerance to collagen type II and allows development of arthritis in mice. *J. Immunol.* **2007**, *179*, 1431–1437. [CrossRef]
84. Wang, D.; Malo, D.; Hekimi, S. Elevated mitochondrial reactive oxygen species generation affects the immune response via hypoxia-inducible factor-1α in long-LivedMclk1 $\pm$ mouse mutants. *J. Immunol.* **2010**, *184*, 582–590. [CrossRef]
85. Morgan, M.J.; Liu, Z.G. Crosstalk of reactive oxygen species and NF-κB signaling. *Cell Res.* **2011**, *21*, 103–115. [CrossRef]
86. Suh, J.; Rabson, A.B. NF-kappaB activation in human prostate cancer: Important mediator or epiphenomenon? *J. Cell. Biochem.* **2004**, *91*, 100–117. [CrossRef]
87. Staal, J.; Beyaert, R. Inflammation and NF-κB Signaling in Prostate Cancer: Mechanisms and Clinical Implications. *Cells* **2018**, *7*, 122. [CrossRef] [PubMed]
88. Kim, J.; Surh, Y.J. The role of Nrf2 in cellular innate immune response to inflammatory injury. *Toxicol. Res.* **2009**, *25*, 159–173. [CrossRef] [PubMed]
89. Battino, M.; Giampieri, F.; Pistollato, F.; Sureda, A.; de Oliveira, M.R.; Pittalà, V.; Fallarino, F.; Nabavi, S.F.; Atanasov, A.G.; Nabavi, S.M. Nrf2 as regulator of innate immunity: A molecular Swiss army knife! *Biotechnol. Adv.* **2018**, *36*, 358–370. [CrossRef]
90. Yu, S.; Khor, T.O.; Cheung, K.L.; Li, W.; Wu, T.Y.; Huang, Y.; Foster, B.A.; Kan, Y.W.; Kong, A.N. Nrf2 expression is regulated by epigenetic mechanisms in prostate cancer of TRAMP mice. *PLoS ONE* **2010**, *5*, e8579. [CrossRef]
91. Oh, B.; Figtree, G.; Costa, D.; Eade, T.; Hruby, G.; Lim, S.; Elfiky, A.; Martine, N.; Rosenthal, D.; Clarke, S.; et al. Oxidative stress in prostate cancer patients: A systematic review of case control studies. *Prostate Int.* **2016**, *4*, 71–87. [CrossRef]
92. Battisti, V.; Maders, L.D.; Bagatini, M.D.; Reetz, L.G.; Chiesa, J.; Battisti, I.E.; Gonçalves, J.F.; Duarte, M.M.; Schetinger, M.R.; Morsch, V.M. Oxidative stress and antioxidant status in prostate cancer patients: Relation to Gleason score, treatment and bone metastasis. *Biomed. Pharmacother.* **2011**, *65*, 516–524. [CrossRef]
93. Akanji, M.A.; Fatinukun, H.D.; Rotimi, D.E.; Afolabi, B.L.; Adeyemi, O.S. The Two Sides of Dietary Antioxidants in Cancer Therapy. In *Antioxidants—Benefits, Sources, Mechanisms of Action*; IntechOpen: London, UK, 2020.
94. Heinonen, O.P.; Albanes, D.; Virtamo, J.; Taylor, P.R.; Huttunen, J.K.; Hartman, A.M.; Haapakoski, J.; Malila, N.; Rautalahti, M.; Ripatti, S.; et al. Prostate cancer and supplementation with alpha-tocopherol and beta-carotene: Incidence and mortality in a controlled trial. *J. Natl. Cancer Inst.* **1998**, *90*, 440–446. [CrossRef]
95. Fleshner, N.E.; Klotz, L.H. Diet, androgens, oxidative stress and prostate cancer susceptibility. *Cancer Metastasis Rev.* **1998**, *17*, 325–330. [CrossRef] [PubMed]
96. Lonn, E.; Bosch, J.; Yusuf, S.; Sheridan, P.; Pogue, J.; Arnold, J.M.; Ross, C.; Arnold, A.; Sleight, P.; Probstfield, J.; et al. Effects of long-term vitamin E supplementation on cardiovascular events and cancer: A randomized controlled trial. *JAMA* **2005**, *293*, 1338–1347.
97. Kirsh, V.A.; Hayes, R.B.; Mayne, S.T.; Chatterjee, N.; Subar, A.F.; Dixon, L.B.; Albanes, D.; Andriole, G.L.; Urban, D.A.; Peters, U.; et al. Supplemental and dietary vitamin E, β-carotene, and vitamin C intakes and prostate cancer risk. *J. Natl. Cancer Inst.* **2006**, *98*, 245–254. [CrossRef]
98. Algotar, A.M.; Stratton, M.S.; Ahmann, F.R.; Ranger-Moore, J.; Nagle, R.B.; Thompson, P.A.; Slate, E.; Hsu, C.H.; Dalkin, B.L.; Sindhwani, P.; et al. Phase 3 clinical trial investigating the effect of selenium supplementation in men at high-risk for prostate cancer. *Prostate* **2013**, *73*, 328–335. [CrossRef] [PubMed]

99. Vance, T.M.; Azabdaftari, G.; Pop, E.A.; Lee, S.G.; Su, L.J.; Fontham, E.T.; Bensen, J.T.; Steck, S.E.; Arab, L.; Mohler, J.L.; et al. Intake of dietary antioxidants is inversely associated with biomarkers of oxidative stress among men with prostate cancer. *Br. J. Nutr.* **2016**, *115*, 68–74. [CrossRef] [PubMed]
100. Rago, V.; Di Agostino, S. Novel Insights into the Role of the Antioxidants in Prostate Pathology. *Antioxidants* **2023**, *12*, 289. [CrossRef] [PubMed]
101. Mokbel, K. Breath of Danger: Unveiling PM2.5's Stealthy Impact on Cancer Risks. *Anticancer Res.* **2024**, *44*, 1365–1368. [CrossRef]
102. Schichlein, K.D.; Smith, G.J.; Jaspers, I. Protective effects of inhaled antioxidants against air pollution-induced pathological responses. *Respir. Res.* **2023**, *24*, 187. [CrossRef]
103. Price, D.K. Efficacy of androgen deprivation therapy and the role of oxidative stress. *Ann. Oncol.* **2017**, *28*, 451–453. [CrossRef]
104. Tam, N.N.; Gao, Y.; Leung, Y.K.; Ho, S.M. Androgenic regulation of oxidative stress in the rat prostate: Involvement of NAD(P)H oxidases and antioxidant defense machinery during prostatic involution and regrowth. *Am. J. Pathol.* **2003**, *163*, 2513–2522. [CrossRef]
105. Höll, M.; Koziel, R.; Schäfer, G.; Pircher, H.; Pauck, A.; Hermann, M.; Klocker, H.; Jansen-Dürr, P.; Sampson, N. ROS signaling by NADPH oxidase 5 modulates the proliferation and survival of prostate carcinoma cells. *Mol. Carcinog.* **2016**, *55*, 27–39. [CrossRef]
106. Markevych, I.; Schoierer, J.; Hartig, T.; Chudnovsky, A.; Hystad, P.; Dzhambov, A.M.; de Vries, S.; Triguero-Mas, M.; Brauer, M.; Nieuwenhuijsen, M.J.; et al. Exploring pathways linking greenspace to health: Theoretical and methodological guidance. *Environ. Res.* **2017**, *158*, 301–317. [CrossRef]
107. Demoury, C.; Thierry, B.; Richard, H.; Sigler, B.; Kestens, Y.; Parent, M.E. Residential greenness and risk of prostate cancer: A case-control study in Montreal, Canada. *Environ. Int.* **2017**, *98*, 129–136. [CrossRef]

antioxidants

MDPI

Article

Seasonal Variation in $PM_{2.5}$ Composition Modulates Oxidative Stress and Neutrophilic Inflammation with Involvement of TLR4 Signaling

Duo Wang [1], Zirui Zeng [2], Aya Nawata [3], Ryoko Baba [4], Ryuji Okazaki [1], Tomoaki Okuda [5] and Yasuhiro Yoshida [6,*]

1 Department of Radiobiology and Hygiene Management, Institute of Industrial Ecological Sciences, University of Occupational and Environmental Health, Japan, 1-1 Iseigaoka, Yahatanishi-ku, Kitakyushu 807-8555, Japan; ryuji-o@med.uoeh-u.ac.jp (R.O.)
2 The First Department of Internal Medicine, School of Medicine, University of Occupational and Environmental Health, Japan, 1-1 Iseigaoka, Yahatanishi-ku, Kitakyushu 807-8555, Japan
3 Department of Pathology and Oncology, School of Medicine, University of Occupational and Environmental Health, Japan, 1-1 Iseigaoka, Yahatanishi-ku, Kitakyushu 807-8555, Japan; aya.y0116@gmail.com
4 Department of Anatomy, School of Medicine, University of Occupational and Environmental Health, Japan, 1-1 Iseigaoka, Yahatanishi-ku, Kitakyushu 807-8555, Japan
5 Department of Applied Chemistry, Faculty of Science and Technology, Keio University, 3-14-1 Hiyoshi, Kohoku-ku, Yokohama 223-8522, Japan
6 Department of Immunology and Parasitology, School of Medicine, University of Occupational and Environmental Health, Japan, 1-1 Iseigaoka, Yahatanishi-ku, Kitakyushu 807-8555, Japan
* Correspondence: freude@med.uoeh-u.ac.jp; Tel.: +81-936917431

Abstract

Seasonal fluctuations in the chemical composition of fine particulate matter ($PM_{2.5}$) are known to influence its toxicological properties; however, their integrated biological effects remain incompletely understood. In this study, $PM_{2.5}$ was continuously collected over two consecutive years at a single urban site in Japan and classified by season. The samples were comprehensively characterized for ionic species, metals, carbonaceous fractions, and polycyclic aromatic hydrocarbons (PAHs), and their pulmonary effects were evaluated in vivo following intratracheal administration in mice. Seasonal $PM_{2.5}$ exhibited pronounced compositional differences, with higher levels of secondary inorganic aerosol components in summer and enrichment of PAHs and mineral-associated components in winter. These seasonal differences translated into distinct biological responses. Reactive oxygen species (ROS) production (1.6–2.7-fold increase) and bronchoalveolar lavage (BAL) neutrophil infiltration were strongly associated with PAH-rich $PM_{2.5}$, whereas interleukin-1α (IL-1α) showed robust positive correlations with mineral components, including K^+, Ca^{2+}, and Mg^{2+}, which were predominantly enriched in winter $PM_{2.5}$. In contrast, secondary inorganic aerosol species displayed a limited capacity to induce IL-1α. Compared with summer samples, winter $PM_{2.5}$ induced significantly higher levels of ROS production and IL-1α (approximately 1.5–2.6-fold increase). Using TLR2- and TLR4-deficient mice, we further demonstrated that $PM_{2.5}$-induced increases in BAL cell counts, ROS, IL-6, and TNF-α were partially attenuated in TLR4 knockout mice, indicating a contributory but not exclusive role for TLR4 signaling in $PM_{2.5}$-driven pulmonary inflammation. Collectively, these findings demonstrate that seasonal variations in $PM_{2.5}$ composition, not particle mass alone, critically shape oxidative stress and innate immune responses in the lungs. In particular, winter $PM_{2.5}$ enriched in mineral-associated components preferentially activates IL-1α-mediated alarmin pathways, underscoring the importance of the particle composition in determining seasonal air pollution toxicity.

Keywords: reactive oxygen species (ROS); particulate matter 2.5 ($PM_{2.5}$); lung inflammation; seasonality; air pollution toxicity; innate immune response

1. Introduction

Exposure to particulate matter (PM) poses serious risks to human health [1]. Major PM sources include vehicle emissions, industrial activities, construction operations, and natural events such as wildfires and volcanic eruptions [2,3]. PM varies widely in size and composition, and it is typically classified according to aerodynamic diameter. Among these, particles smaller than 2.5 μm has been extensively linked to adverse respiratory and systemic health effects [4–6]. Because of their small size, $PM_{2.5}$ can penetrate deep into the respiratory tract and reach the alveoli, where they contribute to infections, airway inflammation, and chronic lung diseases [7–9].

The physicochemical characteristics of $PM_{2.5}$ differ substantially depending on sampling location [10,11], season [12], and year [13]. Therefore, understanding $PM_{2.5}$ toxicity requires direct experimental evaluation. Several studies have compared seasonal $PM_{2.5}$ effects. Melzi et al. showed that summer and winter $PM_{2.5}$ differ in their capacity to induce oxidative stress, inflammation, and DNA damage in cell lines [14]. Farina et al. reported that heme oxygenase-1 (HO-1), a key antioxidant and stress-response enzyme, was markedly increased following exposure to aerosolized summer PM in mice [15]. Marchetti et al. used $PM_{2.5}$ collected over four seasons and demonstrated that biological responses correlated positively with PAHs and metals characteristic of combustion-derived pollution [16]. The use of $PM_{2.5}$ samples collected over two consecutive years enhances the robustness of seasonal analyses by reducing the influence of interannual variability in meteorological conditions and emission sources, thereby enabling identification of consistent and reproducible seasonal patterns in particle composition and toxicity [17]. However, no study has continuously collected $PM_{2.5}$ over two full years and examined its detailed biological effects in animal models.

Various studies have also examined metal components of $PM_{2.5}$, including Pb, Cu, Cd, and Ni [18]. For example, $PM_{2.5}$ analysis in Puerto Rico revealed higher levels of Ni and V in industrial areas, implicating metal pollution in local respiratory symptoms [19]. However, there remains a lack of integrated analyses linking year-round $PM_{2.5}$ composition with biological responses—particularly oxidative stress—and their interrelationships.

Neutrophils and macrophages express Toll-like receptors (TLRs) that recognize pathogen-associated molecular patterns such as lipopolysaccharide (LPS). TLR2 recognizes lipoproteins and glycolipids, while TLR4 triggers intracellular signaling upon LPS binding, leading to pro-inflammatory cytokine production [20]. We previously showed that murine neutrophils endocytose PM and that this process is diminished in TLR4-deficient mice [21]. We also reported that LPS attached to PM_{10} suppresses splenocyte immune responses [22] and that LPS levels bound to $PM_{2.5}$ strongly influence PM-induced immunosuppression [23]. These findings indicate that the quantity and nature of PM-adsorbed constituents critically shape immune responses.

$PM_{2.5}$ exposure is widely known to induce reactive oxygen species (ROS) [24–28]. Once deposited in the lungs, $PM_{2.5}$ generates ROS directly through redox-active components and indirectly through inflammatory cell activation, overwhelming antioxidant defenses and causing lipid, protein, and DNA damage [29]. ROS serves as a key upstream signal that activates pathways leading to cytokine production, including IL-6 and TNF-α. Our laboratory previously demonstrated that neutrophil endocytosis of 1 μm PM stimulates IL-6 and TNF-α release [21].

https://doi.org/10.3390/antiox15010089

In this study, we collected $PM_{2.5}$ continuously over two years from a single site in Japan and categorized samples into four seasons per year. We analyzed $PM_{2.5}$ composition and evaluated biological effects following intratracheal instillation in mice. We further examined correlations between seasonal $PM_{2.5}$ characteristics and ROS production.

2. Materials and Methods

2.1. Sampling and Preparation of $PM_{2.5}$

The sampling site was located in an urban residential area approximately 15 km southwest of central Tokyo [30]. Aerosol samples were collected by large cyclones (flow rates 1200 L/min) on the rooftop of a 22 m building at Keio University between February 2021 and February 2023, following previously described protocols [31,32]. $PM_{2.5}$ samples were collected for a total 10 samples, among which $PM_{2.5}$ samples collected twice between February and April 2021 were combined as PM-A1 to correspond to samples collected during the same period in 2022. All samples were suspended in PBS at 10 mg/mL.

2.2. Analysis of $PM_{2.5}$ Content

Collected particles were characterized using ion chromatography (Cl^-, $NO_3{}^-$, $SO_4{}^{2-}$, Na^+, $NH_4{}^+$, K^+, Mg^{2+}, Ca^{2+}), thermal–optical analysis for OC1–4 and EC1–3, high-performance liquid chromatography (HPLC) for polycyclic aromatic hydrocarbons (PAHs, including acenaphthene, fluorene, phenanthrene, anthracene, fluoranthene, pyrene, benz[a]anthracene, chrysene, benzo[b]fluoranthene, benzo[k]fluoranthene, benzo[a]pyrene, dibenz[a,h]anthracene, benzo[g,h,i]perylene, indeno[1,2,3-cd]pyrene), and ICP-MS for metals (Al, Si, Ti, V, Cr, Mn, Fe, Ni, Cu, Zn, Pb), following established methodologies [32,33]. Endotoxin levels were quantified using the manufacturer's protocol (Associates of Cape Cod).

Quality Assurance and Quality Control (QA/QC)

Quality assurance and quality control (QA/QC) procedures were implemented for all chemical analyses of $PM_{2.5}$ samples. Water-soluble ions (Cl^-, $NO_3{}^-$, $SO_4{}^{2-}$, Na^+, $NH_4{}^+$, K^+, Mg^{2+}, Ca^{2+}) were quantified by ion chromatography, and analytical accuracy was verified using certified reference material CRM#28 (Urban Aerosols, NIES, Tsukuba, Japan). Limits of detection (LOD) for each ion species were determined to be five times the standard deviation of replicate analyses of standard solutions, and the coefficients of variation for repeated measurements were below 7%.

Elemental concentrations were determined by inductively coupled plasma–mass spectrometry (ICP-MS) following microwave acid digestion. Quantification was performed using multi-point calibration curves, and analytical accuracy was assessed using certified reference materials, yielding recovery rates between 87% and 97%. Instrument calibration and blank corrections were routinely performed [32].

Carbonaceous fractions (OC and EC) were analyzed using a thermal–optical method following the IMPROVE protocol. PAHs were measured by HPLC. Endotoxin and β-glucan contents were determined using commercial assay kits according to the manufacturers' instructions. Detailed analytical procedures have been described previously [31].

2.3. Mice and Intratracheal Administration of $PM_{2.5}$

BALB/c, TLR2 KO, and TLR4 KO mice (male, 7–11 weeks old) were obtained from Japan SLC (Hamamatsu, Japan). $PM_{2.5}$ was suspended at 1 mg/mL in PBS and administered intratracheally (100 μg/100 μL/mouse) under 5% sevoflurane anesthesia. BALF was collected 24 h post-administration.

https://doi.org/10.3390/antiox15010089

2.4. Measurement of BAL Cell Number and ROS Production

BALF was collected by cannulating the trachea and gently instilling sterile PBS (1.0 mL per instillation) into the lungs. After centrifuging, BALF was separated into fluids and BAL cells. The fluids were applied for subsequent analysis. BAL cells were pelleted, resuspended, and counted. ROS production was assessed using a DCFH-DA assay (Dojindo, Kumamoto, Japan), with fluorescence measured on a plate reader following established protocols [34].

2.5. Flow Cytometry

BAL cells were stained with PE-anti-F4/80 and VioletFluor450-anti-Gr-1 (San Diego, CA, USA) at 4 °C for 30 min, washed, and analyzed using a CytoFLEX cytometer. Gating strategy was shown as Supplementary Figure S1.

2.6. Enzyme-Linked Immunosorbent Assay (ELISA)

BALF cytokines (IL-6, TNF-α, IL-1α, IL-12) were quantified using commercial ELISA kits (BioLegend, San Diego, CA, USA), following the manufacturer's instructions.

2.7. Pathology Analysis

Lungs were fixed, paraffin-embedded, sectioned at 5 μm, and stained with hematoxylin and eosin. Ten non-overlapping 200× fields were scored 0–4 for inflammation severity according to published criteria [35–37].

2.8. Statistics

Results are expressed as mean ± SD. Correlation analyses were performed to evaluate the relationships between $PM_{2.5}$ chemical components and biological endpoints, including BAL cellular responses, cytokine levels (IL-6, TNF-α, IL-1α, and IL-12), and ROS production. Pearson correlation was employed due to the study's focus on linear associations, while noting that potential non-linear relationships cannot be excluded and warrant further investigation in future studies. Statistical significance was assessed by one-way ANOVA with Fisher's LSD test, with $p < 0.05$ considered significant.

3. Results

3.1. $PM_{2.5}$ Collected During the Summer (PM-C) Showed Elevated Sulfur (S) and Reduced Calcium (Ca) and OCP Levels

As shown in Figure 1A, $PM_{2.5}$ was collected between February 2021 and February 2023 and classified into five seasonal periods (PM-A to PM-E), enabling inter-seasonal comparisons of particle composition. The proportions of major ionic components (Cl^-, NO_3^-, SO_4^{2-}, Na^+, NH_4^+, K^+, Mg^{2+}, Ca^{2+}) are summarized in Figure 1B. Among these, Ca^{2+} showed the highest relative abundance in PM-A1 (13.9%) and PM-A2 (14.7%), while SO_4^{2-} and NO_3^- consistently dominated the anionic fraction, together accounting for more than 60% across all periods. Crustal elements, including Fe (>17%) and Al (>26%), were also present at high proportions in all samples (Figure 1C).

Clear seasonal variation was observed in several components. During the summer period (PM-C), Ca concentrations tended to be lower (12.7% and 17.3%), whereas S concentrations were markedly higher (13.3% and 19.1%). Although Fe concentrations were generally higher in winter (PM-E) than in summer (PM-C) across both years, Al did not show a consistent seasonal pattern (Pearson correlation coefficient $r = -0.58$). Given the limited number of seasonal composite samples, seasonal trends were evaluated using descriptive statistics and exploratory correlation analysis.

https://doi.org/10.3390/antiox15010089

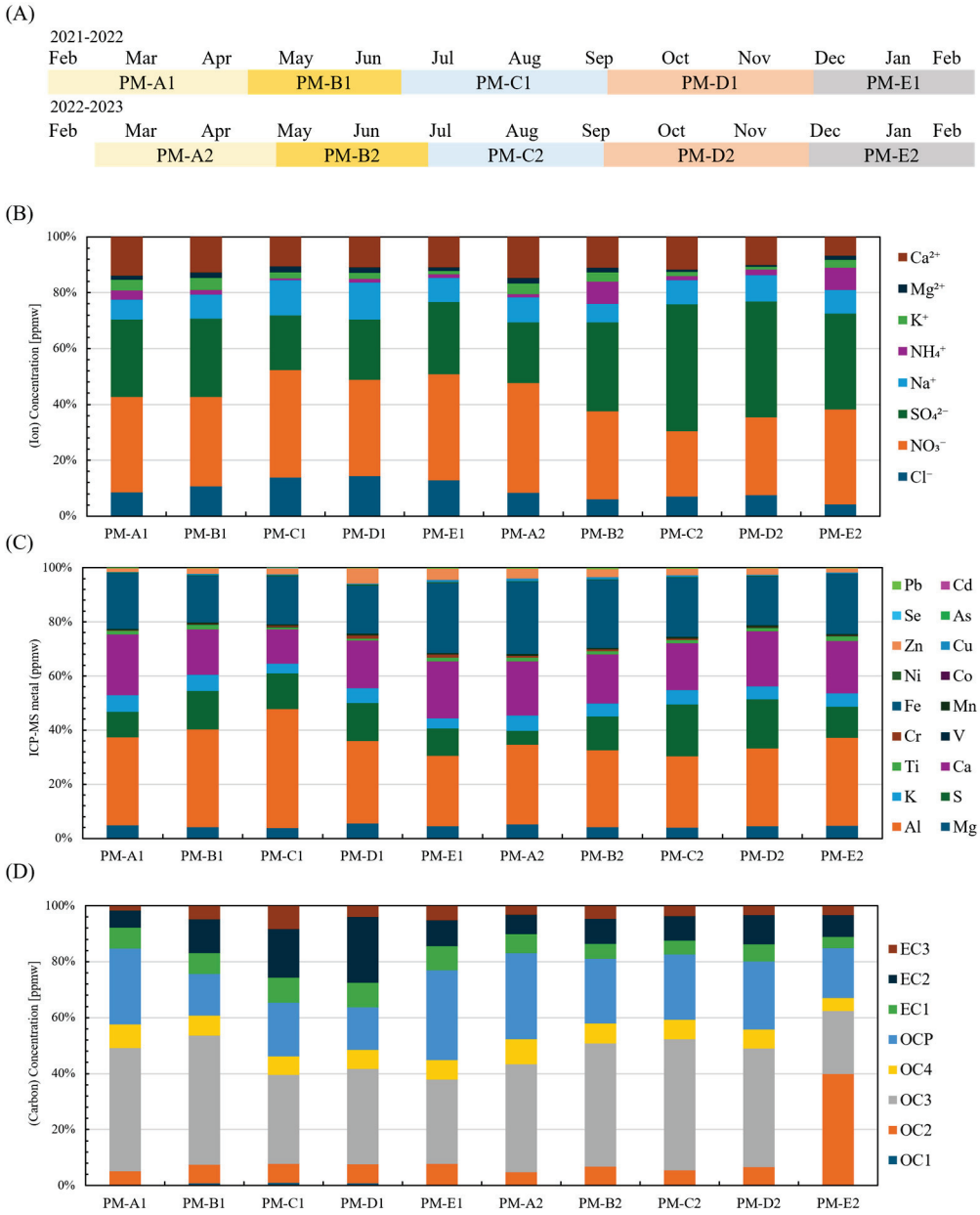

Figure 1. $PM_{2.5}$ collected during the summer (PM-C) showed elevated sulfur, reduced calcium, and decreased OCP levels. (**A**) Sampling periods for $PM_{2.5}$ collected from February 2021 to February 2023, divided into five seasonal periods per year (PM-A to PM-E). The numeral 1 after A to E indicates PM collected in 2021−2022 (PM-A1 to PM-E1), and 2 indicates PM collected in 2022−2023 (PM-A2 to PM-E2). (**B**) Relative proportions of major water-soluble ions (Cl^-, NO_3^-, SO_4^{2-}, Na^+, NH_4^+, K^+, Mg^{2+}, Ca^{2+}) in each $PM_{2.5}$ sample. (**C**) Elemental composition of $PM_{2.5}$ samples, including crustal elements and heavy metals. (**D**) Carbonaceous fractions of $PM_{2.5}$ determined by thermal–optical analysis, showing the distribution of organic carbon (OC1–OC4) and elemental carbon (EC1–EC3).

Figure 1D shows the distribution of carbonaceous fractions determined by thermal–optical analysis. Organic carbon (OC, >65.3%) accounted for a larger proportion than elemental carbon (EC, <34.7%), with OC3 being the most abundant fraction across seasons (22.5–47%). Pyrolyzed organic carbon (OCP) exhibited a modest increase during autumn and winter.

https://doi.org/10.3390/antiox15010089

3.2. Intratracheal Administration of $PM_{2.5}$ to Mice Increased BAL Cell Numbers and ROS Production

To evaluate the biological effects of $PM_{2.5}$, each seasonal sample was administered intratracheally to mice, and BAL cell counts and ROS production were quantified. Although some variability was observed across sampling periods, $PM_{2.5}$ exposure consistently increased BAL cell numbers throughout the entire two-year collection period (Figure 2A).

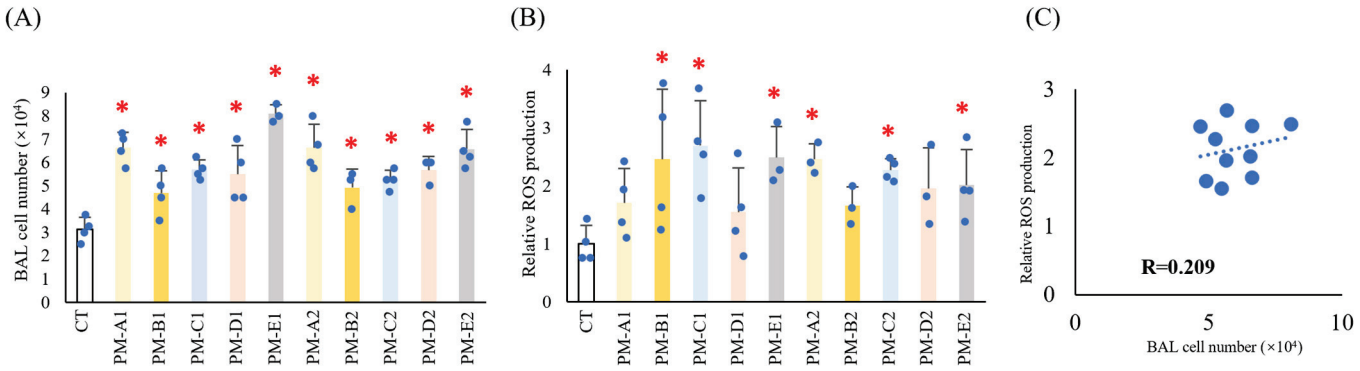

Figure 2. Intratracheal administration of $PM_{2.5}$ to mice increased BAL cell numbers and ROS production. $PM_{2.5}$ was collected from February 2021 to February 2023 as indicated. BALB/c mice were intratracheally administered with PBS (CT) or $PM_{2.5}$ (100 μg/100 μL/mouse, n = 3–4) and dissected 24 h after administration. (**A**,**B**) BALF was collected, and BAL cell numbers were counted (**A**) and ROS production was measured using a DCFH-DA ROS Assay Kit (**B**). (**C**) The correlation between BAL cell numbers and ROS production, along with the correlation coefficient, was analyzed. The CT group (PBS, control) was set as 1.0. * $p < 0.05$ compared with CT.

ROS production was also induced by all $PM_{2.5}$ samples, with particularly notable increases during PM-C and PM-E in both years (Figure 2B; PM-C1 and PM-C2, PM-E1 and PM-E2).

Correlation analysis revealed a weak (r = 0.21) but positive association between BAL cell numbers and ROS production (Figure 2C). Inclusion of the PBS-treated control group (CT) further strengthened this correlation (Supplementary Figure S2A), indicating that ROS generation is proportional to the magnitude of cellular infiltration induced by seasonal $PM_{2.5}$

3.3. $PM_{2.5}$ Administration Increased the Population of Neutrophil in BAL Cells

As shown in Figure 3A, intratracheal administration of seasonal $PM_{2.5}$ increased the total BAL cell numbers and markedly altered the composition of immune cell populations in the lung. Flow cytometric analysis demonstrated a clear increase in Gr-1$^+$ neutrophils following $PM_{2.5}$ exposure, accompanied by a relative decrease in F4/80$^+$ macrophages compared with PBS-treated controls. These findings indicate that $PM_{2.5}$ induces a shift toward neutrophil-dominant infiltration in the airways. The remaining cells, categorized as "other cells," are expected to include lymphocytes and alveolar macrophages, with minor contributions from eosinophils and monocytes.

Correlation analysis (r = 0.47) further revealed that the proportion of Gr-1$^+$ neutrophils was positively associated with ROS production (Figure 3B), suggesting that neutrophils are a major contributor to PM-induced oxidative activity. In contrast, the proportion of F4/80$^+$ macrophages showed no correlation (r = −0.13) with ROS (Figure 3C), consistent with the observation that macrophage abundance decreases following PM exposure.

https://doi.org/10.3390/antiox15010089

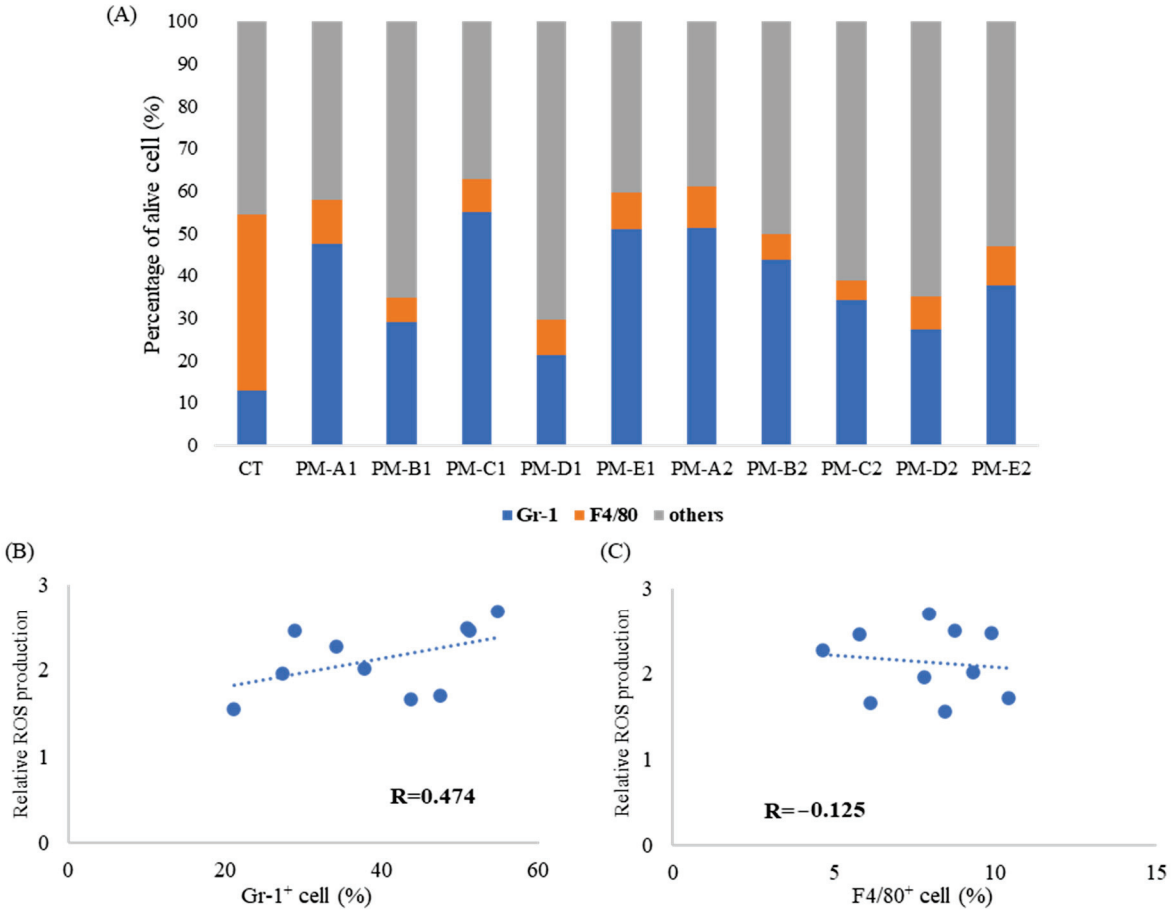

Figure 3. $PM_{2.5}$ administration increased the population of neutrophil in BAL cells. PBS (CT) or PM shown in Figure 1A (100 μg/100 μL/mouse, *n* = 3–4) was administered intratracheally to BALB/c mice, and the mice were sacrificed 24 h after administration. (**A**) BAL cells were stained with each antigen-specific antibody and then analyzed by flow cytometry. The results show the proportions of $Gr\text{-}1^+$ cells, $F4/80^+$ cells, and remaining viable cells. (**B**,**C**) Correlations between $Gr\text{-}1^+$ cells (**B**) or $F4/80^+$ cells (**C**) and ROS production were analyzed. R represents the correlation coefficient.

When the PBS control group (CT) was included, the positive correlation between neutrophil proportion and ROS production became even stronger (Supplementary Figure S2B). Under alternative analytical conditions, however, the correlation between neutrophils and ROS was reversed (Supplementary Figure S2C), highlighting the sensitivity of correlation patterns to data normalization and analytical parameters.

3.4. $PM_{2.5}$ Administration Induced Inflammatory Cytokine Production

To assess the inflammatory responses triggered by seasonal $PM_{2.5}$, cytokine levels in BALF were quantified by ELISA. IL-6 and TNF-α levels were elevated following nearly all $PM_{2.5}$ exposures, although the degree of induction varied across seasonal samples (Figure 4A). In contrast, IL-1α levels increased exclusively in response to PM-A samples in both years, indicating a season-specific pattern of IL-1α release. IL-12 levels remained largely unchanged regardless of $PM_{2.5}$ exposure.

Correlation analysis revealed positive associations between ROS production and the levels of IL-6 (r = 0.30) and TNF-α (r = 0.46), supporting the concept that oxidative stress drives downstream pro-inflammatory cytokine production. Conversely, IL-1α and IL-12 showed no meaningful correlation with ROS (r = 0.15 and 0.01, respectively), suggesting that their regulation is governed by distinct upstream mechanisms independent of oxidative activity (Figure 4B).

https://doi.org/10.3390/antiox15010089

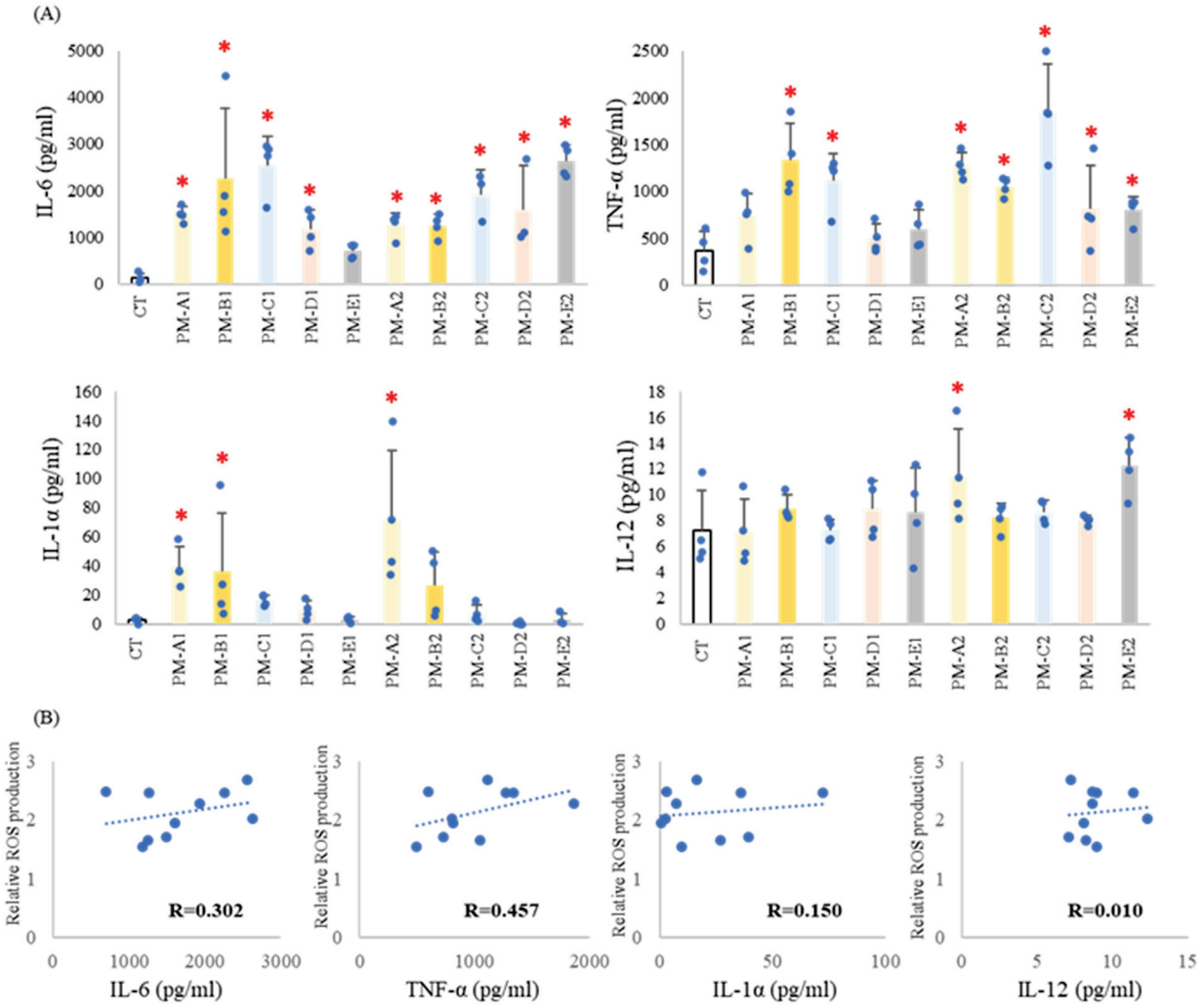

Figure 4. $PM_{2.5}$ administration induced inflammatory cytokine production. PBS (CT) or $PM_{2.5}$ (100 μg/100 μL/mouse, n = 3–4) were intratracheally administered to BALB/c mice, and mice were sacrificed 24 h after administration. BALF was collected, and cytokine levels were measured by ELISA. (**A**) The results showed IL-6, TNF-α, IL-1α, and IL-12 levels in BALF. CT, control group; * $p < 0.05$ compared with PBS. (**B**) The correlation between the mean cytokine concentration and ROS production in each group was analyzed. R represents the correlation coefficient.

Collectively, these findings indicate that most cytokine responses to $PM_{2.5}$ align with patterns of ROS induction, while IL-1α behaves uniquely, showing both seasonal specificity and limited dependence on oxidative signaling pathways.

3.5. Mineral and Carbonaceous $PM_{2.5}$ Components Drive Distinct Cellular Responses

Correlation analysis revealed that specific chemical constituents of $PM_{2.5}$ were closely associated with distinct biological outcomes (Table 1). BAL cell counts showed a moderate positive correlation with nitrate (NO_3^-; r = 0.55) and a strong positive correlation with PAHs (r = 0.72), indicating that nitrate-rich and combustion-derived particles promote cellular infiltration into the airways.

ROS production displayed a moderate inverse correlation with ammonium (NH_4^+; r = –0.41) and a moderate positive correlation with BAL cell counts (r = 0.21), suggesting that reductions in secondary inorganic aerosol components coincide with increases in PM-induced oxidative activity.

https://doi.org/10.3390/antiox15010089

Table 1. Pearson correlation matrix between $PM_{2.5}$ chemical components and pulmonary oxidative and inflammatory responses.

	Cl^-	NO_3^-	SO_4^{2-}	Na^+	NH_4^+	K^+	Mg^{2+}	Ca^{2+}	BAL CELL
BAL CELL	0.11	0.55	−0.25	−0.13	−0.09	−0.23	−0.12	−0.04	
ROS	0.17	−0.08	−0.05	0.20	−0.41	0.23	0.25	0.25	0.21
IL-6	−0.23	−0.16	0.16	0.17	0.16	0.17	0.09	−0.39	−0.40
TNF-α	−0.30	−0.48	0.41	−0.19	−0.17	0.15	−0.13	0.31	−0.48
IL-1α	−0.06	0.40	−0.45	−0.25	−0.12	0.80	0.51	0.81	−0.03
IL-12	−0.43	0.19	0.02	−0.10	0.34	0.22	0.11	−0.28	0.22
	Mg	Al	S	K	Ca	Ti	V	Cr	Mn
BAL CELL	0.30	−0.27	−0.58	−0.29	0.58	0.04	0.65	0.32	0.29
ROS	−0.57	0.53	0.19	−0.02	−0.71	0.14	−0.35	−0.19	−0.59
IL-6	−0.45	0.70	0.30	−0.08	−0.56	0.26	−0.24	−0.62	−0.55
TNF-α	−0.57	0.04	0.29	0.18	−0.41	0.26	−0.06	−0.29	−0.22
IL-1α	0.24	0.12	−0.69	0.53	0.13	0.25	0.14	−0.15	−0.04
IL-12	0.37	−0.22	−0.38	0.17	0.20	0.43	0.72	−0.07	0.32
	Fe	Co	Ni	Cu	Zn	As	Se	Cd	Pb
BAL CELL	0.53	0.57	0.16	0.21	0.15	−0.46	−0.39	0.04	−0.15
ROS	−0.27	−0.36	−0.15	0.14	−0.24	−0.25	−0.07	−0.14	−0.04
IL-6	−0.51	−0.60	−0.51	−0.59	−0.66	0.00	−0.14	−0.08	−0.47
TNF-α	0.07	−0.40	−0.26	0.31	−0.34	0.09	0.13	−0.32	0.34
IL-1α	0.33	0.15	−0.23	0.41	−0.04	−0.17	−0.64	−0.76	0.21
IL-12	0.42	0.38	−0.14	0.14	0.08	−0.15	−0.19	−0.01	0.14
	OC1	OC2	OC3	OC4	OCP	EC1	EC2	EC3	OC	EC
BAL CELL	−0.34	0.21	−0.57	0.10	0.69	0.22	−0.33	−0.16	0.22	−0.22
ROS	0.42	−0.20	0.27	0.05	−0.31	0.08	0.10	0.53	−0.21	0.21
IL-6	0.49	0.51	−0.17	−0.53	−0.64	−0.32	0.05	0.29	−0.03	0.03
TNF-α	−0.14	−0.21	0.54	0.17	−0.04	−0.38	−0.29	0.12	0.26	−0.26
IL-1α	−0.12	−0.34	0.35	0.78	0.29	0.13	−0.30	−0.22	0.24	−0.24
IL-12	−0.22	0.69	−0.48	−0.29	−0.04	−0.49	−0.24	−0.29	0.35	−0.35

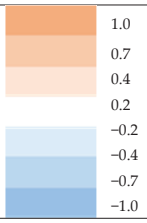

Values represent Pearson correlation coefficients (r). Positive and negative correlations are indicated by warm and cool colors, respectively. Color shading indicates the strength and direction of correlations, with orange representing positive correlations and blue representing negative correlations. Darker shading corresponds to higher absolute correlation coefficients (0.7, 0.4, and 0.2). Abbreviations: bronchoalveolar lavage (BAL), reactive oxygen species (ROS), interleukin-6 (IL-6), tumor necrosis factor-α (TNF-α), interleukin-1α (IL-1α), interleukin-12 (IL-12), organic carbon (OCP), elemental carbon (EC), and pyrolyzed organic carbon (OCP).

Cytokine responses varied substantially by chemical species. IL-6 and IL-12 lacked strong correlations with any major constituent, implying that their induction reflects integrative inflammatory signaling rather than dependence on a single chemical driver. In contrast, TNF-α exhibited a strong negative correlation with PAHs (r = –0.62), suggesting that PAH-rich particles may suppress TNF-α production in this model.

Notably, IL-1α showed the most distinct pattern among cytokines: it strongly correlated with multiple mineral ions, including K^+ (r = 0.80), Ca^{2+} (r = 0.81), and Mg^{2+} (r = 0.51). These findings indicate that mineral-rich particles—typically enriched in primary, crustal, and combustion-derived PM—serve as potent inducers of IL-1α release, distinguishing them from secondary inorganic components such as sulfate and ammonium.

3.6. Seasonal Peaks in PAHs Are Reproducible Across Years, Whereas Endotoxin Levels Fluctuate Substantially

Analysis of seasonal PAH concentrations revealed a highly reproducible pattern across the two-year sampling period (Table 2). In both years, PAH levels were consistently highest during period E, with moderately elevated concentrations during period A. Periods B and C repeatedly showed lower PAH abundance, demonstrating stable seasonal differences in the contribution of combustion-derived $PM_{2.5}$ components.

https://doi.org/10.3390/antiox15010089

Table 2. PAH and endotoxin levels in $PM_{2.5}$ samples collected across different seasons.

A1.	PM-A1	PM-B1	PM-C1	PM-D1	PM-E1	PM-A2	PM-B2	PM-C2	PM-D2	PM-E2
PAHs (ng/mg)	11.8	7.9	7.5	10.5	17.9	8.8	11.2	9.1	12.9	15.4
Endotoxin (EU/mg)	4.2	3.5	1.1	3.1	2.9	3.1	12.4	6.6	6.7	2.3

Abbreviation: polycyclic aromatic hydrocarbons (PAHs).

In contrast, endotoxin levels displayed pronounced interannual variability. While seasons such as A and D showed comparable endotoxin levels between the two years, periods B and C differed markedly, with substantially higher endotoxin abundance observed in the second year. These findings indicate that biologically derived constituents of $PM_{2.5}$, such as endotoxin, are more sensitive to year-to-year environmental fluctuations than chemically derived species like PAHs.

Together, the reproducible PAH pattern and the variable endotoxin levels highlight the differing environmental drivers of combustion-related versus biologically derived PM components.

3.7. PAH-Rich $PM_{2.5}$ Enhances Cellular Infiltration While Endotoxin Drives Oxidative and Pro-Inflammatory Responses

Correlation analyses demonstrated that PAH-rich $PM_{2.5}$ was strongly associated with enhanced cellular infiltration into the airways. BAL cell counts showed a robust positive correlation with PAH concentrations (r = 0.72), indicating that combustion-derived particles are potent drivers of inflammatory cell recruitment. In contrast, endotoxin levels exhibited a moderate negative correlation with BAL cell counts (r = –0.45), suggesting that endotoxin-rich $PM_{2.5}$ does not promote cellular infiltration to the same extent as PAH-rich samples (Table 3).

Table 3. Pearson correlation analysis between $PM_{2.5}$ PAH and endotoxin levels with *inflammatory or oxidative stress indicators*.

	PAHs	Endotoxin
BAL CELL	**0.72**	**−0.45**
ROS	**−0.20**	**−0.50**
IL-6	**−0.25**	**−0.28**
TNF-α	**−0.62**	**0.22**
IL-1α	**−0.50**	**−0.03**
IL-12	**0.21**	**−0.24**

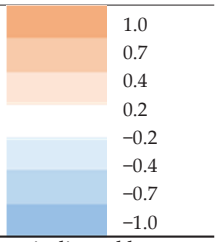

Values represent Pearson correlation coefficients (r). Positive and negative correlations are indicated by warm and cool colors, respectively. Color shading indicates the strength and direction of correlations, with orange representing positive correlations and blue representing negative correlations. Darker shading corresponds to higher absolute correlation coefficients (0.7, 0.4, and 0.2). Abbreviations: polycyclic aromatic hydrocarbons (PAHs), bronchoalveolar lavage (BAL), reactive oxygen species (ROS), interleukin-6 (IL-6), tumor necrosis factor-α (TNF-α), interleukin-1α (IL-1α), and interleukin-12 (IL-12).

ROS production showed a moderate negative correlation with endotoxin levels (r = –0.50), consistent with the idea that endotoxin-containing PM may trigger oxidative responses through pathways independent of cellular infiltration. Pro-inflammatory cytokines, including IL-6 and IL-12, exhibited only weak negative correlations with both PAHs and endotoxin, suggesting that their induction reflects integrated inflammatory signaling rather than dependence on specific PM constituents.

TNF-α displayed a strong negative correlation with PAHs (r = –0.62), supporting the hypothesis that PAH-rich particles suppress TNF-α production, a trend consistent with

earlier analytical findings. IL-1α exhibited a moderate negative correlation with PAHs (r = –0.50) and no meaningful association with endotoxin, indicating that its regulation is driven predominantly by mineral-rich primary particles rather than combustion-related or biologically derived components.

Overall, these results highlight divergent roles of PAHs and endotoxin in shaping pulmonary responses: PAHs primarily enhance cellular infiltration, whereas endotoxin influences oxidative and select cytokine pathways through distinct mechanisms.

3.8. BAL Cell Counts and ROS Production Induced by $PM_{2.5}$ Administration in TLR4 KO Mice Were Lower than Those in WT Mice

Because PM-C2 induced the highest TNF-α production among all $PM_{2.5}$ samples, this sample was selected for downstream mechanistic analyses. PM-C2 was intratracheally administered to BALB/c (WT), TLR2 KO, and TLR4 KO mice to evaluate the involvement of TLR signaling pathways in PM-induced pulmonary inflammation.

PM-C2 increased BAL cell counts and ROS production in all mouse strains; however, both responses were markedly attenuated in TLR4 KO mice compared with WT controls (Figure 5A). This partial reduction indicates that TLR4 contributes substantially, but not exclusively, to PM-induced cellular infiltration and oxidative activation.

Histopathological examination revealed PM-induced inflammatory changes throughout multiple lung regions, including bronchioles and alveolar spaces (Figure 5B). Interestingly, despite showing reduced BAL cell counts and ROS production, TLR4 KO mice exhibited higher inflammation scores—specifically increased hemorrhage, bronchiolitis, and inflammatory cell accumulation—relative to WT mice (Figure 5C).

These findings suggest a dual role for TLR4: while it facilitates PM-induced inflammatory activation, it may also contribute to resolution or containment of lung injury. Loss of TLR4 thus reduces acute cellular and oxidative responses but predisposes the lung to dysregulated or prolonged inflammation following $PM_{2.5}$ exposure.

3.9. IL-6 and TNF-α Levels in TLR4 KO Mice Were Lower than Those in WT Mice

To further examine the contribution of the TLR4 signaling pathway to $PM_{2.5}$-induced inflammation, IL-6 and TNF-α levels were quantified in the BALF of WT and TLR4 KO mice following PM-C2 administration. Both cytokines were markedly reduced in TLR4 KO mice compared with WT controls (Figure 6), reinforcing the conclusion that TLR4 plays a key role in promoting pro-inflammatory cytokine responses to $PM_{2.5}$.

These findings, together with the reduced BAL cell infiltration and ROS production observed in TLR4 KO mice, demonstrate that TLR4 regulates multiple facets of the pulmonary inflammatory response. However, the heightened histopathological inflammation observed in TLR4 KO mice (Section 3.8) suggests that TLR4 also contributes to injury resolution, indicating a dual and context-dependent function during PM-induced lung inflammation.

https://doi.org/10.3390/antiox15010089

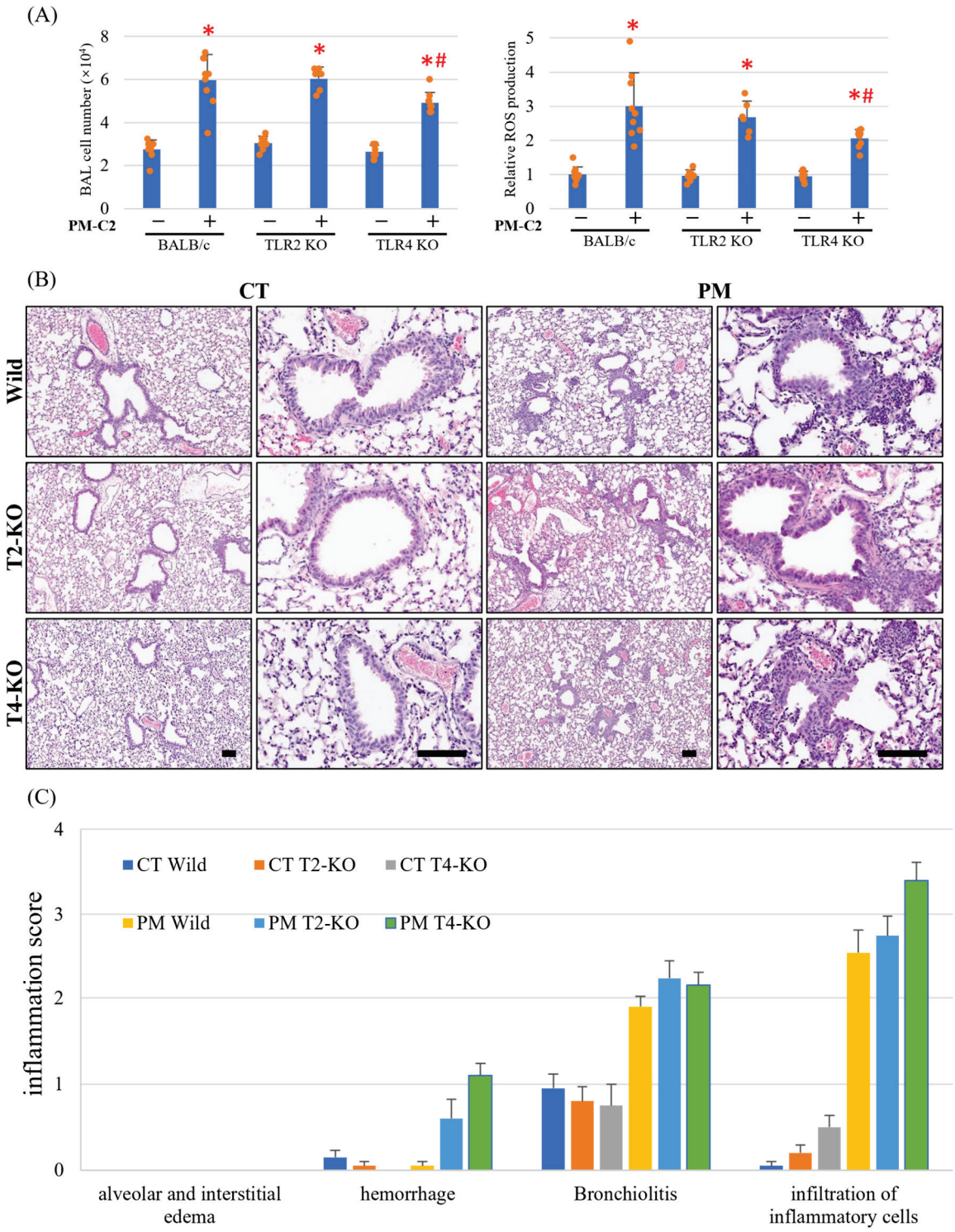

Figure 5. BAL cell counts and ROS production induced by $PM_{2.5}$ administration in TLR4 KO mice were lower than those in WT mice. PBS (CT) or PM-C2 (100 μg/100 μL per mouse) was intratracheally administered to BALB/c, TLR2 KO, and TLR4 KO mice, and the mice were dissected 24 h after administration. (**A**) BALF was collected, BAL cell numbers were counted, and ROS production was measured using the DCFH-DA ROS Assay Kit. The results showed the relative fluorescence intensity of ROS production. (**B**,**C**) Lung samples were fixed and stained with hematoxylin and eosin. Representative photo is shown including black scale bar (200 μm). The severity of inflammation was scored in 10 fields of view, averaged, and summarized as a bar graph with error bars. Pathological images and graphs presented here are from a representative mouse in each experimental group (**C**). * $p < 0.05$ compared with CT of each mouse strain; # $p < 0.05$ compared with PM-C2-administered WT. WT;BALB/c mouse.

https://doi.org/10.3390/antiox15010089

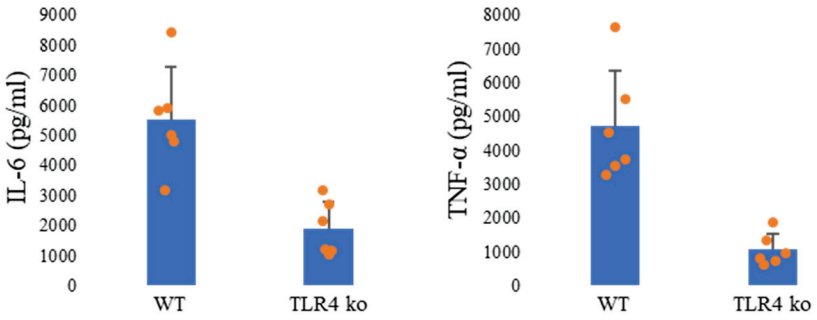

Figure 6. IL-6 and TNF-α levels in TLR4 KO mice were lower than those in WT mice. PBS (CT) or PM-C2 (100 μg/100 μL/mouse, *n* = 6) was intratracheally administered to BALB/c or TLR4 KO mice, and the mice were dissected 24 h after administration. BALF was collected, and IL-6 and TNF-α levels were measured by ELISA. WT;BALB/c mouse.

4. Discussion

Airborne PM has emerged as a significant environmental issue because of its adverse effects on human health, which fluctuate with seasonal changes and human activities. Although monitoring efforts commonly emphasize PM concentrations, the chemical makeup of these particles is equally critical [38].

In this study, we systematically analyzed $PM_{2.5}$ collected over two consecutive years from a single urban site in Japan and demonstrated that both its chemical composition and biological effects varied markedly by season. Seasonal fluctuations in $PM_{2.5}$ characteristics, including oxidative potential and toxicity, have been widely reported in previous studies [12,13]. Consistent with these reports, we observed clear seasonal patterns in the present work, including elevated sulfur levels in summer and increased PAH concentrations in winter [39]. Importantly, these seasonal trends are consistent with observations reported in other regions outside Japan. Studies conducted in Europe, North America, and East Asia have similarly shown higher contributions of secondary sulfate in summer and increased levels of PAHs and combustion-related components during winter, reflecting enhanced photochemical activity in warmer seasons and the accumulation of combustion emissions under stagnant meteorological conditions in colder months [40]. These parallels suggest that the seasonal variability observed in the present study reflects common atmospheric processes rather than region-specific phenomena. These differences likely reflect seasonal variations in secondary aerosol formation and the accumulation of combustion-derived pollutants.

It is well investigated that $PM_{2.5}$ administration induces systemic inflammation and ROS production [41]. Biologically, $PM_{2.5}$ collected in summer (PM-C) and winter (PM-E) induced the highest levels of ROS production and BAL cell infiltration. Combustion-derived components such as PAHs and elemental carbon (EC) possess strong intrinsic redox activity, which contributes to ROS generation and oxidative stress in lung tissue [26,27]. The correlation analysis further suggested that multiple chemical constituents, including nitrates, vanadium, iron, and OCP fractions, are involved in shaping $PM_{2.5}$-induced inflammatory responses. Notably, the direction and magnitude of these correlations were sensitive to the normalization strategy applied, as shown in Supplementary Figure S2. This analytical sensitivity underscores the need for cautious interpretation of correlation strength and direction and supports the use of these analyses primarily as exploratory and hypothesis-generating rather than confirmatory. Although individual components such as PAHs and mineral constituents were analyzed separately in this study, interactive or synergistic effects among $PM_{2.5}$ components may further modulate toxicity and warrant investigation in future studies. Mechanistically, several of the identified constituents have been implicated in $PM_{2.5}$-induced inflammatory responses in previous studies. Transition

https://doi.org/10.3390/antiox15010089

metals such as iron and vanadium can catalyze redox reactions, leading to excessive ROS generation and activation of oxidative stress-responsive signaling pathways. PAHs and carbonaceous fractions, including EC and organic carbon, are known to induce epithelial injury and macrophage activation through both oxidative and receptor-mediated mechanisms, thereby promoting the release of pro-inflammatory cytokines and chemokines. These findings underscore the importance of particle composition, rather than mass concentration alone, in determining the health effects of ambient $PM_{2.5}$. While $PM_{2.5}$ mass is commonly used as a regulatory metric, our results support the growing body of evidence that specific chemical constituents and their combinations play a decisive role in driving biological responses. Such compositional insights may contribute to more refined risk assessment strategies and targeted mitigation policies aimed at reducing the most toxic components of ambient particulate matter.

A strong association was observed between ROS levels and the proportion of neutrophils in BAL cells. Neutrophils are known to be major sources of ROS in PM-induced pulmonary inflammation [21], and excessive ROS can activate redox-sensitive transcription factors such as NF-κB, leading to the production of pro-inflammatory cytokines including IL-6 and TNF-α [28,42]. In line with these mechanisms, PM-C2, one of the samples with the strongest ROS-inducing capacity, elicited the highest levels of TNF-α. In addition, PAHs strongly correlated with BAL cell counts in the present study. PAHs are known to activate the aryl hydrocarbon receptor (AhR) and can be enzymatically converted into redox-active quinone intermediates, thereby amplifying oxidative stress and inflammatory signaling [7,43]. Our results support the notion that $PM_{2.5}$-induced oxidative stress and neutrophil-driven inflammation are central mechanisms contributing to pulmonary injury, highlighting the importance of chemical composition in shaping these biological responses. It should be noted that ambient $PM_{2.5}$ represents a complex mixture of multiple PAH species rather than isolated compounds, and human exposure occurs predominantly under such mixed conditions. While certain PAHs classified as Group B2 by the U.S. EPA exhibit higher toxic potency at the individual compound level, the present study was designed to evaluate the integrated biological effects of environmentally relevant PAH mixtures within seasonal $PM_{2.5}$ samples. Our findings therefore reflect the combined influence of co-existing PAHs and other particle-associated components, which may interact to modulate oxidative stress and inflammatory responses. This mixture-based perspective is particularly relevant for assessing real-world health effects of ambient particulate matter.

Although intracellular ROS production was assessed using DCFH-DA, a widely applied probe for oxidative stress, this method does not distinguish between specific ROSs and their cellular sources. Thus, the observed signals should be interpreted as an index of overall oxidative burden rather than individual ROS. Given that $PM_{2.5}$ components such as transition metals and organic compounds can generate distinct ROS through different mechanisms, future studies employing more specific probes or complementary approaches will be necessary to delineate the precise ROS and cellular origins involved.

Previous studies have identified TLR4 as a key receptor mediating the recognition of environmental particles and subsequent pro-inflammatory signaling, primarily through the activation of NF-κB and ROS-generating pathways [42,44]. To further investigate the involvement of innate immune signaling pathways in PM-driven inflammation, we compared the effects of $PM_{2.5}$ exposure in wild-type, TLR2-deficient, and TLR4-deficient mice. TLR4 is known to recognize pathogen-associated molecules such as LPS, as well as environmental pollutants including PAHs and certain metals [36,42]. In our study, TLR4 knockout mice exhibited significantly lower BAL cell counts, ROS production, and cytokine levels than wild-type mice, supporting the idea that TLR4 partially mediates the inflammatory response to $PM_{2.5}$.

https://doi.org/10.3390/antiox15010089

Interestingly, histopathological analysis revealed more severe inflammatory changes in TLR4-deficient mice compared with wild-type animals, despite reduced BAL cellularity and cytokine levels. This apparent paradox is consistent with previous studies demonstrating dual roles for TLR4, not only as a pro-inflammatory receptor but also as a critical regulator of inflammation resolution and tissue protection [45,46]. In the absence of TLR4 signaling, impaired resolution processes—such as defective clearance of damaged cells, delayed removal of inhaled particles, or dysregulated termination of inflammatory signaling—may contribute to persistent tissue injury [47]. In addition, TLR4 has been implicated in maintaining epithelial barrier integrity and coordinating appropriate cell death pathways, including apoptosis versus necrotic or lytic forms of cell death. Disruption of these processes could exacerbate local tissue damage and histopathological inflammation, even in the context of attenuated cytokine production.

Collectively, these findings suggest that TLR4 plays a dual role in pulmonary responses to $PM_{2.5}$, contributing both to the initiation of inflammatory signaling and to its subsequent resolution. Consequently, TLR4 deficiency may predispose the lung to dysregulated or non-resolving inflammation, resulting in enhanced histopathological injury despite reduced conventional inflammatory readouts.

While the chemical composition of $PM_{2.5}$ is known to vary spatially depending on emission sources and meteorological conditions, the present study analyzed $PM_{2.5}$ samples collected from a single urban area. Consequently, the biological responses observed here may differ in regions with distinct particle compositions, and caution should be exercised when extrapolating these findings to other geographical settings.

Although intratracheal instillation offers a well-controlled and reproducible exposure paradigm, it does not fully recapitulate real-life inhalation exposure. In particular, differences in particle deposition patterns, clearance kinetics, and the temporal dynamics of inflammatory responses should be considered when extrapolating these findings to environmental conditions. Accordingly, the seasonal differences observed in this study are not directly predictive of health effects associated with airborne inhalation exposure and should be interpreted in the context of these limitations.

One of the key findings of this study is the strong positive correlation between IL-1α—an alarmin derived from epithelial cells and macrophages that induces particulate matter-induced pulmonary inflammation—and several mineral components, such as K, Ca, and Mg. These species are enriched in combustion-derived primary particles and are typically more abundant in winter $PM_{2.5}$, reflecting biomass burning, soil resuspension, and mixed combustion sources. In fact, $PM_{2.5}$ induced the highest levels of IL-1α in winter. The preferential association of IL-1α with these components suggests that mineral-rich primary particles may be particularly potent in triggering IL-1α-mediated alarmin responses. This interpretation is consistent with mechanistic studies demonstrating that micro- and nanoparticles, including silica, can induce alveolar macrophage death and subsequent IL-1α release, thereby initiating acute lung inflammation [48,49]. Human exposure studies have similarly shown that inhalation of organic dust elevates BALF IL-1α [50], further supporting the notion that particle composition critically determines IL-1α-dependent pathways.

In contrast, IL-1α showed inverse correlations with secondary inorganic aerosol components such as sulfate and sulfur, which are more abundant in summer and represent photochemically generated secondary particles. This negative association suggests that secondary inorganic aerosols have comparatively weak capacity to induce IL-1α release, despite contributing substantially to $PM_{2.5}$ mass in warm seasons. Such seasonal divergence in IL-1α responsiveness is consistent with prior observations that winter $PM_{2.5}$

exhibits stronger oxidative and inflammatory potential than summer $PM_{2.5}$, largely due to differences in carbonaceous and metal constituents [51].

IL-1α is produced by multiple lung cell types, most notably epithelial cells and alveolar macrophages, each contributing differently to particle-induced lung injury. Epithelial-derived IL-1α primarily functions as an alarmin, being rapidly released upon cellular stress or damage, whereas macrophage-derived IL-1α reflects active inflammatory signaling following particle phagocytosis. The distinct seasonal behavior of IL-1α observed in this study may therefore reflect differences in the relative contribution of these cellular sources, potentially driven by seasonal variability in $PM_{2.5}$ composition and toxicity. Although the present study does not directly resolve the cellular origin of IL-1α, this distinction represents an important mechanistic consideration and warrants further investigation in future studies.

The identification of IL-1α as a sensitive and seasonally responsive marker of $PM_{2.5}$-induced lung inflammation may have important translational implications for environmental health research. As an alarmin predominantly released upon epithelial injury, IL-1α could serve as an early sentinel indicator reflecting the inflammatory potential of particulate matter before overt immune cell recruitment becomes evident. From a human exposure perspective, seasonal variation in IL-1α responses may aid in risk stratification by highlighting periods during which specific $PM_{2.5}$ compositions exert heightened biological activity. Furthermore, IL-1α-centered responses may provide a mechanistic bridge between particle composition and downstream inflammatory outcomes, supporting its potential utility as a biomarker in exposure assessment studies. Future investigations integrating human biomonitoring data, such as airway or circulating IL-1α levels, together with compositional analyses of ambient PM, would help clarify its applicability for evaluating population-level susceptibility and seasonal health risks associated with air pollution.

Taken together, these findings support a model in which IL-1α functions as an early sentinel of lung injury preferentially activated by combustion-related, mineral-rich primary particles, whereas secondary inorganic aerosols exert modest effects on this alarmin pathway. Because IL-1α not only signals tissue injury but also amplifies downstream inflammatory cascades, the enhanced activation of IL-1α by winter $PM_{2.5}$ may represent a key mechanism linking seasonal variations in PM composition to the worsening of respiratory symptoms. These results highlight the importance of particle composition—beyond mass concentration alone—in determining the health effects of ambient $PM_{2.5}$ and underscore IL-1α as a sensitive biomarker for evaluating the toxicity of primary combustion particles.

5. Conclusions

Taken together, our findings provide new insight into how seasonal shifts in $PM_{2.5}$ composition shape oxidative stress, neutrophil-mediated inflammation, and innate immune signaling in the lungs. By integrating two full years of data on chemically characterized $PM_{2.5}$ with in vivo functional analyses, this study highlights the importance of particle composition, rather than mass concentration alone, in determining biological toxicity.

PAH-rich particles, which consistently peak in winter, strongly promoted cellular infiltration, whereas mineral-rich primary particles showed a distinct capacity to induce IL-1α, an early alarmin that amplifies downstream inflammatory cascades. In contrast, secondary inorganic aerosols contributed minimally to IL-1α-driven pathways, underscoring composition-specific biological effects among seasonal $PM_{2.5}$ species.

Mechanistically, ROS generation tightly correlated with neutrophil recruitment and cytokine production, positioning oxidative stress as a key upstream driver of PM-induced inflammation. Experiments using TLR-deficient mice further demonstrated that TLR4 partially mediates PM-induced cellular and cytokine responses, while simultaneously

https://doi.org/10.3390/antiox15010089

influencing the resolution of tissue injury, revealing a dual, context-dependent role for this receptor.

Overall, this work emphasizes the need for the consideration of seasonal and compositional variability in regulatory and health-risk frameworks for $PM_{2.5}$. Such mechanistic insights may also inform the development of targeted interventions that mitigate PM-induced oxidative lung injury, particularly during high-risk winter pollution events.

Importantly, although this study was conducted using $PM_{2.5}$ collected at a single urban site in Japan, the observed relationships between seasonal particle composition and inflammatory responses are consistent with atmospheric processes and emission patterns reported globally. Similar seasonal enrichment of combustion-derived PAHs in winter and secondary aerosols in summer has been documented in many regions worldwide, suggesting that the composition-dependent biological effects identified here may be broadly applicable to other urban and industrialized areas. In addition, previously established in vitro experimental systems using differentiated neutrophils [52] provide a complementary platform for dissecting the underlying molecular mechanisms, including the contribution of TLR4 signaling. Application of these systems to seasonal $PM_{2.5}$ samples represents an important and logical extension of the present findings.

Supplementary Materials: The following supporting information can be downloaded at: https://www.mdpi.com/article/10.3390/antiox15010089/s1. Figure S1: Intratracheal administration of increased the population of Gr-1^+ cell and decreased population of F4/80^+ cell in BAL cell. Figure S2: Intratracheal administration of $PM_{2.5}$ increases BAL cell and correlates with enhanced ROS production.

Author Contributions: Conceptualization, D.W. and Y.Y.; methodology, D.W., A.N., R.B. and T.O.; validation, R.O.; formal analysis, D.W. and Z.Z.; investigation, D.W.; data curation, D.W. and Y.Y.; writing—original draft preparation, D.W.; writing—review and editing, Y.Y.; and funding acquisition, D.W., T.O. and Y.Y. All authors have read and agreed to the published version of the manuscript.

Funding: This research was funded by a Grant-in-Aid for Challenging Research (Exploratory) [grant number 20K21738 to Y. Yoshida], a Grant-in-Aid for Scientific Research (B) [grant number 24K03068 to T. Okuda], a Grant-in-Aid for Scientific Research (C) [grant number 22K09060 to D. Wang], a UOEH Grant-in-Aid for Priority Research in the field of Occupational Medicine [grant number 2022-8 to D. Wang], and a Fund for the Promotion of Joint International Research (International Collaborative Research) [grant number 23KK0195 to T. Okuda].

Institutional Review Board Statement: The experimental protocols were approved by the Ethics Review Committee for Animal Experimentation and the Ethics Committee of Animal Care and Experimentation (admission numbers: AE15-012) at the University of Occupational and Environmental Health from 7 March 2025 Experiments were performed according to the Institutional Guidelines for Animal Experiments (Law Number 105 and Notification Number 6) of the Japanese government.

Informed Consent Statement: Not applicable.

Data Availability Statement: The original contributions presented in this study are included in the article/Supplementary Materials. Further inquiries can be directed to the corresponding author.

Acknowledgments: We appreciate the help of all laboratory members in the management of laboratory and teaching technologies.

Conflicts of Interest: The authors declare no conflicts of interest.

References

1. Gavito-Covarrubias, D.; Ramirez-Diaz, I.; Guzman-Linares, J.; Limon, I.D.; Manuel-Sanchez, D.M.; Molina-Herrera, A.; Coral-Garcia, M.A.; Anastasio, E.; Anaya-Hernandez, A.; Lopez-Salazar, P.; et al. Epigenetic mechanisms of particulate matter exposure: Air pollution and hazards on human health. *Front. Genet.* **2023**, *14*, 1306600. [CrossRef]

2. Naidja, L.; Ali-Khodja, H.; Khardi, S. Sources and levels of particulate matter in North African and Sub-Saharan cities: A literature review. *Environ. Sci. Pollut. Res. Int.* **2018**, *25*, 12303–12328. [CrossRef]
3. Kim, K.H.; Kabir, E.; Kabir, S. A review on the human health impact of airborne particulate matter. *Environ. Int.* **2015**, *74*, 136–143. [CrossRef]
4. Yoshida, Y. Oxidative Stress Induced by Air Pollution. *Antioxidants* **2024**, *13*, 1393. [CrossRef]
5. Thangavel, P.; Park, D.; Lee, Y.C. Recent Insights into Particulate Matter ($PM_{2.5}$)-Mediated Toxicity in Humans: An Overview. *Int. J. Environ. Res. Public Health* **2022**, *19*, 7511. [CrossRef]
6. Krittanawong, C.; Qadeer, Y.K.; Hayes, R.B.; Wang, Z.; Virani, S.; Thurston, G.D.; Lavie, C.J. $PM_{2.5}$ and Cardiovascular Health Risks. *Curr. Probl. Cardiol.* **2023**, *48*, 101670. [CrossRef]
7. Liu, Y.; Yuan, Q.; Zhang, X.; Chen, Z.; Jia, X.; Wang, M.; Xu, T.; Wang, Z.; Jiang, J.; Ma, Q.; et al. Fine particulate matter ($PM_{2.5}$) induces inhibitory memory alveolar macrophages through the AhR/IL-33 pathway. *Cell. Immunol.* **2023**, *386*, 104694. [CrossRef]
8. Mantecca, P.; Farina, F.; Moschini, E.; Gallinotti, D.; Gualtieri, M.; Rohr, A.; Sancini, G.; Palestini, P.; Camatini, M. Comparative acute lung inflammation induced by atmospheric PM and size-fractionated tire particles. *Toxicol. Lett.* **2010**, *198*, 244–254. [CrossRef] [PubMed]
9. Jia, H.; Liu, Y.; Guo, D.; He, W.; Zhao, L.; Xia, S. $PM_{2.5}$-induced pulmonary inflammation via activating of the NLRP3/caspase-1 signaling pathway. *Environ. Toxicol.* **2021**, *36*, 298–307. [CrossRef] [PubMed]
10. Lin, Y.; Zou, J.; Yang, W.; Li, C.Q. A Review of Recent Advances in Research on $PM_{2.5}$ in China. *Int. J. Environ. Res. Public Health* **2018**, *15*, 438. [CrossRef] [PubMed]
11. Wei, S.; Semple, S. Exposure to fine particulate matter ($PM_{2.5}$) from non-tobacco sources in homes within high-income countries: A systematic review. *Air Qual. Atmos. Health* **2023**, *16*, 553–566. [CrossRef]
12. Pietrogrande, M.C.; Demaria, G.; Colombi, C.; Cuccia, E.; Dal Santo, U. Seasonal and Spatial Variations of PM_{10} and $PM_{2.5}$ Oxidative Potential in Five Urban and Rural Sites across Lombardia Region, Italy. *Int. J. Environ. Res. Public Health* **2022**, *19*, 7778. [CrossRef]
13. Viegi, G.; Baldacci, S.; Maio, S.; Fasola, S.; Annesi-Maesano, I.; Pistelli, F.; Carrozzi, L.; La Grutta, S.; Forastiere, F. Health effects of air pollution: A Southern European perspective. *Chin. Med. J.* **2020**, *133*, 1568–1574. [CrossRef]
14. Melzi, G.; Massimi, L.; Frezzini, M.A.; Iulini, M.; Tarallo, N.; Rinaldi, M.; Paglione, M.; Nozza, E.; Crova, F.; Valentini, S.; et al. Redox-activity and in vitro effects of regional atmospheric aerosol pollution: Seasonal differences and correlation between oxidative potential and in vitro toxicity of PM_1. *Toxicol. Appl. Pharmacol.* **2024**, *485*, 116913. [CrossRef] [PubMed]
15. Farina, F.; Sancini, G.; Mantecca, P.; Gallinotti, D.; Camatini, M.; Palestini, P. The acute toxic effects of particulate matter in mouse lung are related to size and season of collection. *Toxicol. Lett.* **2011**, *202*, 209–217. [CrossRef] [PubMed]
16. Marchetti, S.; Hassan, S.K.; Shetaya, W.H.; El-Mekawy, A.; Mohamed, E.F.; Mohammed, A.M.F.; El-Abssawy, A.A.; Bengalli, R.; Colombo, A.; Gualtieri, M.; et al. Seasonal Variation in the Biological Effects of $PM_{2.5}$ from Greater Cairo. *Int. J. Mol. Sci.* **2019**, *20*, 4970. [CrossRef]
17. Becker, S.; Dailey, L.A.; Soukup, J.M.; Grambow, S.C.; Devlin, R.B.; Huang, Y.C. Seasonal variations in air pollution particle-induced inflammatory mediator release and oxidative stress. *Environ. Health Perspect.* **2005**, *113*, 1032–1038. [CrossRef]
18. Giannetto, M.; Alfieri, E.; Giugliano, M.; Lonati, G.; Mori, G.; Pizzol, M. Analysis of voltammetric data for the evaluation of seasonal changes of the Ni, Cd, Pb and Cu content in atmospheric particulate $PM_{2.5}$. *Ann. Chim.* **2005**, *95*, 857–865. [CrossRef]
19. Figueroa, D.A.; Rodriguez-Sierra, C.J.; Jimenez-Velez, B.D. Concentrations of Ni and V, other heavy metals, arsenic, elemental and organic carbon in atmospheric fine particles ($PM_{2.5}$) from Puerto Rico. *Toxicol. Ind. Health* **2006**, *22*, 87–99. [CrossRef] [PubMed]
20. Akira, S.; Takeda, K.; Kaisho, T. Toll-like receptors: Critical proteins linking innate and acquired immunity. *Nat. Immunol.* **2001**, *2*, 675–680. [CrossRef]
21. Miyake, T.; Wang, D.; Matsuoka, H.; Morita, K.; Yasuda, H.; Yatera, K.; Kanazawa, T.; Yoshida, Y. Endocytosis of particulate matter induces cytokine production by neutrophil via Toll-like receptor 4. *Int. Immunopharmacol.* **2018**, *57*, 190–199. Erratum in *Int. Immunopharmacol.* **2018**, *61*, 405. [CrossRef]
22. Song, Y.; Ichinose, T.; He, M.; He, C.; Morita, K.; Yoshida, Y. Lipopolysaccharide attached to urban particulate matter 10 suppresses immune responses in splenocytes while particulate matter itself activates NF-kappaB. *Toxicol. Res.* **2016**, *5*, 1445–1452. [CrossRef]
23. He, C.; Song, Y.; Ichinose, T.; He, M.; Morita, K.; Wang, D.; Kanazawa, T.; Yoshida, Y. Lipopolysaccharide levels adherent to $PM_{2.5}$ play an important role in particulate matter induced-immunosuppressive effects in mouse splenocytes. *J. Appl. Toxicol.* **2018**, *38*, 471–479. [CrossRef]
24. Suo, D.; Zeng, S.; Zhang, J.; Meng, L.; Weng, L. $PM_{2.5}$ induces apoptosis, oxidative stress injury and melanin metabolic disorder in human melanocytes. *Exp. Ther. Med.* **2020**, *19*, 3227–3238. [CrossRef]
25. Kurlawala, Z.; Singh, P.; Hill, B.G.; Haberzettl, P. Fine Particulate Matter ($PM_{2.5}$)-Induced Pulmonary Oxidative Stress Contributes to Changes in the Plasma Lipidome and Liver Transcriptome in Mice. *Toxicol. Sci.* **2023**, *192*, 209–222. [CrossRef] [PubMed]
26. Barzgar, F.; Sadeghi-Mohammadi, S.; Aftabi, Y.; Zarredar, H.; Shakerkhatibi, M.; Sarbakhsh, P.; Gholampour, A. Oxidative stress indices induced by industrial and urban $PM_{2.5}$-bound metals in A549 cells. *Sci. Total Environ.* **2023**, *877*, 162726. [CrossRef]

27. Cao, J.; Qin, G.; Shi, R.; Bai, F.; Yang, G.; Zhang, M.; Lv, J. Overproduction of reactive oxygen species and activation of MAPKs are involved in apoptosis induced by $PM_{2.5}$ in rat cardiac H9c2 cells. *J. Appl. Toxicol.* **2016**, *36*, 609–617. [CrossRef] [PubMed]
28. Shi, F.; Zhang, Z.; Wang, J.; Wang, Y.; Deng, J.; Zeng, Y.; Zou, P.; Ling, X.; Han, F.; Liu, J.; et al. Analysis by Metabolomics and Transcriptomics for the Energy Metabolism Disorder and the Aryl Hydrocarbon Receptor Activation in Male Reproduction of Mice and GC-2spd Cells Exposed to $PM_{2.5}$. *Front. Endocrinol.* **2021**, *12*, 807374. [CrossRef] [PubMed]
29. Jakubczyk, K.; Dec, K.; Kaldunska, J.; Kawczuga, D.; Kochman, J.; Janda, K. Reactive oxygen species—Sources, functions, oxidative damage. *Pol. Merkur. Lekarski* **2020**, *48*, 124–127.
30. Jing, W.; Saito, K.; Okamoto, T.; Saito, H.; Sugimoto, K.; Nishita-Hara, C.; Hara, K.; Hayashi, M.; Hasegawa, S.; Okuda, T. Characterization of Elemental Composition and Valence State of Cyclone-collected Aerosol Particles Using EDXRF and XAFS at Three Sites in Japan. *Asian J. Atmos. Environ.* **2023**, *16*, 2021137. [CrossRef]
31. Onishi, T.; Honda, A.; Tanaka, M.; Chowdhury, P.H.; Okano, H.; Okuda, T.; Shishido, D.; Terui, Y.; Hasegawa, S.; Kameda, T.; et al. Ambient fine and coarse particles in Japan affect nasal and bronchial epithelial cells differently and elicit varying immune response. *Environ. Pollut.* **2018**, *242*, 1693–1701. [CrossRef]
32. Alimov, Z.B.; Youn, H.; Iwata, A.; Nakano, K.; Okamoto, T.; Sasaki, A.; Katori, T.; Okuda, T. Comparison of the Chemical Characteristics and Toxicity of $PM_{2.5}$ Collected Using Different Sizes of Cyclones. *Asian J. Atmos. Environ.* **2022**, *16*, 2022062. [CrossRef]
33. Okuda, T. Measurement of the specific surface area and particle size distribution of atmospheric aerosol reference materials. *Atmos. Environ.* **2013**, *75*, 1–5. [CrossRef]
34. Zeng, Z.; Yoshida, Y.; Wang, D.; Fujii, Y.; Shen, M.; Mimura, T.; Tanaka, Y. Inflammatory Cytokines and Chemokines Are Synergistically Induced in a ROS-Dependent Manner by a Co-Culture of Corneal Epithelial Cells and Neutrophil-like Cells in the Presence of Particulate Matter. *Antioxidants* **2024**, *13*, 467. [CrossRef]
35. Baer, B.; Putz, N.D.; Riedmann, K.; Gonski, S.; Lin, J.; Ware, L.B.; Toki, S.; Peebles, R.S., Jr.; Cahill, K.N.; Bastarache, J.A. Liraglutide pretreatment attenuates sepsis-induced acute lung injury. *Am. J. Physiol. Lung Cell. Mol. Physiol.* **2023**, *325*, L368–L384. [CrossRef]
36. He, M.; Ichinose, T.; Yoshida, Y.; Arashidani, K.; Yoshida, S.; Takano, H.; Sun, G.; Shibamoto, T. Urban $PM_{2.5}$ exacerbates allergic inflammation in the murine lung via a TLR2/TLR4/MyD88-signaling pathway. *Sci. Rep.* **2017**, *7*, 11027. [CrossRef] [PubMed]
37. Duan, R.; Huang, K.; Yu, T.; Chang, C.; Chu, X.; Huang, Y.; Zheng, Z.; Ma, L.; Li, B.; Yang, T. Interleukin-2/anti-interleukin-2 complex attenuates inflammation in a mouse COPD model by expanding $CD4^+$ $CD25^+$ $Foxp3^+$ regulatory T cells. *Int. Immunopharmacol.* **2024**, *131*, 111849. [CrossRef] [PubMed]
38. Chen, Y.J.; Li, M.H.; Gu, F.Y.; Chen, Y.C.; Chan, H.L.; Chou, H.C. Evaluate the impact of $PM_{2.5}$ in different macrophage types under the influence of seasonal changes and anthropogenic activities. *Biochimie* **2025**, *239*, 109–126. [CrossRef] [PubMed]
39. Li, J.; Zhang, G.; Li, X.D.; Qi, S.H.; Liu, G.Q.; Peng, X.Z. Source seasonality of polycyclic aromatic hydrocarbons (PAHs) in a subtropical city, Guangzhou, South China. *Sci. Total Environ.* **2006**, *355*, 145–155. [CrossRef]
40. Bell, M.L.; Dominici, F.; Ebisu, K.; Zeger, S.L.; Samet, J.M. Spatial and temporal variation in $PM_{2.5}$ chemical composition in the United States for health effects studies. *Environ. Health Perspect.* **2007**, *115*, 989–995. [CrossRef]
41. Kim, M.J.; Kim, J.M.; Lee, H.L.; Heo, H.J. Ethyl Acetate Fraction from *Eucommia ulmoides* Ameliorates Particulate Matter $(PM)_{2.5}$-Induced Intestinal Damage by Restoring Barrier Integrity and Regulating Inflammatory Responses. *J. Microbiol. Biotechnol.* **2025**, *35*, e2504002. [CrossRef] [PubMed]
42. Zhang, L.; Xu, F.; Yang, Y.; Yang, L.; Wu, Q.; Sun, H.; An, Z.; Li, J.; Wu, H.; Song, J.; et al. $PM_{2.5}$ exposure upregulates pro-inflammatory protein expression in human microglial cells via oxidant stress and TLR4/NF-kappaB pathway. *Ecotoxicol. Environ. Saf.* **2024**, *277*, 116386. [CrossRef] [PubMed]
43. Julaton, T.; Taclendo, A.; Oyong, G.; Rempillo, O.; Galvez, M.C.; Vallar, E. In Silico Insights on the Pro-Inflammatory Potential of Polycyclic Aromatic Hydrocarbons and the Prospective Anti-Inflammatory Capacity of Andrographis paniculata Phytocompounds. *Int. J. Environ. Res. Public Health* **2022**, *19*, 8588. [CrossRef]
44. Kim, J.; Park, H.M.; Lim, C.M.; Jeon, K.B.; Kim, S.; Lee, J.; Lee, J.; Hong, J.T.; Oh, D.K.; Yang, Y.; et al. Specialized pro-resolving mediator 7S MaR1 inhibits IL-6 expression via modulating ROS/p38/ERK/NF-kappaB pathways in PM_{10}-exposed keratinocytes. *BMB Rep.* **2024**, *57*, 490–496. [CrossRef] [PubMed]
45. Lu, Y.C.; Yeh, W.C.; Ohashi, P.S. LPS/TLR4 signal transduction pathway. *Cytokine* **2008**, *42*, 145–151. [CrossRef]
46. Kawasaki, T.; Kawai, T. Toll-like receptor signaling pathways. *Front. Immunol.* **2014**, *5*, 461. [CrossRef]
47. Hoshino, Y.; Mio, T.; Nagai, S.; Miki, H.; Ito, I.; Izumi, T. Cytotoxic effects of cigarette smoke extract on an alveolar type II cell-derived cell line. *Am. J. Physiol. Lung Cell. Mol. Physiol.* **2001**, *281*, L509–L516. [CrossRef]
48. Kuroda, E.; Ozasa, K.; Temizoz, B.; Ohata, K.; Koo, C.X.; Kanuma, T.; Kusakabe, T.; Kobari, S.; Horie, M.; Morimoto, Y.; et al. Inhaled Fine Particles Induce Alveolar Macrophage Death and Interleukin-1alpha Release to Promote Inducible Bronchus-Associated Lymphoid Tissue Formation. *Immunity* **2016**, *45*, 1299–1310. [CrossRef]

49. Rabolli, V.; Badissi, A.A.; Devosse, R.; Uwambayinema, F.; Yakoub, Y.; Palmai-Pallag, M.; Lebrun, A.; De Gussem, V.; Couillin, I.; Ryffel, B.; et al. The alarmin IL-1alpha is a master cytokine in acute lung inflammation induced by silica micro- and nanoparticles. *Part. Fibre Toxicol.* **2014**, *11*, 69. [CrossRef]
50. Wang, Z.; Larsson, K.; Palmberg, L.; Malmberg, P.; Larsson, P.; Larsson, L. Inhalation of swine dust induces cytokine release in the upper and lower airways. *Eur. Respir. J.* **1997**, *10*, 381–387. [CrossRef]
51. Tuet, W.Y.; Chen, Y.; Fok, S.; Gao, D.; Weber, R.J.; Champion, J.A.; Ng, N.L. Chemical and cellular oxidant production induced by naphthalene secondary organic aerosol (SOA): Effect of redox-active metals and photochemical aging. *Sci. Rep.* **2017**, *7*, 15157. [CrossRef] [PubMed]
52. Wang, D.; Sennari, Y.; Shen, M.; Morita, K.; Kanazawa, T.; Yoshida, Y. ERK is involved in the differentiation and function of dimethyl sulfoxide-induced HL-60 neutrophil-like cells, which mimic inflammatory neutrophils. *Int. Immunopharmacol.* **2020**, *84*, 106510. [CrossRef] [PubMed]

antioxidants

MDPI

Article

Protective Effects of Thyme Leaf Extract Against Particulate Matter-Induced Pulmonary Injury in Mice

Jae-Kyoung Lee [1,2,†], Khawaja Muhammad Imran Bashir [3,†], Hye-Rim Park [4], Jin-Gwan Kwon [4], Beom-Rak Choi [4], Jae-Suk Choi [3,*] and Sae-Kwang Ku [5,*]

[1] Hongsamdan Co., Ltd., Gongju 32511, Republic of Korea; jklee@hongsamdan.com
[2] Department of Food Regulatory Science, College of Science and Technology, Korea University, Sejong 30019, Republic of Korea
[3] Department of Seafood Science and Technology, The Institute of Marine Industry, Gyeongsang National University, Tongyeong 53064, Republic of Korea; imranbashir@gnu.ac.kr
[4] Nutracore Co., Ltd., Suwon 16514, Republic of Korea; hrpark@nutracore.co.kr (H.-R.P.); jgkwon@nutracore.co.kr (J.-G.K.); brchoi@nutracore.co.kr (B.-R.C.)
[5] Department of Anatomy and Histology, College of Korean Medicine, Daegu Haany University, Gyeongsan 38610, Republic of Korea
* Correspondence: jsc1008@gnu.ac.kr (J.-S.C.); gucci200@dhu.ac.kr (S.-K.K.); Tel.: +82-55-772-9142 (J.-S.C.); +82-53-819-1549 (S.-K.K.)
† These authors contributed equally to this work.

Abstract: Airborne particulate matter (PM), particularly $PM_{2.5}$, contributes to pulmonary injury by inducing oxidative stress and inflammation. Thyme (*Thymus vulgaris* L.) contains bioactive compounds with anti-inflammatory, antioxidant, and expectorant properties. Here, we evaluated the dose-dependent protective effects of thyme extract (TV) against $PM_{2.5}$-induced pulmonary injury in mice, using dexamethasone (DEXA) as a reference anti-inflammatory drug. Subacute pulmonary injury was induced in male Balb/c mice via intranasal administration of $PM_{2.5}$ (1 mg/kg, twice at 48 h intervals). Mice received oral TV (50, 100, or 200 mg/kg) or DEXA (0.75 mg/kg) daily for 10 days. Assessments included lung weight, serum AST/ALT, bronchoalveolar lavage fluid (BALF) leukocyte counts, cytokines (TNF-α, IL-6), chemokines, oxidative stress markers (ROS, lipid peroxidation, antioxidant enzymes), histopathology, and mRNA expression of genes related to inflammation (PI3K/Akt, MAPK, and NF-κB), mucus production (MUC5AC, MUC5B), and apoptosis (Bcl-2, Bax). Exposure to $PM_{2.5}$ caused oxidative stress, pulmonary inflammation, mucus hypersecretion, and histopathological changes. TV treatment dose-dependently reduced leukocyte infiltration, cytokine/chemokine release, ROS generation, and mucus overproduction, while enhancing antioxidant defenses and improving tissue pathology. Effects were comparable but slightly less potent than DEXA. Notably, unlike DEXA, TV reduced mucus hyperplasia and enhanced expectorant activity. No hepatotoxicity was observed. These results indicate that thyme extract could serve as a promising natural candidate for alternative respiratory therapeutics or functional food development.

Keywords: antioxidant defense; dexamethasone; expectorant activity; mucus secretion; pulmonary protective effect; respiratory-protective food ingredient; *Thymus vulgaris* L.

1. Introduction

Air pollution in East Asia, particularly in China, Korea, and Japan, has emerged as a serious public health crisis, largely due to fine dust exposure that threatens both human health and regional climate stability [1–3]. Beijing, the capital of China, lies at the heart of

this crisis, experiencing large quantities of particulate matter (PM) during spring due to dust storms originating from northwest China, Mongolia, and the Loess Plateau [4]. The situation is further exacerbated by local emissions from industries, vehicular traffic, and coal combustion. Beijing is recognized as one of the most polluted cities globally [5], drawing international attention during the 2008 Olympic Games and prompting the government to implement stricter pollution control measures thereafter [5]. Ground measurements have revealed that the majority of PM has an aerodynamic diameter of 2.5 μm ($PM_{2.5}$), consisting primarily of mineral dust, polycyclic aromatic hydrocarbons (PAHs), and inorganic substances such as sulfates, nitrates, ammonium, and elemental carbon [6]. An excellent overview of $PM_{2.5}$ fluctuations and their environmental consequences in Beijing is provided by Lv et al. [7].

Epidemiological studies have repeatedly shown that PM infiltrates deep in lung tissues, inducing damage and contributing to cardiopulmonary diseases [1–3]. Among these, asthma is a chronic inflammatory condition closely linked to air pollutants. According to WHO estimates (2017), approximately 235 million people worldwide are asthmatic, with PM exposure recognized as a key risk factor [8]. Over 70% of inhaled PM deposits below the trachea, with approximately 22% reaching the alveoli [9], thereby elevating oxidative stress in epithelial and lung tissues and inducing inflammation [5,10]. Following exposure, cellular stress markers such as catalase (CAT), superoxide dismutase (SOD), reactive oxygen species (ROS), glutathione peroxidase (GPx), and heme oxygenase-1 (HO-1) are upregulated [11], together with pro-inflammatory cytokines including tumor necrosis factor-α (TNF-α) and interleukin-6 (IL-6) [12]. Schaumann et al. [10] further highlighted the health risks of industrial PM exposure, showing strong associations with childhood asthma and increased lung inflammation.

Among available treatments, dexamethasone (DEXA), a synthetic glucocorticoid with potency 4–5 times higher than prednisolone and 20–30 times greater than hydrocortisone [13], has shown strong anti-inflammatory efficacy in respiratory disorders [14,15] including $PM_{2.5}$-induced pulmonary injury [16]. In earlier studies, water-soluble DEXA administered orally at 0.75 mg/kg was employed as a standard drug for therapeutic evaluation [14–16]. In addition, the Balb/c mouse model used in the present study has been extensively validated as an appropriate system for replicating $PM_{2.5}$-induced subacute pulmonary injuries. Earlier studies demonstrated that intranasal instillation of $PM_{2.5}$ reproduces hallmark features of human dust-induced pulmonary disorders, including inflammatory cell infiltration, oxidative stress, airway remodeling, and mucus overproduction [1–3]. Thus, this model provides a suitable platform to evaluate preventive and therapeutic interventions against air pollution–induced lung injury.

Given growing environmental and health concerns, there is an urgent need to identify novel preventive and therapeutic strategies against PM-mediated lung injury [2,3]. Medicinal plants offer a promising source of antioxidants and bioactive molecules [17,18], with potential applications in respiratory protection [1–3,16]. Thyme (*Thymus vulgaris* L.), a member of the Lamiaceae family native to Southern and Eastern Europe, is one such candidate [19]. Its pharmacological activities, which include antioxidant, anti-inflammatory, antimicrobial, immunomodulatory, and metabolic effects, are largely attributed to its polyphenolic constituents, particularly phenolic acids and flavonoids [20–25]. High-performance liquid chromatography (HPLC) analyses of thyme leaf extracts have identified phenolic acids such as rosmarinic acid, methyl rosmarinate, cinnamic acid, caffeic acid, protocatechuic acid, and chlorogenic acid, as well as flavonoids including luteolin, quercetin, apigenin, ferulic acid, zeaxanthin, naringenin, and thymonin [21,26]. Methanolic extracts of thyme leaves have demonstrated antioxidant capacities exceeding those of natural and synthetic antioxidants, including α-tocopherol and BHA [26]. In addition, thyme contains vitamins, particularly C

(ascorbic acid), A (retinol), and B6 (pyridoxine, 100 g providing approximately 27% of the daily recommended intake), as well as other minor vitamins such as E, folic acid, and K [27], along with chlorophyll, which may contribute to supportive detoxifying and anticancer effects [20,25].

The present study evaluated the dose-dependent protective effects of thyme extract (TV; 50, 100, and 200 mg/kg) against $PM_{2.5}$-induced pulmonary injury in mice and compared its efficacy with DEXA (0.75 mg/kg). TV was administered orally once daily for 10 days, one hour after each $PM_{2.5}$ intranasal instillation (1 mg/kg at 48 h intervals), to explore its capability as an innovative respiratory protectant and functional food ingredient.

2. Materials and Methods

2.1. Animal Husbandry

A total of 88 healthy male Balb/cAnNCrlOri (Balb/c) mice (SPF/VAF inbred strain, 6 weeks old at receipt; OrientBio, Seongnam, Republic of Korea) were housed for a 7-day acclimation period before the experiment. All animals used in the study were wild-type with no prior genetic modification or experimental treatment. A total of four mice were placed per polycarbonate cage in a controlled environment (temperature: 20–25 °C; humidity: 30–35%; 12 h light/dark cycle) with ad libitum access to feed (Purinafeed, Seongnam, Republic of Korea) and water. Following acclimatization, the mice were randomly assigned to six groups (n = 10 per group; total = 60). Body weights were recorded one day prior to the first $PM_{2.5}$ instillation (intact control: 20.26 ± 0.62 g, range 19.40–21.30 g; $PM_{2.5}$-treated: 20.27 ± 0.78 g, range 18.70–21.80 g). All experimental procedures were performed in accordance with international guidelines for the care and use of laboratory animals and were approved by the Institutional Animal Care and Use Committee of Daegu Haany University, Gyeongsan, Republic of Korea (Approval No. DHU2022-013; approved on 22 February 2022).

Experimental groups were as follows (n = 10 per group):

1. Intact control: Distilled water (10 mL/kg, p.o.) + saline (0.1 mL/kg, intranasal)
2. $PM_{2.5}$ control: Distilled water (10 mL/kg, p.o.) + $PM_{2.5}$ (1 mg/kg, intranasal)
3. DEXA: DEXA 0.75 mg/kg (11.40 mg/kg as DEXA-water soluble, p.o.) + $PM_{2.5}$ (1 mg/kg, intranasal)
4. TV_{200}: TV 200 mg/kg (p.o.) + $PM_{2.5}$ (1 mg/kg, intranasal)
5. TV_{100}: TV 100 mg/kg (p.o.) + $PM_{2.5}$ (1 mg/kg, intranasal)
6. TV_{50}: TV 50 mg/kg (p.o.) + $PM_{2.5}$ (1 mg/kg, intranasal)

2.2. Induction of Pulmonary Injury by $PM_{2.5}$

Subacute pulmonary injury was induced by intranasal instillation of $PM_{2.5}$ suspensions (NIST 1650b; 10 mg/mL in physiological saline; Sigma-Aldrich, St. Louis, MO, USA). Mice received 0.1 mL/kg (equivalent to 1 mg/kg) twice at 48 h intervals (Day 0 and Day 2), administered 1 h before test article treatment, using micropipettes with yellow tips [1–3]. The suspensions were sonicated for 30 min prior to instillation to prevent particle aggregation. Intact control mice received physiological saline (0.1 mL/kg, intranasal) on the same schedule to account for stress associated with intranasal dosing.

2.3. Preparations and Administration of Test Articles

The fresh leaf extract of thyme (*Thymus vulgaris* L.; TV extract) was prepared, standardized, and supplied by Plantex (Saint Michel Sur Orge, France) and spray-dried by NUTRACORE (Suwon, Republic of Korea). A detailed extract preparation methodology has been presented in Figure S1. A voucher specimen was deposited in the herbarium of the Medical Research Center for Herbal Convergence on Liver Disease, Daegu Haany

University, Gyeongsang, Republic of Korea. In addition, a crude drug reference sample was obtained from the National Institute of Food and Drug Safety Evaluation (NIFDS), Ministry of Food and Drug Safety (MFDS), Republic of Korea. The authenticity of the harvested material was confirmed by comparing its HPLC fingerprint with that of the official reference sample.

The thyme aqueous extract (coded as Batch No. TV-P2118) was a yellowish-brown powder. The extract was prepared in distilled water at concentrations of 20, 10, and 5 mg/mL, which corresponded to doses of 200, 100, and 50 mg/kg body weight for administration. The extract was administered orally by gavage at 10 mL/kg once daily for 10 consecutive days, 1 h after each test article exposure. The highest dose (200 mg/kg) was determined based on preliminary screening results, while the lower doses were established using a twofold serial dilution. Samples were kept at −20 °C until further use.

The dexamethasone-water soluble formulation (Sigma-Aldrich, St. Louis, MO, USA) contained 66 mg/g of dexamethasone. For administration, the white powder was prepared in distilled water at 0.075 mg/mL, equivalent to a dexamethasone dose of 0.75 mg/kg (1.14 mg/mL as DEXA-water soluble). The solution was administered orally at 10 mL/kg once daily for 10 days, 1 h post–$PM_{2.5}$ exposure. The dose level was selected based on previously established anti-inflammatory experimental models [14–16]. Dexamethasone solutions were stored at 4 °C until use. For vehicle control groups (intact and $PM_{2.5}$-treated), distilled water was administered in equal volumes to minimize handling-related stress.

2.4. Determination of Test Article by HPLC

The quantification of rosmarinic acid present in *Thymus vulgaris* leaf extracts was carried out using an Agilent 1260 Infinity II high-performance liquid chromatography (HPLC) system (Agilent Technologies, Inc., Santa Clara, CA, USA). The instrument was equipped with a UV–Vis detector and a CAPCELL PAK C_{18} UGII column (4.6 mm × 250 mm, 5 μm particle size; CELLACHROM™, Daejeon, Republic of Korea). Both the rosmarinic acid standard and the TV extract were dissolved in methanol and subsequently filtered using a 0.45 μm membrane filter prior to analysis. The chromatographic separation was performed at a column temperature of 30 °C, and rosmarinic acid was monitored at a detection wavelength of 330 nm. The mobile phase consisted of 0.05% trifluoroacetic acid in water (A) and acetonitrile (B). The elution profile was as follows: 0–40 min, 75% A and 25% B (*v*/*v*); 40–50 min: 5% A and 95% B; all gradients were linear. Calibration was performed using rosmarinic acid standard (R4033; Sigma-Aldrich, St. Louis, MO, USA). Each sample was injected at a volume of 10 μL, and the flow rate was maintained at 0.35 mL/min. Quantification was performed by comparing the sample peak areas with those of the standard, and the concentration was determined from the corresponding calibration curve.

2.5. Changes in Body Weight

Body weights were measured daily, starting one day before the first $PM_{2.5}$ nasal instillation and oral administration of test articles, and continued for the duration of the experiment using an electronic balance (Precisa Instrument, Dietikon, Switzerland). To reduce individual differences, body weight gain was determined from the day of the first oral administration to 24 h following the 10th administration (Equation (1)).

$$\text{Body weight gain (g)} = \text{Body weight at 24 h after last administration} - \text{Body weight at initial } PM_{2.5} \text{ instillation and test article administration} \quad (1)$$

2.6. Serum AST and ALT Assessment

At 24 h following the final administration of test substances, approximately 1 mL of blood was collected from the vena cava under anesthesia using 2–3% isoflurane (Hana Pharm., Hwasung, Republic of Korea) in a gas mixture of 70% N_2O and 28.5% O_2, delivered via a rodent inhalation system equipped with a ventilator (Surgivet, Waukesha, WI, USA; Harvard Apparatus, Cambridge, UK). Blood samples were centrifuged at 12,500 rpm for 10 min at 4 °C in clot-activated serum tubes (Gyrozen, Daejeon, Republic of Korea), and serum was stored at −150 °C (Sanyo, Tokyo, Japan) until analysis. Levels of aspartate transaminase (AST) and alanine transaminase (ALT) were measured in IU/L using an automated analyzer (Dri-Chem NX500i, Fuji Medical Systems, Tokyo, Japan).

2.7. Lung Weight Measurement

Lungs were excised under inhalation anesthesia 24 h after the last treatment and weighed on an electronic balance (Precisa Instrument, Dietikon, Switzerland). Absolute wet lung weights (g) were recorded, and relative lung weights (% of body weight) were calculated using Equation (2) to account for inter-individual differences:

$$\text{Relative lung weight (\%)} = (\text{Absolute lung wet weight}/\text{Body weight at sacrifice}) \times 100 \quad (2)$$

2.8. Lung Collection and Gross Examination

Following lung excision, the left secondary bronchus and right lower secondary bronchus were ligated using 3-0 nylon (AILEE, Busan, Republic of Korea). Lobar allocation was as follows: right upper and middle lobes for bronchoalveolar lavage fluid (BALF) collection; right lower lobes for assays of matrix metalloproteinases (MMPs), substance P, acetylcholine (ACh), ROS, lipid peroxidation, antioxidant enzymes, and cytokines; and left lobes for gross morphological evaluation, histopathology, and real-time RT-PCR. Gross morphology was photographed with a digital camera (FinePix S700; Fujifilm, Tokyo, Japan), and the proportion of congested areas (%) was quantified from images using an automated image analyzer (iSolution FL v9.1; IMT i-Solution, Burnaby, BC, Canada).

2.9. BALF Collection and Cytology

After ligation, 1 mL of physiological saline was instilled via a 20 G tracheal cannula and aspirated; this process was repeated twice per animal. BALF samples were pooled, as previously described [14,28] with minor modifications. Total cell counts were determined using an automated cell counter (Countess C10281; Invitrogen, Carlsbad, CA, USA) with trypan blue exclusion. Leukocyte differentials (lymphocytes, neutrophils, eosinophils, monocytes) were obtained using a hematology analyzer (Cell-DYN 3700; Abbott Laboratories, Abbott Park, IL, USA).

2.10. Lung Homogenate Preparation

Right lower lung lobes were homogenized in normal saline using a bead beater (Taco™Pre; GeneResearch Biotechnology, Taichung, Taiwan) and an ultrasonic disruptor (Madell Technology, Ontario, CA, USA). Homogenates were stored at −150 °C until further analyses.

2.11. Quantification of Cytokines, MMP, Substance P and ACh

Lung homogenates were centrifuged at 12,500 rpm for 30 min at 4 °C (Gyrozen, Daejeon, Republic of Korea). Supernatants were analyzed for TNF-α, IL-6, chemokines (CXCL-1, CXCL-2), MMP-9, MMP-12, substance P, and ACh using ELISA kits (MyBioSource, San Diego, CA, USA), following manufacturer instructions. Absorbance was read at 450 nm using a microplate reader (Sunrise, Tecan, Männedorf, Switzerland).

2.12. Lipid Peroxidation Assay

Lung homogenates were centrifuged at 12,000× *g* for 15 min at 4 °C as described by Kavutcu et al. [29]. Lipid peroxidation was determined by measuring malondialdehyde (MDA) levels using the thiobarbituric acid assay, with absorbance at 525 nm (OPTIZEN POP, Mecasys, Daejeon, Republic of Korea), and expressed as nM MDA per mg protein [30]. Protein concentrations were determined by the Lowry method [31] using BSA as a standard.

2.13. ROS Measurement

ROS levels in lung homogenates were quantified using the DCFDA probe (Abcam, Cambridge, MN, USA). Fluorescence intensity was measured at 490/520 nm (Versa-Max™; Molecular Devices, Sunnyvale, CA, USA) and normalized to protein content, expressed as RFU/μg protein [32].

2.14. Assessment of Antioxidant Enzymes

Lung homogenates were mixed with 25% trichloroacetic acid (Merck, West Point, CA, USA) and centrifuged at 4200 rpm for 40 min at 4 °C. Glutathione (GSH) content was measured at 412 nm using 2-nitrobenzoic acid [33]. CAT activity was measured at 240 nm via H_2O_2 decomposition [34], and SOD activity was assessed by inhibition of nitroblue tetrazolium reduction [35], read at 560 nm. Enzyme activities were expressed as U/mg protein. All reagents were obtained from Sigma-Aldrich (St. Louis, MO, USA).

2.15. Real-Time RT-PCR

The mRNA expression of mucins (MUC5AC, MUC5B), nuclear factor kappa-light-chain-enhancer of activated B cells (NF-κB), p38 mitogen-activated protein kinase (p38 MAPK), phosphatase and tensin homolog (PTEN), phosphoinositide 3-kinase (PI3K), protein kinase B (Akt), B-cell leukemia/lymphoma 2 (Bcl-2), and BCL2 associated x (Bax) gene was measured using real-time RT-PCR [36,37]. RNA was extracted using Trizol (Invitrogen, Carlsbad, CA, USA), treated with DNase I (Thermo Fisher Scientific, Rockford, IL, USA), and reverse transcribed with a High-Capacity cDNA Kit (Thermo Fisher Scientific). PCR amplification was performed on an ABI StepOnePlus system (50 cycles: 95 °C for 1 min; 95 °C for 15 s; 55–65 °C for 20 s; 72 °C for 30 s). β-actin was used as a reference gene, and relative expression was calculated using the $2^{-\Delta\Delta Cq}$ method [38]. Primer sequences are listed in Table S1.

2.16. Histopathology

Left lung lobes were fixed in 10% neutral-buffered formalin for 24 h, embedded in paraffin, and sectioned at 3–4 μm. Sections were stained with hematoxylin and eosin (H&E) for general morphology and periodic acid–Schiff (PAS) for mucus-producing cells [14,39,40]. Slides were examined under light microscopy (Eclipse 80i; Nikon, Tokyo, Japan) with imaging via ProgRes™ C5 camera (Jenoptik, Jena, Germany) and analyzed using iSolution FL software (v9.1). Parameters measured included alveolar surface area, septal thickness, inflammatory cell density, PAS-positive goblet cell counts, and the percentage of PAS-positive cell areas. At least 10 fields per group were evaluated in a blinded manner.

2.17. Statistical Analysis

Data are presented as mean ± SD (n = 10). Levene's test was used to assess homogeneity of variance. Datasets with equal variance were analyzed by one-way ANOVA followed by Tukey's HSD test, while datasets with unequal variance were analyzed using Dunnett's T3 test [41,42]. Statistical significance was set at $p < 0.05$. Analyses were conducted using SPSS v18.0 (SPSS Inc., Chicago, IL, USA). Percentage changes relative to vehicle control or $PM_{2.5}$ control were calculated using Equations (3) and (4) [14,28,40]:

$$\% \text{ change vs. vehicle control} = [(PM_{2.5} \text{ control} - \text{vehicle control})/\text{vehicle control}] \times 100 \quad (3)$$

$$\% \text{ change vs. } PM_{2.5} \text{ control} = [(\text{Treatment} - PM_{2.5} \text{ control})/PM_{2.5} \text{ control}] \times 100 \quad (4)$$

3. Results

3.1. Rosmarinic Acid Content in TV Extract

HPLC analysis determined that the concentration of rosmarinic acid in the TV extract was 7.2 mg/g. Quantification was performed by comparing the relative peak area of the extract to that of the standard solution, as shown in Figure 1.

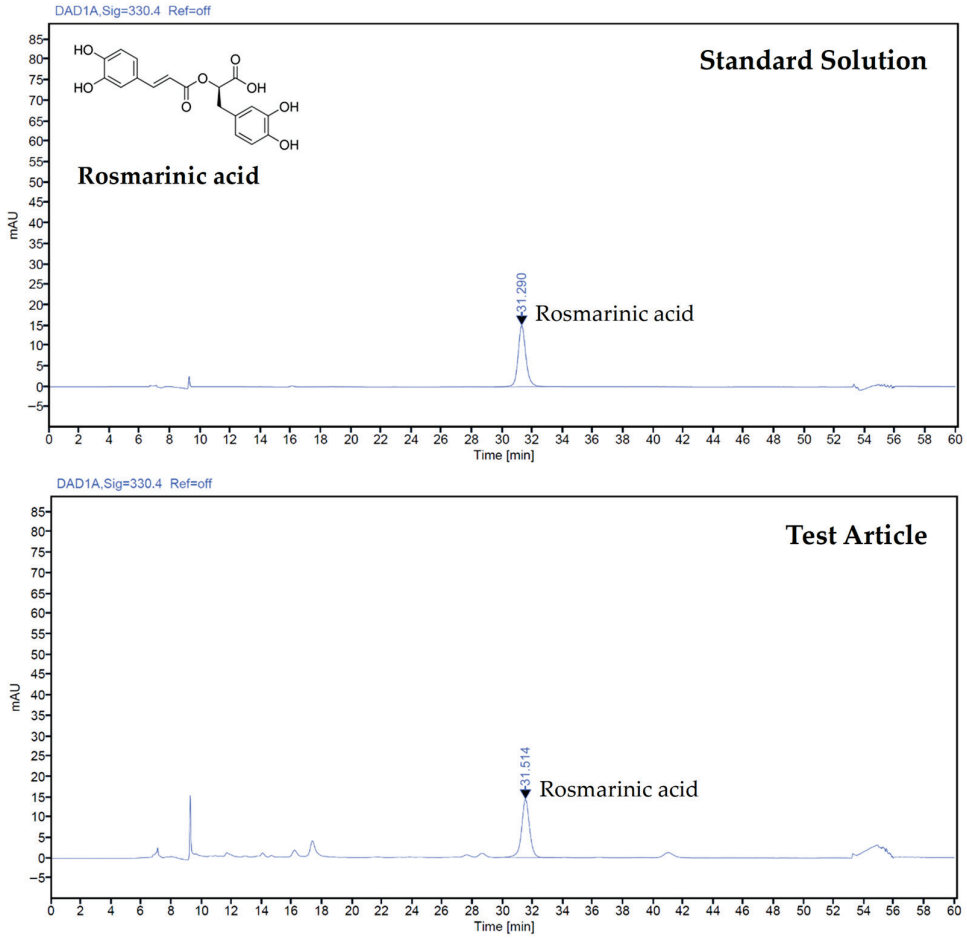

Figure 1. HPLC chromatograms of rosmarinic acid in the standard solution and the *Thymus vulgaris* L. leaf extract (TV extract).

3.2. Body Weight Changes

Body weights or gains did not show a significant change in $PM_{2.5}$-treated mice compared with intact vehicle controls over the experimental period of 10 days, except for DEXA 0.75 mg/kg-treated mice, which showed significant decreases in body weight ($p < 0.01$) from day 3 and reduced weight gains throughout the experimental period (Table S2 and Figure 2). TV treatment at 200, 100, and 50 mg/kg did not significantly alter body weights or gains compared with $PM_{2.5}$ controls. Body weight gains in $PM_{2.5}$ controls changed by 1.23% relative to intact controls, whereas changes in DEXA and TV-treated groups were −202.44%, 7.32%, 1.22%, and −2.44%, respectively.

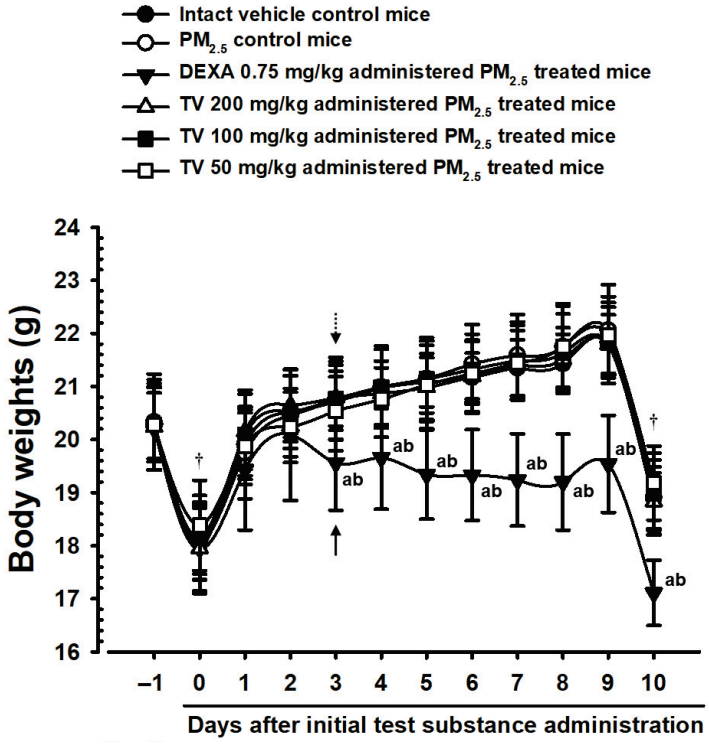

Figure 2. Body weight trends in intact or $PM_{2.5}$-treated pulmonary-injured mice. Values represent means ± SD for 10 mice per group. $PM_{2.5}$ refers to Diesel Particulate Matter NIST 1650b; DEXA indicates dexamethasone treatment; TV refers to thyme (*Thymus vulgaris* L.) leaf extract; THSD denotes Tukey's Honest Significant Difference test. Body weights were monitored from one day prior to the first administration (Day-1) until 24 h after the 10th administration (Day-10). All mice were fasted overnight before the initial administration and at sacrifice. Arrows in the figure indicate significant decreases in body weight following DEXA administration (0.75 mg/kg) relative to intact vehicle control (†), and dot arrows indicate reductions compared with $PM_{2.5}$ control mice. Significant differences are indicated as follows: [a] $p < 0.01$ vs. intact vehicle control (THSD test); [b] $p < 0.01$ vs. $PM_{2.5}$ control (THSD test).

3.3. Gross Lung Inspections and Weights

$PM_{2.5}$ exposure induced notable lung focal congestion and enlargement, with significant increases ($p < 0.01$) in absolute, and relative lung weights, and gross congestional area compared with intact controls (Table S3 and Figure 3). Oral TV treatment dose-dependently reduced these parameters, with inhibitory effects slightly lower than DEXA 0.75 mg/kg. Gross congestional areas in $PM_{2.5}$ controls increased by 3770.21%, while DEXA, TV 200, 100, and 50 mg/kg treatments reduced this by −87.72%, −75.60%, −62.46%, and −40.09%, respectively. Similar trends were observed for absolute and relative lung weights.

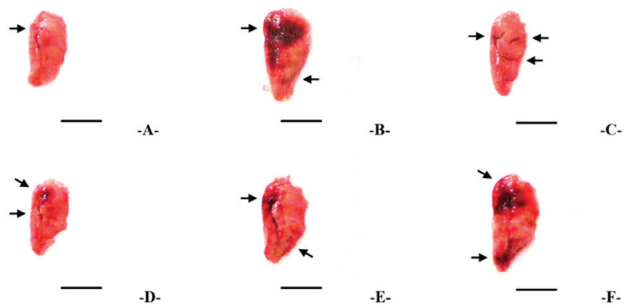

Figure 3. Representative gross lung images showing congestion in left lung lobes of each treatment group. Treatments are designated as follows: (**A**)—intact vehicle control (distilled water orally, saline

intranasal), (**B**)—$PM_{2.5}$ control (distilled water orally, $PM_{2.5}$ intranasal), (**C**)—DEXA (0.75 mg/kg orally, $PM_{2.5}$ intranasal), (**D**)—TV_{200} (200 mg/kg TV orally, $PM_{2.5}$ intranasal), (**E**)—TV_{100} (100 mg/kg TV orally, $PM_{2.5}$ intranasal), (**F**)—TV_{50} (50 mg/kg TV orally, $PM_{2.5}$ intranasal). $PM_{2.5}$ refers to Diesel Particulate Matter NIST 1650b; DEXA indicates dexamethasone treatment; TV refers to thyme (*Thymus vulgaris* L.) leaf extract; Congested regions are highlighted with arrows. Scale bars = 6.00 mm.

3.4. BALF Cytology

$PM_{2.5}$ exposure caused marked pulmonary inflammation, with notable increase ($p < 0.01$) in BALF total cells, leukocytes, eosinophils, neutrophils, lymphocytes, and monocytes compared with intact controls (Table 1). Total cell numbers increased by 715.63%, total leukocytes by 777.05%, lymphocytes by 908.82%, neutrophils by 750.43%, eosinophils by 13,354.55%, and monocytes by 404.62%. Oral supply of TV (200—50 mg/kg) significantly and dose-dependently inhibited these elevations, demonstrating strong anti-inflammatory activity, although slightly lower than DEXA 0.75 mg/kg. This indicates that TV effectively mitigates $PM_{2.5}$-induced immune cell recruitment and pulmonary inflammatory responses.

Table 1. Cytological analysis of BALF in intact or $PM_{2.5}$-treated pulmonary-injured mice.

Groups	Total Cells	Total Leukocytes	Differential Counts			
			Lymphocytes	Neutrophils	Eosinophils	Monocytes
Controls						
Intact vehicle	9.60 ± 2.95	6.10 ± 1.73	3.40 ± 1.17	1.15 ± 0.34	0.01 ± 0.01	1.30 ± 0.87
$PM_{2.5}$	78.30 ± 12.36 ^{c}	53.50 ± 13.18 ^{c}	34.30 ± 10.08 ^{c}	9.78 ± 2.82 ^{c}	1.48 ± 0.23 ^{c}	6.56 ± 1.43 ^{a}
Reference						
DEXA	18.60 ± 3.72 ^{cd}	11.60 ± 2.41 ^{cd}	7.30 ± 2.50 ^{cd}	2.13 ± 0.40 ^{cd}	0.04 ± 0.03 ^{d}	1.95 ± 0.68 ^{b}
Test article–TV						
200 mg/kg	33.80 ± 10.49 ^{cd}	19.50 ± 4.86 ^{cd}	12.70 ± 3.20 ^{cd}	3.79 ± 1.11 ^{cd}	0.17 ± 0.08 ^{cd}	2.65 ± 0.76 ^{b}
100 mg/kg	44.30 ± 6.70 ^{cd}	24.40 ± 3.84 ^{cd}	15.20 ± 2.94 ^{cd}	4.44 ± 0.80 ^{cd}	0.67 ± 0.27 ^{cd}	3.54 ± 1.09 ^{ab}
50 mg/kg	54.10 ± 7.55 ^{cd}	29.50 ± 6.45 ^{cd}	18.80 ± 4.98 ^{ce}	5.38 ± 1.33 ^{cd}	0.85 ± 0.22 ^{cd}	4.33 ± 1.19 ^{ab}

Values represent means ± SD for 10 mice per group. Unit: $\times 10^4$ cells/mL; $PM_{2.5}$ refers to Diesel Particulate Matter NIST 1650b; DEXA indicates dexamethasone treatment; TV refers to thyme (*Thymus vulgaris* L.) leaf extract; BALF: Bronchoalveolar lavage fluid; THSD denotes Tukey's Honest Significant Difference test; DT3 indicates Dunnett's T3 test. Statistical significance is indicated as follows: ^{a,c} $p < 0.01$ vs. intact vehicle control; ^{b,d,e} $p < 0.01$ or $p < 0.05$ vs. $PM_{2.5}$ control, depending on THSD or Dunnett's T3 tests.

3.5. Changes in AST and ALT Levels

No markable differences in serum AST and ALT amounts were observed in $PM_{2.5}$-exposed mice or any treatment group, suggesting that neither $PM_{2.5}$ exposure nor TV administration caused hepatotoxicity under the study conditions (Figure 4). AST changes were minimal (0.57% in $PM_{2.5}$ control vs. intact control), and ALT changes were similarly negligible (0.60%), confirming systemic safety of TV treatments.

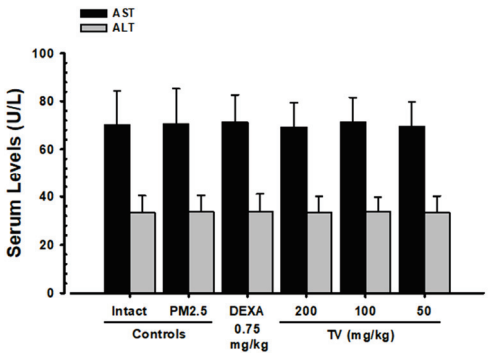

Figure 4. Serum AST and ALT levels in intact and $PM_{2.5}$-exposed mice. Values represent means ± SD for 10 mice per group. $PM_{2.5}$ refers to Diesel Particulate Matter NIST 1650b; DEXA indicates dexamethasone treatment; TV refers to thyme (*Thymus vulgaris* L.) leaf extract; AST refers to aspartate aminotransferase; ALT indicates alanine aminotransferase.

3.6. Lung Cytokine Levels

$PM_{2.5}$ exposure significantly elevated pro-inflammatory cytokines: IL-6 (1431.86%), TNF-α (683.29%), CXCL1 (1003.30%), and CXCL2 (1058.36%) compared with intact controls (Table 2). TV treatment dose-dependently reduced these elevations, indicating suppression of local pulmonary inflammation. For instance, TNF-α levels decreased by 62.32%, 53.44%, and 40.83% in TV 200, 100, and 50 mg/kg groups, respectively, while DEXA achieved a 71.43% reduction. These data highlight TV's potential to modulate cytokine-mediated inflammatory signaling pathways in $PM_{2.5}$-induced lung injury.

Table 2. Lung cytokine content in intact or $PM_{2.5}$-treated mice.

Groups	Lung Contents (pg/mL)			
	TNF-α	IL-6	CXCL1	CXCL2
Controls				
Intact vehicle	29.21 ± 8.72	27.88 ± 11.74	30.37 ± 10.35	16.88 ± 4.30
$PM_{2.5}$	228.82 ± 51.32 [a]	427.08 ± 54.81 [a]	340.54 ± 85.86 [a]	195.53 ± 26.07 [a]
Reference				
DEXA	65.37 ± 16.34 [ab]	75.42 ± 13.54 [ab]	113.70 ± 29.25 [ab]	61.49 ± 20.30 [ab]
Test article—TV				
200 mg/kg	86.22 ± 17.23 [ab]	130.08 ± 45.34 [ab]	156.66 ± 28.26 [ab]	89.69 ± 14.28 [ab]
100 mg/kg	106.55 ± 19.58 [ab]	197.58 ± 57.64 [ab]	187.38 ± 29.10 [ab]	109.88 ± 18.15 [ab]
50 mg/kg	135.41 ± 18.90 [ab]	262.57 ± 52.84 [ab]	210.09 ± 35.64 [ac]	124.70 ± 23.26 [ab]

Values represent means ± SD for 10 mice per group. $PM_{2.5}$ refers to Diesel Particulate Matter NIST 1650b; DEXA indicates dexamethasone treatment; TV refers to thyme (*Thymus vulgaris* L.) leaf extract; TNF refers to tumor necrosis factor; IL indicates interleukin; CXCL refers to the chemokine (C-X-C motif) ligand; THSD denotes Tukey's Honest Significant Difference test; DT3 indicates Dunnett's T3 test. Statistical significance is indicated as follows: [a] $p < 0.01$ vs. intact vehicle; [b] $p < 0.01$, [c] $p < 0.05$ vs. $PM_{2.5}$ control.

3.7. MMP-9 and MMP-12 Contents

Noticeable elevations in $PM_{2.5}$-induced lung MMP-9 (511.48%) and MMP-12 (467.50%) were observed, reflecting extracellular matrix remodeling and potential tissue damage (Figure 5). TV treatment dose-dependently reduced MMP-9 by 57.32%, 48.19%, and 39.66%, and MMP-12 by 57.65%, 46.61%, and 37.16% at 200, 100, and 50 mg/kg, respectively. These findings suggest that TV may protect against $PM_{2.5}$-induced lung tissue remodeling.

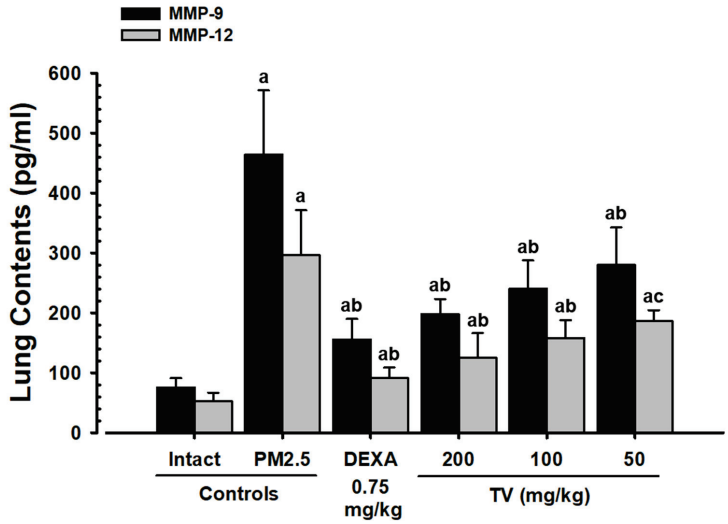

Figure 5. Lung MMP content in intact or $PM_{2.5}$-treated mice. Values represent means ± SD for 10 mice per group. $PM_{2.5}$ refers to Diesel Particulate Matter NIST 1650b; DEXA indicates dexamethasone treatment; TV refers to thyme (*Thymus vulgaris* L.) leaf extract; MMP indicates matrix metalloproteinase; DT3 refers to Dunnett's T3 test. Statistical significance is indicated as follows: [a] $p < 0.01$ vs. intact vehicle; [b] $p < 0.01$, [c] $p < 0.05$ vs. $PM_{2.5}$ control (DT3 test).

3.8. Lung Substance P and ACh Content

$PM_{2.5}$ exposure markedly increased lung substance P (187.12%) and ACh (101.37%), contributing to airway hyperreactivity and mucus secretion (Figure 6). DEXA significantly reduced these levels (−42.16% and −28.50%, respectively). Interestingly, TV treatment dose-dependently increased substance P (49.65–115.24%) and ACh (63.55–166.24%), suggesting a modulatory effect on pulmonary neuroimmune signaling that may support mucus clearance and bronchodilation.

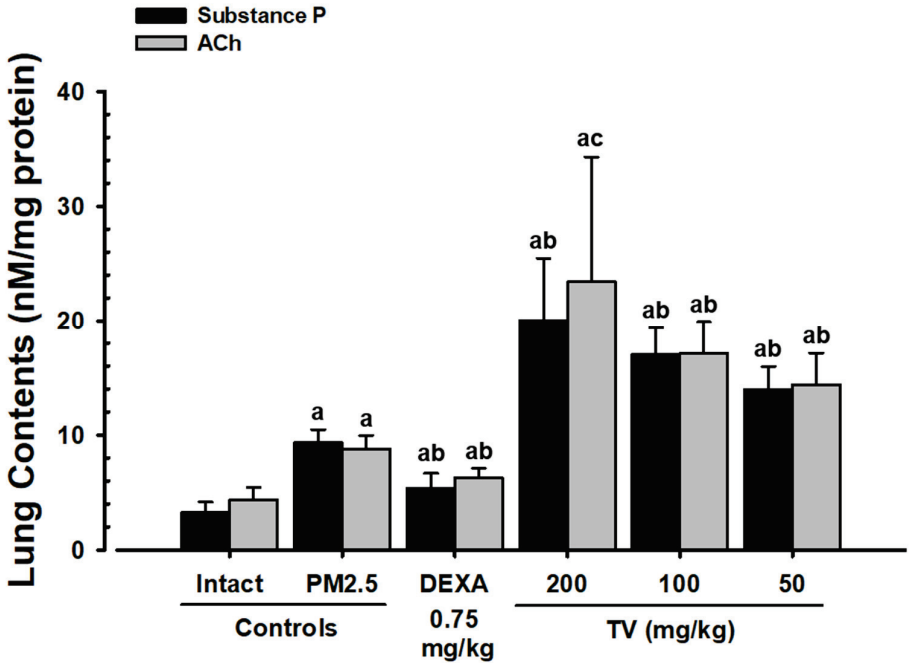

Figure 6. Substance P and ACh content in intact or $PM_{2.5}$-treated mice. Values represent means ± SD for 10 mice per group. $PM_{2.5}$ refers to Diesel Particulate Matter NIST 1650b; DEXA indicates dexamethasone treatment; TV refers to thyme (*Thymus vulgaris* L.) leaf extract; Ach indicates acetylcholine; DT3 refers to Dunnett's T3 test. Statistical significance is indicated as follows: [a] $p < 0.01$ vs. intact vehicle; [b] $p < 0.01$, [c] $p < 0.05$ vs. $PM_{2.5}$ control (DT3 test).

3.9. Lung Lipid Peroxidation and Antioxidant Defense

$PM_{2.5}$ caused pronounced oxidative stress, reflected by elevated MDA (287.91%) and ROS (441.81%) levels, along with depletion of antioxidant defenses (GSH −85.02%, SOD −79.77%, CAT −85.31%). TV treatment dose-dependently suppressed ROS and MDA levels while restoring GSH content and SOD/CAT activities, highlighting its potent antioxidant activity (Table 3). The effects were slightly lower than DEXA but clearly protective against $PM_{2.5}$-induced oxidative lung injury.

Table 3. Lung MDA, GSH content, and CAT/SOD activities in intact or $PM_{2.5}$-treated mice.

Groups	Lung Contents (nM/mg Protein)			Lung Enzyme Activity (U/mg Protein)	
	MDA	ROS	GSH	SOD	CAT
Controls					
Intact vehicle	3.56 ± 1.34	23.31 ± 10.58	41.96 ± 12.99	322.80 ± 47.80	70.10 ± 13.24
$PM_{2.5}$	19.31 ± 2.80 [a]	90.43 ± 10.05 [a]	6.29 ± 1.93 [d]	65.30 ± 19.27 [d]	10.30 ± 2.11 [d]
Reference					

Table 3. *Cont.*

Groups	Lung Contents (nM/mg Protein)			Lung Enzyme Activity (U/mg Protein)	
	MDA	ROS	GSH	SOD	CAT
DEXA	6.75 ± 1.70 ^{bc}	41.35 ± 10.05 ^{ac}	19.17 ± 3.97 ^{de}	188.60 ± 41.95 ^{de}	38.20 ± 12.77 ^{de}
Test article—TV					
200 mg/kg	8.92 ± 2.44 ^{ac}	48.72 ± 11.29 ^{ac}	15.95 ± 2.47 ^{de}	166.10 ± 27.13 ^{de}	30.80 ± 10.78 ^{de}
100 mg/kg	10.70 ± 2.18 ^{ac}	59.25 ± 10.12 ^{ac}	13.95 ± 2.21 ^{de}	145.70 ± 29.81 ^{de}	23.20 ± 7.71 ^{de}
50 mg/kg	12.36 ± 1.72 ^{ac}	64.21 ± 12.31 ^{ac}	12.47 ± 2.87 ^{de}	120.00 ± 14.91 ^{de}	18.90 ± 5.26 ^{de}

Values represent means ± SD for 10 mice per group. $PM_{2.5}$ refers to Diesel Particulate Matter NIST 1650b; DEXA indicates dexamethasone treatment; TV refers to thyme (*Thymus vulgaris* L.) leaf extract; MDA refers to malondialdehyde; ROS indicates reactive oxygen species; GSH means glutathione; CAT refers to catalase; SOD stands for superoxide dismutase; THSD denotes Tukey's Honest Significant Difference test; DT3 indicates Dunnett's T3 test. Statistical significance is indicated as follows: ^{a} $p < 0.01$, ^{b} $p < 0.05$ vs. intact vehicle, ^{c} $p < 0.01$ vs. $PM_{2.5}$ control (THSD test); ^{d} $p < 0.01$ vs. intact vehicle, ^{e} $p < 0.01$ vs. $PM_{2.5}$ control (DT3 test).

3.10. Mucus Production Genes

Significant upregulation of MUC5AC (396.59%) and MUC5B (183.86%) mRNA was observed in $PM_{2.5}$ controls, consistent with hypersecretory airway responses (Table 4). TV treatment dose-dependently suppressed these expressions, suggesting a regulatory effect on mucus production and potential improvement of airway clearance. DEXA exhibited slightly stronger inhibitory effects but did not enhance expectoration-related features, unlike TV.

Table 4. Lung mRNA expression in intact or $PM_{2.5}$-treated mice.

Groups	Controls		Reference	Test Article—TV		
	Intact Vehicle	$PM_{2.5}$	DEXA	200 mg/kg	100 mg/kg	50 mg/kg
MUC5AC	1.00 ± 0.05	4.96 ± 0.75 ^{a}	2.19 ± 0.35 ^{ab}	2.46 ± 0.42 ^{ab}	2.87 ± 0.27 ^{ab}	3.35 ± 0.63 ^{ab}
MUC5 B	1.00 ± 0.07	2.85 ± 0.23 ^{a}	1.76 ± 0.33 ^{ab}	1.85 ± 0.25 ^{ab}	2.01 ± 0.22 ^{ab}	2.16 ± 0.24 ^{ab}
NF-κB	1.00 ± 0.04	8.63 ± 0.89 ^{a}	2.09 ± 0.41 ^{ab}	3.93 ± 1.10 ^{ab}	4.82 ± 1.08 ^{ab}	5.87 ± 1.21 ^{ab}
p38 MAPK	1.00 ± 0.06	7.27 ± 1.02 ^{a}	2.72 ± 0.79 ^{ab}	3.79 ± 0.87 ^{ab}	4.33 ± 0.80 ^{ab}	5.06 ± 0.90 ^{ab}
PTEN	1.00 ± 0.06	0.27 ± 0.10 ^{a}	0.70 ± 0.10 ^{ab}	0.66 ± 0.12 ^{ab}	0.60 ± 0.09 ^{ab}	0.51 ± 0.05 ^{ab}
PI3 K	1.00 ± 0.05	6.34 ± 1.06 ^{a}	2.26 ± 0.74 ^{ab}	2.69 ± 0.40 ^{ab}	3.25 ± 0.75 ^{ab}	4.07 ± 0.72 ^{ab}
Akt	1.00 ± 0.06	5.09 ± 1.31 ^{a}	1.74 ± 0.38 ^{ab}	2.06 ± 0.47 ^{ab}	2.36 ± 0.45 ^{ab}	3.05 ± 0.42 ^{ab}
Bcl-2	1.00 ± 0.06	0.38 ± 0.07 ^{a}	0.69 ± 0.14 ^{ab}	0.60 ± 0.08 ^{ab}	0.55 ± 0.08 ^{ab}	0.50 ± 0.04 ^{ab}
Bax	1.00 ± 0.05	6.93 ± 1.28 ^{a}	2.67 ± 0.71 ^{ab}	3.56 ± 0.75 ^{ab}	3.72 ± 0.83 ^{ab}	4.64 ± 0.70 ^{ab}

Values represent means ± SD for 10 mice per group. $PM_{2.5}$ refers to Diesel Particulate Matter NIST 1650b; DEXA indicates dexamethasone treatment; TV refers to thyme (*Thymus vulgaris* L.) leaf extract; RT-PCR refers to reverse transcription polymerase chain reaction; NF-κB indicates nuclear factor kappa-light-chain-enhancer of activated B cells; MAPK means mitogen-activated protein kinases; PTEN refers to phosphatase and tensin homolog; PI3K stands for phosphoinositide 3-kinase; Akt denotes protein kinase B; Bcl-2 stands for B-cell lymphoma 2; Bax refers to Bcl-2-associated X protein; THSD denotes Tukey's Honest Significant Difference test; DT3 indicates Dunnett's T3 test. Statistical significance is indicated as follows: ^{a} $p < 0.01$ vs. intact vehicle; ^{b} $p < 0.01$ vs. $PM_{2.5}$ control (DT3 test).

3.11. Oxidative Stress- and Inflammation-Related Genes

$PM_{2.5}$ exposure significantly increased NF-κB (763.66%), p38 MAPK (625.95%), PI3K (534.23%), and Akt (408.69%) mRNA expressions while decreasing PTEN (−72.60%), reflecting heightened oxidative stress and inflammatory signaling (Table 4). TV treatment dose-dependently reversed these changes, indicating suppression of pro-inflammatory pathways and partial restoration of protective PTEN signaling. These results suggest TV modulates critical molecular pathways underlying $PM_{2.5}$-induced pulmonary injury.

3.12. Apoptosis-Related Genes

$PM_{2.5}$ induced a pro-apoptotic shift with decreased Bcl-2 (−62.19%) and increased Bax (590.04%) mRNA expression (Table 4). TV treatment dose-dependently normalized these expressions, demonstrating anti-apoptotic effects and potential protection of alveolar epithelial integrity.

3.13. Lung Histopathology

Histopathological analysis confirmed $PM_{2.5}$-induced lung injury, including alveolar septal thickening, inflammatory cell infiltration, and hyperplasia of PAS+ mucus-producing cells, resulting in decreased alveolar surface area (−53.39%). TV treatment dose-dependently reduced septal thickening and inflammatory infiltration, partially restored ASA, and increased PAS+ cell numbers, their occupied percentages, and secondary bronchus mucosa thickness, suggesting both protective and expectorant effects (Figure 7; Table 5). DEXA mainly reduced inflammation but did not affect mucus hyperplasia, highlighting the complementary benefit of TV in maintaining airway clearance.

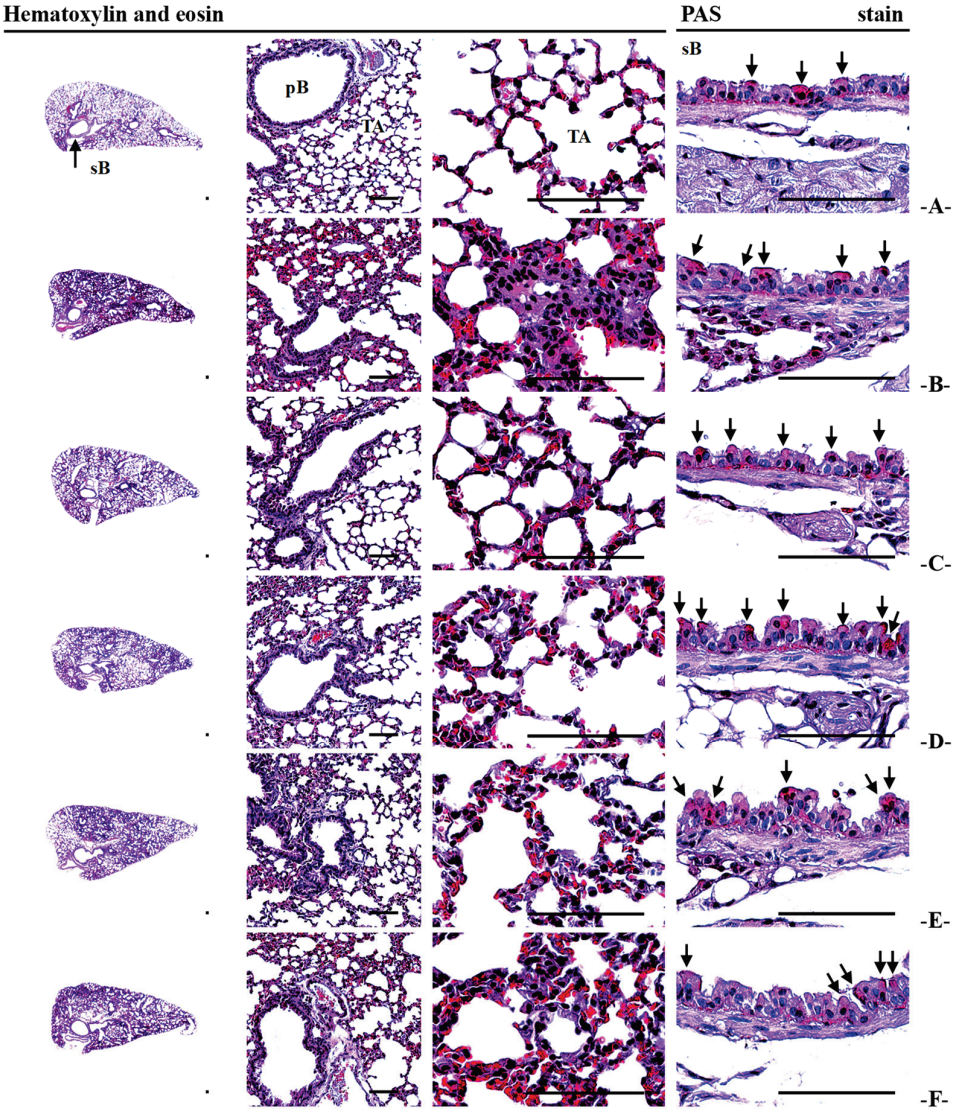

Figure 7. Representative histopathological profiles of left lung lobes in intact and $PM_{2.5}$-treated mice. Treatments are designated as follows: (**A**)—intact vehicle control (distilled water orally, saline intranasal),

(**B**)—$PM_{2.5}$ control (distilled water orally, $PM_{2.5}$ intranasal), (**C**)—DEXA (0.75 mg/kg orally, $PM_{2.5}$ intranasal), (**D**)—TV_{200} (200 mg/kg TV orally, $PM_{2.5}$ intranasal), (**E**)—TV_{100} (100 mg/kg TV orally, $PM_{2.5}$ intranasal), (**F**)—TV_{50} (50 mg/kg TV orally, $PM_{2.5}$ intranasal). $PM_{2.5}$ refers to Diesel Particulate Matter NIST 1650b; DEXA indicates dexamethasone treatment; TV refers to thyme (*Thymus vulgaris* L.) leaf extract; ASA stands for alveolar surface area; PAS indicates periodic acid Schiff; sB denotes secondary bronchus; pB refers to primary bronchiole; TA stands for terminal respiratory bronchiole-alveoli. PAS+ mucus-producing cells are highlighted with arrows. Scale bars = 200 μm.

Table 5. Histomorphometrical analysis of lung—Left lobe tissue in intact or $PM_{2.5}$-treated mice.

Groups	Mean ASA (%/mm²)	Mean Alveolar Septal Thickness (μm)	Mean Thickness of SB (μm)	Mean IF Cell Numbers Infiltrated in AR (×10 Cells/mm²)	PAS-Positive Cells on the SB	
					Numbers (Cells/mm²)	Percentages (%/Epithelium)
Controls						
Intact vehicle	82.66 ± 8.04	4.09 ± 1.46	13.71 ± 1.20	56.80 ± 12.19	24.00 ± 2.98	1.23 ± 0.44
$PM_{2.5}$	38.53 ± 6.10 [a]	38.32 ± 3.41 [d]	19.63 ± 1.46 [d]	883.90 ± 168.40 [d]	39.60 ± 3.75 [d]	4.87 ± 0.68 [d]
Reference						
DEXA	72.16 ± 8.12 [bc]	12.44 ± 4.89 [de]	18.95 ± 2.77 [d]	128.40 ± 31.00 [de]	38.80 ± 7.44 [d]	4.65 ± 0.99 [d]
Test article—TV						
200 mg/kg	67.79 ± 8.16 [ac]	15.97 ± 2.54 [de]	28.08 ± 1.83 [de]	193.60 ± 47.41 [de]	84.60 ± 10.46 [de]	20.00 ± 4.00 [de]
100 mg/kg	60.39 ± 7.96 [ac]	19.14 ± 3.27 [de]	25.88 ± 1.45 [de]	331.00 ± 83.95 [de]	63.80 ± 10.04 [de]	12.84 ± 3.25 [de]
50 mg/kg	54.81 ± 5.57 [ac]	27.78 ± 4.94 [de]	23.81 ± 0.77 [de]	583.00 ± 98.91 [de]	53.00 ± 6.75 [de]	7.56 ± 0.90 [de]

Values represent means ± SD for 10 mice per group. $PM_{2.5}$ refers to Diesel Particulate Matter NIST 1650b; DEXA indicates dexamethasone treatment; TV refers to thyme (*Thymus vulgaris* L.) leaf extract; ASA refers to alveolar surface area; AR indicates alveolar region; SB means secondary bronchus mucosa; IF stands for inflammatory; PAS denotes periodic acid Schiff; THSD refers to Tukey's Honest Significant Difference test; DT3 indicates Dunnett's T3 test. Statistical significance is indicated as follows: [a] $p < 0.01$, [b] $p < 0.05$ vs. intact vehicle, [c] $p < 0.01$ vs. $PM_{2.5}$ control (THSD test); [d] $p < 0.01$ vs. intact vehicle, [e] $p < 0.01$ vs. $PM_{2.5}$ control (DT3 test).

4. Discussion

Particulate matter has emerged as a major environmental health issue due to its profound effects on human respiratory and systemic health. Among its fractions, fine particles < 2.5 μm in diameter ($PM_{2.5}$) are particularly dangerous, as they can penetrate deep into the lung, accumulate in the alveoli, and evade mucociliary clearance [43–46]. The harmful effects of $PM_{2.5}$ are further amplified by adsorbed toxic substances such as organic compounds, heavy metals, and sulfates, which enhance oxidative stress and inflammatory signaling in pulmonary tissues [47,48]. Epidemiological studies have linked chronic $PM_{2.5}$ exposure to a spectrum of health-related problems, including cardiovascular disorders, lung cancer, chronic obstructive pulmonary disease (COPD), and asthma, highlighting the critical necessity for both preventive and treatment strategies [49,50].

In this study, repeated intranasal instillation of $PM_{2.5}$ in Balb/c mice induced classic features of pulmonary injury, including lung congestion, increased lung weight, and leukocyte infiltration in BALF. In parallel, there was upregulation of chemokines (CXCL1, CXCL2) and inflammatory cytokines (IL-6, TNF-α), as well as increased expression of matrix metalloproteinases (MMP-9, MMP-12), which contribute to extracellular matrix degradation and airway remodeling [51,52]. $PM_{2.5}$ also triggered oxidative stress, evidenced by elevated ROS and lipid peroxidation, alongside depletion of endogenous antioxidant systems such as CAT, GSH, and SOD. These results support previous studies indicating that oxidative stress plays a key role in mediating $PM_{2.5}$-induced lung toxicity [53–55].

Treatment with *T. vulgaris* (TV) extract demonstrated robust protective effects across multiple pathological dimensions. TV restored antioxidant defenses by replenishing GSH, SOD, and CAT levels while reducing ROS and MDA accumulation, highlighting its potent free-radical scavenging activity. This effect is likely attributable to bioactive constituents such as rosmarinic acid, which has well-documented antioxidant properties [56–58]. In parallel, TV suppressed key inflammatory signaling pathways, including p38 MAPK,

PI3K/Akt, and NF-κB, while restoring PTEN expression, thereby reducing the transcription of chemokines and pro-inflammatory genes. Consequently, TV significantly decreased BALF leukocyte infiltration and systemic pulmonary inflammation, aligning with earlier studies on the anti-inflammatory activity of thyme and its bioactive components [19,21–23,59–61].

$PM_{2.5}$ exposure also induced apoptotic imbalance, with decreased Bcl-2 and increased Bax expression, contributing to epithelial cell death and alveolar structural damage. TV treatment effectively restored this apoptotic balance, enhancing Bcl-2 and reducing Bax expression, thus preserving alveolar integrity. Histopathological evaluation further confirmed that TV reduced alveolar septal thickening, inflammatory infiltration, and mucus cell hyperplasia, demonstrating comprehensive tissue-level protection.

A particularly notable finding was the mucoregulatory effect of TV. $PM_{2.5}$ exposure enhanced expression of mucin-related genes (MUC5AC, MUC5B), as well as secretagogue substances P and ACh, promoting mucus hypersecretion and impaired airway clearance. TV extract dose-dependently suppressed these changes, reducing alveolar septal thickness and mucin-related gene expressions while facilitating airway clearance—increasing P and ACh contents and PAS+ cell proliferation and hypertrophy. This dual action—limiting excessive mucus while enhancing expectoration—is clinically significant for respiratory diseases such as COPD and asthma, where impaired mucociliary clearance exacerbates pathology [62]. However, future studies should include physiological measurements of substance P and ACh to better elucidate the relationship between the effects of the TV extract and the modulation of bronchiolar hyperresponsiveness, with mucin distributions throughout airways.

Comparison with DEXA (0.75 mg/kg) revealed important therapeutic distinctions. While DEXA strongly suppressed inflammation, it did not fully mitigate mucus cell hyperplasia or bronchial thickening, and systemic adverse effects, including reductions in body weight, were noted. In contrast, TV exhibited broader pulmonary protection by combining anti-inflammatory, antioxidant, anti-apoptotic, and mucoregulatory effects without adverse systemic outcomes, highlighting its potential as a safer, multi-target therapeutic strategy. Collectively, these findings suggest that TV confers comprehensive protection against $PM_{2.5}$-induced pulmonary injury. By simultaneously targeting oxidative stress, inflammation, apoptosis, and mucus hypersecretion, TV provides a broader protective profile than conventional anti-inflammatory drugs, supporting its prospective role as a natural therapeutic or functional food candidate for protecting respiratory function.

Nevertheless, several limitations should be acknowledged. This study employed a subacute 10-day $PM_{2.5}$ exposure model, providing valuable insights into short-term pulmonary responses, but it may not fully capture the complexity of chronic human exposure. While the current findings suggest a regulatory effect of TV extract on airway mediators such as substance P and ACh, complementary physiological assessments of bronchiolar responsiveness would further strengthen the mechanistic understanding of these effects. Phytochemical characterization in this study focused on rosmarinic acid as a representative marker; however, identification and quantification of other polyphenolic constituents present in TV extract warrant further investigation. A more comprehensive phytochemical analysis using advanced techniques such as UHPLC-ESI-MS or HPLC-PDA would enable a clearer delineation of the bioactive components responsible for the observed effects. Future studies could also explore chronic exposure models, include pharmacokinetic evaluations of individual constituents, and perform comparative analyses with standard therapeutic agents such as mucolytics and bronchodilators to better define the clinical relevance and translational potential of *T. vulgaris* leaf extract.

5. Conclusions

The present study demonstrated that oral administration of standardized *T. vulgaris* extract (TV extract at 200—50 mg/kg) provided dose-dependent protective effects under conditions of $PM_{2.5}$-induced subacute pulmonary damage in Balb/c mice. TV significantly reduced oxidative stress, inflammatory cytokines, MMP activity, and apoptosis, while restoring antioxidant defenses and normalizing PI3K/Akt and p38 MAPK signaling. Unlike dexamethasone (DEXA, 0.75 mg/kg), which exhibited stronger anti-inflammatory effects, TV additionally exerted unique mucolytic–expectorant activities by increasing substance P and ACh levels, reducing MUC5AC and MUC5B expression, and alleviating PAS+ cell hyperplasia and mucosal thickening, thereby promoting mucus clearance. Histopathology and gross examinations confirmed that TV alleviated $PM_{2.5}$-induced lung congestion, cellular infiltration, and septal thickening, while serum AST and ALT analysis indicated no hepatotoxicity. Collectively, these findings suggest that although TV was slightly less potent than DEXA in suppressing inflammation, its combined antioxidant, anti-inflammatory, anti-apoptotic, and mucoregulatory actions, together with a favorable safety profile, highlight its efficacy as a natural respiratory-protective agent and functional food ingredient against $PM_{2.5}$-induced pulmonary injury.

Supplementary Materials: The following supporting information can be downloaded at: https://www.mdpi.com/article/10.3390/antiox14111343/s1, Figure S1. Schematic diagram of the manufacturing process for Thymus vulgaris leaf extract; Table S1. Oligonucleotides used for quantitative RT-PCR; Table S2. Body weight gains in intact or $PM_{2.5}$-treated pulmonary-injured mice; Table S3. Lung weights and gross inspections in intact or $PM_{2.5}$-treated pulmonary injured mice.

Author Contributions: Conceptualization, S.-K.K.; methodology, J.-K.L., J.-S.C. and S.-K.K.; software, S.-K.K.; validation, K.M.I.B., J.-S.C. and S.-K.K.; formal analysis, J.-K.L., K.M.I.B., H.-R.P., J.-G.K., B.-R.C., J.-S.C. and S.-K.K.; investigation, J.-S.C. and S.-K.K.; resources, S.-K.K.; data curation, J.-K.L., K.M.I.B., H.-R.P., J.-G.K. and B.-R.C.; writing—original draft preparation, J.-K.L., K.M.I.B. and J.-S.C.; writing—review and editing, K.M.I.B., J.-S.C. and S.-K.K.; visualization, K.M.I.B., J.-S.C. and S.-K.K.; supervision, J.-S.C. and S.-K.K.; project administration, S.-K.K.; funding acquisition, S.-K.K. All authors have read and agreed to the published version of the manuscript.

Funding: This research was supported by a grant (Graduate School Education Program of Regulatory Sciences for Functional Food, 21153MFDS604) from the Ministry of Food and Drug Safety in 2021.

Institutional Review Board Statement: The animal study protocol was approved by the Animal Experiment Ethics Committee of Daegu Haany University [Approval No.: DHU2022-013; Approval Date: 22 February 2022].

Informed Consent Statement: Not applicable.

Data Availability Statement: The original contributions presented in this study are included in the article/Supplementary Materials. Further inquiries can be directed to the corresponding authors.

Conflicts of Interest: Author Jae-Kyoung Lee is employed by Hongsamdan Co., Ltd. Authors Hye-Rim Park, Jin-Gwan Kwon, and Beom-Rak Choi are employed by Nutracore Co., Ltd. The remaining authors declare that this research was conducted without any commercial or financial relationships that could be construed as potential conflicts of interest.

Abbreviations

The following abbreviations are used in this manuscript:

ACh	Acetylcholine
ALT	Alanine transaminase

ASA	Alveolar surface area
AST	Aspartate transaminase
BALF	Bronchoalveolar lavage fluid
Bax	BCL2 associated x
Bcl-2	B-cell leukemia/lymphoma 2
CAT	Catalase
CXCL-1	Chemokine (C-X-C Motif) Ligand 1
CXCL-2	Chemokine (C-X-C Motif) Ligand 2
DCFDA	Dichlorodihydrofluorescein diacetate
DEXA	Dexamethasone
ELISA	Enzyme-linked immunosorbent assay
GPx	Glutathione peroxidase
H&E	Hematoxylin and eosin
HO-1	Heme oxygenase-1
IL-6	Interleukin-6
MAPK	Mitogen-activated protein kinase
MDA	Malondialdehyde
MMPs	Matrix metalloproteinases
MUC5AC	Mucin 5AC
MUC5B	Mucin 5B
NF-κB	Kappa-light-chain-enhancer of activated B cells
p38 MAPK	p38 mitogen-activated protein kinase
PAS	Periodic acid-Schiff
PI3K/Akt	Phosphoinositide 3-kinase/Protein kinase B
PM	Particulate matter
PTEN	Phosphatase and tensin homolog
ROS	Reactive oxygen species
SOD	Superoxide dismutase
TNF-α	Tumor necrosis factor-α
TV	Thyme (*Thyme vulgaris* L.) leaf extract

References

1. Fernando, I.P.S.; Jayawardena, T.U.; Kim, H.S.; Lee, W.W.; Vaas, A.P.J.P.; De Silva, H.I.C.; Abayaweera, G.S.; Nanayakkara, C.M.; Abeytunga, D.T.U.; Lee, D.S.; et al. Beijing urban particulate matter-induced injury and inflammation in human lung epithelial cells and the protective effects of fucosterol from *Sargassum binderi* (Sonder ex J. Agardh). *Environ. Res.* **2019**, *172*, 150–158. [CrossRef]
2. Lee, W.; Ku, S.K.; Kim, J.E.; Cho, S.H.; Song, G.Y.; Bae, J.S. Inhibitory effects of protopanaxatriol type ginsenoside fraction (Rgx365) on particulate matter-induced pulmonary injury. *J. Toxicol. Environ. Health A* **2019**, *82*, 338–350. [CrossRef]
3. Lee, W.; Ku, S.K.; Kim, J.E.; Cho, S.H.; Song, G.Y.; Bae, J.S. Inhibitory effects of black ginseng on particulate matter-induced pulmonary injury. *Am. J. Chin. Med.* **2019**, *47*, 1237–1251. [CrossRef]
4. Zhuang, G.; Guo, J.; Yuan, H.; Zhao, C. The compositions, sources, and size distribution of the dust storm from China in spring of 2000 and its impact on the global environment. *Chin. Sci. Bull.* **2001**, *46*, 895–900. [CrossRef]
5. Wang, W.; Primbs, T.; Tao, S.; Simonich, S.L. Atmospheric particulate matter pollution during the 2008 Beijing Olympics. *Environ. Sci. Technol.* **2009**, *43*, 5314–5320. [CrossRef] [PubMed]
6. Huang, X.F.; He, L.Y.; Hu, M.; Zhang, Y.H. Annual variation of particulate organic compounds in PM2.5 in the urban atmosphere of Beijing. *Atmos. Environ.* **2006**, *40*, 2449–2458. [CrossRef]
7. Lv, B.; Zhang, B.; Bai, Y. A systematic analysis of PM2.5 in Beijing and its sources from 2000 to 2012. *Atmos. Environ.* **2016**, *124*, 98–108. [CrossRef]
8. Nunes, C.; Pereira, A.M.; Morais-Almeida, M. Asthma costs and social impact. *Asthma Res. Pract.* **2017**, *3*, 1. [CrossRef]
9. Wang, G.; Huang, L.; Gao, S.; Gao, S.; Wang, L. Measurements of PM10 and PM2.5 in urban area of Nanjing, China and the assessment of pulmonary deposition of particle mass. *Chemosphere* **2002**, *48*, 689–695. [CrossRef]
10. Schaumann, F.; Borm, P.J.; Herbrich, A.; Knoch, J.; Pitz, M.; Schins, R.P.; Luettig, B.; Hohlfeld, J.M.; Heinrich, J.; Krug, N. Metal-rich ambient particles (particulate matter 2.5) cause airway inflammation in healthy subjects. *Am. J. Respir. Crit. Care Med.* **2004**, *170*, 898–903. [CrossRef]

11. Wang, F.; Wang, R.; Liu, H. The acute pulmonary toxicity in mice induced by *Staphylococcus aureus*, particulate matter, and their combination. *Exp. Anim.* **2019**, *68*, 159–168. [CrossRef]
12. Pozzi, R.; De Berardis, B.; Paoletti, L.; Guastadisegni, C. Inflammatory mediators induced by coarse (PM2.5-10) and fine (PM2.5) urban air particles in RAW 264.7 cells. *Toxicology* **2003**, *183*, 243–254. [CrossRef]
13. Dubashynskaya, N.V.; Bokatyi, A.N.; Skorik, Y.A. Dexamethasone conjugates: Synthetic approaches and medical prospects. *Biomedicines* **2021**, *9*, 341. [CrossRef] [PubMed]
14. Min, B.G.; Park, S.M.; Choi, Y.W.; Ku, S.K.; Cho, I.J.; Kim, Y.W.; Byun, S.H.; Park, C.A.; Park, S.J.; Na, M.; et al. Effects of *Pelargonium sidoides* and Coptis Rhizoma 2 : 1 mixed formula (PS + CR) on ovalbumin-induced asthma in mice. *Evid. Based Complement. Alternat. Med.* **2020**, *2020*, 9135637. [CrossRef]
15. Piao, C.H.; Fan, Y.J.; Nguyen, T.V.; Song, C.H.; Chai, O.H. Mangiferin alleviates ovalbumin-induced allergic rhinitis via Nrf2/HO-1/NF-κB signaling pathways. *Int. J. Mol. Sci.* **2020**, *21*, 3415. [CrossRef] [PubMed]
16. Wang, P.; Liu, H.; Fan, X.; Zhu, Z.; Zhu, Y. Effect of San'ao decoction on aggravated asthma mice model induced by PM2.5 and TRPA1/TRPV1 expressions. *J. Ethnopharmacol.* **2019**, *236*, 82–90. [CrossRef] [PubMed]
17. Kim, H.S.; Park, S.I.; Choi, S.H.; Song, C.H.; Park, S.J.; Shin, Y.K.; Han, C.H.; Lee, Y.J.; Ku, S.K. Single oral dose toxicity test of blue honeysuckle concentrate in mice. *Toxicol. Res.* **2015**, *31*, 61–68. [CrossRef]
18. Devipriya, D.; Gowri, S.; Nideesh, T.R. Hepatoprotective effect of *Pterocarpus marsupium* against carbon tetrachloride induced damage in albino rats. *Anc. Sci. Life.* **2007**, *27*, 19–25. [PubMed Central]
19. Figueira, L.W.; de Oliveira, J.R.; Camargo, S.E.A.; de Oliveira, L.D. *Curcuma longa* L. (turmeric), *Rosmarinus officinalis* L. (rosemary), and *Thymus vulgaris* L. (thyme) extracts aid murine macrophages (RAW 264.7) to fight *Streptococcus mutans* during in vitro infection. *Arch. Microbiol.* **2020**, *202*, 2269–2277. [CrossRef]
20. El-Qudah, J.M. Contents of chlorophyll and carotenoid pigments in common thyme (*Thymus vulgaris* L.). *World Appl. Sci. J.* **2014**, *29*, 1277–1281.
21. de Oliveira, J.R.; de Jesus, D.; Figueira, L.W.; de Oliveira, F.E.; Soares, C.P.; Camargo, S.E.; Jorge, A.O.; de Oliveira, L.D. Biological activities of *Rosmarinus officinalis* L. (rosemary) extract as analyzed in microorganisms and cells. *Exp. Biol. Med.* **2017**, *242*, 625–634. [CrossRef]
22. de Oliveira, J.R.; de Jesus Viegas, D.; Martins, A.P.R.; Carvalho, C.A.T.; Soares, C.P.; Camargo, S.E.A.; Jorge, A.O.C.; de Oliveira, L.D. *Thymus vulgaris* L. extract has antimicrobial and anti-inflammatory effects in the absence of cytotoxicity and genotoxicity. *Arch. Oral Biol.* **2017**, *82*, 271–279. [CrossRef]
23. El-Newary, S.A.; Shaffie, N.M.; Omer, E.A. The protection of *Thymus vulgaris* leaves alcoholic extract against hepatotoxicity of alcohol in rats. *Asian Pac. J. Trop. Med.* **2017**, *10*, 361–371. [CrossRef]
24. Nagoor Meeran, M.F.; Javed, H.; Al Taee, H.; Azimullah, S.; Ojha, S.K. Pharmacological properties and molecular mechanisms of thymol: Prospects for its therapeutic potential and pharmaceutical development. *Front. Pharmacol.* **2017**, *8*, 380. [CrossRef] [PubMed]
25. Waheed, M.; Hussain, M.B.; Saeed, F.; Afzaal, M.; Ahmed, A.; Irfan, R.; Akram, N.; Ahmed, F.; Hailu, G.G. Phytochemical profiling and therapeutic potential of thyme (*Thymus* spp.): A medicinal herb. *Food Sci. Nutr.* **2024**, *12*, 9893–9912. [CrossRef] [PubMed]
26. Sharangi, A.B.; Guha, S. Wonders of leafy spices: Medicinal properties ensuring human health. *Sci. Int.* **2013**, *1*, 312–317. [CrossRef]
27. Dauqan, E.M.; Abdullah, A. Medicinal and functional values of thyme (*Thymus vulgaris* L.) herb. *J. Appl. Biol. Biotechnol.* **2017**, *5*, 17–22. [CrossRef]
28. Ku, S.K.; Kim, J.W.; Cho, H.R.; Kim, K.Y.; Min, Y.H.; Park, J.H.; Kim, J.S.; Park, J.H.; Seo, B.I.; Roh, S.S. Effect of β-glucan originated from *Aureobasidium pullulans* on asthma induced by ovalbumin in mouse. *Arch. Pharm. Res.* **2012**, *35*, 1073–1081. [CrossRef]
29. Kavutcu, M.; Canbolat, O.; Oztürk, S.; Olcay, E.; Ulutepe, S.; Ekinci, C.; Gökhun, I.H.; Durak, I. Reduced enzymatic antioxidant defense mechanism in kidney tissues from gentamicin-treated guinea pigs: Effects of vitamins E and C. *Nephron* **1996**, *72*, 269–274. [CrossRef] [PubMed]
30. Jamall, I.S.; Smith, J.C. Effects of cadmium on glutathione peroxidase, superoxidase dismutase and lipid peroxidation in the rat heart: A possible mechanism of cadmium cardiotoxicity. *Toxicol. Appl. Pharmacol.* **1985**, *80*, 33–42. [CrossRef]
31. Lowry, O.H.; Rosenbrough, N.J.; Farr, A.L.; Randall, R.J. Protein measurement with the Folin phenol reagent. *J. Biol. Chem.* **1951**, *193*, 265–275. [CrossRef] [PubMed]
32. He, J.; Xu, Q.; Jing, Y.; Agani, F.; Qian, X.; Carpenter, R.; Li, Q.; Wang, X.R.; Peiper, S.S.; Lu, Z.; et al. Reactive oxygen species regulate ERBB2 and ERBB3 expression via miR-199a/125b and DNA methylation. *EMBO Rep.* **2012**, *13*, 1116–1122. [CrossRef] [PubMed]
33. Sedlak, J.; Lindsay, R.H. Estimation of total, protein-bound, and nonprotein sulfhydryl groups in tissue with Ellman's reagent. *Anal. Biochem.* **1968**, *25*, 192–205. [CrossRef]

34. Aebi, H. Catalase. In *Methods in Enzymatic Analysis*; Bergmeyer, H.U., Ed.; Academic Press: New York, NY, USA, 1974; pp. 673–686. [CrossRef]
35. Sun, Y.; Larry, W.O.; Ying, L. A simple method for clinical assay of superoxide dismutase. *Clin. Chem.* **1988**, *34*, 497–500. [CrossRef] [PubMed]
36. Deng, X.; Rui, W.; Zhang, F.; Ding, W. PM2.5 induces Nrf2-mediated defense mechanisms against oxidative stress by activating PIK3/AKT signaling pathway in human lung alveolar epithelial A549 cells. *Cell Biol. Toxicol.* **2013**, *29*, 143–157. [CrossRef]
37. Jin, Y.; Wu, W.; Zhang, W.; Zhao, Y.; Wu, Y.; Ge, G.; Ba, Y.; Guo, Q.; Gao, T.; Chi, X.; et al. Involvement of EGF receptor signaling and NLRP12 inflammasome in fine particulate matter-induced lung inflammation in mice. *Environ. Toxicol.* **2017**, *32*, 1121–1134. [CrossRef]
38. Livak, K.J.; Schmittgen, T.D. Analysis of relative gene expression data using real-time quantitative PCR and the $2^{-\Delta\Delta CT}$ method. *Methods* **2001**, *25*, 402–408. [CrossRef]
39. Abdelaziz, R.R.; Elmahdy, M.K.; Suddek, G.M. Flavocoxid attenuates airway inflammation in ovalbumin-induced mouse asthma model. *Chem. Biol. Interact.* **2018**, *292*, 15–23. [CrossRef]
40. Morton, J.; Snider, T.A. Guidelines for collection and processing of lungs from aged mice for histological studies. *Pathobiol. Aging Age-Related Dis.* **2017**, *7*, 1313676. [CrossRef]
41. Lee, S.; Lee, D.K. What is the proper way to apply the multiple comparison test? *Korean J. Anesthesiol.* **2018**, *71*, 353–360. [CrossRef] [PubMed]
42. Sauder, D.C.; DeMars, C.E. An updated recommendation for multiple comparisons. *Adv. Methods Pract. Psychol. Sci.* **2019**, *2*, 26–44. [CrossRef]
43. de Kok, T.M.; Engels, L.G.; Moonen, E.J.; Kleinjans, J.C. Inflammatory bowel disease stimulates formation of carcinogenic N-nitroso compounds. *Gut* **2005**, *54*, 731. [CrossRef]
44. Pope, C.A., 3rd; Dockery, D.W. Health effects of fine particulate air pollution: Lines that connect. *J. Air Waste Manag. Assoc.* **2006**, *56*, 709–742. [CrossRef] [PubMed]
45. Sun, Y.; Yin, Y.; Zhang, J.; Yu, H.; Wang, X.; Wu, J.; Xue, Y. Hydroxyl radical generation and oxidative stress in *Carassius auratus* liver, exposed to pyrene. *Ecotoxicol. Environ. Saf.* **2008**, *71*, 446–453. [CrossRef] [PubMed]
46. Wu, S.; Deng, F.; Hao, Y.; Wang, X.; Zheng, C.; Lv, H.; Lu, X.; Wei, H.; Huang, J.; Qin, Y.; et al. Fine particulate matter, temperature, and lung function in healthy adults: Findings from the HVNR study. *Chemosphere* **2014**, *108*, 168–174. [CrossRef]
47. Kelly, F.J.; Fussell, J.C. Size, source and chemical composition as determinants of toxicity attributable to ambient particulate matter. *Atmos. Environ.* **2012**, *60*, 504–526. [CrossRef]
48. Yang, S.; Fang, D.; Chen, B. Human health impact and economic effect for PM2.5 exposure in typical cities. *Appl. Energy* **2019**, *249*, 316–325. [CrossRef]
49. Brook, R.D.; Rajagopalan, S.; Pope, C.A., 3rd; Brook, J.R.; Bhatnagar, A.; Diez-Roux, A.V.; Holguin, F.; Hong, Y.; Luepker, R.V.; Mittleman, M.A.; et al. American heart association council on epidemiology and prevention, council on the kidney in cardiovascular disease, and council on nutrition, physical activity and metabolism. Particulate matter air pollution and cardiovascular disease: An update to the scientific statement from the American Heart Association. *Circulation* **2010**, *121*, 2331–2378. [CrossRef]
50. Guo, H.; Chang, Z.; Wu, J.; Li, W. Air pollution and lung cancer incidence in China: Who are faced with a greater effect? *Environ. Int.* **2019**, *132*, 105077. [CrossRef]
51. Atkinson, J.J.; Senior, R.M. Matrix metalloproteinase-9 in lung remodeling. *Am. J. Respir. Cell Mol. Biol.* **2003**, *28*, 12–24. [CrossRef]
52. Barnes, P.J. Immunology of asthma and chronic obstructive pulmonary disease. *Nat. Rev. Immunol.* **2008**, *8*, 183–192. [CrossRef]
53. Donaldson, K.; Tran, L.; Jimenez, L.A.; Duffin, R.; Newby, D.E.; Mills, N.; MacNee, W.; Stone, V. Combustion-derived nanoparticles: A review of their toxicology following inhalation exposure. *Part. Fibre Toxicol.* **2005**, *2*, 10. [CrossRef]
54. Gangwar, R.S.; Bevan, G.H.; Palanivel, R.; Das, L.; Rajagopalan, S. Oxidative stress pathways of air pollution mediated toxicity: Recent insights. *Redox. Biol.* **2020**, *34*, 101545. [CrossRef] [PubMed]
55. Garcia, A.; Santa-Helena, E.; De Falco, A.; de Paula, R.J.; Gioda, A.; Gioda, C.R. Toxicological effects of fine particulate matter (PM2.5): Health risks and associated systemic injuries-systematic review. *Water Air Soil Pollut.* **2023**, *234*, 346. [CrossRef]
56. Escobar, A.; Pérez, M.; Romanelli, G.; Blustein, G. Thymol bioactivity: A review focusing on practical applications. *Arab. J. Chem.* **2020**, *13*, 9243–9269. [CrossRef]
57. Mateus, A.R.S.; Serrano, C.; Almeida, C.; Soares, A.; Rolim Lopes, V.; Sanches-Silva, A. Beyond thymol and carvacrol: Characterizing the phenolic profiles and antioxidant capacity of *Portuguese oregano* and thyme for food applications. *Appl. Sci.* **2024**, *14*, 8924. [CrossRef]
58. Spyrou, S.; Bellou, M.G.; Papanikolaou, A.; Nakou, K.; Kontogianni, V.G.; Chatzikonstantinou, A.V.; Stamatis, H. Evaluation of antioxidant, antibacterial and enzyme-inhibitory properties of dittany and thyme extracts and their application in hydrogel preparation. *BioChem* **2024**, *4*, 166–188. [CrossRef]

59. El-Nekeety, A.A.; Mohamed, S.R.; Hathout, A.S.; Hassan, N.S.; Aly, S.E.; Abdel-Wahhab, M.A. Antioxidant properties of *Thymus vulgaris* oil against aflatoxin-induce oxidative stress in male rats. *Toxicon* **2011**, *57*, 984–991. [CrossRef]
60. Ocaña, A.; Reglero, G. Effects of thyme extract oils (from *Thymus vulgaris*, *Thymus zygis*, and *Thymus hyemalis*) on cytokine production and gene expression of oxLDL-stimulated THP-1-macrophages. *J. Obes.* **2012**, *2012*, 104706. [CrossRef]
61. Kensara, O.A.; El-Sawy, N.A.; El-Shemi, A.G.; Header, E.A. *Thymus vulgaris* supplementation attenuates blood pressure and aorta damage in hypertensive rats. *J. Med. Plants Res.* **2013**, *7*, 669–676.
62. Fahy, J.V.; Dickey, B.F. Airway mucus function and dysfunction. *N. Engl. J. Med.* **2010**, *363*, 2233–2247. [CrossRef] [PubMed]

antioxidants

MDPI

Article

Alterations of the Intestinal Barrier and Inflammatory Response, Caused by Chronic Ozone Exposure in a Rat Model

Alfredo Miranda-Martínez, Erika Rodríguez-Martínez, Marlen Valdés-Fuentes and Selva Rivas-Arancibia *

Departamento de Fisiología, Facultad de Medicina, Universidad Nacional Autónoma de México, Mexico City 04510, Mexico; fisiomedicina@gmail.com (A.M.-M.); arodriguez@facmed.unam.mx (E.R.-M.); marlen_valdes@ciencias.unam.mx (M.V.-F.)

* Correspondence: srivas@unam.mx; Tel.: +52-5556232500

Abstract: Ozone pollution is a significant public health problem due to its association with chronic diseases. This study examines the effects of repeated exposure to low doses of ozone on intestinal barrier function in rats. Seventy-two male Wistar rats were divided into six groups. The control group was exposed to normal air, while the ozone groups received a dose of 0.25 ppm for four hours daily for periods of 7, 15, 30, 60, and 90 days, respectively. After treatment, the duodenum, jejunum, and colon were removed and analyzed by biochemical assays, Western blot, immunohistochemistry, and histological techniques. The results indicated an increase in oxidized lipids and structural alterations in the duodenum and jejunum after 7 days of ozone exposure. The result showed changes in haptoglobin, IL-1β, and IL-6. In addition, increased immunoreactivity varied according to intestinal structure and the duration of ozone exposure in the duodenum, jejunum, and colon. In conclusion: Ozone exposure causes an increase in proinflammatory cytokines that leads to a loss of regulation of the immune response in the duodenum, jejunum, and colon of rats, as well as structural changes that alter the intestinal barrier and perpetuate a state of chronic inflammation characteristic of inflammatory bowel diseases.

Keywords: ozone exposure; oxidative stress; intestinal barrier; inflammation; intestinal permeability

1. Introduction

Air pollution is a public health concern, especially in highly industrialized and urbanized regions [1–3]. Ozone (O_3) is one of the most abundant and highly reactive pollutants. Upon entering the body, it generates reactive oxygen species (ROSs) that oxidize and damage macromolecules, including lipids, proteins, and nucleic acids [4,5]. The increase in ROSs produced secondary to repeated exposure to environmental ozone pollution causes alterations at multiple levels, both molecular and in organs and systems, and ultimately induces degenerative processes in the body. Physiologically, ROSs are produced as part of cellular metabolism, mainly by mitochondria, the endoplasmic reticulum, and peroxisomes [6]. ROSs are also important signalers of cell differentiation and proliferation mechanisms, migration, angiogenesis, and modulators of the immune system in the defense against inflammatory components and responses [7,8].

Immune system cells recognize oxidized molecules, particularly lipids, as pathogens through Toll-like receptors (TLRs) and initiate cell signaling pathways that activate the synthesis and release of inflammatory mediators [9,10]. Inflammatory responses involve complex signaling pathways where interactions between pro-inflammatory and anti-inflammatory mediators regulate the immune response. During the oxidation–reduction

balance, an inflammatory response is established during which pro- and anti-inflammatory cytokines act in a finely coordinated response to enable successful recovery from injuries, trauma, sepsis, and infections, aiding in the removal of harmful stimuli and the initiation of healing processes, contributing to the restoration of tissue homeostasis [11,12]. Therefore, the inflammatory response is reparative and self-limiting.

Chronic inflammation occurs when the body is unable to regulate inflammatory processes over time [13]. Research indicates that a loss of redox balance contributes to the dysregulation of inflammatory responses and plays a significant role in the development of various health issues, including neurodegenerative diseases [14–17], cardiovascular diseases [18], endothelial dysfunction [19], cancer, metabolic syndrome [20], obesity [21], and COVID-19 [22].

In animal models, chronic and repeated exposure to low doses of O_3 has been shown to increase oxidative molecules and weaken antioxidant systems, leading to a sustained inflammatory response that intensifies with continued exposure [23]. Additionally, this exposure causes mitochondrial and endoplasmic reticulum swelling, decreases ATP production in mitochondria, alters the structural conformation of proteins, and impairs tissue repair capacity [23–25].

In the gastrointestinal tract, various ROSs are produced as antimicrobial agents and redox signaling molecules. These ROSs are generated by epithelial cells, endothelial cells, and innate immune cells to protect the intestinal epithelium [26]. The intestine plays a crucial role in coordinating digestion, absorption, secretion, and the activities of the microbiota, immune system, endocrine system, and peripheral nervous system. These functions can be influenced by diet, exercise, medication, chronic oxidative stress, and factors such as exposure to environmental pollutants, among others [27,28]. The functions that the gut performs though its constant exposure to food, microbiota, and pathogens indicated that it has a highly specialized immune system associated with it. This system ranges from maintaining tissue integrity and repairing tissue injuries to absorbing food and water and eliminating pathogenic invaders [29,30].

Under normal physiological conditions, the intestine produces various cytokines, hormones, neurotransmitters, and enzymes essential for its proper functioning [31]. However, when the intestinal barrier loses its selective permeability, large molecules can enter the bloodstream. The immune system perceives these substances as threats, triggering inflammatory responses. When these responses become chronically unregulated, they are associated with inflammatory intestinal disorders and extraintestinal autoimmune diseases, such as rheumatoid arthritis and multiple sclerosis, as well as metabolic conditions like diabetes and obesity [32]. We are interested in studying the effects of repeated exposure to low doses of O_3 on the intestinal barrier and the changes in the inflammatory interleukin-1 beta (IL-1β) and interleukin-6 (IL-6) in the duodenum, jejunum, and colon of rats.

2. Materials and Methods

The experiments conducted in this study strictly adhered to the guidelines set forth by the Mexican Official Standard NOM-062-ZOO-1999 [33], which specifies the technical requirements for the production, care, and use of laboratory animals. International guidelines on animal ethics and management were also followed to minimize both the number of animals used and their suffering. The Ethics Committee of the UNAM Faculty of Medicine approved all animal experiments [34]. A total of 72 male Wistar rats, weighing 250 g, were individually housed in transparent acrylic cages with laboratory animal chow (LabDiet, México City, Mexico), water ad libitum, and a constant temperature of 21 °C, with 12 h of light and 12 h of darkness. They were randomly divided into six experimental groups (n = 12); After O_3 exposure, the animals were deeply anesthetized with sodium pentobarbital at a dose of

50 mg/kg, as described in NOM-033-SAG-ZOO-2014 guidelines [35]. The tissues of six subjects from each group were kept frozen at −80 °C for TBARS and Western blot techniques, while the samples from the other six animals (duodenum, jejunum, and colon) were collected and fixed in 10% formaldehyde for immunohistochemical and histologic techniques.

2.1. Exposure to O_3

Animal exposure to O_3 was carried out for 4 h daily following the methodology of Pereira et al., 2006 [36] and Rivas-Arancibia et al., 2010 [15]. Briefly, an air compressor (5 L/s) connected to an O_3 generator was used, which supplied 0.25 parts per million (ppm) of O_3 constantly. O_3 levels were monitored throughout the experiment with an O_3 monitor (PCI O_3 and Control Systems, West Caldwell, NJ, USA). A control group was exposed to air free of O_3, and the other groups received one of the following treatments of O_3 for 7, 15, 30, 60, and 90 days, respectively.

2.2. TBARS

To evaluate oxidative stress levels, malondialdehyde (MDA) content was measured using the thiobarbituric acid reactive substances (TBARS) test. Tissues were removed and washed with PBS solution. Tissue fragments were homogenized in a mixture of PBS + Butylhydroxytoluene (Sigma 34750, St. Louis, MO, USA) (5 mM) in 1 mL of acetonitrile and centrifuged at 5000× *g* for 3 min at 4 °C. Supernatants were recovered, and total protein quantification was performed using Micro BCA (Thermo Scientific 23235, Waltham, MA, USA). Then, 100 µL of each tissue was incubated in a 1:1 solution of sulfosalicylic acid (3%) at 4 °C overnight. The samples were resuspended and centrifuged at 11,000 rpm for 3 min. An amount of 190 µL of thiobarbituric acid (TBA) solution, prepared with 4% TBA, 20% trichloroacetic acid, and HCl, was added to 10 µL of the supernatant. The mixture was incubated at 95 °C for 60 min. The reaction was measured at 532 nm in a plate spectrophotometer (Biotek, Winooski, VT, USA). Tetraethoxypropane (Sigma T-9889, St. Louis, MO, USA) was used as a standard to make the calibration curve [37].

2.3. Western Blot

To determine the relative content of haptoglobin and the interleukins IL-1β and IL-6, Western blot assays were performed on duodenum, jejunum, and colon tissue. Samples were processed in a protein lysis buffer supplemented with a protease inhibitor cocktail (Roche 11836170001, Basel, Switzerland) and then quantified using a protein quantification kit (Thermo Scientific 23235, Waltham, MA, USA). 100 µg of protein for IL-1β and IL-6, and 40 µg of protein for haptoglobin were separated by electrophoresis in sodium dodecyl sulfate polyacrylamide gels (SDS-PAGE 12% and 10%, respectively). The membranes were then transferred to PVDF (Millipore Sigma ISEQ00010, Burlington, MA, USA). Membranes were blocked with 5% skim milk powder in TBST (TBS + 0.01% Tween 20) for 60 min at room temperature. The following antibodies were used: against haptoglobin (sc-390962, Santa Cruz Biotechnology, Dallas, TX, USA) at 1:1000; against IL-1β (sc-7884, Santa Cruz Biotechnology, USA) at 1:1000, and against IL-6 (ab6672, Abcam, Cambridge, MA, USA) at 1:1000. The membranes were left overnight at 4 °C. As a loading control, an antibody against β-actin (GTX110564, Genetex, Irvine, CA, USA) at a dilution of 1:1000 was used under the same incubation conditions. The membranes were rinsed with TBST and subsequently incubated with horseradish peroxidase-conjugated anti-rabbit IgG (sc-2357, Santa Cruz Biotechnology USA, for IL-1β and IL-6) and anti-mouse IgG (sc-2005, Santa Cruz Biotechnology USA, for haptoglobin) for 1 h at 1:10,000, followed by three washes with TBST. PVDF membranes were stained with three antibodies (actin, IL-1β, and IL-6), washed with a low-pH glycine–HCl buffer (Gly-HCl, 0.1 M, pH 2.2) to remove antibodies from the membrane, and then reused. Different molecular weight antibodies were utilized to

reuse membranes following a stripping protocol. The membranes were developed using Immobilon® Forte Western HRP Substrate reagent (Millipore WBLUF0500, Burlington, MA, USA), and images were digitized using GelCapture software (v 7.0.5, DNR Bio Imaging System, Lincolnshire, IL, USA). Band density was read using Image Studio software (v 5.2.5, LI-COR Bioscience, Lincoln, NE, USA).

2.4. Immunohistochemistry

To study the localization of haptoglobin, IL-1β, and IL-6, immunohistochemistry experiments were performed in the duodenum, jejunum, and colon. The tissues were dehydrated and embedded in paraffin blocks, and 5-µm-thick cross-sections were made and mounted on slides. The tissues were deparaffinized and hydrated, and an antigen retrieval reagent (Biocare Medical DV2004, Pacheco, CA, USA) was used. Peroxidase activity was inhibited with 3% H_2O_2, and blocking was performed to reduce background (Background Sniper, 4plus Detection, Biocare Medical, BS966, USA). To identify the localization of haptoglobin, the slides were incubated overnight at 4 °C with antibodies against haptoglobin (sc-390962, Santa Cruz Biotechnology, USA) at 1:200 dilution, and against IL-6 (ab6672, ABCAM, USA) at 1:200 dilution, and IL-1β (sc-7884, Santa Cruz Biotechnology, USA) at 1:200 dilution. They were incubated with biotinylated secondary antibody (Biocare Medical STU700, USA). Streptavidin (Biocare Medical STHRP700, USA) was then used, and the slides were developed with 3,3-diaminobenzidine substrate chromogen (Biocare Medical DS854H, USA) and counterstained with hematoxylin. Each slide was analyzed with an Olympus BX41 microscope (Olympus, Tokyo, Japan), and photographs were taken with a digital camera (Evolution-QImagin MediaCybernetics, Rockville, MD, USA).

2.5. Hematoxylin and Eosin (H-E) Histological Technique

The sections were placed on slides, and the tissues were subsequently rehydrated in a train using xylene for 2 min, followed by re-immersion in a second bath of xylene for another 2 min. Next, tissues were passed through a train of alcohols: 100%, 96%, 70%, and 50% for 2 min at each concentration. Finally, they were washed with distilled water. The slides were then immersed in hematoxylin for 3 min, rinsed with running water for 1 min, placed in alcohol for 1 min, and washed with water for 1 min. They were then immersed in 2% eosin for 45 s. The slides were then dehydrated and rinsed in 95% alcohol for 1 min, followed by absolute alcohol for 2 min. This step was repeated, and then the slides were placed in xylene for 2 min, followed by another 2 min in xylene. Finally, mounting medium was applied to each sample, and a coverslip was placed over it to be observed under an Olympus BX41 microscope (Olympus, Japan). Photographs were then taken using a digital camera (Evolution-QImagin MediaCybernetics, USA).

2.6. Statistical Analysis

Western blot data were analyzed using the Kolmogorov–Smirnov normality test. The data were subsequently analyzed using the Kruskal–Wallis test to compare all groups. Mann–Whitney U tests were performed to compare the control group with each of the treated groups. Differences were considered statistically significant if $p \leq 0.05$. All statistical analyses were performed using GraphPad Prism® version 5.00 (GraphPad Software, San Diego, CA, USA). TBARS and Western blot results are presented as medians and interquartile ranges for non-parametric variables. Western blot data were analyzed using the Kolmogorov–Smirnov normality test. The data were subsequently analyzed using the Kruskal–Wallis test to compare all groups. Mann–Whitney U tests were performed to compare the control group with each of the treated groups. Differences were considered statistically significant if $p \leq 0.05$. All statistical analyses were performed using GraphPad Prism® version 5.00 (GraphPad Software, USA). TBARS and Western blot results are

presented as medians and interquartile ranges for non-parametric variables. Each figure shows representative data from each experiment (n = 6).

3. Results

3.1. Oxidative Stress Status in the Duodenum, Jejunum, and Colon of the Rat

To evaluate the effects of O_3 exposure on ROS, lipid oxidation assays were performed in the three specific regions of the intestine. In the duodenum, a significant decrease in MDA levels was observed at 30 days, followed by an increase at 60 days of exposure when compared to the control group (see Figure 1A). The jejunum exhibited significant increases in the amounts of oxidized lipids at 7, 15, 60, and 90 days compared to the control group (refer to Figure 1B). In the colon, elevated levels of oxidized lipids were detected at 7, 15, 30, and 60 days in comparison to the control group (Figure 1C).

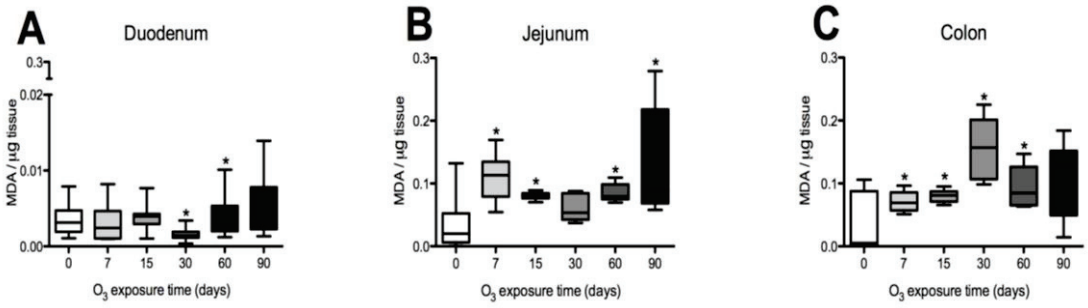

Figure 1. Effect of O_3 exposure on lipid oxidation in the duodenum, jejunum, and colon of rats. The x-axis shows the duration of exposure to O_3, and the y-axis shows MDA levels in μM MDA/μg tissue. In the duodenum, the results show a significant decrease in MDA at 30 days and an increase at 60 days compared to the control group (**A**). In the jejunum, there was a significant increase in MDA at 7, 15, 60, and 90 days of exposure to O_3 compared to the control group (**B**). In the colon, statistically significant increases in MDA were observed at 7, 15, 30, and 60 days compared to the control group (**C**). * $p \leq 0.05$.

3.2. Western Blot Results in Duodenum, Jejunum, and Colon

Haptoglobin Content in Rat Duodenum, Jejunum, and Colon

To evaluate the effects of different low-dose O treatments on tight junctions and to observe changes in intestinal permeability and immune response, haptoglobin content was determined. The results indicate that in the duodenum there is a significant increase in haptoglobin at 7 and 15 days of exposure to O_3 (Figure 2A); in the jejunum, a significant increase is presented at 7, 15, 30, and 90 days of exposure to (Figure 2B); and in the colon, increases in haptoglobin are observed at 7 and 15 days of exposure to O_3 (Figure 2C) compared to their respective control groups ($p < 0.05$).

3.3. L-1β Content in the Duodenum, Jejunum, and Colon of Rats

To evaluate the effects of low-dose O_3 treatments on the immune response, IL-1β content was determined in different regions of the intestine. The results show that the duodenum showed a significant increase after 60 days of exposure to O_3 (Figure 3A). The jejunum did not show significant results (Figure 3B), and the colon did after 30 days of exposure to O_3 (Figure 3C), compared to the control groups.

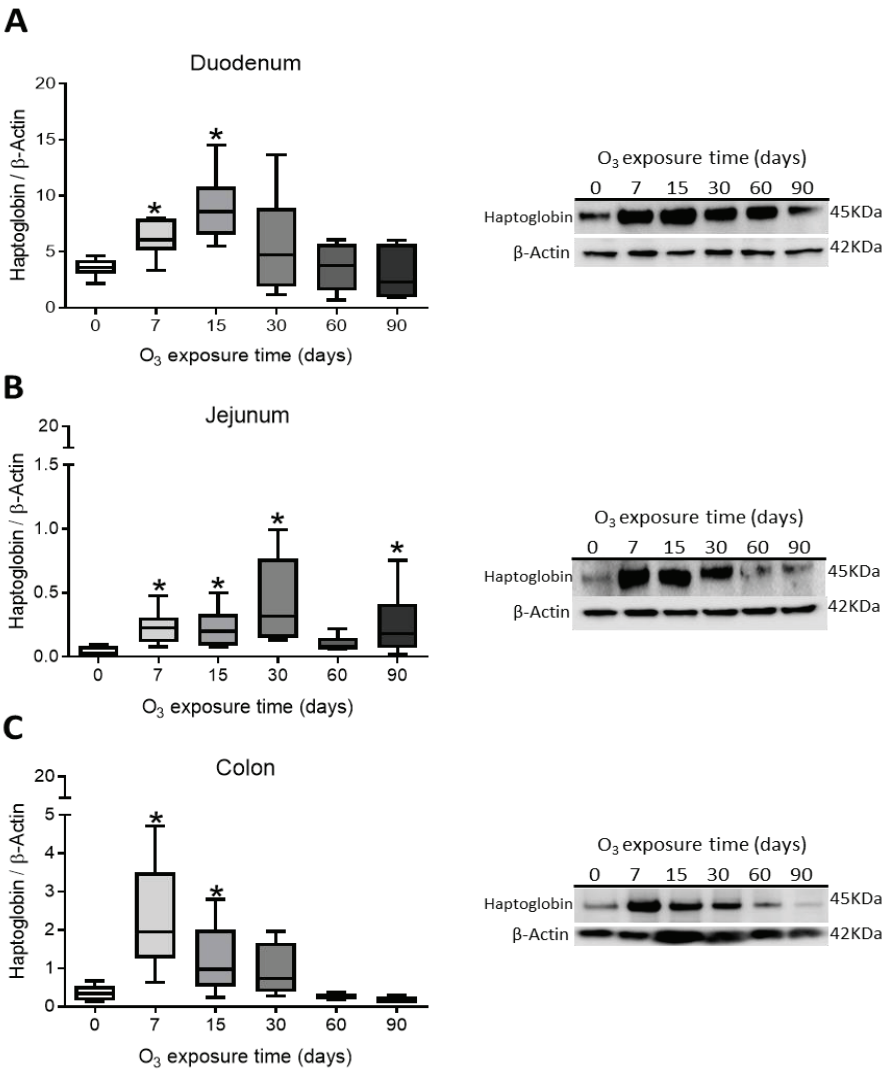

Figure 2. Effect of O_3 exposure on haptoglobin content in the duodenum, jejunum, and colon of rats. The *x*-axis shows the time of exposure of animals to O_3, and the *y*-axis shows the relative haptoglobin content expressed in arbitrary units. β-Actin was used as a loading control. The results in the duodenum show a significant increase in haptoglobin levels at 7 and 15 days compared to the control group (**A**). In the jejunum, there is a significant increase in haptoglobin at 7, 15, 30, and 90 days of exposure to O_3 compared to the control group (**B**). In the colon, haptoglobin levels increased at 7 and 15 days compared to the control group (**C**) (* $p < 0.05$).

3.4. IL-6 Content in Rat Duodenum, Jejunum, and Colon

IL-6 content was assessed in the three intestinal regions. The results indicate no statistically significant differences in the duodenum (Figure 4A), jejunum (Figure 4B), and colon (Figure 4C) compared to their respective control groups.

3.5. Immunohistochemical Test Results

Immunohistochemistry Against Haptoglobin

Haptoglobin in the Duodenum

The analysis of duodenal images after exposure to O_3 reveals that the villi in control animals show immunoreactivity against haptoglobin primarily at the edges and in the cells of the lamina propria. These villi maintain a regular shape and exhibit a parallel arrangement of Brunner's glands. However, after 7 days of exposure, there is an increase in immunoreactive labeling within the lamina propria. By 15, 60, and 90 days, aggregates

of immune system cells become apparent, and their immunoreactivity against haptoglobin increases. In contrast to the control animals, the enterocytes in the exposed animals display intense labeling in the cytoplasm. Additionally, the continuity of the epithelium is disrupted, and the arrangement of goblet cells becomes disorganized (Figure 5).

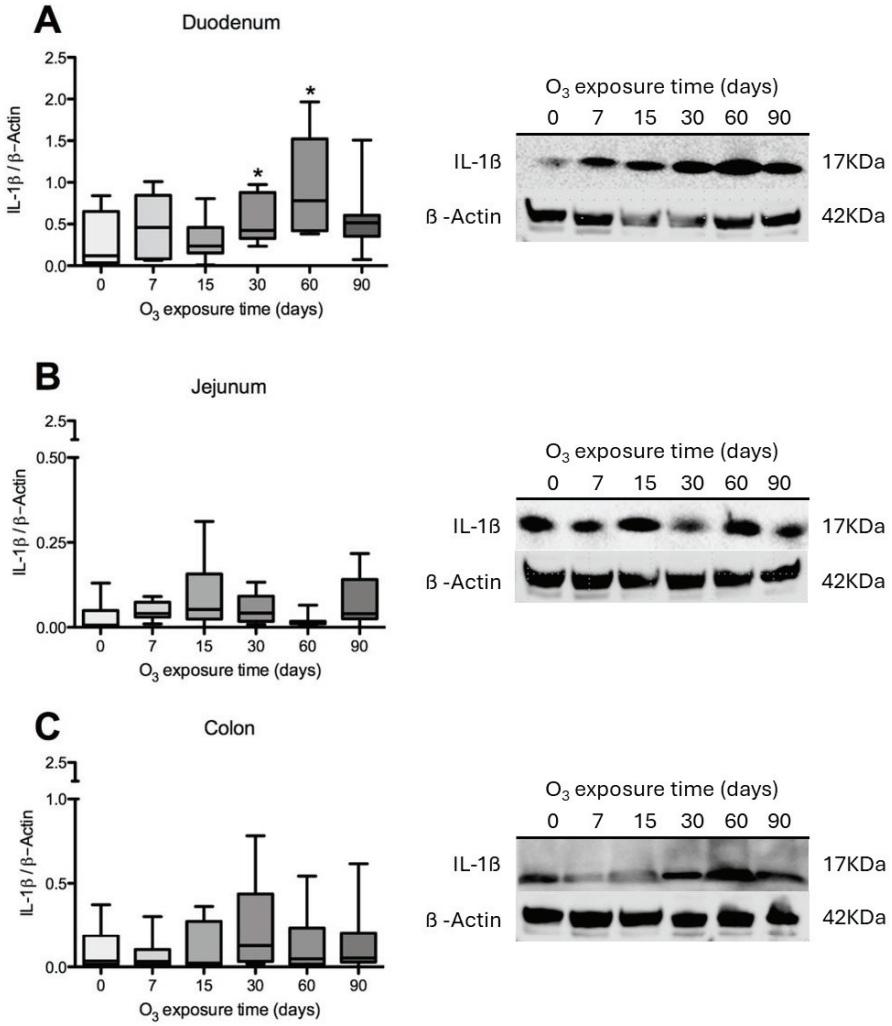

Figure 3. Effect of O_3 exposure on IL-1β content in the duodenum, jejunum, and colon of rats. The *x*-axis shows the time of exposure of animals to O_3, and the *y*-axis shows the relative content of interleukin IL-1β, expressed in arbitrary units. β-Actin was used as a loading control. The results show an increase in IL-1β in the duodenum at 30 days compared to the control group (**A**). In the jejunum, no statistically significant results were found when compared to the control group (**B**). In the colon, a statistically significant increase in IL-1β was observed at 30 days of exposure compared to the control group (**C**). * $p \leq 0.05$.

3.6. Haptoglobin in the Jejunum

Haptoglobin is found on the surface of enterocytes and in the lamina propria cells of the jejunum, similar to its presence in the duodenum. In control animals, immunoreactivity can be observed in the cells surrounding the crypts of Lieberkühn. However, in specimens exposed to O_3, there is an increase in the number of haptoglobin-immunoreactive cells within the lamina propria. The infiltration of immune system cells and changes in the intestinal epithelium's structure mark this condition. Additionally, after 30, 60, and 90 days of O_3 exposure, alterations in the arrangement of enterocytes are evident, along with a more intense intracellular immunoreactive signal. This pattern differs from that seen in

epithelial cells exposed to O_3 for shorter periods, where haptoglobin is primarily detected in the apical region of the enterocytes (Figure 6).

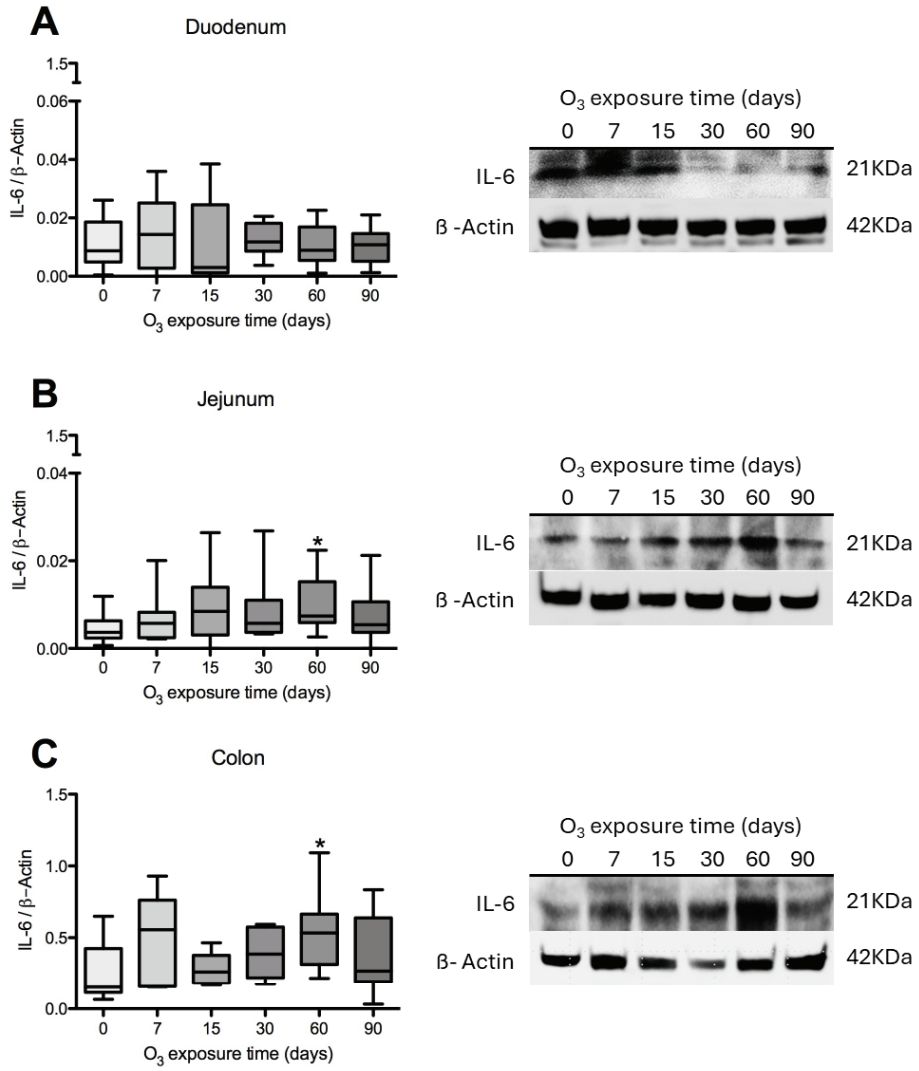

Figure 4. Effect of O_3 exposure on IL-6 content in the duodenum, jejunum, and colon of rats. The *x*-axis shows the time of exposure of animals to O_3, and the *y*-axis shows the relative IL-6 content, expressed in arbitrary units. β-Actin was used as a loading control. The results in the duodenum (**A**), jejunum (**B**), and colon (**C**) did not show significant differences when compared with their respective control groups. * $p \leq 0.05$.

3.7. Haptoglobin in the Colon

Haptoglobin is located in the apical zone of colonic enterocytes in the colon, where it regulates the function of intestinal tight junctions. An increase in the number of cells in the lamina propria that exhibit immunoreactivity against haptoglobin was observed after 60 and 90 days of O_3 exposure. Additionally, after 90 days of exposure, a noticeable discontinuity in the colonic epithelium was found, indicating that repeated exposure to O_3 significantly impacts epithelial tight junctions and may have adverse effects on the overall function of the gastrointestinal system (Figure 7).

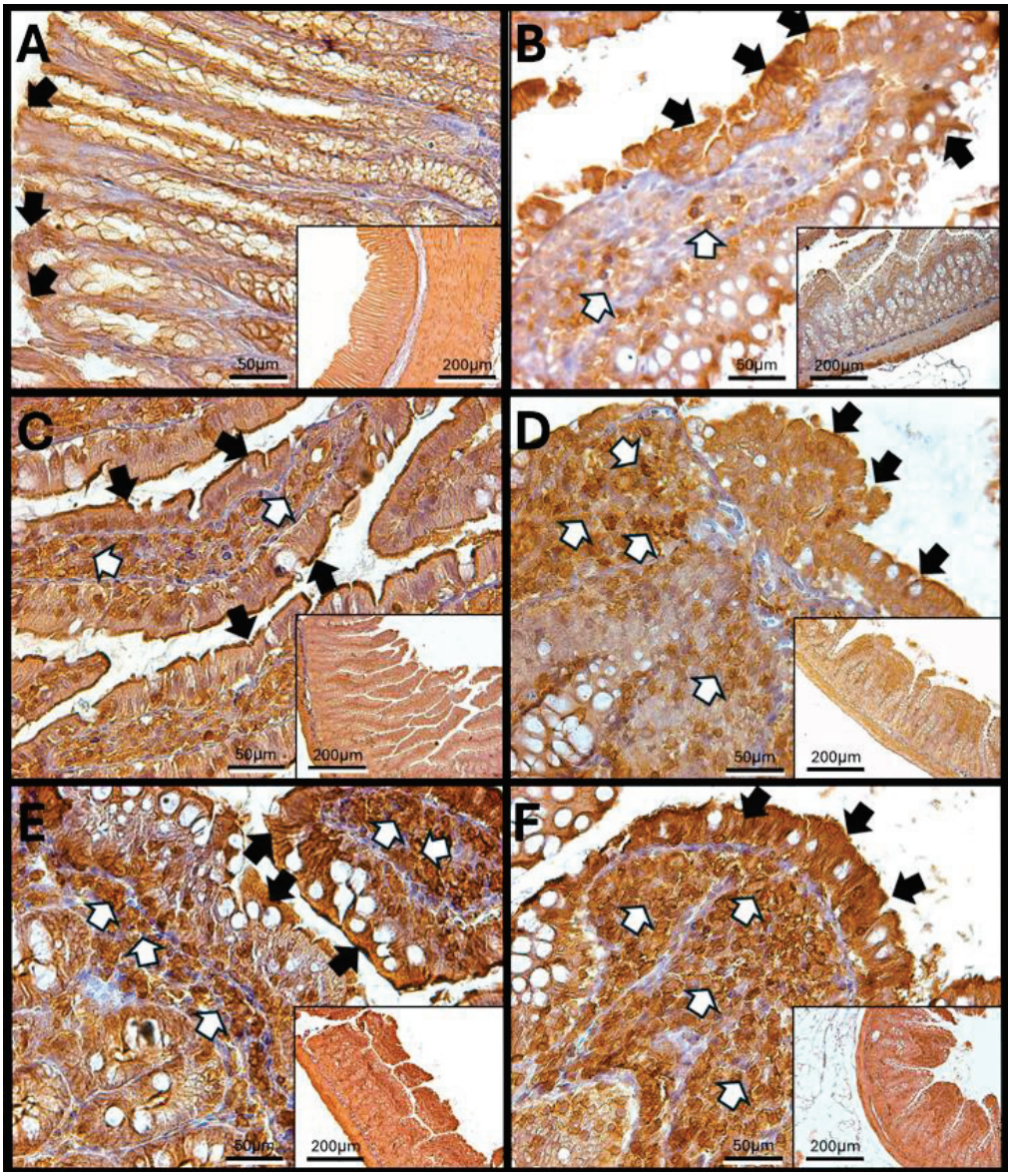

Figure 5. Effect of chronic exposure to low doses of ozone on haptoglobin immunoreactivity in the duodenum of rats. (**A**) Control group, (**B**) 7 days, (**C**) 15 days, (**D**) 30 days, (**E**) 60 days, and (**F**) 90 days post-treatment. The black arrows (➡) indicate immunoreactivity in the simple columnar epithelium, while the white arrows (⇨) mark immunoreactivity in the cells of the lamina propria of the duodenum. Notably, there is an increase in immunoreactivity in both regions at 30 days (**D**), 60 days (**E**), and 90 days (**F**), whereas a decrease is observed at 15 days (**C**) compared to the control group. The micrographs are presented at magnifications of 40× (scale bar = 50 µm) and 10× (scale bar = 200 µm), respectively.

3.8. Immunohistochemistry Against IL-1β

3.8.1. IL-1β in Rat Duodenum

The duodenum of control animals (A) shows IL-1β staining in enterocytes, as well as around the crypts and Brunner's glands. With increasing exposure time to O_3, a significant rise in the staining signal is observed in the lamina propria of the tissue, which increases from 7 to 90 days of exposure to O_3. Additionally, changes in the structure of the duodenal villi and infiltration of immune cells are noted. IL-1β staining is also present in the muscular layer of the duodenum across the different experimental groups. These findings suggest a more comprehensive and complex immune response (Figure 8).

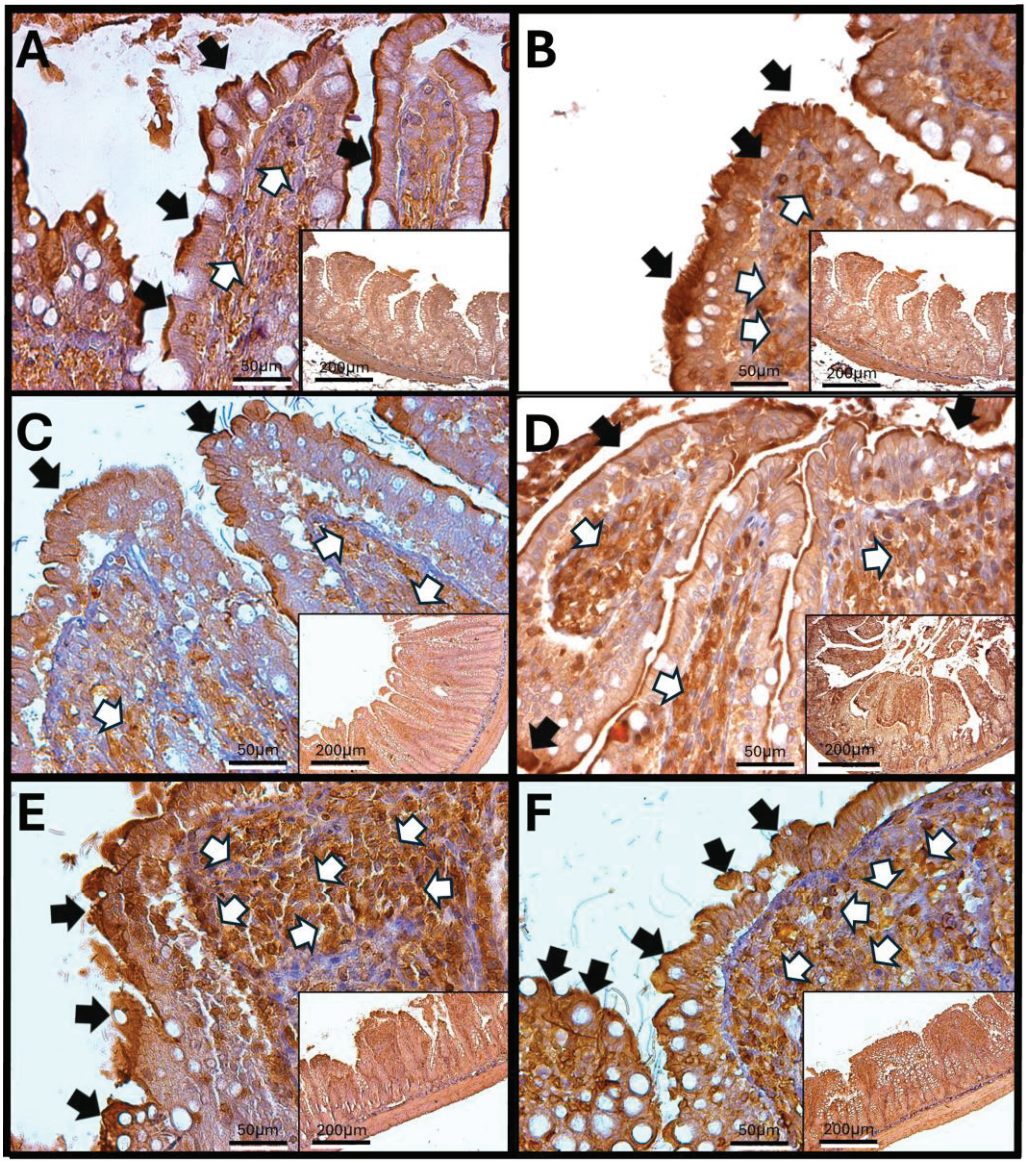

Figure 6. Effect of chronic exposure to low doses of ozone on haptoglobin immunoreactivity in the jejunum of rats. (**A**) Control group, (**B**) 7 days, (**C**) 15 days, (**D**) 30 days, (**E**) 60 days, and (**F**) 90 days after treatment. The black arrows (➥) indicate immunoreactivity in the simple columnar epithelium, and the white arrows (⇨) indicate immunoreactivity in the cells of the lamina propria of the jejunum. Note the increase in immunoreactivity in both regions in (**C**–**F**), as well as a decrease at 7 days (**C**) compared to the control. The micrographs are shown at magnifications of 40× (bar = 50 µm) and 10× (bar = 200 µm), respectively.

3.8.2. IL-1β in the Rat Jejunum

IL-1β in the rat jejunum shows immunoreactive signals in the enterocytes and cells of the lamina propria. In addition to the structural changes observed in the intestinal villi of the jejunum, there are increases in IL-1β levels in the lamina propria during the exposure periods, particularly on days 15, 30, and 90 of exposure to O_3. Furthermore, the muscular layer exhibits strong reactivity to IL-1β at various exposure times, indicating an inflammatory response (Figure 9).

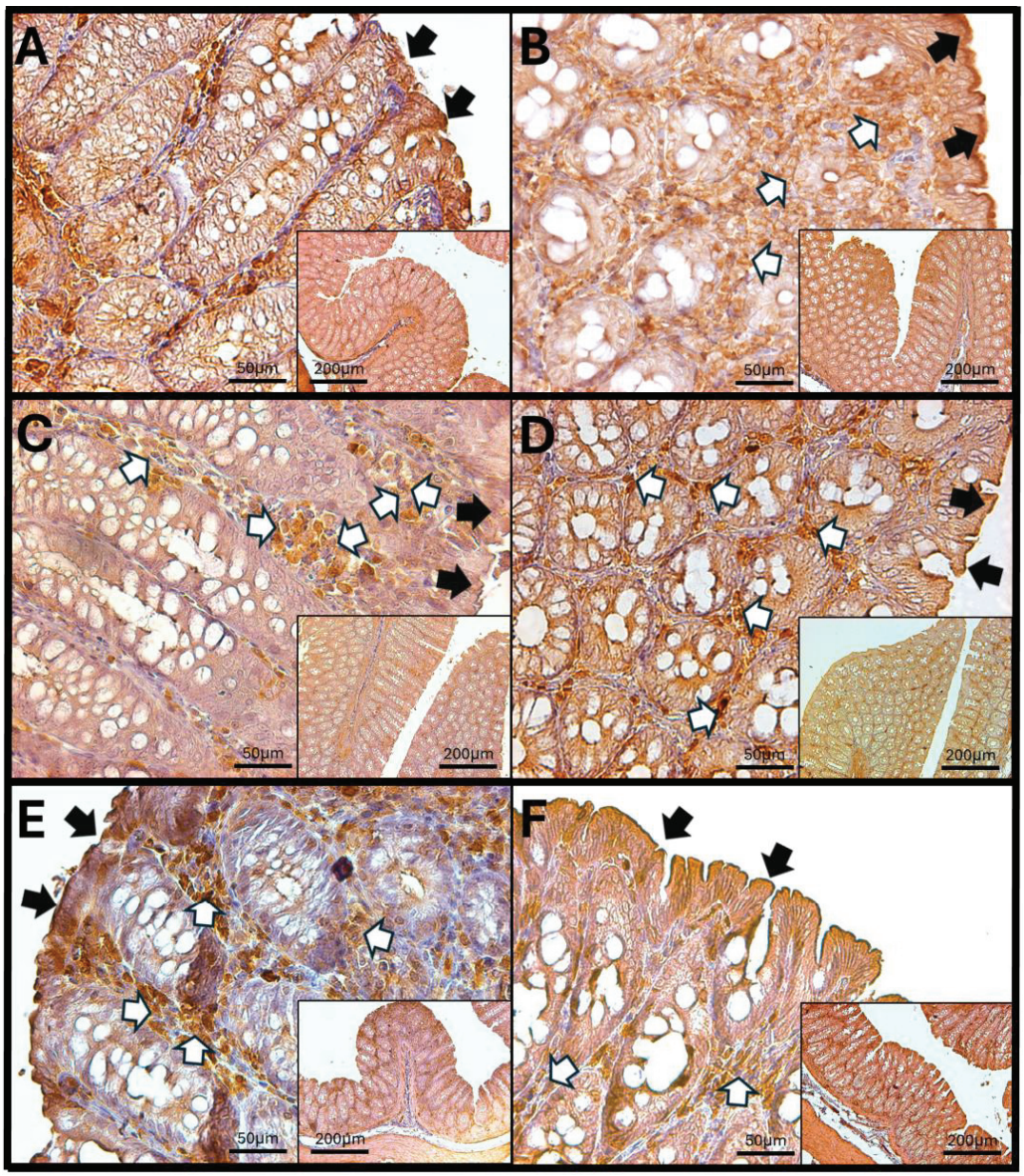

Figure 7. Effect of chronic exposure to low doses of ozone on haptoglobin immunoreactivity in the colon of rats. (**A**) Control group, (**B**) 7 days, (**C**) 15 days, (**D**) 30 days, (**E**) 60 days, and (**F**) 90 days after treatment. The black arrows (➡) indicate immunoreactivity in the simple columnar epithelium, and the white arrows (⇨) indicate immunoreactivity in the cells of the lamina propria of the colon. Note the increase in immunoreactivity in both regions in E, as well as an increase in immunoreactivity in the lamina propria compared to the control. Micrographs (**B**–**D**) show no changes. The micrographs are shown at magnifications of 40× (bar = 50 µm) and 10× (bar = 200 µm), respectively.

3.8.3. IL-1β in the Rat Colon

The results of IL-1β in the rat colon are presented in Figure 10. The micrographs illustrate the presence of IL-1β-reactive cells after exposure to O_3 in the rat colon. IL-1β is distributed in cells within the lamina propria, as well as in enterocytes. An increase in immunoreactivity is observed around the crypts at 15 and 30 days. By 60 and 90 days, disruptions in the composition of the colonic epithelium become evident.

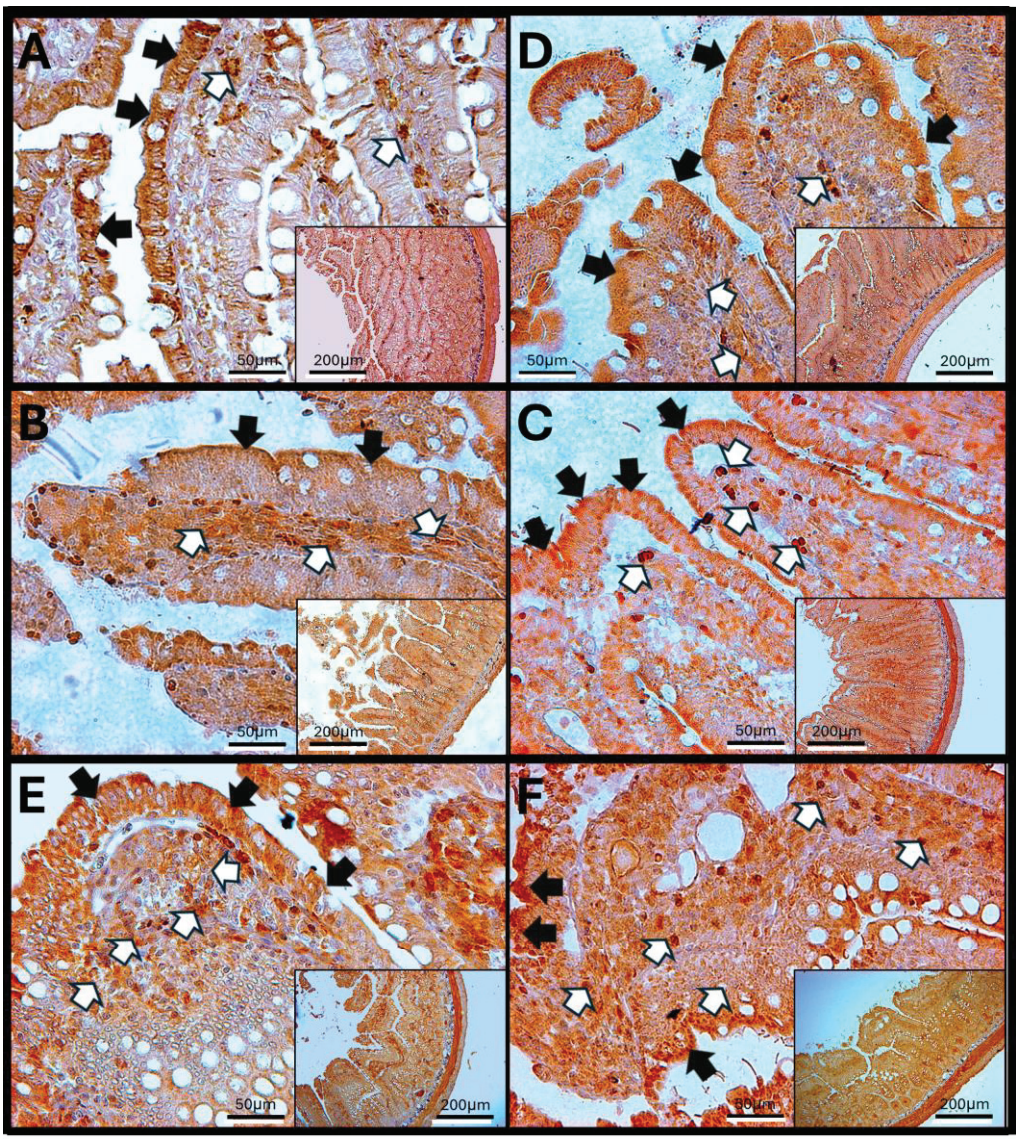

Figure 8. Effect of chronic exposure to low doses of ozone on IL6 immunoreactivity in the duodenum of rats. (**A**) Control group, (**B**) 7 days, (**C**) 15 days, (**D**) 30 days, (**E**) 60 days, and (**F**) 90 days after treatment. The black arrows (➡) indicate immunoreactivity in the simple columnar epithelium, and the white arrows (⇨) indicate immunoreactivity in the cells of the lamina propria of the duodenum. Note the increase in immunoreactivity in both regions in (**B**–**D**,**F**), as well as a decrease in immunoreactivity in the lamina propria in (**E**). Micrographs are shown at a magnification of 40× (bar = 50 µm) and 10× (bar = 200 µm), respectively.

3.9. Immunohistochemistry Against IL-6

Immunohistochemistry for IL-6 was conducted on the duodenum of rats. The results indicate that IL-6 immunoreactivity is present in enterocytes and lamina propria cells of control rats. In animals exposed to O_3 for 7, 15, 30, 60, and 90 days, noticeable alterations in the villi structure and epithelial surface were observed. Additionally, disruptions in the arrangement of goblet cells were evident after 15, 30, and 90 days of O_3 exposure (Figure 11).

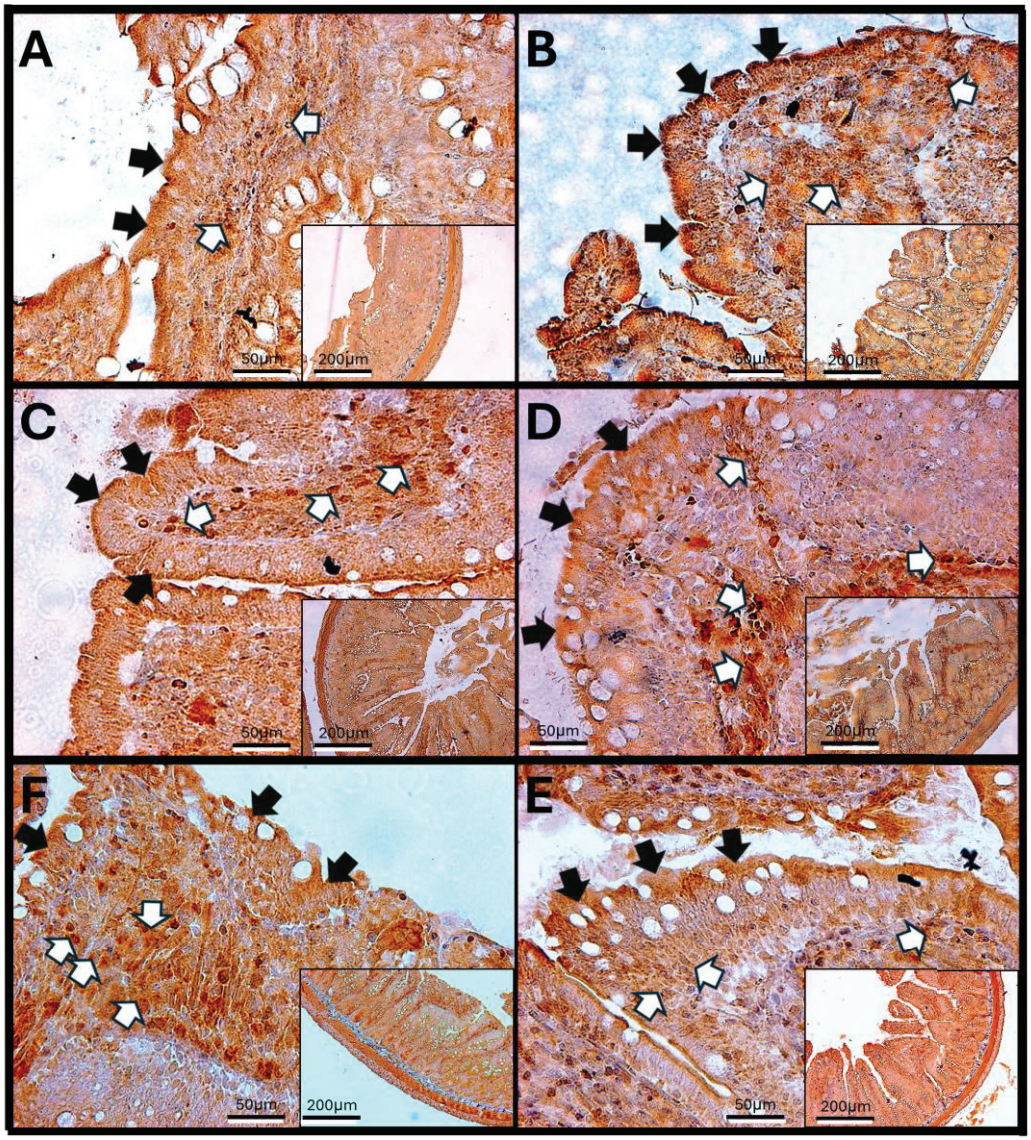

Figure 9. Effect of chronic exposure to low doses of ozone on IL6 immunoreactivity in the jejunum of rats. (**A**) Control group, (**B**) 7 days, (**C**) 15 days, (**D**) 30 days, (**E**) 60 days, and (**F**) 90 days after treatment. The black arrows (➡) indicate immunoreactivity in the simple columnar epithelium, and the white arrows (⇳) indicate immunoreactivity in the lamina propria cells of the jejunum. Note the decrease in immunoreactivity in the columnar epithelium in (**B**,**F**), as well as an increase in immunoreactivity in both regions in (**C**,**D**). In (**E**), a decrease in immunoreactivity is observed in the lamina propria cells with respect to the control. The micrographs are shown at magnifications of 40× (bar = 50 µm) and 10× (bar = 200 µm), respectively.

3.10. IL-6 in Rat Jejunum

In the jejunum of rats, the results show that control animals exhibit IL-6 immunoreactivity in both enterocytes and lamina propria cells. After 7, 30, and 60 days of exposure to O_3, there was noticeable cell infiltration and an increase in IL-6-reactive cells within the lamina propria. Additionally, alterations in the structure of the intestinal villi and significant changes in the epithelial layer were observed (Figure 12).

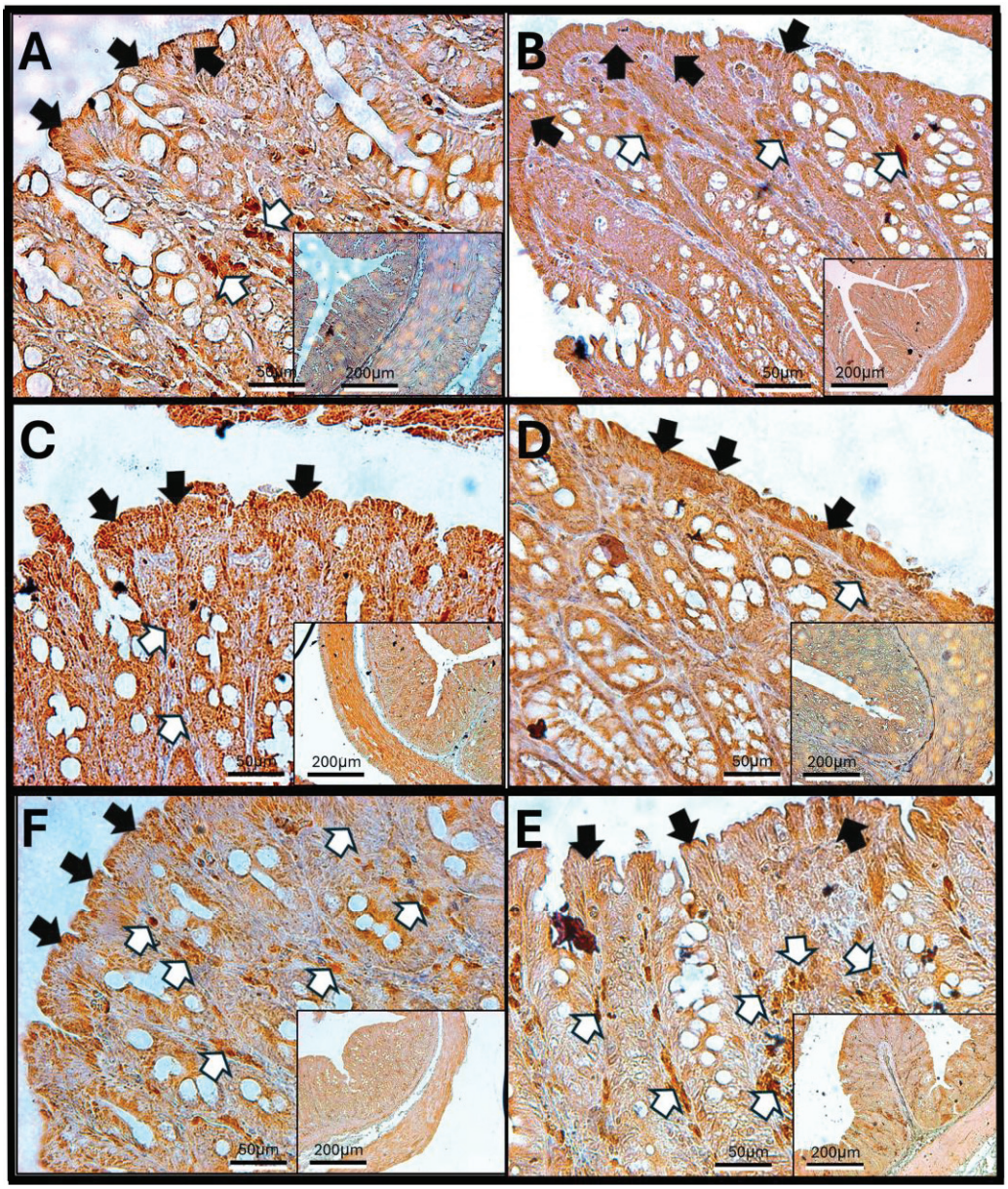

Figure 10. Effect of chronic exposure to low doses of ozone on IL6 immunoreactivity in the colon of rats. (**A**) Control group, (**B**) 7 days, (**C**) 15 days, (**D**) 30 days, (**E**) 60 days, and (**F**) 90 days after treatment. The black arrows (➡) indicate immunoreactivity in the simple columnar epithelium, and the arrows (⇨) indicate immunoreactivity in the lamina propria cells of the colon. Note a decrease in immunoreactivity in both the simple columnar epithelium and the lamina propria cells in (**B**), as well as a decrease in the columnar epithelium in (**E**) with respect to the control. Micrographs are shown at magnifications of 40× (bar = 50 µm) and 10× (bar = 200 µm), respectively.

3.11. IL-6 Immunoreactivity in the Rat Colon

The results of IL-6 immunoreactivity in the rat colon show variations depending on the duration of exposure to O_3. IL-6 is detected in enterocytes and the lamina propria, with its expression increasing at 60 and 90 days of treatment compared to control animals. Additionally, there is a noted loss of epithelial continuity (Figure 13).

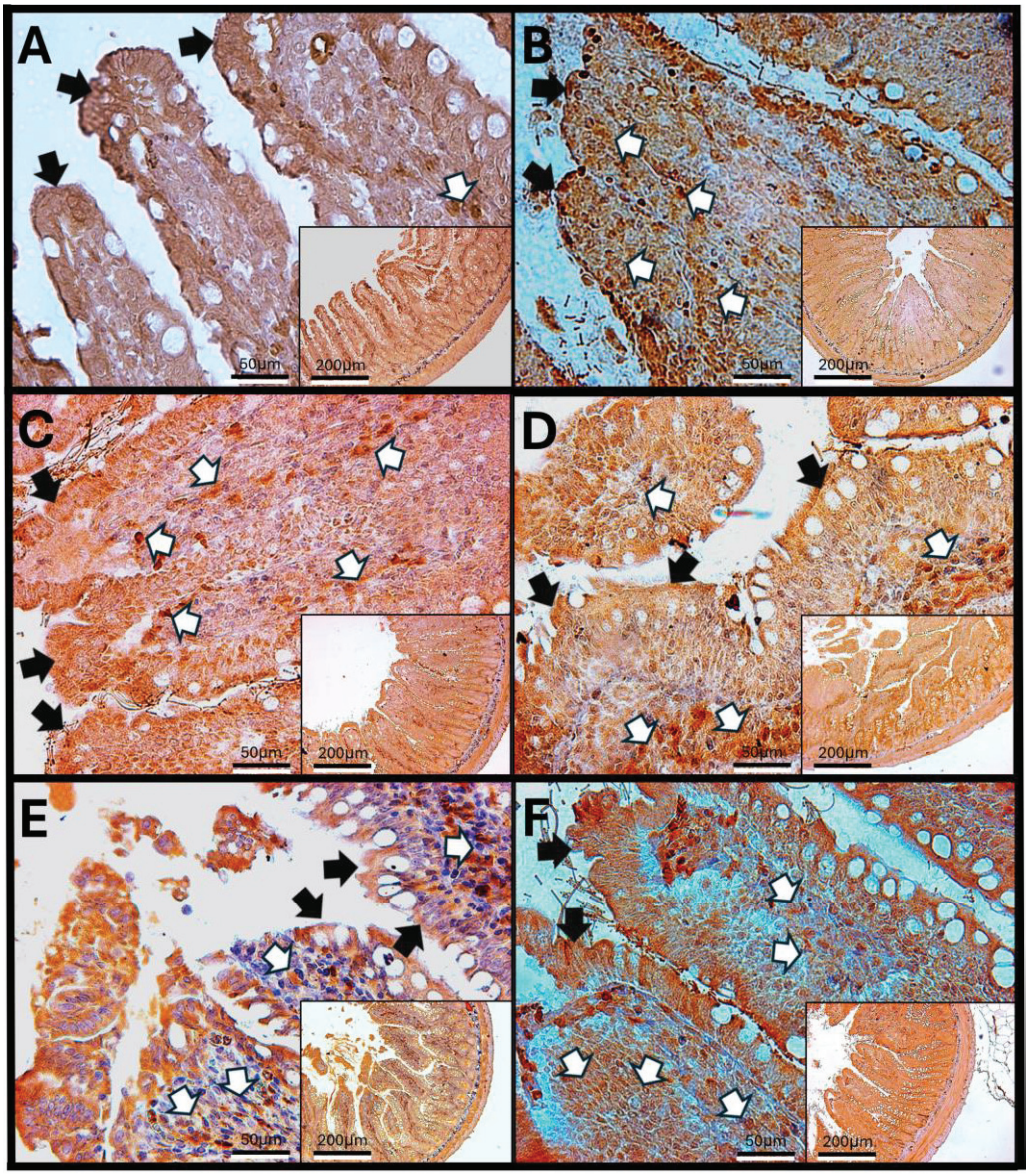

Figure 11. Effect of chronic exposure to low doses of ozone on IL-1β immunoreactivity in the duodenum of rats. (**A**) Control group, (**B**) 7 days, (**C**) 15 days, (**D**) 30 days, (**E**) 60 days, and (**F**) 90 days after treatment. The black arrows (➡) indicate immunoreactivity in the simple white columnar epithelium, and the arrows (⇨) indicate immunoreactivity in the lamina propria cells of the duodenum. Note a decrease in immunoreactivity in the columnar epithelium in (**B**), as well as an increase in immunoreactivity in the lamina propria cells in (**B**–**F**) with respect to the control. The micrographs are shown at magnifications of 40× (bar = 50 µm) and 10× (bar = 200 µm), respectively.

3.12. Results of H-E Staining in the Duodenum, Jejunum, and Colon of the Rat

H-E of the duodenum. In the histology of the duodenum of control animals, the structure of the villi is normal with a parallel arrangement, and no alterations are observed in the lamina propria or Brunner's glands. However, at 7, 15, 30, 60, and 90 days of exposure to O_3, atrophy and loss of villous arrangement are observed as a result of infiltration of immune system cells and distortion in the architecture of goblet cells, in addition to significant alterations in the intestinal epithelium and widening at the mouth of the crypts (Figure 14).

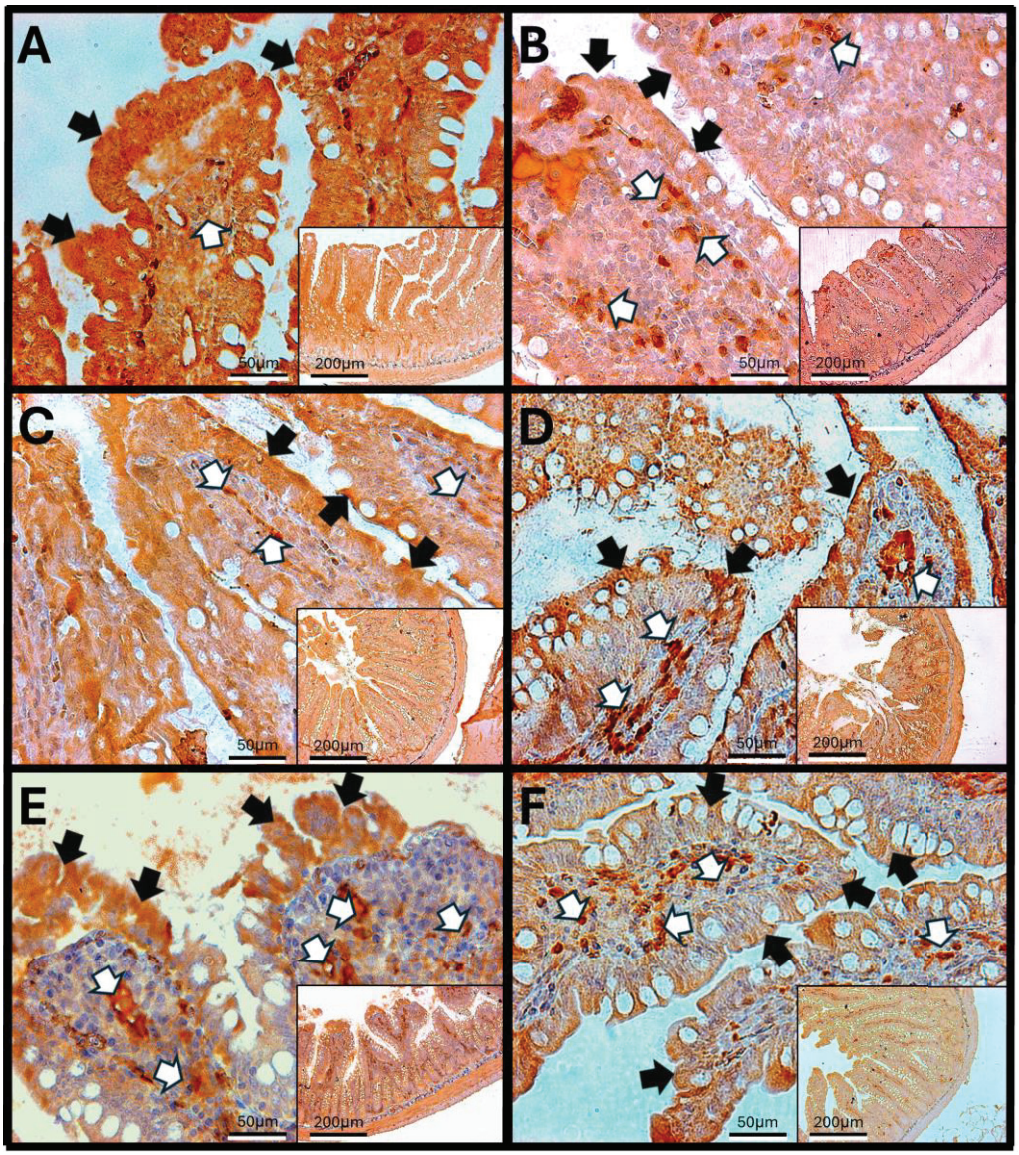

Figure 12. Effect of chronic exposure to low doses of ozone on IL-1β immunoreactivity in the jejunum of rats. (**A**) Control group, (**B**) 7 days, (**C**) 15 days, (**D**) 30 days, (**E**) 60 days, and (**F**) 90 days after treatment. The black arrows (➡) indicate immunoreactivity in the simple columnar epithelium, and the arrows (⇨) indicate immunoreactivity in the lamina propria cells of the jejunum. Note an increase in immunoreactivity in the simple columnar epithelium in (**B**), as well as an increase in immunoreactivity in the lamina propria cells in (**B**–**E**), with respect to the control. The micrographs are shown at magnifications of 40× (bar = 50 µm) and 10× (bar = 200 µm), respectively.

3.13. H-E in Jejunum

The results show that at 7, 15, 30, 60, and 90 days of exposure to O_3, villous atrophy and crypt distortion are evident, as well as basal plasmacytosis processes in the lamina propria (Figure 15). Additionally, erosion lesions are visible on the epithelial surface, accompanied by significant epithelial damage.

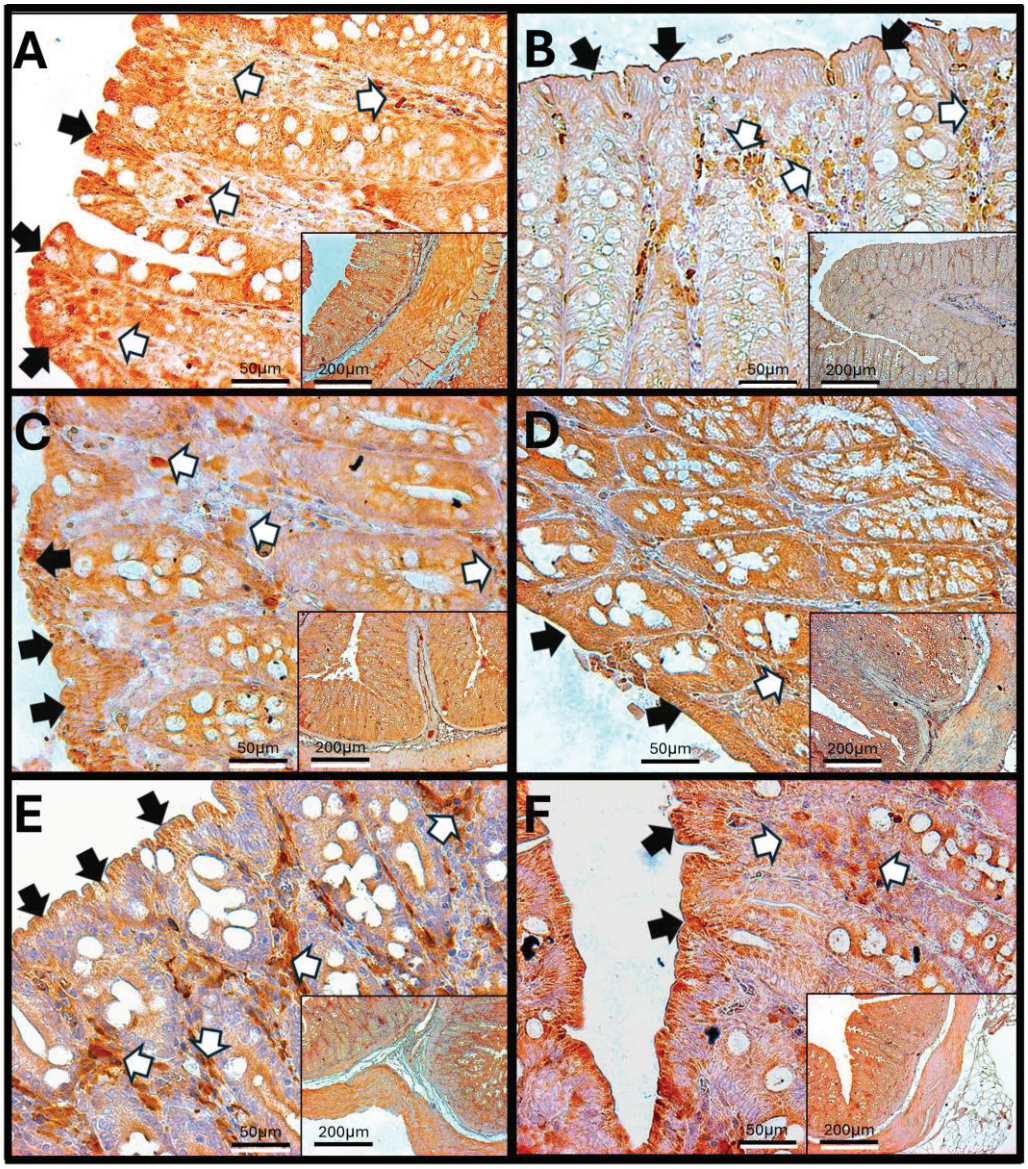

Figure 13. Effect of chronic exposure to low doses of ozone on IL-1β immunoreactivity in the colon of rats. (**A**) Control group, (**B**) 7 days, (**C**) 15 days, (**D**) 30 days, (**E**) 60 days, and (**F**) 90 days after treatment. The black arrows (➡) indicate immunoreactivity in the simple columnar epithelium, and the white arrows (⇳) indicate immunoreactivity in the lamina propria cells of the colon. Note an increase in immunoreactivity in the simple columnar epithelium in (**B**–**D**), as well as a decrease in immunoreactivity in the lamina propria cells in (**B**,**D**) with respect to the control. The micrographs are shown at magnifications of 40× (bar = 50 µm) and 10× (bar = 200 µm), respectively.

3.14. H-E of the Colon

The results show enlargement of Peyer's patches at 30 and 90 days after low-dose O_3 treatment (Figure 16). Also, at the same time, the formation of crypt abscesses, where eosinophils and neutrophils agglomerate, is observed. At 60 days, the loss of normal tissue structure is noticeable, as well as infiltration of immune system cells into the lamina propria.

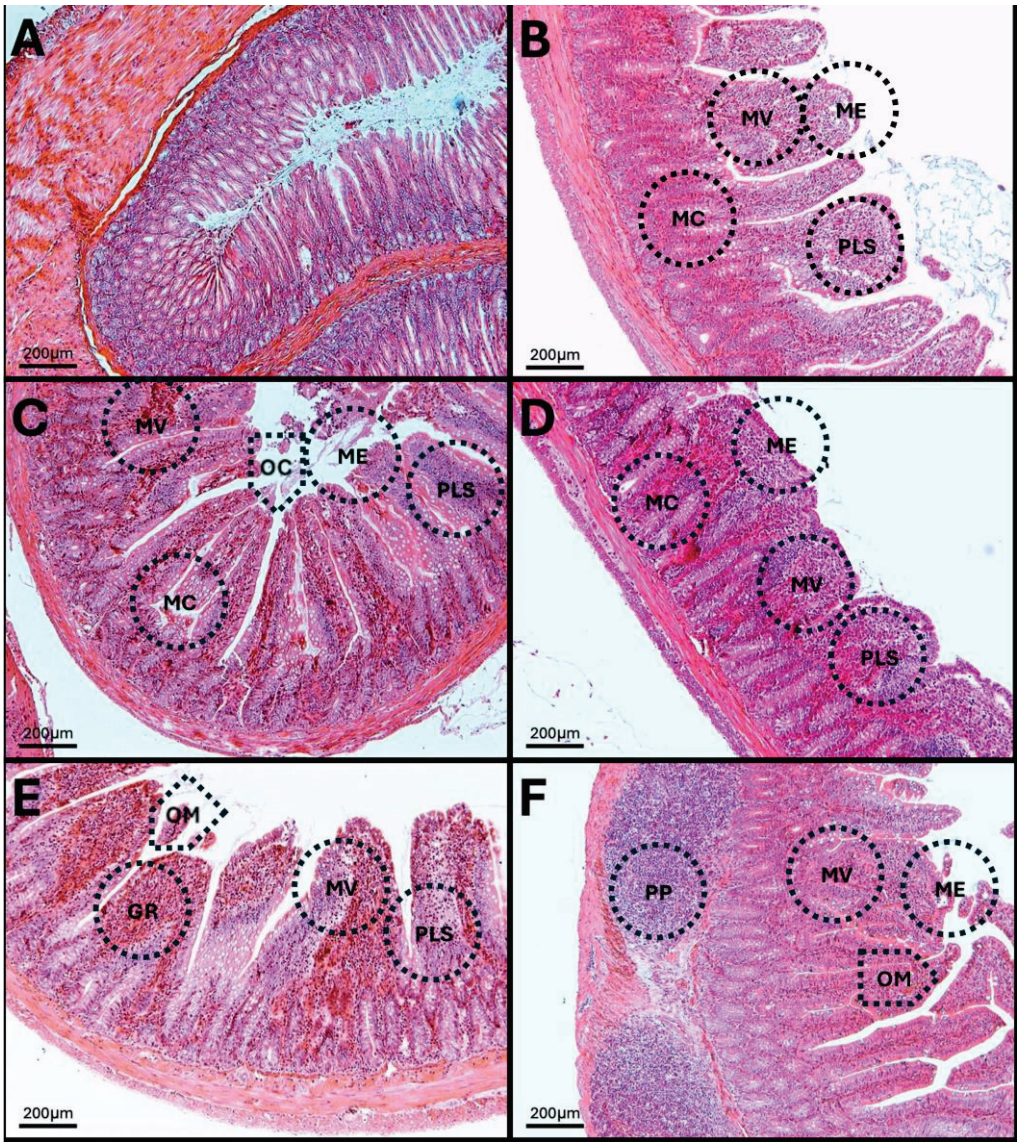

Figure 14. Cellular and structural changes in the duodenum of rats exposed to low doses of O_3. The micrographs show cellular and structural changes in the duodenum of rats chronically exposed to O_3. (**A**) Control group without O_3. Tall villi with unaltered columnar epithelium, in the form of a continuous brush; there are no erosions or loss of continuity. The stroma of the lamina propria appears normal, with few, sparse, and scattered cells. Mucin cells are abundant and uniform. (**B**) O_3 group at 7 days. The subepithelial region shows plasmacytosis (PLS) and vacuoles, which modify the structure of the villi (MV); the epithelial contour is modified (ME). Mucin cells (MC) appear sparse compared to the control group, and some crypts are elongated. (**C**) O_3 group at 15 days. Foci of epithelial erosion and opening of the crypt mouths are visible (OM). Infiltrated lamina propria. Mucin cells are seen in smaller numbers and located toward the surface of the epithelium. (**D**) O_3 group, 30 days old. The epithelium appears cuboidal due to fused villi with a discontinuous surface. Massive infiltration in the lamina propria is observed. Mucin cells are scarce. (**E**) O_3 group, 60 days old. Opening of the crypt mouths is observed. The lamina propria shows marked plasmacytosis (PLS) and granulomas (GR). Isolated, deformed, and small mucous cells are present. (**F**) O_3 group, 90 days old. Columnar epithelium is partially restored, and the crypt mouths are seen wide; there are signs of epithelial erosion. Residual infiltration in the villi and Peyer's patches (PP) are observed in the region. Mucin cells are reorganized into a glandular shape. Each photograph shows the area at 10× (bar = 200 µm).

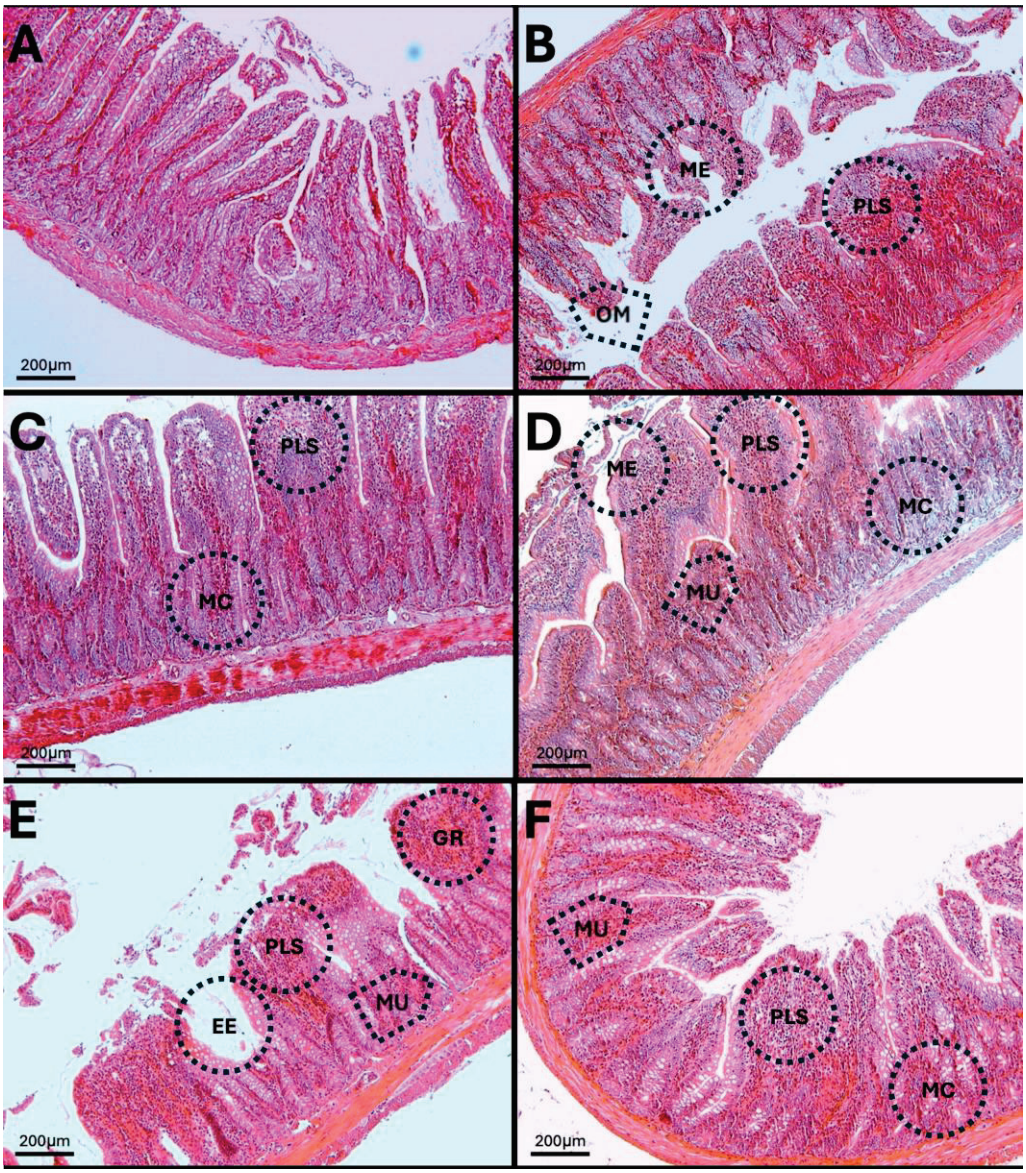

Figure 15. Cellular and structural alterations in the jejunum of rats exposed to low doses of O_3. The micrographs show cellular and structural alterations in the jejunum of rats chronically exposed to O_3. (**A**) Control group without O_3. Tall villi, continuous contour; intact brush border; no evident erosions. Lamina propria stroma with few cells. Abundant and regular mucin cells. (**B**) Seven-day O_3 group. Epithelial contour modified by villous fusion (ME). Subepithelial region with plasmacytosis processes (PLS). Mucin cells (MC) of unequal size. Opening of the crypt mouths are visible (OM). (**C**) Fifteen-day O_3 group. Sites of cellular infiltration are observed in the villi. Decreased number of mucin cells, located mostly in the apical region. (**D**) Thirty-day O_3 group. Fussed epithelium and microulcers (MU). Lamina propria with cellular infiltration. Marked decrease in mucin cells, with crypts showing altered morphology. (**E**) O_3 group, 60 days. Highly eroded epithelium (EE). Ulcerations reaching the muscularis (MU). Massive plasmacytosis (PLS) and granulomas (GR). Small, deformed mucin glands. (**F**) O_3 group, 90 days. Partial restoration of columnar epithelium; presence of small ulcerations (MU). Residual cellular infiltration of the lamina propria. Reappearance of mucin glands in discontinuous rows. Each photograph shows the area at 10× (bar = 200 µm).

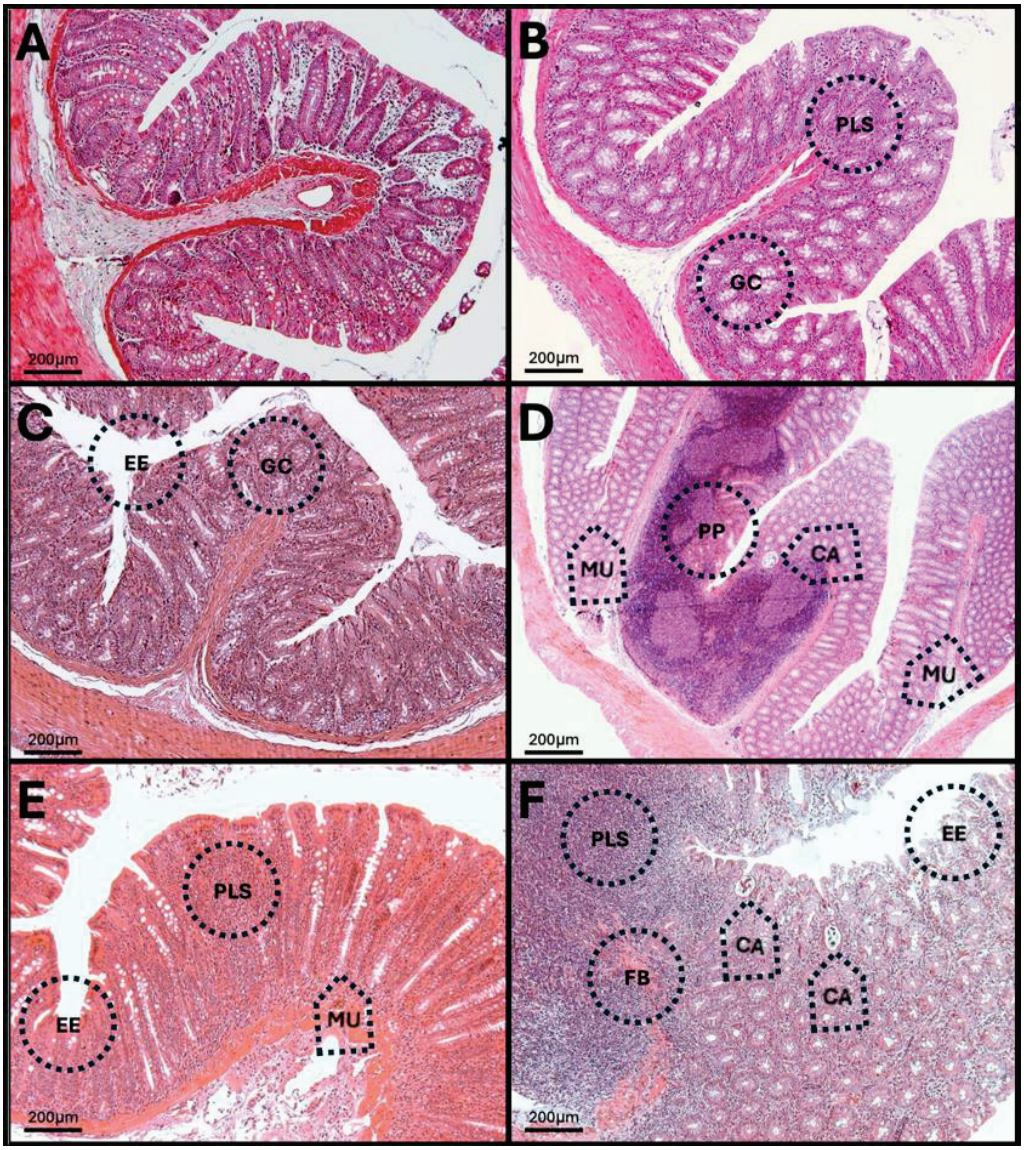

Figure 16. Structural changes in the colon of rats exposed to low doses of O_3. The micrographs show structural changes in the colon of rats chronically exposed to O_3. (**A**) Control group without O_3. Continuous epithelial contour; no erosions. Loose stroma of the lamina propria, abundant cell count. Crypts with numerous, uniform, and dense mucin cells. (**B**) Seven-day O_3 group. The apical contour of the epithelium is preserved. Subepithelial region with a significant number of cells in the lamina propria (PLS). Abundant mucous glands with enlarged mucin cells (MC). (**C**) Fifteen-day O_3 group. Localized foci of epithelial erosion (EE). Increased cell infiltration into the stroma. Mucin cells hyperplasia. (**D**) Thirty-day O_3 group. Presence of microulcers (MU). Enlargement of a Peyer's patch with drainage into the luminal space, altering the structure and arrangement of the mucin glands; a crypt abscess is seen (CA). (**E**) O_3 group, 60 days old. Multiple microulcers (MU) with loss of epithelial continuity; elongated crypts with numerous mucin cells. The lamina propria is undergoing plasmacytosis (PLS). (**F**) O_3 group, 90 days old. Epithelium is undergoing erosion (EE), disrupting its continuity; a large number of infiltrating cells are reaching the luminal space; fibrosis process is seen (FB). The mucin glands are disorganized and discontinuous. Two crypt abscesses (CA) are seen.

4. Discussion

This study uniquely illustrates how ozone pollution impacts the intestinal barrier, potentially explaining the rise in inflammatory bowel and chronic degenerative diseases. Our primary interest was to assess the effects of ozone on the changes in the simple columnar epithelium and lamina propria cells across different intestinal segments due to

oxidative stress. The intestine is considered the primary target organ of the microbiota, given its significant implications for health and the development of degenerative diseases.

This oxidation, resulting from chronic O_3 exposure, leads to the formation of secondary products, such as ROSs, which further amplify oxidative stress and trigger inflammation. Additionally, oxidized lipids (1A, B, C) can be recognized by the immune system as pathogens through TLRs, initiating signaling cascades that activate and enhance inflammatory responses. This response contributes to the establishment of a systemic inflammatory process, as discussed by Miller & Shyy (2017) [38] and Rhoads & Major (2018) [39]. Under both normal and disease conditions, various stimuli can alter the structure of tight junctions (TJs) in the intestine. Factors that influence paracellular permeability include pathogens, growth factors, cytokines, microbiota components, substances in ingested food, digestive enzymes, oxidative stress, and proinflammatory molecules. These factors work together to regulate the opening of intestinal tight junctions [40]. When changes occur in the intestinal epithelium and innate immune cells are activated, the composition of intestinal bacterial populations may also change. These alterations can be linked to variations in mucus production, which helps eliminate pathogens and bacterial metabolites, such as short-chain fatty acids (SCFAs). SCFAs play a crucial role in various processes, including cell proliferation and differentiation, hormone secretion (such as leptin and peptide YY), and the activation of immune and inflammatory responses [41]. Therefore, maintaining a suitable microenvironment and a healthy microbiota composition are essential for the proper functioning of the intestine [42,43].

The increase in reactive oxygen species (ROSs) caused by O_3 exposure, as demonstrated in this study (Figure 1), contributes to the recruitment and accumulation of immune system cells in the lamina propria. This process involves the synthesis and release of zonulin (Figures 5–7), IL-1β (Figures 8–10), and IL-6 (Figures 11–13) by specific immune cells, as demonstrated by Dillon et al., 2010 [44], Shaw et al., 2012 [45], and Yonker et al., 2021 [46,47]. During the early immune response, IL-6 is primarily produced by cells of the innate immune system through the activation of TLRs. IL-6 generally enhances the production of various cytokines and chemokines, including chemokine (C-C motif) ligand 4 (CCL4), ligand 5 (CCL5), ligand 11 (CCL11), ligand 17 (CCL17), as well as intracellular and vascular adhesion molecules like intercellular adhesion molecule 1 (ICAM-1) and vascular cell adhesion molecule 1 (VCAM-1). As a result, IL-6 regulates the growth, differentiation, and circulation of CD4+ and CD8+ T cells, natural killer (NK) cells, dendritic cells, monocytes, and macrophages. This cytokine plays a vital role in signaling for leukocyte translocation and infiltration into sites of inflammation. Additionally, IL-6 promotes the differentiation of monocytes into macrophages by inducing the expression of macrophage colony-stimulating factor receptors on monocytes [48,49]. IL-1β is also crucial in the inflammatory response associated with inflammatory bowel disease (IBD) and other inflammatory conditions [50].

Zonulin, also known as prehaptoglobin-2, is a protein that plays a crucial role in the reversible disassembly of tight junctions in the intestinal epithelium, thereby regulating mucosal permeability [51]. In contrast, prehaptoglobins 1 and 2 are immature molecules; both are glycoproteins that contain a β polypeptide chain. Prehaptoglobin molecules undergo cleavage, resulting in the formation of mature haptoglobin, a glycoprotein that retains the β polypeptide chain. In this study, we utilized an antibody that recognizes the β polypeptide chain found in both types of haptoglobin, 1 and 2. Haptoglobin typically binds to hemoglobin in circulating blood. However, by using an antibody that identifies a common polypeptide chain across these molecules and showing that its immunoreactivity highlights tight tissue junctions similar to those observed in other species, we can conclude that we are detecting the mature haptoglobin present in rats. Haptoglobin, on the other

hand, is part of a family of acute-phase proteins that form a complex with hemoglobin to prevent its oxidation and protect surrounding tissues [52]. It also assists in the elimination of old red blood cells in the liver. Most haptoglobin is produced in the liver, but it can also be found in the lungs, oral epithelium, and colorectal epithelium [53]. Haptoglobin is notable for having distinct biological activities in its precursor form, which differ from the functions of its mature form. In its precursor state, it is involved in the development of various human immunological diseases [54]. As a circulating protein, haptoglobin has antioxidant, anti-inflammatory, and senescent cell elimination effects.

In our research, exposure to low doses of O_3 impacts the presence of haptoglobin in the duodenum (Figure 2A), jejunum (Figure 2B), and colon (Figure 2C), as well as its localization in the duodenum (Figure 5), jejunum (Figure 6), and colon (Figure 7). These changes are influenced by the duration of exposure and the specific intestinal structure being studied. Since zonulin is a precursor molecule of haptoglobin and is often referenced interchangeably in various studies, we used zonulin as a marker for intestinal permeability in the tissue. Zonulin modulates intestinal permeability by regulating the opening of TJs. This mechanism is crucial for the recruitment and activation of innate immune cells in the intestine. Elevated levels of zonulin are implicated in the pathogenesis of autoimmune diseases, such as celiac disease [51], and contribute to the persistence of inflammatory states. Our results indicate significant changes in haptoglobin concentration in the duodenum (Figure 2A) after 7 and 15 days of treatment. In the jejunum (Figure 2B), notable changes are observed at 7, 15, 30, and 90 days of O_3 exposure. The colon (Figure 2C) shows a significant increase at both 7 and 15 days. Furthermore, O_3 treatment leads to alterations in haptoglobin localization, as seen in the duodenum (Figure 5), jejunum (Figure 6), and colon (Figure 7).

A strong relationship exists between ROS and the immune system, as changes in the redox balance can lead to alterations in immune responses. Repeated exposure to low doses of O_3 disrupts this redox balance, leading to a chronic state of oxidative stress that affects interleukins and other pro-inflammatory molecules. Previous studies conducted in our laboratory have shown that reactive oxygen species (ROS) cause the phosphorylation of NF-κB. This process leads to the increased translocation of NF-κB to the nucleus, resulting in the production of pro-inflammatory cytokines. Additionally, some research has demonstrated that changes in the translocation of Nrf2 to the nucleus occur, leading to chronic alterations that disrupt the regulation of antioxidant systems. Together, these two transcription factors highlight the complex relationship between the balance of oxidation and reduction and the inflammatory response [55,56].

The findings of this study show that both IL-1β and IL-6 experience changes in the intestine, with variations based on the region and the treatment with O_3. Specifically, there is a significant increase in IL-1β levels in the duodenum after 60 days of treatment, while in the colon, this increase is observed after 30 days.

Examining the distribution of IL-1β in the duodenum reveals the highest immunoreactivity at 15 and 60 days across different structures, including enterocytes, the lamina propria, villi, and the muscular layer. In the jejunum, more pronounced immunoreactivity is noted at 15, 30, and 90 days compared to the control group. Finally, in the colon, there is an increase in immunoreactivity after 15 days of treatment. IL-1β is a common and versatile proinflammatory cytokine that plays a critical role in the development of intestinal inflammation. Patients with IBD typically have elevated levels of IL-1β, and it is also significant in animal models of intestinal inflammation [50,57]. Although the role of alterations in epithelial TJs in the development of intestinal inflammation associated with IBD is recognized, there are currently no therapeutic agents available that specifically target the treatment of TJs.

ROS play a crucial role in recruiting and accumulating immune cells in the lamina propria. These immune cells synthesize and release key substances, including zonulin, IL-1β, and IL-6. During the early stages of the immune response, innate immune cells activated through TLRs are the primary source of IL-6. Our experimental results indicate that IL-6 levels in the duodenum tend to increase at both 7 and 15 days post-stimulation. In contrast, significant increases in IL-6 levels are observed in the jejunum and colon at 60 days. Specifically, there is an increase in immunoreactivity at 60 and 90 days in the duodenum (see Figure 11), at 30 and 60 days in the jejunum (see Figure 12), and at 30 days in the colon (see Figure 13).

These alterations together generate alterations in the structure and function of intestinal tissue, such as modifications in tight junctions that increase intestinal permeability, distortion in the Liberkühn crypts, atrophy in intestinal villi, widening at the mouth of the crypts, erosion of the epithelium, the formation of eosinophil and neutrophil abscesses in the crypts, and often enlargement of Peyer's patches (Figures 14–16). These changes can result in altered immune responses, characterized by proinflammatory cytokines (Figures 8–13) causing modifications in the structure of the intestinal tract with the consequent synthesis and release of zonulin (Figures 5–7), to the detriment of intestinal permeability; this allows the passage of microbial debris and antigens from the luminal space to the basolateral layer, perpetuating a state of unregulated intestinal permeability, inflammation and dysbiosis, similar to what occurs in IBD, which are chronic inflammatory disorders of the gastrointestinal tract that have complex interactions between genetic predisposition, environmental factors, intestinal microbiota, and the immune system [57].

Finally, human inhalation of pollutants involves a complex mixture of suspended particles and gases, which can produce ozone in the troposphere when exposed to ultraviolet light. While some researchers have explored the effects of environmental pollution on the health of individuals exposed to these gases, they have not been able to pinpoint the specific impact of any single pollutant. As a result, there are no human studies that provide a clear understanding of the effects of ozone pollution on its own. However, using animal models allows us to investigate its effects and determine how chronic oxidative stress contributes to human health issues associated with this pollutant.

5. Conclusions

In conclusion, repeated exposure to low doses of O_3 causes increased oxidative stress, an increase in proinflammatory cytokines that leads to a loss of regulation of the immune response in the duodenum, jejunum, and colon of rats, as well as structural changes that alter the intestinal barrier and perpetuate a state of chronic inflammation characteristic of inflammatory bowel diseases.

Author Contributions: Conceptualization, S.R.-A.; Formal analysis, A.M.-M., E.R.-M., M.V.-F. and S.R.-A.; Funding acquisition, S.R.-A.; Investigation, A.M.-M., E.R.-M., M.V.-F. and S.R.-A.; Methodology, A.M.-M., E.R.-M. and M.V.-F.; Resources, S.R.-A.; Writing—original draft, A.M.-M., E.R.-M., M.V.-F. and S.R.-A.; Writing—review and editing, S.R.-A. All authors have read and agreed to the published version of the manuscript.

Funding: Project funded by Dirección General de Asuntos del Personal Académico-UNAM (PAPIIT IN204324) to S.R-A.

Institutional Review Board Statement: The study was conducted in accordance with the Declaration of Helsinki. The animal study protocol was approved by the Ethics Committee of the Facultad de Medicina, UNAM and based on Comité Interno para el Cuidado y Uso de Animales de Laboratorio. División de Investigación. Facultad de Medicina 2018 (CICUAL) Registry 019-2023 [34], approved 1 August 2023. The project was approved with registration number FM/DI/063/2023.

Informed Consent Statement: Not applicable.

Data Availability Statement: The data in this work will be available when required.

Acknowledgments: Alfredo Miranda-Martínez received a Secretaría de Ciencias, Humanidades, Tecnología e Innovación (Secihti)postdoctoral fellowship, CVU 385286. The authors thank Pamela Barragán-Reséndiz for her technical assistance and Eduardo Hernández-Orozco for his support with ozone model supervision. The authors have reviewed and edited the output and take full responsibility for the content of this publication.

Conflicts of Interest: The authors declare no conflicts of interest.

Abbreviations

The following abbreviations are used in this manuscript:

ATP	Adenosine triphosphate
CCL4	Chemokine (C-C motif) ligand 4
CCL5	Chemokine (C-C motif) ligand 5
CCL11	Chemokine (C-C motif) ligand 11
CCL17	Chemokine (C-C motif) ligand 17
CA	Crypt abscess
ME	Modified epithelial
EE	Eroded epithelium
FB	Fibrosis
MC	Mucin cells
GR	Granulomas
H2O2	Hydrogen peroxide
H-E	Hematoxylin and eosin
IBD	Inflammatory bowel disease
ICAM-1	Intercellular adhesion molecule 1
IL-1β	Interleukin-1 beta
IL-6	Interleukin-6
MDA	Malondialdehyde
MU	Micro ulcers
MV	Modify villi
NK	Natural killer cells
OM	Opening crypt
O3	Ozone
ppm	Parts per million
PP	Peyer's patches
PLS	Plasmacytosis
PreHp-2	Prehaptoglobin-2
ROS	Reactive oxygen species
SDS-PAGE	Sodium Dodecyl Sulfate Polyacrylamide Gel Electrophoresis
SCFAs	Short-chain fatty acids
TBARS	Thiobarbituric acid reactive substances
TBA	Thiobarbituric acid
TJs	Tight junctions
TLRs	Toll-like receptors
VCAM-1	Vascular cell adhesion molecule 1

References

1. Manisalidis, I.; Stavropoulou, E.; Stavropoulos, A.; Bezirtzoglou, E. Environmental and Health Impacts of Air Pollution: A Review. *Front. Public Health* **2020**, *8*, 14. [CrossRef]

2. Waxman, M.; Manczak, E.M. Air Pollution's Hidden Toll: Links Between Ozone, Particulate Matter, and Adolescent Depression. *Int. J. Environ. Res. Public Health* **2024**, *21*, 1663. [CrossRef] [PubMed]
3. Bista, S.; Chatzidiakou, L.; Jones, R.L.; Benmarhnia, T.; Postel-Vinay, N.; Chaix, B. Associations of air pollution mixtures with ambulatory blood pressure: The MobiliSense sensor-based study. *Environ. Res.* **2023**, *227*, 115720. [CrossRef]
4. Zhang, J.J.; Wei, Y.; Fang, Z. Ozone Pollution: A Major Health Hazard Worldwide. *Front. Immunol.* **2019**, *10*, 2518. [CrossRef]
5. Liu, C.; Chen, R.; Sera, F.; Vicedo-Cabrera, A.M.; Guo, Y.; Tong, S.; Lavigne, E.; Correa, P.M.; Ortega, N.V.; Achilleos, S.; et al. Interactive effects of ambient fine particulate matter and ozone on daily mortality in 372 cities: Two stage time series analysis. *Bmj* **2023**, *383*, e075203. [CrossRef] [PubMed]
6. Wang, Y.; Chen, Y.; Zhang, X.; Lu, Y.; Chen, H. New insights in intestinal oxidative stress damage and the health intervention effects of nutrients: A review. *J. Funct. Foods* **2020**, *75*, 104248. [CrossRef]
7. Forman, H.J.; Zhang, H. Targeting oxidative stress in disease: Promise and limitations of antioxidant therapy. *Nat. Rev. Drug Discov.* **2021**, *20*, 689–709. [CrossRef]
8. Sadiq, I.Z. Free Radicals and Oxidative Stress: Signaling Mechanisms, Redox Basis for Human Diseases, and Cell Cycle Regulation. *Curr. Mol. Med.* **2023**, *23*, 13–35. [CrossRef]
9. Andrés, C.M.C.; Pérez de la Lastra, J.M.; Juan, C.A.; Plou, F.J.; Pérez-Lebeña, E. The Role of Reactive Species on Innate Immunity. *Vaccines* **2022**, *10*, 1735. [CrossRef]
10. Solleiro-Villavicencio, H.; Hernández-Orozco, E.; Rivas-Arancibia, S. Effect of exposure to low doses of ozone on interleukin 17A expression during progressive neurodegeneration in the rat hippocampus. *Neurol. (Engl. Ed.)* **2021**, *36*, 673–680. [CrossRef] [PubMed]
11. Lugrin, J.; Rosenblatt-Velin, N.; Parapanov, R.; Liaudet, L. The role of oxidative stress during inflammatory processes. *Biol. Chem.* **2014**, *395*, 203–230. [CrossRef]
12. Megha, K.B.; Joseph, X.; Akhil, V.; Mohanan, P.V. Cascade of immune mechanism and consequences of inflammatory disorders. *Phytomedicine* **2021**, *91*, 153712. [CrossRef]
13. Medzhitov, R. The spectrum of inflammatory responses. *Science* **2021**, *374*, 1070–1075. [CrossRef]
14. Merelli, A.; Repetto, M.; Lazarowski, A.; Auzmendi, J. Hypoxia, Oxidative Stress, and Inflammation: Three Faces of Neurodegenerative Diseases. *J. Alzheimers Dis.* **2021**, *82*, S109–S126. [CrossRef]
15. Rivas-Arancibia, S.; Guevara-Guzmán, R.; López-Vidal, Y.; Rodríguez-Martínez, E.; Zanardo-Gomes, M.; Angoa-Pérez, M.; Raisman-Vozari, R. Oxidative stress caused by ozone exposure induces loss of brain repair in the hippocampus of adult rats. *Toxicol. Sci.* **2010**, *113*, 187–197. [CrossRef]
16. Calderón-Garcidueñas, L.; González-Maciel, A.; Kulesza, R.J.; González-González, L.O.; Reynoso-Robles, R.; Mukherjee, P.S.; Torres-Jardón, R. Air Pollution, Combustion and Friction Derived Nanoparticles, and Alzheimer's Disease in Urban Children and Young Adults. *J. Alzheimers Dis.* **2019**, *70*, 343–360. [CrossRef]
17. Calderón-Garcidueñas, L.; Torres-Jardón, R.; Kulesza, R.J.; Mansour, Y.; González-González, L.O.; Gónzalez-Maciel, A.; Reynoso-Robles, R.; Mukherjee, P.S. Alzheimer disease starts in childhood in polluted Metropolitan Mexico City. A major health crisis in progress. *Environ. Res.* **2020**, *183*, 109137. [CrossRef]
18. Vekic, J.; Stromsnes, K.; Mazzalai, S.; Zeljkovic, A.; Rizzo, M.; Gambini, J. Oxidative Stress, Atherogenic Dyslipidemia, and Cardiovascular Risk. *Biomedicines* **2023**, *11*, 2897. [CrossRef]
19. Zhang, Y.; Shi, J.; Ma, Y.; Yu, N.; Zheng, P.; Chen, Z.; Wang, T.; Jia, G. Association between Air Pollution and Lipid Profiles. *Toxics* **2023**, *11*, 894. [CrossRef]
20. Chatterjee, S. Oxidative stress, inflammation, and disease. In *Oxidative Stress and Biomaterials*; Elsevier: Amsterdam, The Netherlands, 2016; pp. 35–58.
21. Bondia-Pons, I.; Ryan, L.; Martinez, J.A. Oxidative stress and inflammation interactions in human obesity. *J. Physiol. Biochem.* **2012**, *68*, 701–711. [CrossRef]
22. Beltrán-García, J.; Osca-Verdegal, R.; Pallardó, F.V.; Ferreres, J.; Rodríguez, M.; Mulet, S.; Sanchis-Gomar, F.; Carbonell, N.; García-Giménez, J.L. Oxidative Stress and Inflammation in COVID-19-Associated Sepsis: The Potential Role of Anti-Oxidant Therapy in Avoiding Disease Progression. *Antioxidants* **2020**, *9*, 936. [CrossRef]
23. Rodríguez-Martínez, E.; Martínez, F.; Espinosa-García, M.T.; Maldonado, P.; Rivas-Arancibia, S. Mitochondrial dysfunction in the hippocampus of rats caused by chronic oxidative stress. *Neuroscience* **2013**, *252*, 384–395. [CrossRef]
24. Rodríguez-Martínez, E.; Nava-Ruiz, C.; Escamilla-Chimal, E.; Borgonio-Perez, G.; Rivas-Arancibia, S. The Effect of Chronic Ozone Exposure on the Activation of Endoplasmic Reticulum Stress and Apoptosis in Rat Hippocampus. *Front. Aging Neurosci.* **2016**, *8*, 245. [CrossRef]
25. Rivas-Arancibia, S.; Hernández-Orozco, E.; Rodríguez-Martínez, E.; Valdés-Fuentes, M.; Cornejo-Trejo, V.; Pérez-Pacheco, N.; Dorado-Martínez, C.; Zequeida-Carmona, D.; Espinosa-Caleti, I. Ozone Pollution, Oxidative Stress, Regulatory T Cells and Antioxidants. *Antioxidants* **2022**, *11*, 1553. [CrossRef]

26. Campbell, E.L.; Colgan, S.P. Control and dysregulation of redox signalling in the gastrointestinal tract. *Nat. Rev. Gastroenterol. Hepatol.* **2019**, *16*, 106–120. [CrossRef]
27. Junges, V.M.; Closs, V.E.; Nogueira, G.M.; Gottlieb, M.G.V. Crosstalk between Gut Microbiota and Central Nervous System: A Focus on Alzheimer's Disease. *Curr. Alzheimer Res.* **2018**, *15*, 1179–1190. [CrossRef]
28. Ojeda, J.; Ávila, A.; Vidal, P.M. Gut Microbiota Interaction with the Central Nervous System throughout Life. *J. Clin. Med.* **2021**, *10*, 1299. [CrossRef]
29. Gieryńska, M.; Szulc-Dąbrowska, L.; Struzik, J.; Mielcarska, M.B.; Gregorczyk-Zboroch, K.P. Integrity of the Intestinal Barrier: The Involvement of Epithelial Cells and Microbiota-A Mutual Relationship. *Animals* **2022**, *12*, 145. [CrossRef]
30. Hitch, T.C.A.; Hall, L.J.; Walsh, S.K.; Leventhal, G.E.; Slack, E.; de Wouters, T.; Walter, J.; Clavel, T. Microbiome-based interventions to modulate gut ecology and the immune system. *Mucosal Immunol.* **2022**, *15*, 1095–1113. [CrossRef]
31. Dicks, L.M.T. Gut Bacteria and Neurotransmitters. *Microorganisms* **2022**, *10*, 1838. [CrossRef]
32. Chelakkot, C.; Ghim, J.; Ryu, S.H. Mechanisms regulating intestinal barrier integrity and its pathological implications. *Exp. Mol. Med.* **2018**, *50*, 1–9. [CrossRef]
33. Estados Unidos Mexicanos-Secretaría de Agricultura Ganadería, Desarrollo Rural, Pesca y Alimentación. Especificaciones técnicas para la producción, cuidado y uso de los animales de laboratorio. In *Norma Oficial Mexicana (NOM-062-ZOO-1999)*; Gobernación, S.d., Ed.; Diario Oficial de la Federación-SEGOB: Ciudad de México, Mexico, 2001; Volume 107, pp. 107–165.
34. CICUAL (Comité Interno para el Cuidado y Uso de Animales de Laboratorio). In. División de Investigación, Facultad de Medicina: Ciudad de México, Mexico, 2018. Available online: https://di.facmed.unam.mx/comisiones/ManualCICUAL.pdf (accessed on 12 August 2025).
35. Estados Unidos Mexicanos-Secretaría de Agricultura Ganadería; Desarrollo Rural Pesca y Alimentación. Métodos Para Dar Muerte a Los Animales Domésticos y Silvestres. In *NORMA Oficial Mexicana NOM-033-SAG/ZOO-2014*; Gobernación, S.d., Ed.; Diario Oficial de la Federación-SEGOB: Ciudad de México, Mexico, 2015.
36. Pereyra-Muñoz, N.; Rugerio-Vargas, C.; Angoa-Pérez, M.; Borgonio-Pérez, G.; Rivas-Arancibia, S. Oxidative damage in substantia nigra and striatum of rats chronically exposed to ozone. *J. Chem. Neuroanat.* **2006**, *31*, 114–123. [CrossRef]
37. Fuentes-Venado, C.E.; Terán-Pérez, G.; Espinosa-Hernández, V.M.; Martínez-Herrera, E.; Segura-Uribe, J.J.; Mercadillo, R.E.; Pinto-Almazán, R.; Guerra-Araiza, C. Nutritional Status Influences Oxidative Stress and Insulin Resistance in Preschool Children. *Metab. Syndr. Relat. Disord.* **2021**, *19*, 513–523. [CrossRef]
38. Miller, Y.I.; Shyy, J.Y. Context-Dependent Role of Oxidized Lipids and Lipoproteins in Inflammation. *Trends Endocrinol. Metab.* **2017**, *28*, 143–152. [CrossRef]
39. Rhoads, J.P.; Major, A.S. How Oxidized Low-Density Lipoprotein Activates Inflammatory Responses. *Crit. Rev. Immunol.* **2018**, *38*, 333–342. [CrossRef]
40. Van Spaendonk, H.; Ceuleers, H.; Witters, L.; Patteet, E.; Joossens, J.; Augustyns, K.; Lambeir, A.M.; De Meester, I.; De Man, J.G.; De Winter, B.Y. Regulation of intestinal permeability: The role of proteases. *World J. Gastroenterol.* **2017**, *23*, 2106–2123. [CrossRef]
41. Vinolo, M.A.; Rodrigues, H.G.; Nachbar, R.T.; Curi, R. Regulation of inflammation by short chain fatty acids. *Nutrients* **2011**, *3*, 858–876. [CrossRef]
42. Larabi, A.; Barnich, N.; Nguyen, H.T.T. New insights into the interplay between autophagy gut microbiota inflammatory responses, i.n.IBD. *Autophagy* **2020**, *16*, 38–51. [CrossRef]
43. Mostafavi Abdolmaleky, H.; Zhou, J.R. Gut Microbiota Dysbiosis, Oxidative Stress, Inflammation, and Epigenetic Alterations in Metabolic Diseases. *Antioxidants* **2024**, *13*, 985. [CrossRef]
44. Dillon, S.M.; Rogers, L.M.; Howe, R.; Hostetler, L.A.; Buhrman, J.; McCarter, M.D.; Wilson, C.C. Human Intestinal Lamina Propria CD1c+ Dendritic Cells Display an Activated Phenotype at Steady State and Produce IL-23 in Response to TLR7/8 Stimulation. *J. Immunol.* **2010**, *184*, 6612–6621. [CrossRef] [PubMed]
45. Shaw, M.H.; Kamada, N.; Kim, Y.-G.; Núñez, G. Microbiota-induced IL-1β, but not IL-6, is critical for the development of steady-state TH17 cells in the intestine. *J. Exp. Med.* **2012**, *209*, 251–258. [CrossRef]
46. Yonker, L.M.; Gilboa, T.; Ogata, A.F.; Senussi, Y.; Lazarovits, R.; Boribong, B.P.; Bartsch, Y.C.; Loiselle, M.; Rivas, M.N.; Porritt, R.A.; et al. Multisystem inflammatory syndrome in children is driven by zonulin-dependent loss of gut mucosal barrier. *J. Clin. Investig.* **2021**, *131*, e149633. [CrossRef] [PubMed]
47. Rosser, F.; Balmes, J. Ozone and childhood respiratory health: A primer for US pediatric providers and a call for a more protective standard. *Pediatr. Pulmonol.* **2023**, *58*, 1355–1366. [CrossRef]
48. Smith, J.K. IL-6 and the dysregulation of immune, bone, muscle, and metabolic homeostasis during spaceflight. *NPJ Microgravity* **2018**, *4*, 24. [CrossRef]
49. Madaro, L.; Passafaro, M.; Sala, D.; Etxaniz, U.; Lugarini, F.; Proietti, D.; Alfonsi, M.V.; Nicoletti, C.; Gatto, S.; De Bardi, M.; et al. Denervation-activated STAT3-IL-6 signalling in fibro-adipogenic progenitors promotes myofibres atrophy and fibrosis. *Nat. Cell Biol.* **2018**, *20*, 917–927. [CrossRef]

50. Rawat, M.; Nighot, M.; Al-Sadi, R.; Gupta, Y.; Viszwapriya, D.; Yochum, G.; Koltun, W.; Ma, T.Y. IL1BIncreases Intestinal Tight Junction Permeability by Up-regulation of MIR200C-3p Which Degrades Occludin, m.RNA. *Gastroenterology* **2020**, *159*, 1375–1389. [CrossRef]
51. Fasano, A. Zonulin, regulation of tight junctions, and autoimmune diseases. *Ann. N. Y. Acad. Sci.* **2012**, *1258*, 25–33. [CrossRef]
52. Ajamian, M.; Steer, D.; Rosella, G.; Gibson, P.R. Serum zonulin as a marker of intestinal mucosal barrier function: May not be what it seems. *PLoS ONE* **2019**, *14*, e0210728. [CrossRef]
53. Mariño-Crespo, Ó.; Cuevas-Álvarez, E.; Harding, A.L.; Murdoch, C.; Fernández-Briera, A.; Gil-Martín, E. Haptoglobin expression in human colorectal cancer. *Histol. Histopathol.* **2019**, *34*, 953–963. [CrossRef] [PubMed]
54. Tripathi, A.; Lammers, K.M.; Goldblum, S.; Shea-Donohue, T.; Netzel-Arnett, S.; Buzza, M.S.; Antalis, T.M.; Vogel, S.N.; Zhao, A.; Yang, S.; et al. Identification of human zonulin, a physiological modulator of tight junctions, as prehaptoglobin-2. *Proc. Natl. Acad. Sci. USA* **2009**, *106*, 16799–16804. [CrossRef] [PubMed]
55. Xiao, C.L.; Lai, H.T.; Zhou, J.J.; Liu, W.Y.; Zhao, M.; Zhao, K. Nrf2 Signaling Pathway: Focus on Oxidative Stress in Spinal Cord Injury. *Mol. Neurobiol.* **2025**, *62*, 2230–2249. [CrossRef] [PubMed]
56. Wardyn, J.D.; Ponsford, A.H.; Sanderson, C.M. Dissecting molecular cross-talk between Nrf2 and NF-κB response pathways. *Biochem. Soc. Trans.* **2015**, *43*, 621–626. [CrossRef] [PubMed]
57. Kurti, Z.; Vegh, Z.; Gonczi, L.; Lakatos, P.L. Clinical Risk Factors: Lessons from Epidemiology. In *Biomarkers in Inflammatory Bowel Diseases*; Springer: Cham, Switzerland, 2019; pp. 9–22.

antioxidants

MDPI

Article

A Combined Extract from *Dioscorea bulbifera* and *Zingiber officinale* Mitigates $PM_{2.5}$-Induced Respiratory Damage by NF-κB/TGF-β1 Pathway

In Young Kim [1], Hyo Lim Lee [1], Hye Ji Choi [1], Yeong Hyeon Ju [1], Yu Mi Heo [1], Hwa Rang Na [1], Dong Yeol Lee [2], Won Min Jeong [2] and Ho Jin Heo [1,*]

[1] Division of Applied Life Science (BK21), Institute of Agriculture and Life Science, Gyeongsang National University, Jinju 52828, Republic of Korea; inzero331@gnu.ac.kr (I.Y.K.); gyfla059@gnu.ac.kr (H.L.L.); hjchoi0820@gnu.ac.kr (H.J.C.); ju8172001@gnu.ac.kr (Y.H.J.); yumi@gnu.ac.kr (Y.M.H.); hrna@gnu.ac.kr (H.R.N.)

[2] Research & Development Team, Gyeongnam Anti-Aging Research Institute, Sancheong 52215, Republic of Korea; dylee1984@gari.or.kr (D.Y.L.); jwm5618@gari.or.kr (W.M.J.)

* Correspondence: hjher@gnu.ac.kr; Tel.: +82-55-772-1907

Abstract: This research evaluated the protective role of a combined extract of *Dioscorea bulbifera* and *Zingiber officinale* (DBZO) against respiratory dysfunction caused by particulate matter ($PM_{2.5}$) exposure in BALB/c mice. The bioactive compounds identified in the DBZO are catechin, astragalin, 6-gingerol, 8-gingerol, and 6-shogaol. DBZO ameliorated cell viability and reactive oxygen species (ROS) production in $PM_{2.5}$-stimulated A549 and RPMI 2650 cells. In addition, it significantly alleviated respiratory dysfunction in BALB/c mice exposed to $PM_{2.5}$. DBZO improved the antioxidant systems in lung tissues by modulating malondialdehyde (MDA) content, as well as levels of reduced glutathione (GSH) and superoxide dismutase (SOD). Likewise, DBZO restored mitochondrial dysfunction by improving ROS levels, mitochondrial membrane potential, and ATP production. Moreover, DBZO modulated the levels of neutrophils, eosinophils, monocytes, and lymphocytes (specifically $CD4^+$, $CD8^+$, and $CD4^+IL\text{-}4^+$ T cells) in blood and IgE levels in serum. DBZO was shown to regulate the c-Jun N-terminal kinase (JNK) pathway, nuclear factor kappa B (NF-κB) pathway, and transforming growth factor β (TGF-β)/suppressor of mothers against decapentaplegic (Smad) pathway. Histopathological observation indicated that DBZO mitigates the increase in alveolar septal thickness. These findings indicate that DBZO is a promising natural agent for improving respiratory health.

Keywords: *Dioscorea bulbifera*; *Zingiber officinale*; respiratory dysfunction; oxidative stress; inflammation; fibrosis

1. Introduction

Air quality has deteriorated worldwide due to urbanization and population growth, which has created public health challenges [1]. Among various air pollutants, particulate matter (PM) is particularly recognized for its heightened risk to human health compared to other pollutants [2]. Various studies have reported that exposure to PM can trigger respiratory diseases such as chronic obstructive pulmonary disease (COPD), idiopathic pulmonary fibrosis (IPF), and asthma [3,4]. PM is categorized based on aerodynamic diameter into PM_{10} (particles $\leq$ 10 μm), $PM_{2.5}$ (particles $\leq$ 2.5 μm), and $PM_{0.1}$ (particles $\leq$ 0.1 μm) [5]. Of these, $PM_{2.5}$ is particularly concerning due to its high specific surface area relative to its mass which allows it to adsorb harmful substances such as zinc (Zn), iron (Fe), and polycyclic aromatic hydrocarbons (PAHs) from the atmosphere and enter the body, leading to oxidative stress and inflammatory responses [6]. Inorganic elements attached to $PM_{2.5}$ that enter the body generate reactive oxygen species (ROS) through the Fenton reaction,

inducing oxidative stress, while PAHs are also known to penetrate the body and produce metabolic byproducts that contribute to cellular injury and increased ROS production [7,8]. The overproduction of ROS leads to the depletion of the endogenous antioxidant system, such as reduced glutathione (GSH) and superoxide dismutase (SOD), resulting in increased oxidative stress [9]. It promotes the infiltration of inflammatory cells into the respiratory system and the secretion of chemokines and cytokines, eventually triggering the activation of nuclear factor kappa B (NF-κB) proteins that drive inflammatory responses [10,11]. Furthermore, chronic inflammation has been reported to promote pulmonary fibrosis through the activation of the transforming growth factor-β (TGF-β)/suppressor of mothers against decapentaplegic (Smad) pathway [12]. Against this backdrop, numerous studies are being conducted to explore the relationship between oxidative stress and inflammatory responses and to develop strategies for their mitigation, with natural antioxidants emerging as a primary approach [13–15].

Natural products, rich in antioxidants, have been used for centuries in health and treatment, and play a crucial role in traditional medicine [16]. Among these, *Dioscorea bulbifera* (*D. bulbifera*) and *Zingiber officinale* (*Z. officinale*) are plants traditionally used in Asian medicine for their therapeutic efficacy [17,18]. *D. bulbifera*, also known as air potato, is a member of the *Dioscoreaceae* family and has been traditionally used to treat conditions such as laryngopharyngitis and chest pain [19,20]. It contains various polyphenols and flavonoids, including catechin, quercetin, and kaempferol, which have been reported to exhibit respiratory protective effects through their antioxidant and anti-inflammatory activities [21–23]. Similarly, *Z. officinale*, or ginger, is a member of the *Zingiberaceae* family and has been used to alleviate respiratory diseases such as colds and sore throats [18]. Its biological activity is attributed to bioactive compounds such as gingerol, shogaol, paradol, and zingerone [18]. In particular, gingerol and shogaol have been extensively studied for their antioxidative and anti-inflammatory characteristics, as well as their protective roles in the respiratory system [24]. Previous research has demonstrated that combining herbs with similar biological activities, such as antioxidant and anti-inflammatory properties, can more effectively alleviate pathological symptoms by targeting multiple metabolic pathways than using a single herb [25,26]. This effect is believed to arise from the synergistic interaction among the various bioactive components [25,26]. Thus, this study aimed to investigate the protective properties of a combined extract of *D. bulbifera* and *Z. officinale* (DBZO), each traditionally used in therapies for treating respiratory diseases, in BALB/c mice with $PM_{2.5}$-induced respiratory dysfunction.

2. Materials and Methods

2.1. Preparation of $PM_{2.5}$

$PM_{2.5}$ was purchased from Powder Technology Incorporated (Nominal 0–3 micron arizona test dust, Arden Hills, MN, USA), with an average particle size of 1.06 μm. This particle was used as $PM_{2.5}$ in this study. The components of $PM_{2.5}$ used in this study were identified as Al, Fe, Mg, Mn, Ba, Zn, and Cu [27]. It was dissolved in purified water and used for cell and animal experiments.

2.2. Preparation of DBZO

DBZO extract powder was offered by the Gyeongnam Anti-Aging Research Institute on 23 February 2024. *D. bulbifera* was purchased from local market (Jinju, Republic of Korea) as a fresh sample. It was cut into pieces and dried in a drying oven (JOURI-Q, KEC, Seoul, Republic of Korea) at 45 °C for 48 h. *Z. officinale* was purchased as a dried sample from Donghae (Seoul, Republic of Korea). Next, the dried *D. bulbifera* and *Z. officinale* were combined at a 9:1 ratio. The mixture was then subjected to reflux extraction with 50% ethanol at 90 °C for 4 h. Afterward, it was filtered, concentrated, freeze-dried, and stored at −80 °C until further use.

2.3. Ultra-Performance Liquid Chromatography-Quadrupole Time-of-Flight Mass Spectrometry (UPLC-Q-TOF/MS)

The DBZO used for the analysis was prepared by dissolving it in 50% methanol. The analysis was conducted using UPLC-Q-TOF/MS (Waters, Milford, MA, USA) equipped with an Acquity UPLC BEH C_{18} column (2.1 mm × 100 mm, 1.7 μm; Waters). The column temperature was set to 40 °C and the mobile phase was composed of water containing 0.1% formic acid (solvent A) and acetonitrile containing 0.1% formic acid (solvent B), with a flow rate of 0.35 mL/min. For chromatographic separation, solvent B was initially maintained at 1% for 1 min, then linearly increased to 100% from 1 to 8 min. Solvent B was held at 100% from 8 to 9 min, decreased to 1% from 9 to 9.5 min, and finally maintained at 1% from 9.5 to 12 min. Subsequently, the column eluents were detected using the Q-TOF-MS with positive electrospray ionization (ESI) mode. Mass spectrometry conditions were applied as follows: capillary voltage, 3 kV; ion source temperature, 100 °C; desolvation temperature, 400 °C; cone gas, 30 L/h; desolvation gas, 800 L/h; collision energy, 20–40 eV; and mass range, 50–1500 m/z.

2.4. Cytoprotective Effects of DBZO Against $PM_{2.5}$-Induced A549 and RPMI 2650 Cells

2.4.1. Cell Cultures

A549 cells (KCLB, Seoul, Republic of Korea) and RPMI 2650 cells (ATCC, Manassas, VA, USA) were cultured in RPMI1640 and MEM media, respectively, each supplemented with 10% fetal bovine serum and 1% penicillin/streptomycin. All cells were cultured in an incubator maintained at 37 °C and 5% CO_2.

2.4.2. Cell Viability

A549 and RPMI 2650 cells were plated in a 96-well plate at a density of 1×10^4 cells/well and incubated for 24 h. Then, cells were pre-treated for 30 min with phosphate-buffered saline (PBS), vitamin C (100 μg/mL), or DBZO (at concentrations of 10, 20, 50, 100, and 200 μg/mL). Vitamin C was used as a positive control in this study due to its extensively reported cellular protective effects against oxidative stress [28]. The dose of DBZO was selected based on previous studies reporting non-cytotoxic yet biologically effective ranges [20,29]. After 30 min, cultured cells were treated with PBS or $PM_{2.5}$ (100 μg/mL) and cultured for 24 h. The dose of $PM_{2.5}$ was selected based on previous studies (Figures S1 and S2). Following this, the MTT solution was added to each well for 3 h. The medium was then replaced with dimethyl sulfoxide after it was suctioned. Absorbance was measured at 570 nm (determination wavelength) and 655 nm (reference wavelength) using a microplate reader (Epoch2, BioTek Instruments Inc., Winooski, VT, USA).

2.4.3. Intracellular Oxidative Stress

A549 and RPMI 2650 cells were plated in a 96-well black plate at a density of 1×10^4 cells/well and cultured for 24 h. Then, cells were pre-treated for 30 min with PBS, vitamin C (100 μg/mL), or DBZO (at concentrations of 10, 20, 50, 100, and 200 μg/mL). Vitamin C was used as a positive control in this study due to its extensively reported cellular protective effects against oxidative stress [28]. The dose of DBZO was selected based on previous studies reporting non-cytotoxic yet biologically effective ranges [20,29]. After 30 min, cultured cells were treated with PBS or $PM_{2.5}$ (100 μg/mL) and cultured for 24 h. The dose of $PM_{2.5}$ was selected based on previous studies (Figures S1 and S2). Following this, the DCFH-DA solution was added to each well for 50 min. Fluorescence was measured at 485 nm (excitation wavelength) and 535 nm (emission wavelength) using a fluorometer (Infinite F200, TECAN, Mannedorf, Switzerland).

2.5. Animals

BALB/c mice (6 weeks, male) were purchased from Samtako (Osan, Republic of Korea) and housed under controlled environmental conditions, including a 12 h light/dark cycle, a temperature of 22 ± 2 °C, and a humidity of 50 ± 5%. The mice were randomly divided into

five groups (n = 15 per group) as follows: normal control (NC, clean air exposure + drinking water), normal sample (NS, clean air exposure + DBZO 100 mg/kg of body weight), $PM_{2.5}$ ($PM_{2.5}$ exposure + drinking water), DBZO50 ($PM_{2.5}$ exposure + DBZO 50 mg/kg of body weight), and DBZO100 ($PM_{2.5}$ exposure + DBZO 100 mg/kg of body weight). After an adaptation period of 1 week, the animals were orally administered either clean water or DBZO before exposure to the air in the chamber. Then, the whole bodies of the mice were exposed in a chamber to clean air or $PM_{2.5}$ at a concentration of 500 μg/m^3 for 5 h/day and 5 days/week for 12 weeks. The dose of $PM_{2.5}$ was selected based on previous studies and WHO guidelines [30–33]. After 12 weeks, mice were dissected to collect blood and lung samples for subsequent analyses. All animal experiments were performed with the permission of the Institutional Animal Care and Use Committee (IACUC) of Gyeongsang National University (GNU-240108-M0002, date of approval: 8 January 2024).

2.6. Effects of DBZO Against $PM_{2.5}$-Induced Antioxidant System Dysfunction

2.6.1. Malondialdehyde (MDA) Contents

The lung tissues obtained from the mice were homogenized with PBS. The homogenate was centrifuged at 4 °C, 2356× *g* for 10 min to obtain the supernatants. The supernatants were heated in a water bath set to 95 °C with 1% phosphoric acid and 0.67% thiobarbituric acid. The reactants were measured at 532 nm using a spectrophotometer (UV-1800, Shimadzu, Tokyo, Japan).

2.6.2. Reduced GSH Levels

The lung tissues obtained from the mice were homogenized with 10 mM phosphate buffer, including 1 mM ethylenediamine tetraacetic acid (EDTA), and centrifuged at 4 °C and 10,000× *g* for 15 min. The supernatants were mixed with 5% metaphosphoric acid and re-centrifuged at 4 °C and 2000× *g* for 2 min to obtain supernatant. Subsequently, it was mixed with 0.26 M Tris-HCl (pH 7.5), 0.65 N NaOH, and 1 mg/mL o-phthalaldehyde. Fluorescence was measured at 360 nm (excitation wavelength) and 430 nm (emission wavelength) using a fluorometer (Infinite F200, TECAN).

2.6.3. SOD Levels

The lung tissues obtained from the mice were homogenized with PBS and centrifuged at 4 °C and 400× *g* for 10 min to obtain the pellet. Subsequently, it was mixed with an extraction buffer and then reacted on ice for 30 min. The reactants were centrifuged at 4 °C and 10,000× *g* for 10 min. Afterward, the SOD kit (Dojindo Molecular Tech., Rockville, MD, USA) was used according to the manufacturer's instructions.

2.7. Effects of DBZO Against $PM_{2.5}$-Induced Mitochondrial Dysfunction

2.7.1. Extraction of Mitochondria from Lung Tissue

The lung tissues obtained from the mice were homogenized with mitochondrial isolation (MI) buffer [0.1% bovine serum albumin, 20 mM HEPES sodium salt, 75 mM sucrose, and 215 mM mannitol] containing 1 mM ethylene glycol-bis(β-aminoethyl ether)-N,N,N′,N′-tetraacetic acid (EGTA). The homogenate was centrifuged at 4 °C and 1300× *g* for 5 min to obtain the supernatant. Subsequently, it was re-centrifuged at 4 °C and 13,000× *g* for 10 min to obtain the pellets. Next, the pellet was treated with MI buffer containing 0.1% digitonin and incubated on ice for 5 min. After that, MI buffer containing 1 mM EGTA was added to the reactant and centrifuged at 4 °C and 13,000× *g* for 15 min. The obtained pellet was re-centrifuged at 4 °C and 10,000× *g* for 10 min after adding the MI buffer. Finally, the collected pellet was mixed with MI buffer to obtain the samples for analysis.

2.7.2. ROS Levels

To measure mitochondrial ROS levels, mitochondrial extracts from the lung tissues were mixed with a DCFH-DA solution dissolved in respiration buffer (500 μM EGTA,

1 mM $MgCl_2$, 2 mM KH_2PO_4, 2.5 mM malate, 5 mM pyruvate, 20 mM HEPES, and 125 mM KCl). Fluorescence was measured at 485 nm (excitation wavelength) and 535 nm (emission wavelength) using a fluorometer (Infinite F200, TECAN).

2.7.3. Mitochondrial Membrane Potential

To evaluate mitochondrial membrane potential levels, mitochondrial extracts from lung tissues were mixed in 1,1′,3,3′-Tetraethyl-5,5′,6,6′-tetrachloroimidacarbocyanine iodide (JC-1) solution dissolved in assay buffer (5 mM pyruvate and 5 mM malate). Fluorescence was measured at 535 nm (excitation wavelength) and 590 nm (emission wavelength) using a fluorometer (Infinite F200, TECAN).

2.7.4. ATP Contents

The ATP kit (Promega Corporation, Madison, WI, USA) was used to measure the ATP contents in mitochondrial extracts from lung tissues according to the manufacturer's instructions. Luminescence was measured using a luminometer (Glomax®, Promega Corporation).

2.8. White Blood Cells (WBC) Differential Counting

After dissection, whole blood was obtained from the abdominal vena cava and placed in the ethylenediaminetetraacetic acid dipotassium salt dihydrate (K_2EDTA) tube. Then, WBC (neutrophils, lymphocytes, monocytes, eosinophils, and basophils) were analyzed using SYSMEX XN-V (Sysmex Corporation, Kobe, Japan).

2.9. Flow Cytometry

All materials used in flow cytometry were obtained from BD Bioscience (Franklin Lakes, NJ, USA) except for the PerCP-Cy5.5-conjugated CD8a and PE-conjugated IL-4, which were obtained from BioLegend (San Diego, CA, USA). Additionally, all washing processes were conducted at 4 °C and 126× *g* for 5 min.

After dissection, whole blood was immediately collected from the abdominal vena cava and placed in the heparin tube. The collected blood was stained with BV786-conjugated CD3e (#564379), PE-Cy7-conjugated CD4 (#552775), and PerCP-Cy5.5-conjugated CD8a (#100734) at 4 °C for 30 min. Next, the lysing solution (#349202) was added to lyse the red blood cells, followed by washing the pellet using the stain buffer (#554657). It was then fixed and permeabilized through the fixation/permeabilization solution kit (#554715) at 4 °C for 20 min. Following this, intracellular cytokines were incubated with PE-conjugated IL-4 (#504104) at 4 °C for 30 min, and then washed using the wash buffer provided in the fix/perm kit. Finally, the samples were suspended in the stain buffer and analyzed using the FACSLyric (BD Bioscience). Data were analyzed using FlowJo (version 10.10.0, BD Biosciences).

2.10. Enzyme-Linked Immunosorbent Assay (ELISA)

The serum was obtained by centrifuging whole blood collected in heparin tubes at 4 °C, 10,000× *g* for 15 min. The IgE level in the serum was determined using ELISA kit (Abcam, Cambridge, UK) according to the manufacturer's instructions. Absorbance was measured at 450 nm using a microplate reader (Epoch 2, BioTek Instruments Inc.).

2.11. Hematoxylin-Eosin (H&E) Staining

To observe the morphological changes, the left lungs of mice were fixed in 10% formalin. After dehydration, the lung tissues were embedded in paraffin and cut into sagittal sections (4 μm). The H&E-stained slides were scanned with a Motic EasyScan Pro 6 (Motic, Hong Kong, China), and the alveolar space was analyzed using ImageJ (version 1.54d, National Institutes of Health, Bethesda, MD, USA).

2.12. Western Blot

The lung tissues obtained from the mice were homogenized with ProtinEx™ Animal cell/tissue (GeneAll Biotechnology, Seoul, Republic of Korea) containing 1% protease inhibitor Cocktail kit tissue 2 perfect (Quartett, Berlin, Germany) and centrifuged at 4 °C and 15,928× *g* for 10 min. The obtained supernatants were used in a Bradford assay (Bio-Rad, Hercules, CA, USA) and mixed with 4X sample buffer (Bio-Rad). Using sodium dodecylsulfate polyacrylamide gel electrophoresis, proteins were separated, then transferred onto a polyvinylidene difluoride membrane (Millipore, Burlington, MA, USA). The membrane was treated with 5% skimmed milk at room temperature for 1 h and then incubated with the primary antibody (1:1000) at 4 °C for 12 h. Following three washes, the membrane was incubated with a secondary antibody (1:3000) at room temperature for 1 h. In the final step, the proteins were detected using an ECL ottimo (Translab, Daejeon, Republic of Korea) and iBright CL1500 (Thermo Fisher Scientific, Walthman, MA, USA). The band density was quantified using ImageJ (version 1.54d, National Institutes of Health). The information on the primary and secondary antibodies used is summarized in Table 1.

Table 1. Details of primary and secondary antibodies utilized in this study.

Antibody	Catalog No.	Manufacturer
Anti-mouse IgG	AP124P	Millipore (Billerica)
Anti-rabbit IgG	#7074	Cell Signaling Tech (Danvers, MA, USA)
β-actin	sc-69879	Santa Cruz Biotech (Dallas, TX, USA)
B-cell leukemia/lymphoma 2 (BCl-2)	sc-7382	Santa Cruz Biotech (Dallas)
BCl-2 associated X (BAX)	sc-7480	Santa Cruz Biotech (Dallas)
caspase-3	sc-56053	Santa Cruz Biotech (Dallas)
Interleukin 1β (IL-1β)	sc-515598	Santa Cruz Biotech (Dallas)
IL-33	sc-517600	Santa Cruz Biotech (Dallas)
Matrix metalloproteinase (MMP) -2	sc-13595	Santa Cruz Biotech (Dallas)
MMP-9	sc-13520	Santa Cruz Biotech (Dallas)
Myeloid differentiation primary response 88 (MyD88)	sc-74532	Santa Cruz Biotech (Dallas)
Phospho-c-Jun N-terminal kinases (p-JNK)	sc-6254	Santa Cruz Biotech (Dallas)
p-NF-κB inhibitor α (p-IκB-α)	sc-8404	Santa Cruz Biotech (Dallas)
p-NF-κB	sc-136548	Santa Cruz Biotech (Dallas)
p-Smad2	#3108	Cell Signaling Tech (Danvers)
p-Smad3	sc-517575	Santa Cruz Biotech (Dallas)
TGF-β1	sc-130348	Santa Cruz Biotech (Dallas)
Tumor necrosis factor α (TNF-α)	sc-33639	Santa Cruz Biotech (Dallas)

2.13. Statistics Analysis

All data were shown as mean ± standard deviation. Statistical comparison was performed with one-way analysis of variance (ANOVA). Duncan's multiple range test was used for multiple group comparisons, and Student's *t*-test was used for single comparisons.

3. Results

3.1. Identification of Bioactive Compounds

The results of identifying the bioactive compounds of DBZO through UPLC-Q-TOF/MS are as follows: catechin (retention time (RT), 3.40 min; adduct ion, 291; fragments; 139 and 273), astragalin (kaempferol-3-glucoside) (RT, 3.99 min; adduct ion, 449; fragments; 257, 269, and 287), 6-gingerol (RT, 5.88 min; adduct ion, 317; fragments, 115, 117, and 145), 8-gingerol (RT, 6.66 min; adduct ion, 345; fragments, 115 and 145), and 6-shogaol (RT, 6.82 min; adduct ion, 277; fragments, 94, 122, 137, and 177) (Figure 1 and Table 2) [34–36].

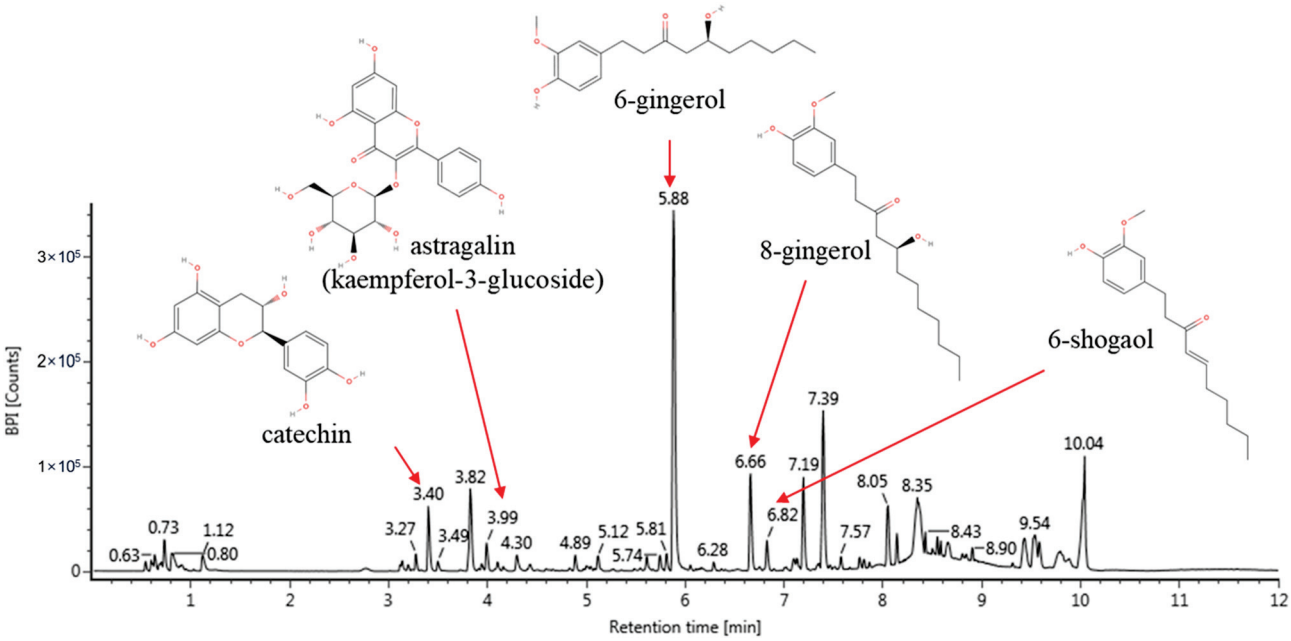

Figure 1. Ultra-performance liquid chromatography quadrupole time-of-flight mass spectrometry (UPLC-Q-TOF/MS) chromatogram of a combined extract from *Dioscorea bulbifera* and *Zingiber officinale* (DBZO).

Table 2. Physiological compounds identified in DBZO using UPLC-Q-TOF/MS analysis.

No.	Retention Time	Proposed Compound	(+) ESI-MS (*m*/*z*)	Fragments (*m*/*z*)
1	3.40	catechin	291	139, 273
2	3.99	astragalin (kaempferol-3-glucoside)	449	257, 269, 287
3	5.88	6-gingerol	317	115, 117, 145
4	6.66	8-gingerol	345	115, 145
5	6.82	6-shogaol	277	94, 122, 137, 177

3.2. Cytoprotective Effects of DBZO Against $PM_{2.5}$-Induced A549 and RPMI 2650 Cells

3.2.1. Cell Viability

The $PM_{2.5}$ treatment reduced cell viability to 61.11% in A549 cells compared to the control (100%). However, the treatment with vitamin C positive control showed an increase in cell viability to 77.38%. Similarly, the treatment with DBZO showed an increase in cell viability, with 61.66% at 10 μg/mL, 68.80% at 20 μg/mL, 74.69% at 50 μg/mL, 83.28% at 100 μg/mL, and 92.61% at 200 μg/mL (Figure 2a).

The $PM_{2.5}$ treatment reduced cell viability to 56.98% in RPMI 2650 cells compared to the control (100%). However, the treatment with vitamin C positive control showed an increase in cell viability to 76.61%. Similarly, the treatment with DBZO showed an increase in cell viability, with 73.25% at 10 μg/mL, 76.77% at 20 μg/mL, 83.93% at 50 μg/mL, 91.90% at 100 μg/mL, and 94.44% at 200 μg/mL (Figure 2b).

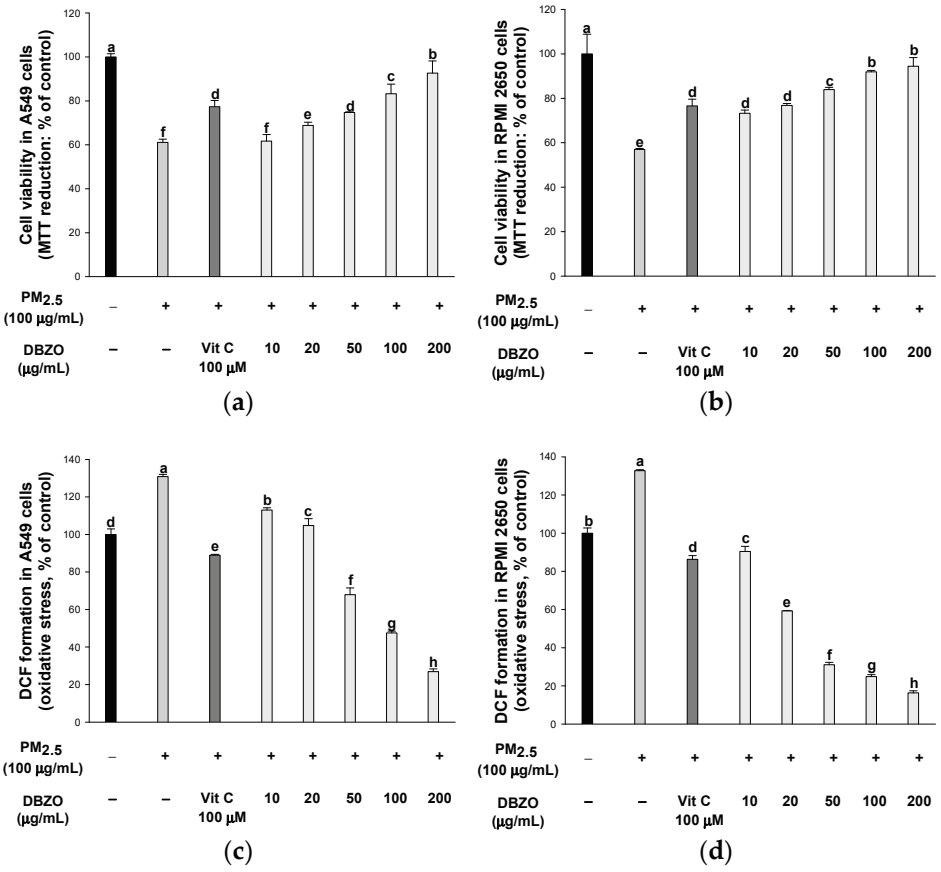

Figure 2. Effects of DBZO of particulate matter ($PM_{2.5}$)-stimulated A549 and RPMI 2650 cells. Cell viability in (**a**) A549 and (**b**) RPMI 2650 cells and intracellular oxidative stress levels in (**c**) A549 and (**d**) RPMI 2650 cells. The results are presented as mean ± SD ($n = 3$). Data were statistically considered at $p < 0.05$, and different small letters represent the statistical differences.

3.2.2. Intracellular Oxidative Stress

The $PM_{2.5}$ treatment increased ROS production to 130.87% in A549 cells compared to the control (100%). However, the treatment with vitamin C positive control reduced ROS production to 88.92%. Similarly, the treatment with DBZO reduced ROS production, with 113.02% at 10 μg/mL, 104.70% at 20 μg/mL, 67.93% at 50 μg/mL, 47.57% at 100 μg/mL, and 26.93% at 200 μg/mL (Figure 2c).

The $PM_{2.5}$ treatment increased ROS production to 132.70% in RPMI 2650 cells compared to the control (100%). However, the treatment with vitamin C positive control reduced ROS production to 86.32%. Similarly, the treatment with DBZO reduced ROS production, with 90.38% at 10 μg/mL, 59.36% at 20 μg/mL, 31.12% at 50 μg/mL, 24.90% at 100 μg/mL, and 16.32% at 200 μg/mL (Figure 2d).

3.3. Effects of DBZO Against $PM_{2.5}$-Induced Antioxidant System Dysfunction

3.3.1. MDA Contents

The $PM_{2.5}$ group (3.01 nmol/mg of protein) showed an increase in MDA contents compared to the NC group (2.48 nmol/mg of protein). However, the DBZO100 group (2.43 nmol/mg of protein) demonstrated a significant reduction in MDA contents compared to the $PM_{2.5}$ group (Figure 3a).

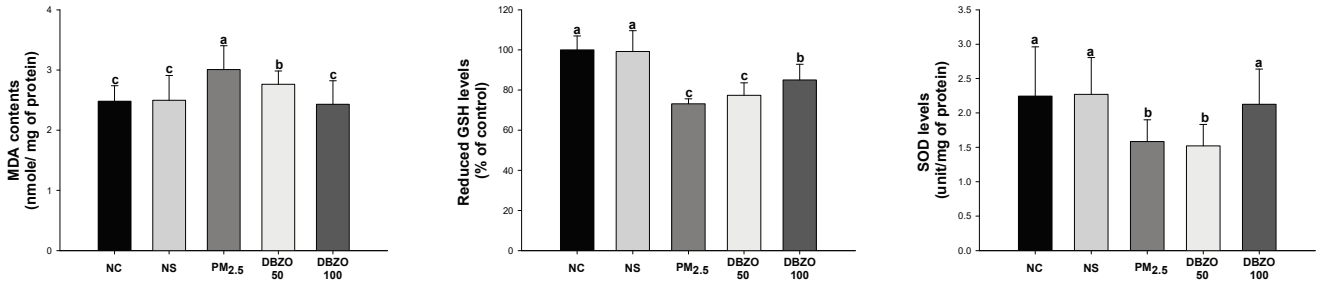

Figure 3. Effects of DBZO on antioxidant system in the lung tissues of $PM_{2.5}$-exposed BALB/c mice. (**a**) Malondialdehyde (MDA) contents, (**b**) reduced glutathione (GSH) levels, and (**c**) superoxide dismutase (SOD) levels. The results are presented as mean ± SD (n = 5). Data were statistically considered at $p < 0.05$, and different small letters represent the statistical differences.

3.3.2. Reduced GSH Levels

The $PM_{2.5}$ group (73.13%) showed a decrease in reduced GSH levels compared to the NC group (100.00%). However, the DBZO100 group (85.02%) exhibited a significant increase in reduced GSH levels compared to the $PM_{2.5}$ group (Figure 3b).

3.3.3. SOD Levels

The $PM_{2.5}$ group (1.59 unit/mg of protein) showed a reduction in SOD levels compared to the NC group (2.25 unit/mg of protein). However, the DBZO100 group (2.13 unit/mg of protein) showed a significant increase in SOD levels compared to the $PM_{2.5}$ group (Figure 3c).

3.4. Effects of DBZO Against $PM_{2.5}$-Induced Mitochondrial Dysfunction

3.4.1. ROS Levels

The $PM_{2.5}$ group (156.20%, $p = 0.031$) showed an increase in ROS levels compared to the NC group (100.00%). However, the DBZO100 group (96.23%, $p = 0.001$) demonstrated a reduction in ROS levels compared to the $PM_{2.5}$ group (Figure 4a).

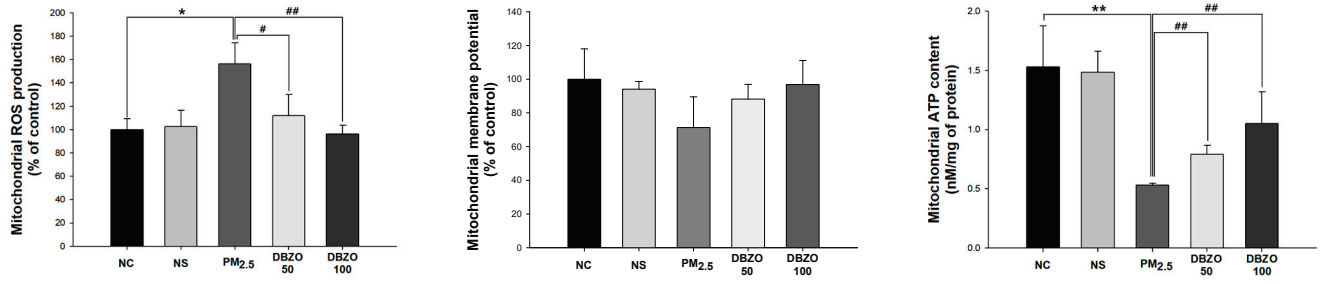

Figure 4. Effects of DBZO on mitochondrial function in lung tissues of $PM_{2.5}$-exposed BALB/c mice. (**a**) Mitochondrial reactive oxygen species (ROS) production, (**b**) mitochondrial membrane potential, and (**c**) mitochondrial ATP content. The results are presented as mean ± SD (n = 4). Data are statistically represented with * = significantly different from the NC group, and # = significantly different from the $PM_{2.5}$ group; * and # = $p < 0.05$ and ** and ## = $p < 0.01$.

3.4.2. Mitochondrial Membrane Potential

The $PM_{2.5}$ group (71.31%, $p = 0.066$) showed a reduction in mitochondrial membrane potential compared to the NC group (100.00%). However, the DBZO100 group (96.83%, $p = 0.069$) showed an increase in mitochondrial membrane potential compared to the $PM_{2.5}$ group. However, there was no significant difference between the groups (Figure 4b).

3.4.3. ATP Content

The $PM_{2.5}$ group (0.53 nM/mg of protein, $p = 0.001$) showed a decrease in ATP content compared to the NC group (1.53 nM/mg of protein). However, the DBZO100 group (1.05 nM/mg of protein, $p = 0.008$) exhibited an increase in ATP content compared to the $PM_{2.5}$ group (Figure 4c).

3.5. Effects of DBZO Against $PM_{2.5}$-Induced Hematological and Biochemical Changes

3.5.1. WBC Differential Counting

The $PM_{2.5}$ group (4.0460 k/μL) showed an increase in total WBC count compared to the NC group (1.6380 k/μL). However, the DBZO100 group (2.8740 k/μL) demonstrated a significant reduction in total WBC count compared to the $PM_{2.5}$ group.

Furthermore, the $PM_{2.5}$ group exhibited elevated levels of neutrophils (0.9327 k/μL), lymphocytes (2.8743 k/μL), and eosinophils (0.1955 k/μL) compared to the NC group (0.3464 k/μL, 1.2477 k/μL, and 0.0078 k/μL, respectively). However, the DBZO100 group (0.5902 k/μL, 2.2140 k/μL, and 0.0258 k/μL, respectively) significantly reduced these levels compared to the $PM_{2.5}$ group. Whereas monocytes and basophil counts showed no significant differences among the NC (0.0298 k/μL and 0.0062 k/μL), $PM_{2.5}$ (0.0396 k/μL and 0.0040 k/μL), and DBZO100 groups (0.0402 k/μL and 0.0037 k/μL) (Table 3).

Table 3. Effects of DBZO on whole blood immune cell number in the blood of $PM_{2.5}$-exposed BALB/c mice.

	Unit: k/μL		
	NC	**$PM_{2.5}$**	**DBZO100**
Total cells	1.6380 ± 0.6489^{c}	4.0460 ± 0.7922^{a}	2.8740 ± 1.0270^{b}
Neutrophils	0.3464 ± 0.1538^{c}	0.9327 ± 0.2122^{a}	0.5902 ± 0.2009^{b}
Lymphocytes	1.2477 ± 0.5594^{c}	2.8743 ± 0.6679^{a}	2.2140 ± 0.8076^{b}
Monocytes	0.0298 ± 0.0158^{a}	0.0396 ± 0.0166^{a}	0.0402 ± 0.0242^{a}
Eosinophils	0.0078 ± 0.0129^{b}	0.1955 ± 0.1562^{a}	0.0258 ± 0.0093^{b}
Basophils	0.0062 ± 0.0057^{a}	0.0040 ± 0.0055^{a}	0.0037 ± 0.0051^{a}

The results are presented as mean ± SD ($n = 5$). Data were statistically considered at $p < 0.05$, and different small letters represent the statistical differences.

3.5.2. Flow Cytometry

The $PM_{2.5}$ group showed increased levels of T cells, including T helper cells (25.52% of T cells), T cytotoxic cells (8.16% of T cells), and T helper 2 cells (1.50% of T helper cells), compared to the NC group (22.4%, 6.15%, and 1.03% of T cells, respectively). In contrast, the DBZO100 group (25.14%, 6.95%, and 0.91% of T cells, respectively) significantly downregulated these T cell levels compared to the $PM_{2.5}$ group (Figure 5a–d).

3.5.3. IgE Analysis Using ELISA

The $PM_{2.5}$ group (6.49 mg/mL) showed an increased IgE levels in serum compared to the NC group (2.99 mg/mL). In contrast, the DBZO100 group (2.12 mg/mL) demonstrated a significantly reduced IgE levels in serum compared to the $PM_{2.5}$ group (Figure 5e).

3.6. Effects of DBZO Against $PM_{2.5}$-Induced Histopathological Changes

A pathological examination of the lung tissue revealed that the NC group exhibited a normal lung architecture with no pathological changes observed (Figure 6a). In contrast, the $PM_{2.5}$ group demonstrated marked histopathological alterations, including alveolar septal thickening due to inflammation and fibrosis, resulting in the collapse of normal alveolar spaces. The DBZO100 group, however, exhibited reduced alveolar septal thickening compared to the $PM_{2.5}$ group, maintaining an alveolar structure similar to that of the NC group. In this regard, quantification of lung structural damage by alveolar area measurements showed that the alveolar area in the $PM_{2.5}$ group (43.35%) increased compared to the NC group (71.96%),

whereas a significant reduction in the alveolar area was observed in the DBZO100 group (62.03%), suggesting a protective effect of DBZO on lung tissue (Figure 6b).

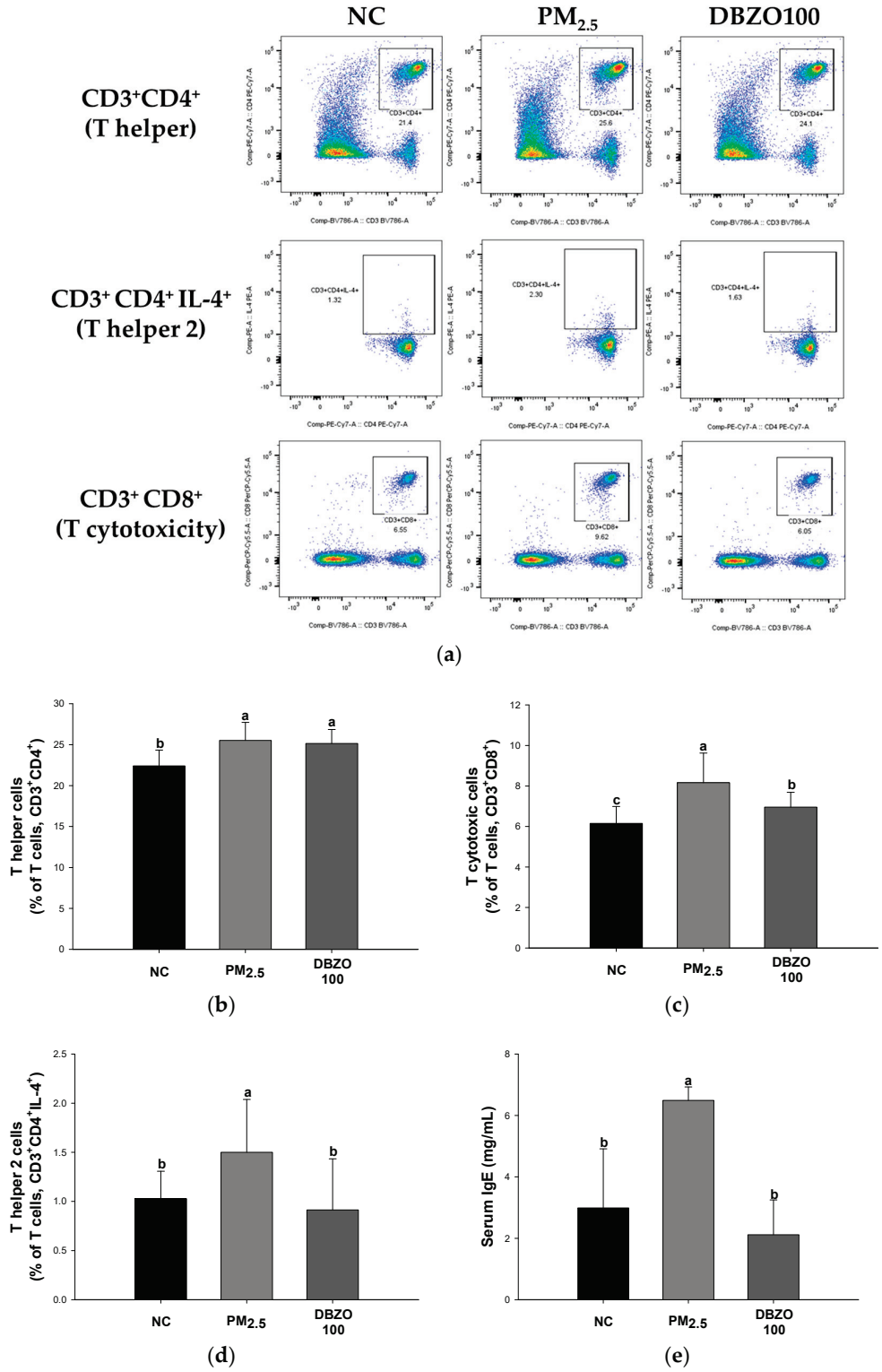

Figure 5. Effects of DBZO on inflammatory cells in whole blood and immunoglobulin E (IgE) levels in serum of $PM_{2.5}$-exposed BALB/c mice. (**a**) Flow cytometry plots, frequency of (**b**) $CD3^+CD4^+$ T cells, (**c**) $CD3^+CD8^+$ T cells, (**d**) $CD3^+CD4^+IL\text{-}4^+$ T cells in whole blood, and (**e**) IgE levels in serum. The results are presented as mean ± SD (**b**–**d**, $n = 5$; e, $n = 3$). Data were statistically considered at $p < 0.05$, and different small letters represent the statistical differences.

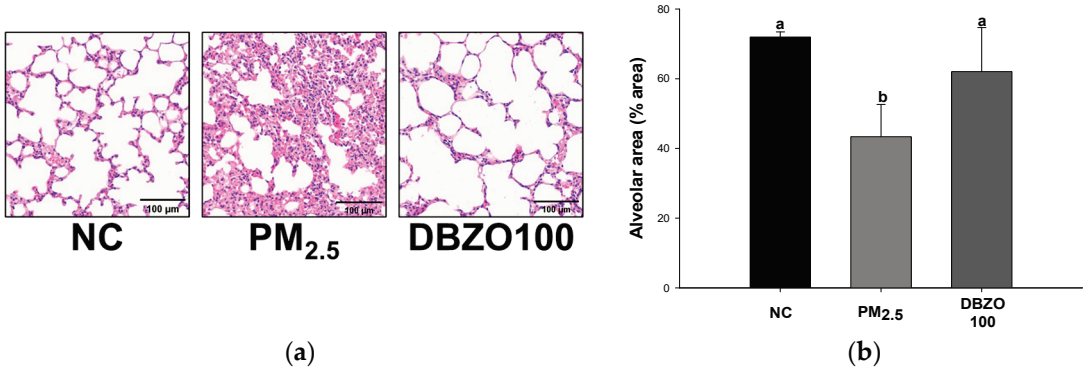

Figure 6. Effects of DBZO on alveolar size in lung tissues of $PM_{2.5}$-exposed BALB/c mice. (**a**) Histopathological sections and (**b**) alveolar area. The results are presented as mean ± SD (n = 3). Data were statistically considered at $p < 0.05$, and different small letters represent the statistical differences.

3.7. Effect of DBZO Against $PM_{2.5}$-Induced Pulmonary Inflammation-Related Factors

The $PM_{2.5}$ group showed a significant upregulation in the expression levels of IL-33 (1.39), MyD88 (1.92), p-IκB-α (1.19), p-NF-κB (1.71), IL-1β (1.64), and TNF-α (1.36) compared to the NC group (1.00). In contrast, the DBZO100 group demonstrated a significant downregulation in the expression levels of IL-33 (1.12), MyD88 (1.38), p-IκB-α (1.10), p-NF-κB (1.16), IL-1β (0.97), and TNF-α (0.83) compared to the $PM_{2.5}$ group (Figure 7).

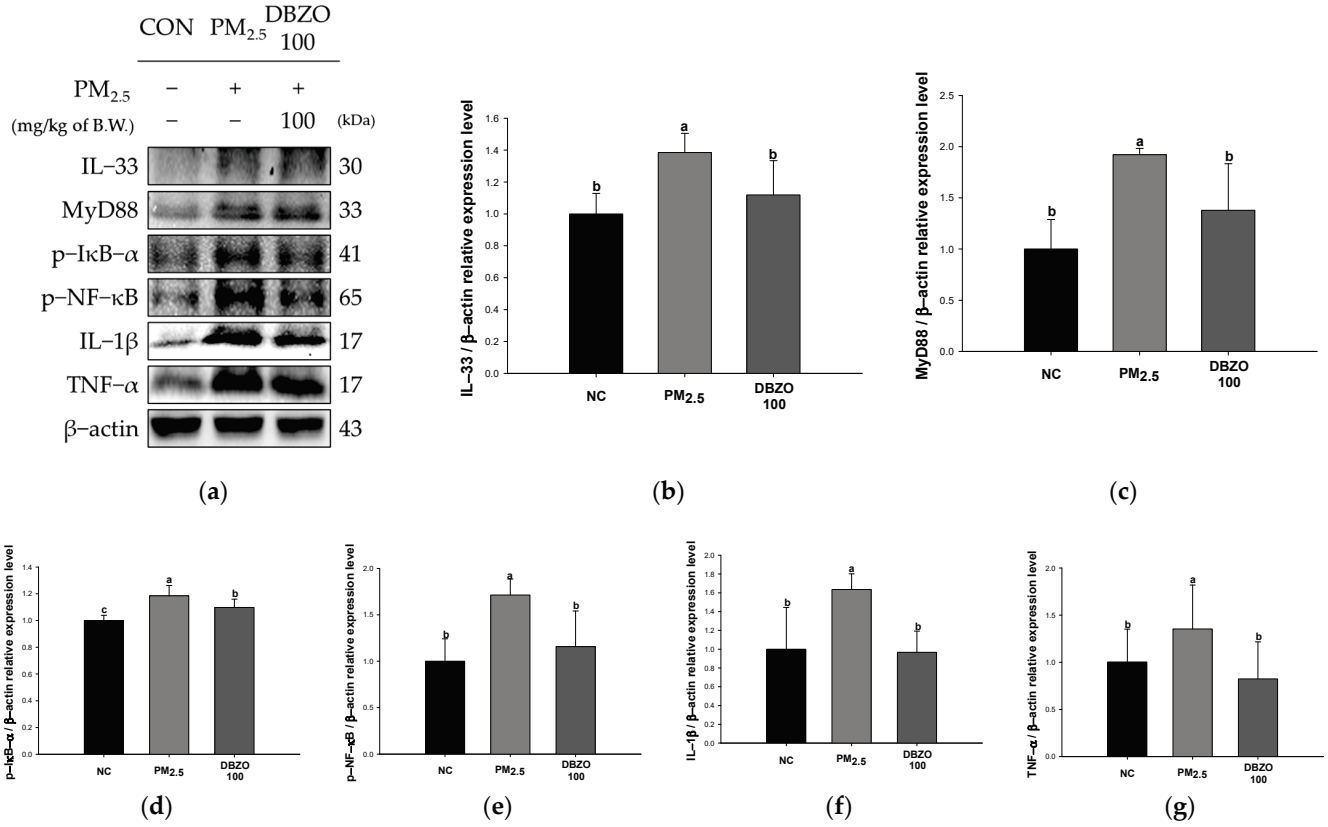

Figure 7. Effects of DBZO on inflammation-related protein expression levels in lung tissues of $PM_{2.5}$-exposed BALB/c mice. (**a**) Western blot images, protein expression levels of (**b**) IL-33, (**c**) MyD88, (**d**) p-IκB-α, (**e**) p-NF-κB, (**f**) IL-1β, and (**g**) TNF-α. The results are presented as mean ± SD (n = 3). Data were statistically considered at $p < 0.05$, and different small letters represent the statistical differences.

3.8. Effect of DBZO Against $PM_{2.5}$-Induced Pulmonary Apoptosis-Related Factors

The $PM_{2.5}$ group showed a significant downregulation in the expression level of BCl-2 (0.67) and a significant upregulation in the expression levels of p-JNK (1.60), BAX (1.38), BAX/BCl-2 ratio (2.34), and caspase-3 (1.83) compared to the NC group (1.00). In contrast, the DBZO100 group demonstrated a significant regulation of expression levels for p-JNK (1.46), BCl-2 (0.94), BAX (1.02), BAX/BCl-2 ratio (1.52), and caspase-3 (1.56) compared to the $PM_{2.5}$ group (Figure 8).

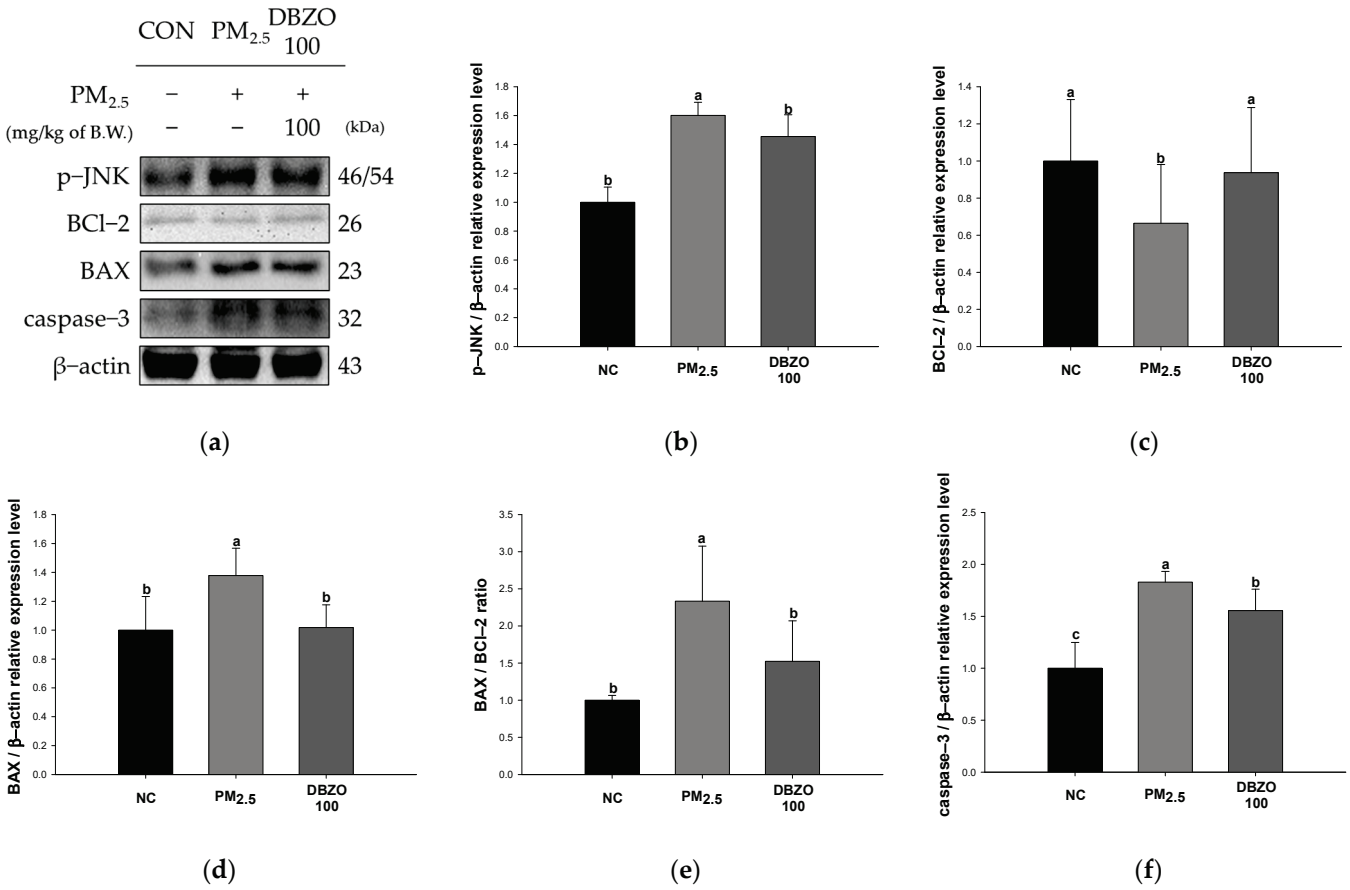

Figure 8. Effects of DBZO on apoptosis-related protein expression levels in lung tissues of $PM_{2.5}$-exposed BALB/c mice. (**a**) Western blot images, protein expression levels of (**b**) p-JNK, (**c**) BCl-2, (**d**) BAX, (**e**) BAX/BCl-2 ratio, and (**f**) caspase-3. The results are presented as mean ± SD (n = 3). Data were statistically considered at $p < 0.05$, and different small letters represent the statistical differences.

3.9. Effect of DBZO Against $PM_{2.5}$-Induced Pulmonary Fibrosis-Related Factors

The $PM_{2.5}$ group showed a significant upregulation in the expression levels of TGF-β1 (1.18), p-Smad2 (1.46), p-Smad3 (1.36), MMP-2 (1.47), and MMP-9 (1.36) compared to the NC group (1.00). In contrast, the DBZO100 group demonstrated a significant downregulation in the expression levels of TGF-β1 (0.93), p-Smad2 (1.17), p-Smad3 (1.13), MMP-2 (1.27), and MMP-9 (1.26) compared to the $PM_{2.5}$ group (Figure 9).

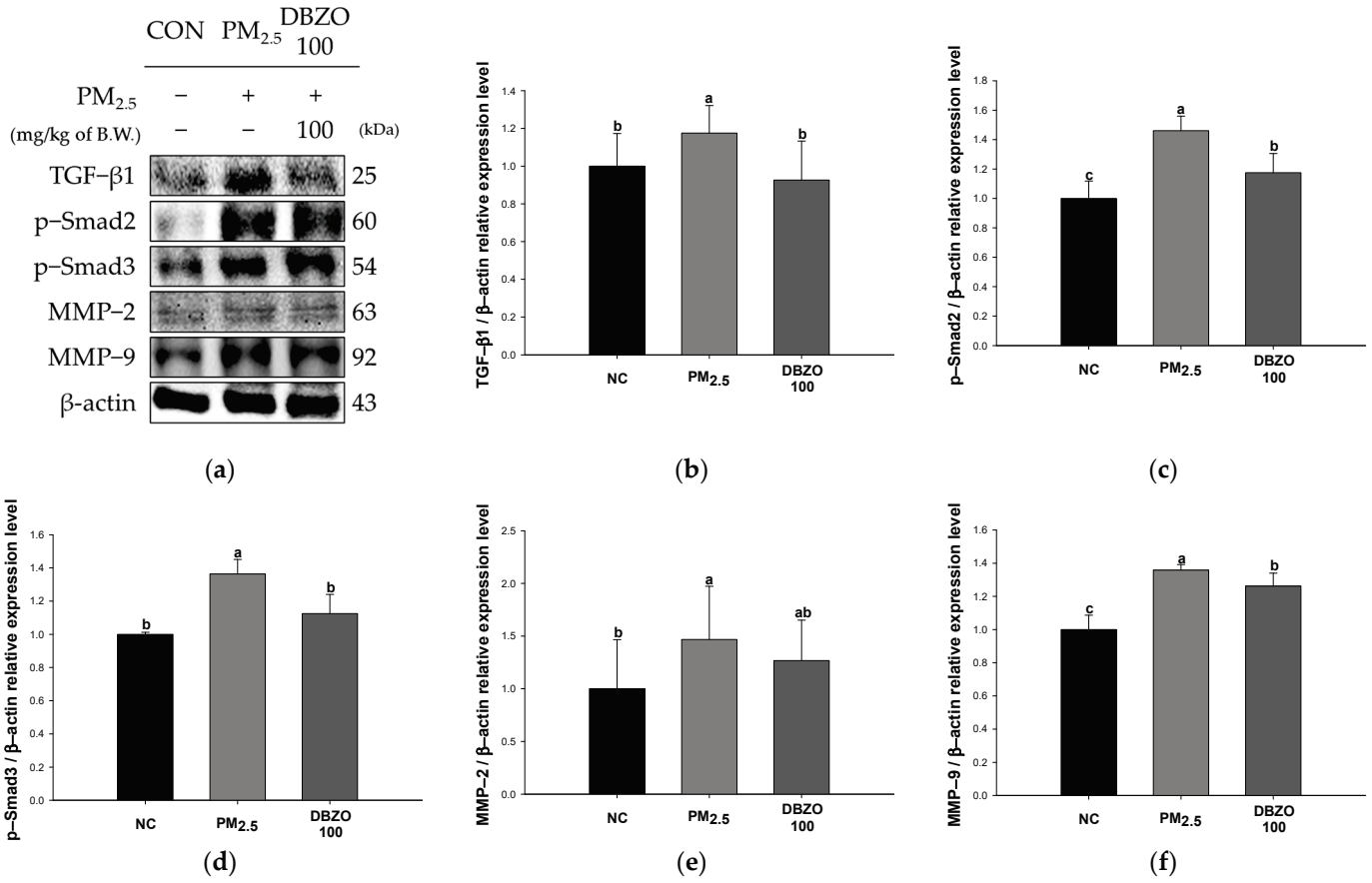

Figure 9. Effects of DBZO on pulmonary fibrosis-related protein expression levels in lung tissues of $PM_{2.5}$-exposed BALB/c mice. (**a**) Western blot images, protein expression levels of (**b**) TGF-β1, (**c**) p-Smad2, (**d**) p-Samd3, (**e**) MMP-2, and (**f**) MMP-9. The results are presented as mean ± SD ($n = 3$). Data were statistically considered at $p < 0.05$, and different small letters represent the statistical differences.

4. Discussion

Air pollution has emerged as a global public health issue, leading to a growing emphasis on research into chronic respiratory diseases [37]. The pathogenesis of these diseases involves a complex interplay of factors such as oxidative stress, mitochondrial dysfunction, and inflammation [3]. Therefore, natural products are being highlighted as therapeutic strategies due to their pharmacological effects, which arise from acting on various targets and simultaneously modulating multiple signaling pathways [38]. In this context, this study examined the protective role of DBZO in mitigating respiratory system damage caused by $PM_{2.5}$ exposure.

D. bulbifera and *Z. officinale* are known for their various biological properties and have a long history of use in traditional medicine [17,18]. To further explore their potential, the present study analyzed DBZO, a combined extract of these two substances, using UPLC-Q-TOF/MS, which led to the identification of five phytochemicals: catechin, astragalin (kaempferol-3-glucoside), 6-gingerol, 8-gingerol, and 6-shogaol (Figure 1 and Table 2) [34–36]. Catechin is a representative bioactive compound reported in *D. bulbifera* [17]. Similarly, 6-gingerol, 8-gingerol, and 6-shogaol are representative bioactive compounds reported in *Z. officinale* [36]. However, astragalin identified through UPLC-Q-TOF/MS in this study has not been previously reported in the root extracts of *D. bulbifera* and *Z. officinale*. Nevertheless, *D. bulbifera* has been reported to contain kaempferol and its glycosides [17]. In this regard, *D. bulbifera* was extracted under the same conditions as DBZO and analyzed using UPLC-Q-TOF/MS, resulting in the confirmation of astragalin

(Figure S3). Catechins and astragalin share a flavonoid backbone and have been reported to possess numerous biological activities, including antioxidant, anti-inflammatory, and anti-diabetic effects [39]. In particular, astragalin has been reported to exhibit protective effects against respiratory diseases such as asthma, COPD, and acute lung injury (ALI) by modulating various signaling pathways, including the nuclear factor erythroid 2-related factor 2 (Nrf2)/heme oxygenase-1 (HO-1), NF-κB, and mitogen-activated protein kinase (MAPK) pathways, thereby suppressing inflammation and oxidative stress [40]. Additionally, gingerol and shogaol, recognized components in *Z. officinale*, exhibit antioxidant and anti-inflammatory properties attributed to their structural features, including alkyl chains and double bonds, and confer various health benefits such as enhanced respiratory health, improved digestion, strengthened immune function, and promoted cardiovascular health [41]. Similarly, secondary metabolites in plants, such as flavonoids, phenolic acids, and fatty acids, are widely found in natural products and have been reported to confer various health advantages by effectively scavenging ROS through their unique structural properties [16,22,39]. Therefore, to assess the protective effects of DBZO on the respiratory system, an in vitro study was conducted using A549 (lung epithelial cells) and RPMI 2650 (nasal epithelial cells) to confirm its protective effects (Figure 2). The epithelial cells in the respiratory system serve as the primary defense against external damage, and this impairment is therefore regarded as a critical factor determining disease severity [42]. In this context, DBZO suggests a positive influence on respiratory health by preventing damage to the respiratory epithelial cells caused by exposure to PM. Therefore, an in vivo study was subsequently conducted using a mouse model chronically exposed to $PM_{2.5}$ to further assess the protective effects of DBZO on the respiratory system.

Oxidative stress is regarded as a primary contributor to the initiation and progression of respiratory diseases [43]. It arises from an imbalance between a diminished antioxidant defense system and increased ROS production in the body [9]. SOD is an initial response element in the antioxidant defense system in the body that catalyzes the reaction that converts $O_2^{\cdot -}$ into H_2O_2, thereby preventing damage to essential biological structures such as DNA, proteins, and cell membranes, and protecting cells from oxidative stress [44]. Meanwhile, GSH is known for its powerful antioxidant properties in removing oxidative stress-causing substances such as $OH\cdot$ and O_2, as well as aiding in the elimination of hydrogen peroxide [9]. However, $PM_{2.5}$ contains various metal compounds such as heavy metals, carbonaceous materials, and PAHs, which are reported to trigger oxidative stress by increasing the production of ROS and compromising the innate antioxidant system in the respiratory system [6]. Consequently, this increases in oxidative stress levels in the body induces protein and lipid peroxidation, leading to elevated levels of MDA, a biomarker for chronic respiratory diseases such as COPD and asthma [45]. In this regard, catechin, a principal bioactive compound of DBZO, has been reported to mediate both a direct antioxidant mechanism by scavenging reactive radicals and an indirect antioxidant effect by inducing antioxidant enzymes such as catalase, SOD, and reduced GSH, or by inhibiting proteins that promote oxidation such as cyclooxygenase and inducible nitric oxide synthase [46]. In addition, another bioactive compound of DBZO, 6-gingerol, has been shown to regulate the levels of GSH, SOD, and MDA in mice exposed to oxidative stress caused by chlorpyrifos [47]. Consistent with these findings, lung tissue from the group treated with DBZO in this study showed modulated levels of GSH, SOD, and MDA compared to the $PM_{2.5}$ group, indicating a recovery from PM-induced oxidative stress (Figure 3). These results indicate that DBZO could help safeguard the respiratory system from oxidative stress caused by PM exposure.

Mitochondria, the primary site of ROS production, are significantly more susceptible to oxidative stress than other cellular components, and their damage is reported to induce various physiological and pathological processes, including respiratory diseases [9,48]. Generally, the mitochondrial respiratory chain maintains a balance between ROS production and elimination, but $PM_{2.5}$ disrupts this equilibrium, resulting in excessive ROS generation [49]. It can damage mitochondrial structural proteins and membrane poten-

tial, ultimately impairing energy metabolism and causing cellular damage [48]. Santos et al. reported that catechins regulate the function of Complex I of the respiratory chain, thereby modulating ATP synthesis capacity in MRC-5 fibroblasts with amiodarone-induced mitochondrial dysfunction [50]. Similarly, Han et al. noted that 6-gingerol exhibits cardioprotective effects by improving mitochondrial membrane damage and edema in a mouse model of cardiac toxicity induced by As_2O_3 [51]. Likewise, in this study, the lung tissue of the group administrated with DBZO exhibited regulated levels of ROS, mitochondrial membrane proteins, and ATP compared to the $PM_{2.5}$ group (Figure 4). Additionally, the increased ROS resulting from oxidative stress and mitochondrial damage can activate the JNK pathway and further exacerbate oxidative stress [43]. JNK plays a crucial role in apoptosis by modulating BCl-2 family proteins, inhibiting BCl-2, an anti-apoptotic protein, while promoting the activation of BAX, a pro-apoptotic protein on the mitochondrial outer membrane, which subsequently increases membrane permeability [52]. Ultimately, this cascade of events leads to apoptosis by activating caspase-3 [53]. Cho et al. noted that astragalin inhibited the expression of p-JNK protein in BEAS-2B cells stimulated to H_2O_2 and concentration-dependently suppressed caspase-3 activity in BEAS-2B cells stimulated to lipopolysaccharide [53]. Furthermore, Han et al. reported that pretreatment of 6-shogaol reduced BAX and caspase-3 in ultraviolet A-stimulated human dermal fibroblast cells in a dose-dependent manner [54]. Similarly, in the lungs of the DBZO-administered group in this study, the expression of apoptosis-related proteins was improved compared to the $PM_{2.5}$ group (Figure 8). These findings indicate that DBZO, which contains various bioactive compounds, may protect the respiratory system from $PM_{2.5}$ exposure by protecting mitochondrial function and regulating the expression of apoptosis-related proteins.

Furthermore, increased ROS production leads to a complex inflammatory response, including the release of inflammatory cytokines and the infiltration of inflammatory cells, thereby accelerating the pathogenesis of respiratory diseases [11,42]. Specifically, excessive ROS production and a depleted antioxidant system induced by $PM_{2.5}$ result in oxidative stress, which mediates the release of IL-33 from pulmonary epithelial cells [42,55]. The released IL-33 activates various immune cells, including neutrophils, eosinophils, basophils, and T cells, a process reported to drive the pathology of pulmonary diseases, including COPD, IPF, and asthma [56]. The activated inflammatory cells then infiltrate lung tissue through chemotaxis and secrete various cytokines and chemokines that amplify the inflammatory response [11]. Moreover, activated T cells stimulate B cells to promote the secretion of immunoglobulins such as IgE, thus sustaining the inflammatory response [57]. 6-Gingerol has been observed to exhibit anti-inflammatory and antioxidant effects by reducing neutrophil accumulation and regulating the NF-κB pathway in a ventilator-induced lung injury mouse model [58]. Astragalin has been reported to significantly reduce the numbers of eosinophils, neutrophils, basophils, and macrophages in the bronchoalveolar lavage fluid of ovalbumin (OVA)-induced mice and to suppress IgE elevation in the NC/Nga mouse model [59,60]. Similarly, this analysis demonstrated that the counts of inflammatory cells and levels of IgE in both blood and serum were altered in the DBZO group in comparison to the $PM_{2.5}$ group (Figure 5 and Table 3). Additionally, released IL-33 is known to bind to its receptor and mediate downstream signaling through the MyD88 protein [56]. Activated MyD88 phosphorylates IκB proteins, facilitating the nuclear translocation of NF-κB, activating the transcription of pro-inflammatory cytokine genes, and leading to increased secretion of TNF-α and IL-1 [11,56]. The secretion of these cytokines induces the recruitment and activation of inflammatory cells, thereby sustaining and amplifying the inflammatory response and promoting the pathogenic process [61]. Catechin has been shown to inhibit thymic stromal lymphopoietin (TSLP), a protein with a role similar to IL-33, in human nasal epithelial cells (HNEpC), in turn suppressing the NF-κB pathway [62]. In addition, ginger extract rich in gingerol and shogaol has been reported to have shown the effect of improving clinical symptoms of the disease with the regulation of IL-33 expression in experimental autoimmune encephalomyelitis mouse models [63]. In this context, the lung tissue of the DBZO group in the present study showed

a significant attenuation of the NF-κB pathway induced by IL-33 compared to the $PM_{2.5}$ group (Figure 7). This suggests that DBZO may protect the respiratory system from $PM_{2.5}$ exposure by inhibiting inflammatory cell infiltration, immunoglobulin secretion, and the expression of inflammation-related proteins.

Chronic exposure to $PM_{2.5}$ induces persistent inflammation and promotes pulmonary fibrosis characterized by diffuse alveolar damage, epithelial cell phenotype changes, and fibroblast proliferation [6,64]. Notably, $PM_{2.5}$ increases the expression of TGF-β1 in lung tissue and induces the phosphorylation of Smad2/3, mediating the classical TGF-β/Smad pathway involved in fibrosis development [6,12]. It induces the activation of fibroblasts and myofibroblasts, leading to an increase in the secretion of extracellular matrix (ECM) components and promoting the progression of fibrosis [65]. Additionally, TGF-β1 regulates the expression of epithelial-to-mesenchymal transition (EMT)-related genes, including MMP-2 and MMP-9, which promote fibrosis [66]. MMP-2 and MMP-9, categorized as gelatinases, degrade various ECM molecules to activate the EMT process, with MMP-9 playing a pivotal role in promoting sustained tissue remodeling by inducing the re-expression of TGF-β1, thereby accelerating ECM accumulation and tissue stiffening, which drives fibrosis progression [66,67]. Wang et al. reported that green tea catechins effectively mitigate liver fibrosis in CCl_4-induced mice by inhibiting the expression of TGF-β, p-Smad2, MMP-2, and MMP-9 [68]. Similarly, Cho et al. reported that astragalin inhibits airway epithelial fibrosis in H_2O_2-exposed BEAS-2B cells and OVA-induced mice [60]. Similarly, Liu et al. reported that 6-gingerol, a functional component of *Z. officinale*, reduces the transcription of fibrosis-related factors such as α-SMA in lung fibroblasts treated with TGF-β1 and has shown effectiveness in reducing inflammation and fibrosis in a bleomycin-induced pulmonary fibrosis mouse model [69]. In this context, the present study revealed that the lung tissue of the DBZO group had a significantly reduced expression of fibrosis-related proteins compared to the $PM_{2.5}$ group (Figure 9). Additionally, histological observations were conducted to examine the impact of the anti-inflammatory and anti-fibrotic properties of DBZO on lung structure and found that DBZO effectively inhibited pulmonary dysfunction and fibrotic changes (Figure 6). In conclusion, these findings indicate that DBZO possesses anti-inflammatory and anti-fibrotic effects, suggesting its potential as a candidate for improving respiratory health.

5. Conclusions

This study indicates that DBZO significantly ameliorates $PM_{2.5}$-induced respiratory dysfunction by regulating oxidative stress and inflammation. DBZO suppressed the production of ROS triggered by $PM_{2.5}$ and mitigated oxidative stress by regulating the levels of antioxidant markers. DBZO has been shown to prevent mitochondrial dysfunction and regulate JNK pathway, thereby inhibiting apoptosis. Moreover, it has been demonstrated to alleviate levels of inflammatory cells and IgE and to reduce the inflammatory response by modulating the NF-κB pathway. Furthermore, DBZO contributed to the anti-fibrotic process in the respiratory system by regulating the TGF-β1/Smad pathway. These effects were confirmed by histopathological observation. The protective effect of DBZO against $PM_{2.5}$-induced respiratory damage is considered to be due to its bioactive compounds such as phytochemicals such as catechin, astragalin, 6-gingerol, 8-gingerol, and 6-shogaol. In conclusion, this study suggests that DBZO can be used as an ingredient in functional foods that improve oxidative stress and inflammation to prevent respiratory dysfunction.

Supplementary Materials: The following supporting information can be downloaded at: https://www.mdpi.com/article/10.3390/antiox13121572/s1, Figure S1: Effects of $PM_{2.5}$ exposure on cell viability in A549 cells. The cells were treated with $PM_{2.5}$ at concentrations of 0, 25, 50, 100, and 200 μg/mL for 4, 12, 24, and 48 h; Figure S2: Effects of $PM_{2.5}$ exposure on apoptosis-related protein expression level in A549 cells. Western blot image (A) and protein expression level of cleaved caspase-3 (B); Figure S3: 50% ethanol extract of *Dioscorea bulbifera* of UPLC-Q/TOF-MS chromatogram (A) and MS fragments chromatogram (B).

Author Contributions: Conceptualization, H.J.H.; methodology, H.L.L. and I.Y.K.; validation, H.L.L.; formal analysis, H.J.C.; investigation, I.Y.K., H.L.L., H.J.C., Y.H.J., Y.M.H. and H.R.N.; resources, W.M.J. and D.Y.L.; data curation, I.Y.K.; writing—original draft preparation, I.Y.K.; writing—review and editing, H.L.L. and H.J.H.; visualization, I.Y.K.; supervision, H.J.H.; project administration, H.J.H.; funding acquisition, H.J.H. All authors have read and agreed to the published version of the manuscript.

Funding: This research received no external funding.

Institutional Review Board Statement: The animal study protocol was approved by the Institutional Animal Care and Use Committee of Gyeongsang National University (protocol code GNU-240108-M0002 and date of approval 8 January 2024).

Informed Consent Statement: Not applicable.

Data Availability Statement: The data presented in this study are available on request from the corresponding author.

Acknowledgments: This study was carried out with the support of Gyeongnam Anti-Aging Research Institute.

Conflicts of Interest: The authors declare no conflicts of interest.

References

1. Darçın, M. Association between air quality and quality of life. *Environ. Sci. Pollut. Res.* **2014**, *21*, 1954–1959. [CrossRef] [PubMed]
2. Kim, K.H.; Kabir, E.; Kabir, S. A review on the human health impact of airborne particulate matter. *Environ. Int.* **2015**, *74*, 136–143. [CrossRef] [PubMed]
3. Kim, H.J.; Choi, M.G.; Park, M.K.; Seo, Y.R. Predictive and prognostic biomarkers of respiratory diseases due to particulate matter exposure. *J. Cancer Prev.* **2017**, *22*, 6–15. [CrossRef] [PubMed]
4. Kyung, S.Y.; Jeong, S.H. Particulate-matter related respiratory diseases. *Tuberc. Respir. Dis.* **2020**, *83*, 116–121. [CrossRef]
5. Flood-Garibay, J.A.; Angulo-Molina, A.; Méndez-Rojas, M.Á. Particulate matter and ultrafine particles in urban air pollution and their effect on the nervous system. *Environ. Sci. Processes. Impacts* **2023**, *25*, 704–726. [CrossRef]
6. Lim, E.Y.; Kim, G.-D. Particulate matter-induced emerging health effects associated with oxidative stress and inflammation. *Antioxidants* **2024**, *13*, 1256. [CrossRef]
7. Lelieveld, S.; Wilson, J.; Dovrou, E.; Mishra, A.; Lakey, P.S.J.; Shiraiwa, M.; Pöschl, U.; Berkemeier, T. Hydroxyl radical production by air pollutants in epithelial lining fluid governed by interconversion and scavenging of reactive oxygen species. *Environ. Sci. Technol.* **2021**, *55*, 14069–14079. [CrossRef]
8. Yu, Y.-Y.; Jin, H.; Lu, Q. Effect of polycyclic aromatic hydrocarbons on immunity. *J. Transl. Autoimmun.* **2022**, *5*, 100177. [CrossRef]
9. Afzal, S.; Abdul Manap, A.S.; Attiq, A.; Albokhadaim, I.; Kandeel, M.; Alhojaily, S.M. From imbalance to impairment: The central role of reactive oxygen species in oxidative stress-induced disorders and therapeutic exploration. *Front. Pharmacol.* **2023**, *14*, 1269581. [CrossRef]
10. Bezerra, F.S.; Lanzetti, M.; Nesi, R.T.; Nagato, A.C.; Silva, C.P.e.; Kennedy-Feitosa, E.; Melo, A.C.; Cattani-Cavalieri, I.; Porto, L.C.; Valenca, S.S. Oxidative stress and inflammation in acute and chronic lung injuries. *Antioxidants* **2023**, *12*, 548. [CrossRef]
11. Wu, W.; Jin, Y.; Carlsten, C. Inflammatory health effects of indoor and outdoor particulate matter. *J. Allergy Clin. Immunol.* **2018**, *141*, 833–844. [CrossRef] [PubMed]
12. Ghafouri-Fard, S.; Askari, A.; Shoorei, H.; Seify, M.; Koohestanidehaghi, Y.; Hussen, B.M.; Taheri, M.; Samsami, M. Antioxidant therapy against TGF-β/SMAD pathway involved in organ fibrosis. *J. Cell. Mol. Med.* **2024**, *28*, e18052. [CrossRef] [PubMed]
13. Victoni, T.; Barreto, E.; Lagente, V.; Carvalho, V.F. Oxidative imbalance as a crucial factor in inflammatory lung diseases: Could antioxidant treatment constitute a new therapeutic strategy? *Oxid. Med. Cell. Longev.* **2021**, *2021*, 6646923. [CrossRef] [PubMed]
14. Shoura, S.M.S.; Naghsh, N.; Moslemi, E.; Kavyani, Z.; Moridpour, A.H.; Musazadeh, V.; Dehghan, P. Can resveratrol supplementation affect biomarkers of inflammation and oxidative stress? An umbrella meta-analysis. *J. Funct. Foods.* **2022**, *99*, 105360. [CrossRef]
15. Ismaeel, G.L.; Abdulhadi, M.A.; Al-Ameer, L.R.; Jumaa, S.S.; Essa, I.M.; Jalil, A.T.; Almulla, A.F.; Ali, R.T. Quercetin for inhibition of inflammatory responses and oxidative stress in lung injury model: A systematic review and meta-analysis. *Egypt. J. Bronchol.* **2023**, *17*, 71. [CrossRef]
16. Li, F.-S.; Weng, J.-K. Demystifying traditional herbal medicine with modern approach. *Nat. plants* **2017**, *3*, 17109. [CrossRef]
17. Yang, M.H.; Yoon, K.D.; Chin, Y.W.; Kim, J.W. Phytochemical and pharmacological profiles of *Dioscorea* species in Korea, China and Japan. *Korean J. Pharmacogn.* **2009**, *40*, 257–279.
18. Sharifi-Rad, M.; Varoni, E.M.; Salehi, B.; Sharifi-Rad, J.; Matthews, K.R.; Ayatollahi, S.A.; Kobarfard, F.; Ibrahim, S.A.; Mnayer, D.; Zakaria, Z.A. Plants of the genus *Zingiber* as a source of bioactive phytochemicals: From tradition to pharmacy. *Molecules* **2017**, *22*, 2145. [CrossRef]
19. Nam, H.-S.; Cho, C.-S.; Kim, C.-J. The effects of *Dioscorea bulbifera* L. on hyperthyroidism of rats. *J. Korean Med.* **2006**, *27*, 169–177.

20. Jung, J.Y.; Lee, J.R.; Byun, S.H.; Jung, J.W.; Kim, Y.H.; Kim, S.C. Inhibitory effect of *Dioscorea bulbifera* MeOH extract on pro-inflammatory mediator in vitro and in vivo. *J. Physiol. Pathol. Korean Med.* **2010**, *24*, 310–318.
21. Chaniad, P.; Tewtrakul, S.; Sudsai, T.; Langyanai, S.; Kaewdana, K. Anti-inflammatory, wound healing and antioxidant potential of compounds from *Dioscorea bulbifera* L. bulbils. *PLoS ONE* **2020**, *15*, e0243632. [CrossRef] [PubMed]
22. Dudala, S.S.; Venkateswarulu, T.C.; Kancharla, S.C.; Kodali, V.P.; Babu, D.J. A review on importance of bioactive compounds of medicinal plants in treating idiopathic pulmonary fibrosis (special emphasis on isoquinoline alkaloids). *Futur. J. Pharm. Sci.* **2021**, *7*, 156. [CrossRef]
23. David, A.V.A.; Arulmoli, R.; Parasuraman, S. Overviews of biological importance of quercetin: A bioactive flavonoid. *Pharmacogn. Rev.* **2016**, *10*, 84–89.
24. Mao, Q.-Q.; Xu, X.-Y.; Cao, S.-Y.; Gan, R.-Y.; Corke, H.; Beta, T.; Li, H.-B. Bioactive compounds and bioactivities of ginger (*Zingiber officinale* Roscoe). *Foods* **2019**, *8*, 185. [CrossRef]
25. Tran, M.N.; Kim, N.S.; Lee, S. Biological network comparison identifies a novel synergistic mechanism of Ginseng Radix-Astragali Radix herb pair in cancer-related fatigue. *J. Ethnopharmacol.* **2024**, *333*, 118447. [CrossRef]
26. Zhang, L.; Virgous, C.; Si, H. Synergistic anti-inflammatory effects and mechanisms of combined phytochemicals. *J. Nutr. Biochem.* **2019**, *69*, 19–30. [CrossRef]
27. Kim, J.M.; Kang, J.Y.; Park, S.K.; Moon, J.H.; Kim, M.J.; Lee, H.L.; Jeong, H.R.; Kim, J.C.; Heo, H.J. Powdered Green Tea (Matcha) Attenuates the Cognitive Dysfunction via the Regulation of Systemic Inflammation in Chronic $PM_{2.5}$-Exposed BALB/c Mice. *Antioxidants* **2021**, *10*, 1932. [CrossRef]
28. Padayatty, S.J.; Katz, A.; Wang, Y.; Eck, P.; Kwon, O.; Lee, J.H.; Chen, S.; Corpe, C.; Dutta, A.; Dutta, S.K.; et al. Vitamin C as an antioxidant: Evaluation of its role in disease prevention. *J. Am. Coll. Nutr.* **2003**, *22*, 18–35. [CrossRef]
29. Hao, S.; Cho, B.O.; Wang, F.; Shin, J.Y.; Shin, D.; Jang, S.I. *Zingiber officinale* attenuates neuroinflammation in LPS-stimulated mouse microglia by AKT/STAT3, MAPK, and NF-κB signaling. *Food Sci. Technol.* **2022**, *42*, e104221. [CrossRef]
30. Ambient (Outdoor) Air Pollution. Available online: https://www.who.int/news-room/fact-sheets/detail/ambient-(outdoor)-air-quality-and-health (accessed on 15 December 2024).
31. List of Most-Polluted Cities by Particulate Matter Concentration. Available online: https://en.wikipedia.org/wiki/List_of_most-polluted_cities_by_particulate_matter_concentration (accessed on 15 December 2024).
32. Lee, H.L.; Kim, J.M.; Go, M.J.; Kim, T.Y.; Joo, S.G.; Kim, J.H.; Lee, H.S.; Kim, H.-J.; Heo, H.J. Protective Effect of Lonicera japonica on $PM_{2.5}$-Induced Pulmonary Damage in BALB/c Mice via the TGF-β and NF-κB Pathway. *Antioxidants* **2023**, *12*, 968. [CrossRef]
33. Kim, T.Y.; Kim, J.M.; Lee, H.L.; Go, M.J.; Joo, S.G.; Kim, J.H.; Lee, H.S.; Jeong, W.M.; Lee, D.Y.; Kim, H.-J.; et al. Codium fragile Suppressed Chronic $PM_{2.5}$-Exposed Pulmonary Dysfunction via TLR/TGF-β Pathway in BALB/c Mice. *Antioxidants* **2023**, *12*, 1743. [CrossRef]
34. Chang, C.L.; Wu, R.T. Quantification of (+)-catechin and (−)-epicatechin in coconut water by LC-MS. *Food Chem.* **2011**, *126*, 710–717. [CrossRef]
35. Hu, Y.; Cheng, Z.; Heller, L.I.; Krasnoff, S.B.; Glahn, R.P.; Welch, R.M. Kaempferol in red and pinto bean seed (*Phaseolus vulgaris* L.) coats inhibits iron bioavailability using an in vitro digestion/human Caco-2 cell model. *J. Agric. Food Chem.* **2006**, *54*, 9254–9261. [CrossRef]
36. Asamenew, G.; Kim, H.W.; Lee, M.K.; Lee, S.H.; Kim, Y.J.; Cha, Y.S.; Yoo, S.M.; Kim, J.B. Characterization of phenolic compounds from normal ginger (*Zingiber officinale* Rosc.) and black ginger (*Kaempferia parviflora* Wall.) using UPLC–DAD–QToF–MS. *Eur. Food Res. Technol.* **2018**, *245*, 653–665. [CrossRef]
37. Lee, J.-E.; Lim, H.J.; Kim, Y.-Y. Publication trends in South Korean research on particulate matter and health effects during two decades (2000–2019). *Toxicol. Res.* **2022**, *38*, 53–62. [CrossRef]
38. Koeberle, A.; Werz, O. Multi-target approach for natural products in inflammation. *Drug Discov. Today* **2014**, *19*, 1871–1882. [CrossRef]
39. Al-Khayri, J.M.; Sahana, G.R.; Nagella, P.; Joseph, B.V.; Alessa, F.M.; Al-Mssallem, M.Q. Flavonoids as potential anti-inflammatory molecules: A review. *Molecules* **2022**, *27*, 2901. [CrossRef]
40. Chen, J.; Zhong, K.; Qin, S.; Jing, Y.; Liu, S.; Li, D.; Peng, C. Astragalin: A food-origin flavonoid with therapeutic effect for multiple diseases. *Front. Pharmacol.* **2023**, *14*, e1265960. [CrossRef]
41. Zick, S.M.; Djuric, Z.; Ruffin, M.T.; Litzinger, A.J.; Normolle, D.P.; Alrawi, S.; Feng, M.R.; Brenner, D.E. Pharmacokinetics of 6-gingerol, 8-gingerol, 10-gingerol, and 6-shogaol and conjugate metabolites in healthy human subjects. *Cancer Epidemiol. Biomark. Prev.* **2008**, *17*, 1930–1936. [CrossRef]
42. Burgoyne, R.A.; Fisher, A.J.; Borthwick, L.A. The role of epithelial damage in the pulmonary immune response. *Cells* **2021**, *10*, 2763. [CrossRef]
43. Thimmulappa, R.K.; Chattopadhyay, I.; Rajasekaran, S. Oxidative stress mechanisms in the pathogenesis of environmental lung diseases. In *Oxidative Stress in Lung Diseases*; Chakraborti, S., Parinandi, N.L., Ghosh, R., Ganguly, N.K., Chakraborti, T., Eds.; Springer: Singapore, 2020; Volume 2, pp. 103–137.
44. Ighodaro, O.M.; Akinloye, O.A. First line defence antioxidants-superoxide dismutase (SOD), catalase (CAT) and glutathione peroxidase (GPX): Their fundamental role in the entire antioxidant defence grid. *Alex. J. Med.* **2018**, *54*, 287–293. [CrossRef]

45. Bartoli, M.L.; Novelli, F.; Costa, F.; Malagrinò, L.; Melosini, L.; Bacci, E.; Cianchetti, S.; Dente, F.L.; Di Franco, A.; Vagaggini, B.; et al. Malondialdehyde in exhaled breath condensate as a marker of oxidative stress in different pulmonary diseases. *Mediators Inflamm.* **2011**, *2011*, 891752. [CrossRef]
46. Bernatoniene, J.; Kopustinskiene, D.M. The role of catechins in cellular responses to oxidative stress. *Molecules* **2018**, *23*, 965. [CrossRef]
47. Abolaji, A.O.; Ojo, M.; Afolabi, T.T.; Arowoogun, M.D.; Nwawolor, D.; Farombi, E.O. Protective properties of 6-gingerol-rich fraction from *Zingiber officinale* (ginger) on chlorpyrifos-induced oxidative damage and inflammation in the brain, ovary and uterus of rats. *Chem. Biol. Interact.* **2017**, *270*, 15–23. [CrossRef]
48. Kowalczyk, P.; Sulejczak, D.; Kleczkowska, P.; Bukowska-Ośko, I.; Kucia, M.; Popiel, M.; Wietrak, E.; Kramkowski, K.; Wrzosek, K.; Kaczyńska, K. Mitochondrial oxidative stress—A causative factor and therapeutic target in many diseases. *Int. J. Mol. Sci.* **2021**, *22*, 13384. [CrossRef]
49. Chew, S.; Kolosowska, N.; Saveleva, L.; Malm, T.; Kanninen, K.M. Impairment of mitochondrial function by particulate matter: Implications for the brain. *Neurochem. Int.* **2020**, *135*, 104694. [CrossRef]
50. Santos, L.F.S.; Stolfo, A.; Calloni, C.; Salvador, M. Catechin and epicatechin reduce mitochondrial dysfunction and oxidative stress induced by amiodarone in human lung fibroblasts. *J. Arrhythmia* **2017**, *33*, 220–225. [CrossRef]
51. Han, X.; Yang, Y.; Zhang, M.; Chu, X.; Zheng, B.; Liu, C.; Xue, Y.; Guan, S.; Sun, S.; Jia, Q. Protective effects of 6-gingerol on cardiotoxicity induced by arsenic trioxide through AMPK/SIRT1/PGC-1α signaling pathway. *Front. Pharmacol.* **2022**, *13*, 1298. [CrossRef]
52. Park, G.B.; Choi, Y.; Kim, Y.S.; Lee, H.K.; Kim, D.; Hur, D.Y. ROS-mediated JNK/p38-MAPK activation regulates Bax translocation in Sorafenib-induced apoptosis of EBV-transformed B cells. *Int. J. Oncol.* **2014**, *44*, 977–985. [CrossRef]
53. Cho, I.-H.; Gong, J.-H.; Kang, M.-K.; Lee, E.-J.; Park, J.H.Y.; Park, S.-J.; Kang, Y.-H. Astragalin inhibits airway eotaxin-1 induction and epithelial apoptosis through modulating oxidative stress-responsive MAPK signaling. *BMC Pulm. Med.* **2014**, *14*, 122. [CrossRef]
54. Han, H.S.; Kim, K.B.; Jung, J.H.; An, I.S.; Kim, Y.-J.; An, S. Anti-apoptotic, antioxidant and anti-aging effects of 6-shogaol on human dermal fibroblasts. *Biomed. Dermatol.* **2018**, *2*, 27. [CrossRef]
55. Berman, R.; Kopf, K.W.; Min, E.; Huang, J.; Downey, G.P.; Alam, R.; Chu, H.W.; Day, B.J. IL-33/ST2 signaling modulates Afghanistan particulate matter induced airway hyperresponsiveness in mice. *Toxicol. Appl. Pharmacol.* **2020**, *404*, 115186. [CrossRef]
56. Griesenauer, B.; Paczesny, S. The ST2/IL-33 axis in immune cells during inflammatory diseases. *Front. Immunol.* **2017**, *8*, 475. [CrossRef]
57. Celebi Sözener, Z.; Cevhertas, L.; Nadeau, K.; Akdis, M.; Akdis, C.A. Environmental factors in epithelial barrier dysfunction. *J. Allergy Clin. Immunol.* **2020**, *145*, 1517–1528. [CrossRef]
58. Kim, J.M.; Heo, H.J. The roles of catechins in regulation of systemic inflammation. *Food Sci. Biotechnol.* **2022**, *31*, 957–970. [CrossRef]
59. Hong, W.; Zhi, F.X.; Kun, T.H.; Hua, F.J.; Ling, L.H.; Fang, F.; Wen, C.; Jie, W.; Yang, L.C. 6-Gingerol attenuates ventilator-induced lung injury via anti-inflammation and antioxidative stress by modulating the PPARγ/NF-κBsignalling pathway in rats. *Int. Immunopharmacol.* **2021**, *92*, 107367. [CrossRef]
60. Cho, I.-H.; Choi, Y.-J.; Gong, J.-H.; Shin, D.; Kang, M.-K.; Kang, Y.-H. Astragalin inhibits autophagy-associated airway epithelial fibrosis. *Respir Res.* **2015**, *16*, 51–58. [CrossRef]
61. Gulati, N.; Chellappan, D.K.; MacLoughlin, R.; Gupta, G.; Singh, S.K.; Oliver, B.G.; Dua, K.; Dureja, H. Advances in nano-based drug delivery systems for the management of cytokine influx-mediated inflammation in lung diseases. *Naunyn-Schmiedeberg's Arch. Pharmacol.* **2024**, *397*, 3695–3707. [CrossRef]
62. Pan, Z.; Zhou, Y.; Luo, X.; Ruan, Y.; Zhou, L.; Wang, Q.; Yan, Y.J.; Liu, Q.; Chen, J. Against NF-κB/thymic stromal lymphopoietin signaling pathway, catechin alleviates the inflammation in allergic rhinitis. *Int. Immunopharmacol.* **2018**, *61*, 241–248. [CrossRef]
63. Jafarzadeh, A.; Mohammadi-Kordkhayli, M.; Ahangar-Parvin, R.; Azizi, V.; Khoramdel-Azad, H.; Shamsizadeh, A.; Ayoobi, A.; Nemati, M.; Hassan, Z.; Moazeni, S. Ginger extracts influence the expression of IL-27 and IL-33 in the central nervous system in experimental autoimmune encephalomyelitis and ameliorates the clinical symptoms of disease. *J. Neuroimmunol.* **2014**, *276*, 80–88. [CrossRef]
64. Camelo, A.; Dunmore, R.; Sleeman, M.A.; Clarke, D.L. The epithelium in idiopathic pulmonary fibrosis: Breaking the barrier. *Front. Pharmacol.* **2014**, *4*, 173. [CrossRef] [PubMed]
65. Khalil, H.; Kanisicak, O.; Prasad, V.; Correll, R.N.; Fu, X.; Schips, T.; Vagnozzi, R.J.; Liu, R.; Huynh, T.; Lee, S.J.; et al. Fibroblast-specific TGF-β-Smad2/3 signaling underlies cardiac fibrosis. *J. Clin. Investig.* **2017**, *127*, 3770–3783. [CrossRef] [PubMed]
66. Agraval, H.; Yadav, U.C.S. MMP-2 and MMP-9 mediate cigarette smoke extract-induced epithelial-mesenchymal transition in airway epithelial cells via EGFR/Akt/GSKβ/β-catenin pathway: Amelioration by fisetin. *Chem. Biol. Interact.* **2019**, *314*, 108846. [CrossRef] [PubMed]
67. Ashraf, S.T.; Obaid, A.; Saeed, M.T.; Naz, A.; Shahid, F.; Ahmad, J.; Ali, A. Formal model of the interplay between TGF-β1 and MMP-9 and their dynamics in hepatocellular carcinoma. *Math. Biosci. Eng.* **2019**, *16*, 3285–3310. [CrossRef]

68. Wang, L.; Yang, G.; Yuan, L.; Yang, Y.; Zhao, H.; Ho, C.-T.; Li, S. Green tea catechins effectively altered hepatic fibrogenesis in rats by inhibiting ERK and Smad1/2 phosphorylation. *J. Agric. Food Chem.* **2018**, *67*, 5437–5445. [CrossRef]
69. Liu, L.; Yu, N.; Leng, W.; Lu, Y.; Xia, X.; Yuan, H. 6-Gingerol, a functional polyphenol of ginger, reduces pulmonary fibrosis by activating Sirtuin1. *Allergol. Immunopathol.* **2022**, *50*, 104–114. [CrossRef]

antioxidants

MDPI

Article

Association Between Oxidative Potential of Particulate Matter Collected by Personal Samplers and Systemic Inflammation Among Asthmatic and Non-Asthmatic Adults

Miguel Santibáñez [1,*], Juan José Ruiz-Cubillán [2], Andrea Expósito [3], Juan Agüero [2], Juan Luis García-Rivero [2], Beatriz Abascal [2], Carlos Antonio Amado [2], Laura Ruiz-Azcona [1], Marcos Lopez-Hoyos [4], Juan Irure [4], Yolanda Robles [5], Ana Berja [5], Esther Barreiro [6,7], Adriana Núñez-Robainas [6,7], José Manuel Cifrián [2] and Ignacio Fernandez-Olmo [3]

[1] Global Health Research Group, Faculty of Nursing, Universidad de Cantabria-Valdecilla Research Institute (IDIVAL), Avenida Valdecilla, s/n, 39008 Santander, Cantabria, Spain; laura.ruiz@unican.es
[2] Division of Pneumology, Hospital Universitario Marqués de Valdecilla, IDIVAL, 39008 Santander, Cantabria, Spain; juanjose.ruizc@scsalud.es (J.J.R.-C.); jagcal@gmail.com (J.A.); jgarcia@separ.es (J.L.G.-R.); beatriz.abascal@scsalud.es (B.A.); amadodiago.carlos@gmail.com (C.A.A.); josemanuel.cifrian@scsalud.es (J.M.C.)
[3] Departamento de Ingenierías Química y Biomolecular, Universidad de Cantabria, Avenida Los Castros, s/n, 39005 Santander, Cantabria, Spain; andreaexpositomonar@gmail.com (A.E.); ignacio.fernandez@unican.es (I.F.-O.)
[4] Division of Immunology, Hospital Universitario Marqués de Valdecilla, IDIVAL, 39008 Santander, Cantabria, Spain; marcos.lopez@scsalud.es (M.L.-H.); juan.irure@scsalud.es (J.I.)
[5] Division of Biochemistry, Hospital Universitario Marqués de Valdecilla, IDIVAL, 39008 Santander, Cantabria, Spain; roblesfla@hotmail.es (Y.R.); anaberj@gmail.com (A.B.)
[6] Pulmonology Department-Muscle Wasting and Cachexia in Chronic Respiratory Diseases and Lung Cancer, IMIM-Hospital del Mar, Department of Medicine and Life Sciences (MELIS), Universitat Pompeu Fabra, Barcelona Biomedical Research Park (PRBB), 08003 Barcelona, Spain; ebarreiro@imim.es (E.B.); adriananunez96@gmail.com (A.N.-R.)
[7] Centro de Investigación en Red de Enfermedades Respiratorias (CIBERES), Instituto de Salud Carlos III (ISCIII), 08034 Barcelona, Spain
* Correspondence: santibanezm@unican.es

Abstract: With the rationale that the oxidative potential of particulate matter (PM-OP) may induce oxidative stress and inflammation, we conducted the ASTHMA-FENOP study in which 44 asthmatic patients and 37 matched controls wore a personal sampler for 24 h, allowing the collection of fine and coarse PM fractions separately, to determine PM-OP by the dithiothreitol (DTT) and ascorbic acid (AA) methods. The levels of Interleukin 6 (IL-6) and the IL-6/IL-10 ratio, as indicators of pro- and anti-inflammatory statuses, were determined by calculating the mean differences (MDs), odds ratios (ORs) and p-trends adjusted for sex, age, study level and body mass index. Positive associations for IL-6 levels in the form of adjusted MDs and ORs were obtained for all PM-OP metrics, reaching statistical significance for both OP-DTT and OP-AA in the fine fraction, with adjusted OR = 5.66; 95%CI (1.46 to 21.92) and 3.32; 95%CI (1.07 to 10.35), respectively, along with statistically significant dose–response patterns when restricting to asthma and adjusted also for clinical variables (adjusted p-trend = 0.029 and 0.01). Similar or stronger associations and dose–response patterns were found for the IL-6/IL-10 ratio. In conclusion, our findings on the effect of PM-OP on systemic inflammation support that asthma is a heterogeneous disease at the molecular level, with PM-OP potentially playing an important role.

Keywords: particulate matter (PM); oxidative potential (OP); asthma; systemic inflammation; interleukin-6

1. Introduction

Among air pollutants, particulate matter (PM) has the greatest impact on human health [1,2]. In this regard, the toxicity of PM, beyond its chemical composition, seems to be related to its capacity to generate reactive oxygen species (ROS). This may alter the balance between oxidants and antioxidants in the cells in favor of the former, leading to oxidative stress [3]. Increased expression of inflammatory cytokines and other molecules, such as cellular adhesion molecules and coagulation factors, may also be involved [2].

The characterization of PM exposure in epidemiological studies is mainly based on the PM mass concentration and chemical composition from filters collected by stationary samplers. However, recent studies have suggested that the oxidative potential (OP) of PM may be a better proxy than the PM mass concentration to account for the exposure to PM in such studies [4]. PM OP is defined as the ability of inhaled components to produce ROS while simultaneously depleting antioxidants [5]. In addition, this characterization is usually not performed on an individual basis. In this sense, the use of personal PM samplers instead of stationary ones allows the collection of particles to which a volunteer has been exposed to in the last 24 h. These personal PM samplers have been used in some studies with the aim of determining the mass and chemical composition of PM [6,7] and, recently, its OP also [5,8–11].

Asthma is currently the most prevalent chronic respiratory disease worldwide, with twice as many cases as Chronic Obstructive Pulmonary Disease (COPD) [12]. There is consistent evidence on the association between air pollution and a higher incidence of asthma [13]. In relation to the clinical course of this disease, there is evidence from meta-analyses and subsequent studies on the effects of airborne PM on the use of rescue medication, visits to emergency departments, and especially, admissions for asthma exacerbations [14,15]. Recently, an intervention reducing the ROS effects of PM2.5 has been shown to alleviate asthma symptoms in a mouse model, suggesting potential translation into clinical practice for PM2.5-induced respiratory complications in patients with asthma [16].

At the molecular level, it is increasingly clear that asthma represents a heterogeneous disease with multiple phenotypes and endotypes [17–19]. Nevertheless, it is well known that the disease is mediated by increased bronchial inflammation and hyperresponsiveness, and it is plausible that there is a response to PM pollution with increased systemic inflammation in addition to epithelial airway inflammation. The reasons why exposure to PM in asthmatic patients is linked to a worsening of their condition, expressed as a greater number of exacerbations and visits to emergency departments, and their possible relationship with the OP of certain components present in PM remain to be studied in depth. Interestingly, Canova et al. [20] measured PM10 OP as depletion of ascorbic acid (AA), glutathione and uric acid in synthetic airway fluid. They conducted a bi-directional case-crossover study in patients admitted to hospital for asthma/COPD exacerbations and compared the OP on the admission day with that on 14 days before/after admission. PM10 was collected by using stationary samplers located near the hospital. The analyses included 160 exacerbations in 151 patients. PM10 OP was not associated with asthma/COPD admissions, but the authors highlight the use of stationary samplers instead of PM personal sampling methods as a main limitation, as the latter are more accurate but difficult to incorporate in a case-crossover design.

Interleukin 6 (IL-6) is one of the major studied mediators of inflammation. It is a cytokine produced by different cell types, with immune cells and adipose tissue being the most important. Besides the fact that it is one of the most commonly analyzed inflammatory mediators in respiratory diseases, there is consistent evidence of an association between obesity and higher IL-6 levels; and IL-6 constitutes an important proatherogenic biomarker, and it is one of the systemic inflammation biomarkers most consistently associated with a risk of cardiovascular morbidity and mortality [21,22].

IL-10 is the most important cytokine with anti-inflammatory properties. It is secreted by a variety of cells, and its anti-inflammatory effect seems to be mediated by inhibiting

the synthesis of many inflammatory proteins, macrophage activation and the antigen presentation [23]. The so-called "Cytokine storm" with abnormal levels of the inflammatory cytokines IL-6 and IL-10 is well known in COVID-19 disease [24], and the balance of pro- and anti-inflammatory statuses, as determined by the IL-6/IL-10 ratio, has been recently established as a consistent marker of severe SARS-CoV-2 infection [25]. In addition, the IL-6/IL-10 ratio seems to perform better than IL-6 alone as a predictor of the severity of primary open-angle glaucoma [26].

We hypothesized that PM may induce oxidative stress and inflammation due to the oxidative capacity of its components, particularly in patients with asthma. With this rationale, we launched the ASTHMA-FENOP study, which included a group of controls without asthma matched by gender and age with asthmatic patients. Our objective was to determine and compare between these two groups the association between the OP of PM by using personal PM samplers and IL-6 levels as a surrogate of systemic inflammation and the IL-6/IL-10 ratio as a surrogate of the balance of pro- and anti-inflammatory statuses.

2. Methods

2.1. Study Design

We conducted a cross-sectional study on 44 adult asthmatic patients in collaboration with the Pneumology Service of Hospital Universitario Marqués de Valdecilla (HUMV) and Hospital de Liencres (HL), based on the following inclusion criteria: (1) Diagnosis of asthma according to GINA criteria [27], at least 12 months prior to the baseline visit. (2) Stable treatment with inhaled corticosteroids (ICS) with/without long-acting β adrenoceptor agonists (LABAs), for the past 3 months. (3) No exacerbations in the 4 weeks prior to study inclusion. Previous diagnosis of confirmed COPD and being treated with oral steroids for other reasons than asthma were exclusion criteria. Thirty-seven controls (without asthma) matched with asthmatic patients by gender and age (±5 years old), were recruited as a comparison group.

Volunteers' residences are shown in Figure S1. Most of them lived in the urban area of Santander, while a second subgroup lived in the Maliaño area (Camargo), near some metallurgical plants, constituting an urban–industrial mixed area. The selection of candidates was based on "a priori" different levels of outdoor PM-bound metals, which are the main drivers of PM-OP. A previous study of the research group at these sites, using PM stationary samplers (see the two red circles in Figure S1), showed higher PM-bound metal levels in the urban-industrial area [28].

2.2. Recruitment Scheme and PM Personal Sampling

The recruitment scheme covered 3 consecutive days, with 1–4 patients per week, from November 2022 to February 2024. After signing the informed consent, each volunteer received a personal sampler upon arrival on the first day (visit 1). PM personal samples were collected for 24 h using a two-stage personal modular impactor (SKC PMI coarse) capable of sampling PM2.5 and PM10–2.5 filters separately, connected to a personal pump (SKC Aircheck XR5000, SKC Inc., Valley View Road Eighty Four, PA, USA) that operated at a flow rate of 3 L per minute (l pm). Thirty-seven and 25 mm diameter polytetrafluoroethylene (PTFE) membrane filters were used to collect PM2.5 and PM10–2.5 samples, respectively. The sampler pumps were programmed to sample for 24 h to prevent mishandling and were returned on the second day's visit. On day 3 (lag1, 25–48 h after returning the personal sampler) FeNO was determined and a blood sample was obtained. The protocol for each volunteer is summarized in Table S1.

2.3. Oxidative Potential Analysis

The PM2.5 and PM10–2.5 filters were extracted with 5 mL of a phosphate buffer (PB) solution (0.0075 M Na_2HPO_4, 0.0025 M NaH_2PO_4) for 24 h at 37 °C and filtered using a syringe cartridge. All samples were stored until OP analysis at 4 °C.

Two OP assays were carried out based on the methodology developed by Expósito et al. [29]: the dithiothreitol (DTT) and AA assays. A microplate reader spectrophotometer (Multiskan Skyhigh microplate spectrophotometer, Thermo Fisher Scientific Inc., Singapore) was used for the OP measurements.

Samples were analyzed in triplicate. The detection limits (D.L.) were calculated by multiplying the standard deviation (SD) of the OP-AA or OP-DTT values of 5 blank filters by the $n - 1$ sample two-tailed Student's t value at 95% confidence level (2.57). Furthermore, the OP-DTT and OP-AA arithmetic mean of blank filters was subtracted from the depletion rate of each PM sample. The D.L., mean of blank filters, and percentage of samples higher than the D.L. are shown in Table S2.

2.4. Cytokine Measurement

Fasting blood samples were collected from all participants on visit 3 (from 8:00–9:00 a.m.) and serum was then separated and stored at −80 °C until assayed. Quantification of cytokine profiles was performed for all samples at the same time utilizing the human IL-6 enzyme-linked immunosorbent assay (ELISA) kit ENZ-KIT178-0001 IL-6 and Human IL-10 ADI-900-036 ELISA kit (Enzo Biochem, Inc., Farmingdale, NY, USA) according to the manufacturer's protocols. Lowest quantification values for IL-6 and IL-10 cytokines were 0.12 and 1.37 pg/mL, respectively. Samples with concentrations below the D.L. (n = 3 for IL-6 and n = 0 for IL-10) were assigned a value equal to half of the lowest quantification limit and were included in the statistical analysis.

2.5. Statistical Analysis

Continuous variables were described as mean and SD and/or median and interquartile ranges (IQR). Statistical differences between groups were compared by using the Student's *t* test (for equal or different variances, depending on the previous result in the Levene test) in the case of mean comparisons. Normality distribution of variables was studied using the Shapiro–Wilk test. Medians were compared using the Mann–Whitney's u test. Categorical and discrete variables were expressed as percentages, and comparisons were performed with the Chi-square test, using Yates' correction or Fisher's exact test, when appropriate.

IL levels and exposure metrics were dichotomously categorized according to their medians and crude and adjusted odds ratios (aORs) with their 95% confidence intervals (CI) were estimated using unconditional logistic regression models. In these models, the ILs binary results (low and high IL levels) were treated as dependent variables and exposures were treated as independent binary variables (0 = lower values; 1 = higher values). Lastly, OP levels were categorized ordinally (low T1, medium T2, high T3) according to tertiles, calculating adjusted dose–response trends (p trends) in addition to aORs. In a parallel approach, adjusted mean differences (MDs) with their 95%CI were calculated using a linear regression model in which the quantitative IL results were treated as the dependent variable, and each OP exposure as a binary variable (0 = lower values; 1 = higher values).

Age (as a continuous variable), sex, study level (ordinally categorized), body mass index (BMI) and FeNO levels were pre-established as confounders to obtain adjusted ORs and MDs. A stratified analysis based on the asthma and non-asthma statuses was pre-established, along with an additional multivariate model for asthmatic patients. In this additional model, results in the Asthma Control Test (ACT), Test of Adherence to Inhalers (TAI), and asthma severity (according to GINA 2023 guideline steps), were also included as confounders.

The level of statistical significance was set at 0.05 and all tests were two-tailed. We used the SPSS statistical software package 22.0 (SPSS, Inc., Chicago, IL, USA) for statistical analyses.

3. Results

3.1. Description of the Sample and Distribution of Results for ILs and OP Levels

The characteristics of asthmatic patients are summarized in Table S3. The overall mean age was 52.45 years; [SD = 17.42], with ages ranging from 18 to 80 years. 56.8% were women (n = 25) and the rest men (n = 19, 43.2%). The mean score on the ACT was 22.16 points; [SD = 3.8] with a median of 23, and an IQR between 20 and 25 points. Based on these scores, 81.8% had their asthma controlled ($\geq$20 points). Adherence to inhaled maintenance therapy was good (TAI 10 items = 50) in the majority of patients (n = 33, 75.0%). Most of the sample (n = 25, 56.8%) was in GINA stage 4 (medium dose maintenance of ICS-long-acting β adrenoceptor agonists (LABAs)).

Mean age and sex were similar for both asthmatic patients and controls (mean = 52.45, 56% female) as a result of matching. Most of volunteers were non-smokers (77.3% and 78.4%) being former smokers the rest. University study level was different between asthmatic patients and control volunteers, with a higher prevalence of University studies in controls ($p < 0.001$). Regarding BMI, 36.4% of asthmatic volunteers were on healthy weight according to WHO classification (cut off points 18.5–24.9). Prevalence of overweight (40.9%, BMI 25–29.9) and obesity (22.7%, BMI $\geq$ 30) was slightly higher among asthmatic volunteers ($p = 0.096$). FeNO median levels (on day 2) were 27 ppb in asthmatic volunteers with a 72.7% having FeNO levels $\geq$ 20 ppb. As expected, FeNO levels were higher among asthmatic patients compared to controls. See Table S4.

The distribution of IL-6 levels and IL-6/IL-10 ratios, and OP results presented positive asymmetry with the mean values greater than the medians. Median levels for IL-6 and IL-6/IL-10 ratios were slightly higher among controls with statistically significant *p* values. Median levels for PM-OP determinations were higher among asthmatic patients compared to controls, yielding statistical significance in some cases. See Table 1.

Table 1. Description of systemic inflammation based on ILs levels and PM-OP metrics as a function of their asthma or control statuses.

	Asthma N = 44		**Non-Asthma N = 37**		**All N = 81**		***p* Value**
Systemic inflammation							
IL-6 pg/mL. Mean [SD]	18.08	32.57	30.33	40.45	23.68	36.66	*0.135*
IL-6 pg/mL. Median [IQR]	5.84	2.06–15.25	10.56	7.86–38.9	9.24	4.08–16.70	*0.009*
IL-10 pg/mL. Mean [SD]	10.95	19.22	5.60	4.15	8.51	14.61	*0.079*
IL-10 pg/mL. Median [IQR]	6.35	3.73–10.18	4.48	3.80–5.32	4.74	3.73–7.40	*0.041*
IL-6/IL-10 ratio. Mean [SD]	3.57	7.77	6.05	8.15	4.70	7.99	*0.166*
IL-6/IL-10 ratio. Median [IQR]	0.95	0.26–2.03	2.44	1.52–8.00	1.52	0.66–3.27	*<0.001*
PM-OP metrics (nmol/min/m^3)							
OP-DTT PM2.5. Mean [SD]	0.30	0.29	0.17	0.25	0.24	0.27	*0.029*
OP-DTT PM2.5. Median [IQR]	0.24	0.15–0.34	0.10	0.03–0.18	0.16	0.1–0.31	*<0.001*
OP-AA PM2.5. Mean [SD]	0.72	1.29	0.34	0.89	0.55	1.14	*0.127*
OP-AA PM2.5. Median [IQR]	0.23	0.12–0.49	0.15	0.06–0.28	0.18	0.07–0.37	*0.027*
OP-DTT PM10–2.5. Mean [SD]	0.18	0.11	0.14	0.11	0.16	0.11	*0.058*
OP-DTT PM10–2.5. Median [IQR]	0.17	0.10–0.26	0.11	0.06–0.19	0.13	0.08–0.22	*0.052*
OP-AA PM10–2.5. Mean [SD]	0.59	1.38	0.17	0.11	0.40	1.04	*0.051*
OP-AA PM10–2.5. Median [IQR]	0.22	0.10–0.55	0.20	0.1–0.20	0.20	0.1–0.39	*0.029*

SD = standard deviation. IQR = interquartile rank.

3.2. Adjusted Associations Between PM-OP, IL-6 and the IL-6/IL-10 Ratio

Positive associations for IL-6 levels in the form of adjusted ORs were obtained for all the PM-OP metrics, reaching statistical significance for both OP-DTT and OP-AA in the fine fraction, with differences between crude and adjusted results (associations were higher after adjusting for confusion) (see Tables S5 and S6, and Figure 1). Overall, volunteers with higher OP-DTT values (above median) had a 5.66 fold increased risk of elevated IL-6 levels: adjusted OR = 5.66; 95%CI (1.46 to 21.92); and those with higher

OP-AA levels a 3.32 fold increased risk: adjusted OR = 3.32; 95%CI (1.07 to 10.35) (see Table S6 and Figure 1). Associations between OP values and the IL-6/IL-10 ratio were even stronger (see Tables S7 and S8), with statistical significance also reached for OP-AA in the coarse fraction: adjusted OR = 5.14; 95%CI (1.13 to 23.40) (see Table S8 and Figure 1). In the form of adjusted MDs, statistically significant positive MDs were also obtained, indicating higher IL6 and IL-6/IL-10 ratio values among those with higher PM-OP exposures (see Tables S9–S12 and Figure 2). When stratifying the analysis into asthma and controls, positive associations in the form of adjusted ORs and adjusted MDs were found in both groups.

Table 2 presents OR results for IL-6 specifically for the 44 asthmatic patients, examining dose–response patterns by classifying exposure according to tertiles, and after adjusting for specific clinical confounders such as the ACT and TAI scores, or GINA stage. Positive dose–response patterns were obtained for all PM-OP metrics (the greater PM-OP, the greater the association for higher IL-6 levels), with statistically significant adjusted p-trends in the fine fraction for both PM-OP metrics (adjusted p-trend = 0.029 for OP-DTT and 0.01 for OP-AA). Dose–response patterns were maintained for the IL-6/IL-10 ratio (See Table 3).

Table 2. Association between PM-OP metrics and IL-6 levels, restricted to asthmatic patients and studying dose–response patterns.

		IL-6 pg/mL (Median)									
***PM-OP$_v$* nmol min^{-1} m^{-3}**	***Cut-Off Point***	**n = 27 ≤9.24**	**n = 17 9.24+**	**OR Crude**	**95%**	**CI**	***p Value***	**aOR**	**95%**	**CI**	***p Value***
OP-DTT PM2.5											
Lower values	≤0.161	12	2	1				1			
Higher values	0.161+	15	15	6.00	1.14	31.53	*0.034*	39.70	2.19	718.60	*0.013*
OP-DTT PM2.5 (Tertiles)											
Low values	≤0.110	4	1	1				1			
Medium values	0.111–0.236	11	7	2.55	0.23	27.71	*0.443*	4.52	0.25	83.26	*0.310*
High values	0.236+	12	9	3.00	0.29	31.63	*0.361*	41.96	1.12	1566.43	*0.043*
Linear p-trend							*0.409*				*0.029*
OP-AA PM2.5											
Lower values	≤0.184	13	5	1				1			
Higher values	0.184+	14	12	2.23	0.62	8.08	*0.223*	3.76	0.75	18.92	*0.108*
OP-AA PM2.5 (Tertiles)											
Low values	≤0.125	8	3	1				1			
Medium values	0.126–0.260	13	3	0.62	0.10	3.82	*0.602*	0.57	0.06	5.62	*0.632*
High values	0.260+	6	11	4.89	0.93	25.67	*0.061*	48.39	2.12	1106.24	*0.015*
Linear p-trend							*0.032*				*0.01*
OP-DTT PM10–2.5											
Lower values	≤0.129	11	6	1				1			
Higher values	0.129+	16	11	1.26	0.36	4.43	*0.718*	1.82	0.36	9.26	*0.469*
OP-DTT PM10–2.5 (Tertiles)											
Low values	≤0.090	6	4	1				1			
Medium values	0.091–0.200	9	6	1.00	0.20	5.12	*1.000*	1.33	0.20	9.02	*0.769*
High values	0.200+	12	7	0.88	0.18	4.21	*0.868*	1.46	0.20	10.90	*0.709*
Linear p-trend							*0.851*				*0.713*
OP-AA PM10–2.5											
Lower values	≤0.200	14	8	1				1			
Higher values	0.200+	13	9	1.21	0.36	4.08	*0.757*	5.16	0.78	34.15	*0.089*
OP-AA PM10–2.5 (Tertiles)											
Low values	≤0.100	7	4	1				1			
Medium values	0.101–0.300	8	5	1.09	0.21	5.76	*0.916*	0.88	0.11	6.85	*0.905*
High values	0.300+	12	8	1.17	0.26	5.33	*0.842*	4.53	0.47	43.47	*0.191*
Linear p-trend							*0.842*				*0.221*

OR = odds ratio. aOR = OR adjusted for age, sex, ACT, TAI, severity of asthma, FeNO levels and BMI according to WHO classification.

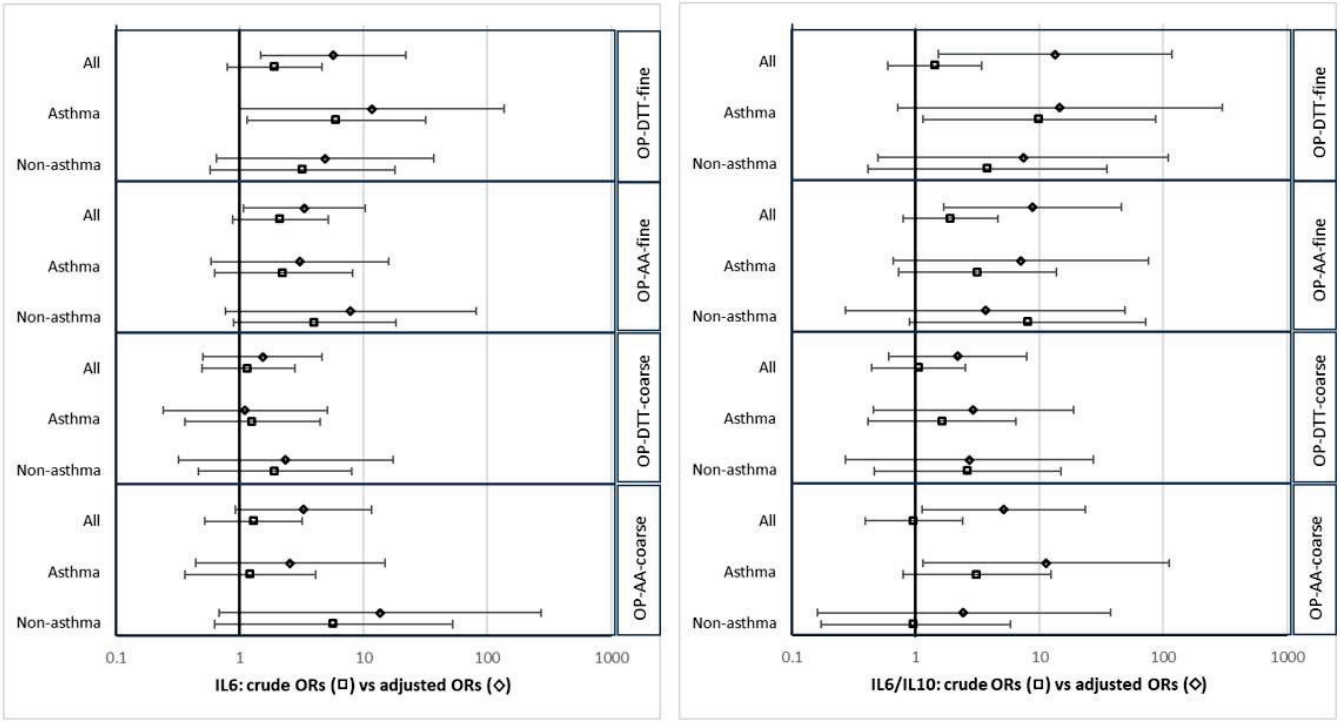

Figure 1. Forest plot of crude and adjusted odds ratios (ORs) between higher values of OP-DTT and OP-AA (for the fine and coarse PM fractions); and higher IL-6 levels (on the **left**) and higher IL-6/IL-10 ratio levels (on the **right**). ORs adjusted for age, sex, educational level, BMI according to WHO classification, and FeNO levels.

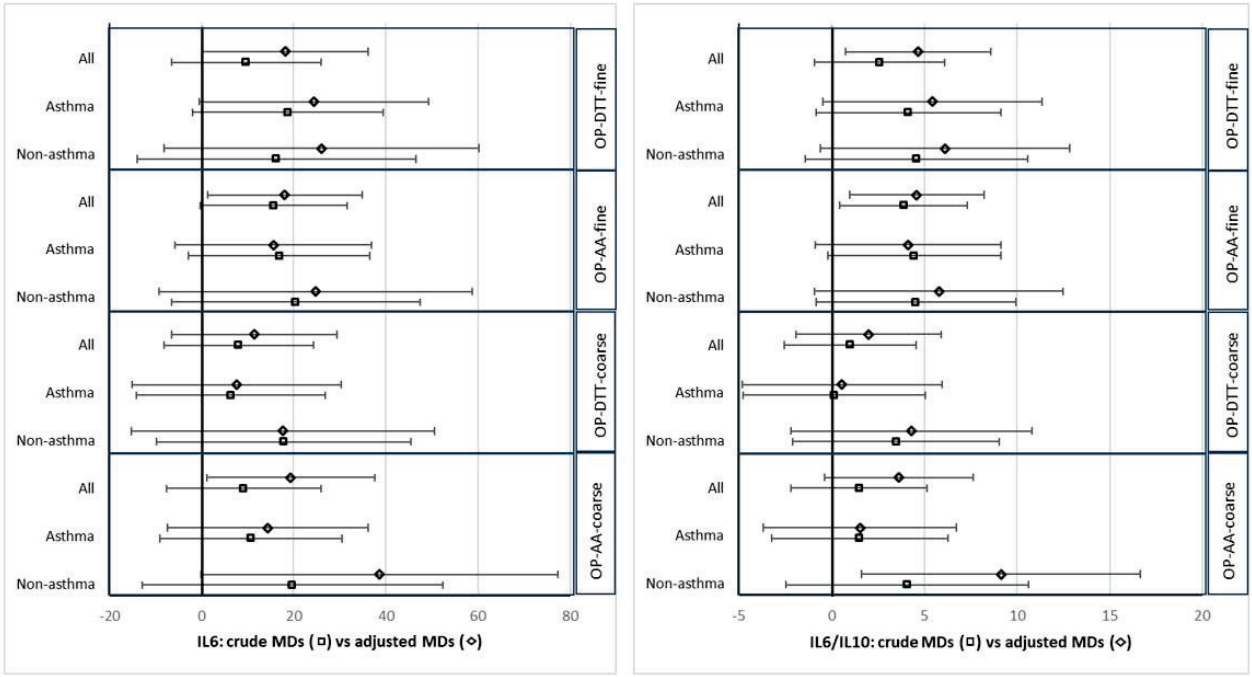

Figure 2. Forest plot of crude and adjusted mean differences (aMDs) between higher values of OP-DTT and OP-AA (for the fine and coarse PM fractions); and IL-6 (on the **left**) and the IL-6/IL-10 ratio levels (on the **right**). MDs adjusted for age, sex, educational level, BMI according to WHO classification, and FeNO levels.

Table 3. Association between PM-OP metrics and the IL-6/IL-10 ratio, restricted to asthmatic patients and studying dose–response patterns.

		IL-6/IL-10 (Median)									
		n = 30	n = 14								
PM-OP$_v$ nmol min^{-1} m^{-3}	*Cut-Off Point*	≤1.52	1.52+	OR Crude	95%	CI	*p Value*	aOR	95%	CI	*p Value*
OP-DTT PM2.5											
Lower values	≤0.161	13	1	1				1			
Higher values	0.161+	17	13	9.94	1.15	86.06	*0.037*	14.65	1.15	186.87	*0.039*
OP-DTT PM2.5 (Tertiles)											
Low values	≤0.110	5	1	1				1			
Medium values	0.111–0.236	14	3	1.07	0.09	12.83	*0.957*	0.51	0.02	10.52	*0.660*
High values	0.236+	11	10	4.55	0.45	45.86	*0.199*	9.39	0.44	198.71	*0.150*
Linear p-trend							*0.063*				*0.074*
OP-AA PM2.5											
Lower values	≤0.184	15	3	1				1			
Higher values	0.184+	15	11	3.67	0.85	15.84	*0.082*	5.20	0.78	34.54	*0.088*
OP-AA PM2.5 (Tertiles)											
Low values	≤0.125	10	1	1				1			
Medium values	0.126–0.260	12	4	2.31	0.21	25.66	*0.496*	6.66	0.25	177.74	*0.258*
High values	0.260+	8	9	11.25	1.17	108.41	*0.036*	33.86	1.08	1066.42	*0.045*
Linear p-trend							*0.015*				*0.018*
OP-DTT PM10–2.5											
Lower values	≤0.129	12	5	1				1			
Higher values	0.129+	18	9	1.20	0.32	4.47	*0.786*	1.30	0.26	6.63	*0.75*
OP-DTT PM10–2.5 (Tertiles)											
Low values	≤0.090	7	3	1				1			
Medium values	0.091–0.200	11	4	0.85	0.14	4.99	*0.856*	0.59	0.08	4.36	*0.607*
High values	0.200+	12	7	1.36	0.26	7.04	*0.713*	1.18	0.17	8.07	*0.867*
Linear p-trend							*0.640*				*0.814*
OP-AA PM10–2.5											
Lower values	≤0.200	17	5	1				1			
Higher values	0.200+	13	9	2.35	0.64	8.73	*0.200*	4.69	0.84	26.26	*0.079*
OP-AA PM10–2.5 (Tertiles)											
Low values	≤0.100	7	4	1				1			
Medium values	0.101–0.300	11	2	0.32	0.05	2.22	*0.248*	0.25	0.03	2.41	*0.232*
High values	0.300+	12	8	1.17	0.26	5.33	*0.842*	2.10	0.28	15.51	*0.467*
Linear p-trend							*0.652*				*0.430*

OR = odds ratio. aOR = OR adjusted for age, sex, ACT, TAI, severity of asthma, FeNO levels and BMI according to WHO classification.

4. Discussion

Among air pollutants, particulate matter (PM) has the greatest impact on human health. We have found an association between the OP of PM and serum IL-6 levels, with positive associations in the form of adjusted MDs and adjusted ORs for all the OP metrics, reaching statistical significance and with well-defined dose–response patterns in the fine fraction. When comparing adults with and without asthma, positive associations were observed in both groups. Lastly, our results were maintained for the IL-6/IL-10 ratio as a surrogate of pro- and anti-inflammatory statuses.

Each PM-OP assay has different sensitivities to the chemical composition of PM. Thus, both OP-DTT and OP-AA are very sensitive to soluble Cu. However, OP-DTT is sensitive to Mn but not to Fe, whereas Fe is an important driver of OP-AA [5]. Regarding the organic species bound to PM, quinones are significant drivers of both OP-DTT and OP-AA, whereas OP-DTT is in general much more sensitive to other organic compounds, particularly photochemically aged organic species. Therefore, PM samples with higher levels of certain transition metals such as Cu, Fe or Mn and some OP-sensitive organic compounds, may result in higher OP values independently of their PM mass concentration. In this way, Weichenthal et al. [30] found that the strength of association between PM2.5 and the risk of acute cardiovascular events was highly influenced by the levels of PM-bound transition metals and S (which is usually correlated with some of these transition metals), because OP metrics were strongly correlated with these metals.

Our results support an association between PM-OP and inflammation as a whole, as we found associations between OP and IL levels for both OP assays (OP-DTT and OP-AA).

However, our findings suggest that the OP of the fine fraction plays a more important role in causing systemic inflammation compared to the coarse fraction. This makes sense, considering that the fine fraction can penetrate deeper into the smaller airways. On the other hand, our results, based predominantly on a population living in a mixed urban-industrial area, showed lower PM-OP levels than those reported in other studies [31]. It is conceivable to extrapolate that stronger associations might have been found in a more exposed population.

When we analyzed PM-OP using the stationary samplers located in Maliaño and Santander (the urban-industrial and urban sites, respectively, as shown in Figure S1), we observed differences, with higher levels of PM-OP and metals in the stationary samples from the urban-industrial site compared to those from the urban site. However, for the personal samples assessed in the present study, no spatial pattern was found, suggesting that work and/or leisure activities (hobbies) outside the place of residence substantially contribute to the individual personal exposure. Therefore, since no differences in the geographic distribution of places of residence were observed between asthmatic and non-asthmatic volunteers, the lower levels of PM-OP in non-asthmatic volunteers may be related to different educational levels (higher university studies in non-asthmatics), indicating different occupations or hobbies. Nevertheless, it is difficult to interpret with a single measurement per person, as in our current cross-sectional approach; so, this is a shortcoming that needs to be improved in future prospective studies.

We have presented both crude results and after adjusting for predefined confounders. Table S13 shows the percentage change in the OR after including each predefined confounding variable for the main analyses. We maintained all the predefined variables in the final multivariate model as stated in the research protocol in order to prevent selective reporting bias. The differences observed between the crude (unadjusted) and adjusted MDs and ORs highlight the importance of controlling for confounding bias using multivariate regression models. Because of this, we included asthma-specific clinical variables such as severity of asthma (GINA stage) and the ACT and TAI results in a multivariate regression model restricted to asthmatic patients. We found a clear dose–response pattern for the OP of the fine fraction, with adjusted ORs that reached statistical significance based on both the OP-DTT and OP-AA methods (adjusted p-trends 0.029 and 0.01, respectively). The dose–response pattern is one of Bradford Hill's classic causality criteria and would therefore support the association between higher OP exposure and elevated IL-6 and IL-6/IL-10 levels. Beyond statistical significance, the existence of a dose–response pattern provides additional support for a real causal association.

Studies evaluating the relationship between PM exposure and blood IL-6 levels have reported mixed results. While most studies [6,21–23,32–35] have found a positive association, others [36–40] have observed no relationship. These contradictory results may be due to the different characteristics of study participants in relation to age, use of healthy volunteers versus volunteers with a disease as inclusion criterion, the study design (observational versus experimental with different compositions and concentrations of PM), the matrix used to determine IL levels (serum, plasma, other matrices…), or the different approaches for controlling confounding bias.

Among these studies, to our knowledge, only three have included asthmatic patients. Urch et al. [34] measured IL-6 blood levels before and after exposures in their experimental study, using a concentrated ambient particle (CAP) facility for PM2.5, in 10 mild asthmatic and 13 non-asthmatic individuals (18–40 years old). They observed an increase in IL-6 blood levels three hours post exposure, but only after CAP alone exposures (without ozone), and the IL-6 increase was associated with increased PM2.5 mass concentration, suggesting a dose–response pattern. The responses of asthmatic and non-asthmatic volunteers were similar. In contrast, Brown et al. [38] found no association between asthmatic children (aged 6–17 years old) living near a major roadway and IL-6 or IL-10 plasma levels. Lastly, Klümper et al. [23] recruited 27 children with asthma and 59 without asthma (all aged 6-year-old). Their findings showed a differential response between the two groups. No

association was found between air pollution and IL-6 or IL-10 in non-asthmatic children. However, the mean ratios for asthmatic children tended to be greater than 1, suggesting that children with asthma are more susceptible to traffic-related air pollution exposure, compared to non-asthmatic children.

An important methodological strength of our study is the use of PM personal samplers, also known as personal environmental monitors (PEM), to characterize the individual PM-OP exposure in each volunteer. It consists of a portable impactor connected to a personal pump. The impactor enabled the separation of fine (PM2.5) and coarse (PM10–2.5) particles and for each particle size the two OP assays (DTT and AA) were performed. As mentioned in the introduction section, there are very few studies that have characterized PM-OP using personal samplers [8–11,41]. To our knowledge, only two studies have utilized PM personal samplers specifically in asthmatic patients. Both studies focused on children, and neither measured PM-OP. In the study by Isiugo et al. [42], the children did not carry the personal samplers. Instead, the personal samplers were placed 48 h outdoors and in the bedrooms of the children's homes (indoors), and only spirometries were performed to determine lung function. In the study published by Delfino et al. [43], 45 children carried personal samplers, but only FeNO was determined. Therefore, our study is the first one on the association between the PM-OP obtained using personal samplers and ILs blood levels. In contrast, an important limitation of our study is the sample size and the statistical power to detect positive associations as statistically significant. Because of this, most of the statistically significant associations observed in the total sample (n = 81), lost statistical significance in the stratified analysis (n = 44 asthmatics and n = 37 controls) with wider 95% CI.

For clinical management, asthmatic patients are classified into type 2-high and type 2-low. In type 2-high asthma, type 2 inflammation is present with its associated cytokines IL-4, IL-5, and IL-13, high levels of blood and/or sputum eosinophils, and elevated FeNO. Type 2-low asthma is defined by the absence of type 2 markers. Both types of inflammation are not mutually exclusive and overlapping phenotypes can occur in asthmatic patients [17–19]. Genome-wide association studies and other basic research have shown an association between IL-6 signaling and asthma [44,45], which is also supported by clinical studies [46]; and there is growing evidence of subgroups of type 2-low asthma where IL-6 plays a major role. These patients might benefit from another biologic targeting IL-6 signaling such as Olamkicept [47]. Our ASTHMA-FENOP study was designed to compare results between asthmatic and non-asthmatic adults, based on the rationale that inflammation in response to PM-OP may differ between these two groups. IL-6 levels (as well as IL-6/IL-10 ratio) were slightly higher in our non-asthmatic compared to asthmatic patients, with medians of 9.24 and 7.86 pg/mL, respectively. However, no big differences were found when comparing the associations between PM-OP and IL-6 levels or the IL-6/IL-10 ratio. This suggests that higher PM-OP increases IL-6 levels and the IL-6/IL-10 ratio in both asthmatic and non-asthmatic adults.

5. Conclusions

We found an independent association between PM-OP and systemic inflammation, as determined by IL-6 levels and the IL-6/IL-10 ratio, in both asthmatic and non-asthmatic volunteers after adjusting for confounding variables; and with a dose-response pattern that suggests causality and supports that asthma is a heterogeneous disease at the molecular level. Future studies with a larger number of subjects will be needed to clarify the association between higher PM-OP exposure and levels of IL-6 and IL-6/IL-10 ratio, as well as their potential clinical implications.

Supplementary Materials: The following supporting information can be downloaded at: https://www.mdpi.com/article/10.3390/antiox13121464/s1, Figure S1: Location of volunteers' residences (blue points) and the two stationary sampling points (urban and urban-industrial) (red points) established by the research group; Table S1: Visit protocol for the volunteers (n = 81); Table S2: PM-OP detection limits (D.L), mean of blank filters, and percentage of samples higher than the D.L.; Table S3: Description of asthmatic patients as a function of gender.; Table S4: Description of

the sample as a function of their asthma or control statuses.; Table S5: Crude association between PM-OP metrics and IL-6 levels, overall and as a function of their asthma or control statuses; Table S6: Adjusted association between PM-OP metrics and IL-6 levels, overall and as a function of their asthma or control statuses.; Table S7: Crude association between PM-OP metrics and the IL-6/IL-10 ratio, overall and as a function of their asthma or control statuses.; Table S8: Adjusted association between PM-OP metrics and the IL-6/IL-10 ratio, overall and as a function of their asthma or control statuses.; Table S9: Crude mean differences (MD) for IL-6 levels, between higher and lower PM-OP values.; Table S10: Adjusted mean differences (aMD) for the IL-6/IL-10 ratio, between higher and lower PM-OP values.; Table S11: Crude mean differences (MD) for IL-6 levels, between higher and lower PM-OP values.; Table S12: Adjusted mean differences (aMD) for the IL-6/IL-10 ratio, between higher and lower PM-OP values.; Table S13: % of change in the OR for high IL-6 levels, after including each predefined confounding variable, in all patients (n = 81).

Author Contributions: M.S.: Conceptualization. Data curation. Formal analysis. Funding acquisition. Investigation. Methodology. Supervision. Writing—original draft. A.E.: Data curation. Formal analysis. Investigation. Methodology. Writing—review and editing. L.R.-A.: Investigation and Formal analysis. I.F.-O.: Conceptualization. Funding acquisition. Investigation. Methodology. Project administration. Resources. Supervision. Validation. Writing—review and editing. J.A., J.J.R.-C., B.A., J.L.G.-R., C.A.A. and J.M.C.: Data curation; Funding acquisition; Investigation; Resources. M.L.-H. and E.B.: Conceptualization. Formal analysis. Investigation. Resources. J.I.: Formal analysis. Investigation. Resources. Data curation. Investigation. Resources. Y.R., A.B. and A.N.-R.: Data curation. Investigation. Resources. All authors have read and agreed to the published version of the manuscript.

Funding: This work was supported by the Spanish Society of Pneumology (SEPAR Nº 1383/23; Nº 1616/24) and the Spanish Ministry of Science and Innovation (Project PID2020-114787RBI00, funded by MCIN/AEI/10.13039/501100011033 and "ERDF A way of making Europe").

Institutional Review Board Statement: The study was conducted in accordance with the Declaration of Helsinki and was approved by the Clinical Research Ethics Committee of Cantabria (CEIC) (internal codes 2020.475 and 2023.412), and the ethics committee of the UC (CEPI) (internal code: 16.2021).

Informed Consent Statement: Informed consent was obtained from all subjects involved in the study.

Data Availability Statement: Data cannot be made publicly available in order to protect patient privacy. The data are available on request from the University of Cantabria Archive (http://repositorio.unican.es/, accessed on 25 November 2024) for researchers who meet the criteria for access to confidential data. Requests may be sent to the Ethics Committee (ceicc@idival.org), or Miguel Santibañez (santibanezm@unican.es).

Conflicts of Interest: The authors declare that they have no known competing financial interests or personal relationships that could have appeared to influence the work reported in this paper.

References

1. Guo, C.; Lv, S.; Liu, Y.; Li, Y. Biomarkers for the adverse effects on respiratory system health associated with atmospheric particulate matter exposure. *J. Hazard. Mater.* **2022**, *421*, 126760. [CrossRef] [PubMed]
2. Kaufman, J.D.; Elkind, M.S.V.; Bhatnagar, A.; Koehler, K.; Balmes, J.R.; Sidney, S.; Burroughs Peña, M.S.; Dockery, D.W.; Hou, L.; Brook, R.D.; et al. Guidance to Reduce the Cardiovascular Burden of Ambient Air Pollutants: A Policy Statement From the American Heart Association. *Circulation* **2020**, *142*, e432–e447; Erratum in *Circulation* **2020**, *142*, e449. [CrossRef] [PubMed]
3. He, R.W.; Shirmohammadi, F.; Gerlofs-Nijland, M.E.; Sioutas, C.; Cassee, F.R. Pro-inflammatory responses to PM0.25 from airport and urban traffic emissions. *Sci. Total Environ.* **2018**, *640–641*, 997–1003. [CrossRef] [PubMed]
4. Weichenthal, S.; Crouse, D.L.; Pinault, L.; Godri-Pollitt, K.; Lavigne, E.; Evans, G.; van Donkelaar, A.; Martin, R.V.; Burnett, R.T. Oxidative burden of fine particulate air pollution and risk of cause-specific mortality in the Canadian Census Health and Environment Cohort (CanCHEC). *Environ. Res.* **2016**, *146*, 92–99. [CrossRef] [PubMed]
5. Bates, J.T.; Fang, T.; Verma, V.; Zeng, L.; Weber, R.J.; Tolbert, P.E.; Abrams, J.Y.; Sarnat, S.E.; Klein, M.; Mulholland, J.A.; et al. Review of Acellular Assays of Ambient Particulate Matter Oxidative Potential: Methods and Relationships with Composition, Sources, and Health Effects. *Environ. Sci. Technol.* **2019**, *53*, 4003–4019. [CrossRef]
6. Zhang, X.; Staimer, N.; Gillen, D.L.; Tjoa, T.; Schauer, J.J.; Shafer, M.M.; Hasheminassab, S.; Pakbin, P.; Vaziri, N.D.; Sioutas, C.; et al. Associations of oxidative stress and inflammatory biomarkers with chemically-characterized air pollutant exposures in an elderly cohort. *Environ. Res.* **2016**, *150*, 306–319. [CrossRef]

7. Brehmer, C.; Norris, C.; Barkjohn, K.K.; Bergin, M.H.; Zhang, J.; Cui, X.; Zhang, Y.; Black, M.; Li, Z.; Shafer, M.; et al. The impact of household air cleaners on the chemical composition and children's exposure to PM2.5 metal sources in suburban Shanghai. *Environ. Pollut.* **2019**, *253*, 190–198. [CrossRef]
8. Brehmer, C.; Norris, C.; Barkjohn, K.K.; Bergin, M.H.; Zhang, J.; Cui, X.; Teng, Y.; Zhang, Y.; Black, M.; Li, Z.; et al. The impact of household air cleaners on the oxidative potential of PM2.5 and the role of metals and sources associated with indoor and outdoor exposure. *Environ. Res.* **2020**, *181*, 108919. [CrossRef]
9. Marsal, A.; Sauvain, J.J.; Thomas, A.; Lyon-Caen, S.; Borlaza, L.J.S.; Philippat, C.; Jaffrezo, J.L.; Boudier, A.; Darfeuil, S.; Elazzouzi, R.; et al. Effects of personal exposure to the oxidative potential of PM2.5 on oxidative stress biomarkers in pregnant women. *Sci. Total Environ.* **2024**, *911*, 168475. [CrossRef]
10. Quinn, C.; Miller-Lionberg, D.D.; Klunder, K.J.; Kwon, J.; Noth, E.M.; Mehaffy, J.; Leith, D.; Magzamen, S.; Hammond, S.K.; Henry, C.S.; et al. Personal Exposure to PM2.5 Black Carbon and Aerosol Oxidative Potential using an Automated Microenvironmental Aerosol Sampler (AMAS). *Environ. Sci. Technol.* **2018**, *52*, 11267–11275. [CrossRef]
11. Secrest, M.H.; Schauer, J.J.; Carter, E.M.; Lai, A.M.; Wang, Y.; Shan, M.; Yang, X.; Zhang, Y.; Baumgartner, J. The oxidative potential of PM2.5 exposures from indoor and outdoor sources in rural China. *Sci. Total Environ.* **2016**, *571*, 1477–1489. [CrossRef]
12. Wang, Z.; Li, Y.; Gao, Y.; Fu, Y.; Lin, J.; Lei, X.; Zheng, J.; Jiang, M. Global, regional, and national burden of asthma and its attributable risk factors from 1990 to 2019: A systematic analysis for the Global Burden of Disease Study 2019. *Respir. Res.* **2023**, *24*, 169. [CrossRef] [PubMed]
13. Jacquemin, B.; Siroux, V.; Sanchez, M.; Carsin, A.E.; Schikowski, T.; Adam, M.; Bellisario, V.; Buschka, A.; Bono, R.; Brunekreef, B.; et al. Ambient air pollution and adult asthma incidence in six European cohorts (ESCAPE). *Environ. Health Perspect.* **2015**, *123*, 613–621. [CrossRef] [PubMed]
14. Fan, J.; Li, S.; Fan, C.; Bai, Z.; Yang, K. The impact of PM2.5 on asthma emergency department visits: A systematic review and meta-analysis. *Environ. Sci. Pollut. Res.* **2016**, *23*, 843–850. [CrossRef] [PubMed]
15. Karakatsani, A.; Analitis, A.; Perifanou, D.; Ayres, J.G.; Harrison, R.M.; Kotronarou, A.; Kavouras, I.G.; Pekkanen, J.; Hämeri, K.; Kos, G.P.; et al. Particulate matter air pollution and respiratory symptoms in individuals having either asthma or chronic obstructive pulmonary disease: A European multicentre panel study. *Environ. Health* **2012**, *11*, 75. [CrossRef]
16. Park, J.; Kim, B.Y.; Park, E.J.; Shin, Y.I.; Ryu, J.H. Photobiomodulation Mitigates PM2.5-Exacerbated Pathologies in a Mouse Model of Allergic Asthma. *Antioxidants* **2024**, *13*, 1003. [CrossRef]
17. Brusselle, G.G.; Koppelman, G.H. Biologic Therapies for Severe Asthma. *N. Engl. J. Med.* **2022**, *386*, 157–171. [CrossRef]
18. Israel, E.; Reddel, H.K. Severe and Difficult-to-Treat Asthma in Adults. *N. Engl. J. Med.* **2017**, *377*, 965–976. [CrossRef]
19. Robinson, D.; Humbert, M.; Buhl, R.; Cruz, A.A.; Inoue, H.; Korom, S.; Hanania, N.A.; Nair, P. Revisiting Type 2-high and Type 2-low airway inflammation in asthma: Current knowledge and therapeutic implications. *Clin. Exp. Allergy* **2017**, *47*, 161–175. [CrossRef]
20. Canova, C.; Minelli, C.; Dunster, C.; Kelly, F.; Shah, P.L.; Caneja, C.; Tumilty, M.K.; Burney, P. PM10 oxidative properties and asthma and COPD. *Epidemiology* **2014**, *25*, 467–468. [CrossRef]
21. Hassanvand, M.S.; Naddafi, K.; Kashani, H.; Faridi, S.; Kunzli, N.; Nabizadeh, R.; Momeniha, F.; Gholampour, A.; Arhami, M.; Zare, A.; et al. Short-term effects of particle size fractions on circulating biomarkers of inflammation in a panel of elderly subjects and healthy young adults. *Environ. Pollut.* **2017**, *223*, 695–704. [CrossRef] [PubMed]
22. Jaafari, J.; Naddafi, K.; Yunesian, M.; Nabizadeh, R.; Hassanvand, M.S.; Shamsipour, M.; Ghanbari Ghozikali, M.; Nazmara, S.; Shamsollahi, H.R.; Yaghmaeian, K. Associations between short term exposure to ambient particulate matter from dust storm and anthropogenic sources and inflammatory biomarkers in healthy young adults. *Sci. Total Environ.* **2021**, *761*, 144503. [CrossRef] [PubMed]
23. Klümper, C.; Krämer, U.; Lehmann, I.; von Berg, A.; Berdel, D.; Herberth, G.; Beckmann, C.; Link, E.; Heinrich, J.; Hoffmann, B.; et al. Air pollution and cytokine responsiveness in asthmatic and non-asthmatic children. *Environ. Res.* **2015**, *138*, 381–390. [CrossRef] [PubMed]
24. Fajgenbaum, D.C.; June, C.H. Cytokine Storm. *N. Engl. J. Med.* **2020**, *383*, 2255–2273. [CrossRef]
25. Azaiz, M.B.; Jemaa, A.B.; Sellami, W.; Romdhani, C.; Ouslati, R.; Gharsallah, H.; Ghazouani, E.; Ferjani, M. Deciphering the balance of IL-6/IL-10 cytokines in severe to critical COVID-19 patients. *Immunobiology* **2022**, *227*, 152236. [CrossRef]
26. Ulhaq, Z.S.; Soraya, G.V.; Hasan, Y.T.N.; Rachma, L.N.; Rachmawati, E.; Shodry, S.; Kusuma, M.A.S. Serum IL-6/IL-10 ratio as a biomarker for the diagnosis and severity assessment of primary-open angle glaucoma. *Eur. J. Ophthalmol.* **2022**, *32*, 2259–2264. [CrossRef]
27. Global Initiative for Asthma. Global Strategy for Asthma Management and Prevention. 2020. Available online: www.ginasthma.org (accessed on 20 November 2021).
28. Hernández-Pellón, A.; Fernández-Olmo, I. Airborne concentration and deposition of trace metals and metalloids in an urban area downwind of a manganese alloy plant. *Atmos. Pollut. Res.* **2019**, *10*, 712–721. [CrossRef]
29. Expósito, A.; Maillo, J.; Uriarte, I.; Santibáñez, M.; Fernandez-Olmo, I. Kinetics of ascorbate and dithiothreitol oxidation by soluble copper, iron, and manganese, and 1,4-naphthoquinone: Influence of the species concentration and the type of fluid. *Chemosphere* **2024**, *361*, 142435. [CrossRef]

30. Weichenthal, S.; Lavigne, E.; Traub, A.; Umbrio, D.; You, H.; Pollitt, K.; Shin, T.; Kulka, R.; Stieb, D.M.; Korsiak, J.; et al. Association of sulfur, transition metals, and the oxidative potential of outdoor with acute cardiovascular events: A case-crossover study of Canadian adults. *Environ. Health Perspect.* **2021**, *129*, 107005. [CrossRef]
31. in't Veld, M.; Pandolfi, M.; Amato, F.; Pérez, N.; Reche, C.; Dominutti, P.; Jaffrezo, J.; Alastuey, A.; Querol, X.; Uzu, G. Discovering oxidative potential (OP) drivers of atmospheric PM10, PM2.5, and PM1 simultaneously in North-Eastern Spain. *Sci. Total Environ.* **2023**, *857*, 159386. [CrossRef]
32. Delfino, R.J.; Staimer, N.; Tjoa, T.; Gillen, D.L.; Polidori, A.; Arhami, M.; Kleinman, M.T.; Vaziri, N.D.; Longhurst, J.; Sioutas, C. Air pollution exposures and circulating biomarkers of effect in a susceptible population: Clues to potential causal component mixtures and mechanisms. *Environ. Health Perspect.* **2009**, *117*, 1232–1238. [CrossRef] [PubMed]
33. Delfino, R.J.; Staimer, N.; Tjoa, T.; Arhami, M.; Polidori, A.; Gillen, D.L.; George, S.C.; Shafer, M.M.; Schauer, J.J.; Sioutas, C. Associations of primary and secondary organic aerosols with airway and systemic inflammation in an elderly panel cohort. *Epidemiology* **2010**, *21*, 892–902. [CrossRef] [PubMed]
34. Urch, B.; Speck, M.; Corey, P.; Wasserstein, D.; Manno, M.; Lukic, K.Z.; Brook, J.R.; Liu, L.; Coull, B.; Schwartz, J.; et al. Concentrated ambient fine particles and not ozone induce a systemic interleukin-6 response in humans. *Inhal. Toxicol.* **2010**, *22*, 210–218. [CrossRef] [PubMed]
35. Liu, L.; Urch, B.; Szyszkowicz, M.; Evans, G.; Speck, M.; Van Huang, A.; Leingartner, K.; Shutt, R.H.; Pelletier, G.; Gold, D.R.; et al. Metals and oxidative potential in urban particulate matter influence systemic inflammatory and neural biomarkers: A controlled exposure study. *Environ. Int.* **2018**, *121 Pt 2*, 1331–1340. [CrossRef]
36. Behbod, B.; Urch, B.; Speck, M.; Scott, J.A.; Liu, L.; Poon, R.; Coull, B.; Schwartz, J.; Koutrakis, P.; Silverman, F.; et al. Endotoxin in concentrated coarse and fine ambient particles induces acute systemic inflammation in controlled human exposures. *Occup. Environ. Med.* **2013**, *70*, 761–767. [CrossRef]
37. Bräuner, E.V.; Møller, P.; Barregard, L.; Dragsted, L.O.; Glasius, M.; Wåhlin, P.; Vinzents, P.; Raaschou-Nielsen, O.; Loft, S. Exposure to ambient concentrations of particulate air pollution does not influence vascular function or inflammatory pathways in young healthy individuals. *Part. Fibre Toxicol.* **2008**, *5*, 13. [CrossRef]
38. Brown, M.S.; Sarnat, S.E.; DeMuth, K.A.; Brown, L.A.; Whitlock, D.R.; Brown, S.W.; Tolbert, P.E.; Fitzpatrick, A.M. Residential proximity to a major roadway is associated with features of asthma control in children. *PLoS ONE* **2012**, *7*, e37044. [CrossRef]
39. Liu, L.; Ruddy, T.; Dalipaj, M.; Poon, R.; Szyszkowicz, M.; You, H.; Dales, R.E.; Wheeler, A.J. Effects of indoor, outdoor, and personal exposure to particulate air pollution on cardiovascular physiology and systemic mediators in seniors. *J. Occup. Environ. Med.* **2009**, *51*, 1088–1098. [CrossRef]
40. Steenhof, M.; Mudway, I.S.; Gosens, I.; Hoek, G.; Godri, K.J.; Kelly, F.J.; Harrison, R.M.; Pieters, R.H.; Cassee, F.R.; Lebret, E.; et al. Acute nasal pro-inflammatory response to air pollution depends on characteristics other than particle mass concentration or oxidative potential: The RAPTES project. *Occup. Environ. Med.* **2013**, *70*, 341–348. [CrossRef]
41. Shang, J.; Zhang, Y.; Schauer, J.J.; Chen, S.; Yang, S.; Han, T.; Zhang, D.; Zhang, J.; An, J. Prediction of the oxidation potential of PM2.5 exposures from pollutant composition and sources. *Environ. Pollut.* **2022**, *293*, 118492. [CrossRef]
42. Isiugo, K.; Jandarov, R.; Cox, J.; Ryan, P.; Newman, N.; Grinshpun, S.A.; Indugula, R.; Vesper, S.; Reponen, T. Indoor particulate matter and lung function in children. *Sci. Total Environ.* **2019**, *663*, 408–417. [CrossRef] [PubMed]
43. Delfino, R.J.; Staimer, N.; Gillen, D.; Tjoa, T.; Sioutas, C.; Fung, K.; George, S.C.; Kleinman, M.T. Personal and ambient air pollution is associated with increased exhaled nitric oxide in children with asthma. *Environ. Health Perspect.* **2006**, *114*, 1736–1743. [CrossRef] [PubMed]
44. Hawkins, G.A.; Robinson, M.B.; Hastie, A.T.; Li, X.; Li, H.; Moore, W.C.; Howard, T.D.; Busse, W.W.; Erzurum, S.C.; Wenzel, S.E.; et al. The IL6R variation Asp(358)Ala is a potential modifier of lung function in subjects with asthma. *J. Allergy Clin. Immunol.* **2012**, *130*, 510–515.e1. [CrossRef] [PubMed]
45. Jevnikar, Z.; Östling, J.; Ax, E.; Calvén, J.; Thörn, K.; Israelsson, E.; Öberg, L.; Singhania, A.; Lau, L.C.K.; Wilson, S.J.; et al. Epithelial IL-6 trans-signaling defines a new asthma phenotype with increased airway inflammation. *J. Allergy Clin. Immunol.* **2019**, *143*, 577–590. [CrossRef]
46. Rincon, M.; Irvin, C.G. Role of IL-6 in asthma and other inflammatory pulmonary diseases. *Int. J. Biol. Sci.* **2012**, *8*, 1281–1290. [CrossRef]
47. El-Husseini, Z.W.; Khalenkow, D.; Lan, A.; van der Molen, T.; Brightling, C.; Papi, A.; Rabe, K.F.; Siddiqui, S.; Singh, D.; Kraft, M.; et al. An epithelial gene signature of trans-IL-6 signaling defines a subgroup of type 2-low asthma. *Respir. Res.* **2023**, *24*, 308. [CrossRef]

antioxidants

MDPI

Article

Photobiomodulation Mitigates $PM_{2.5}$-Exacerbated Pathologies in a Mouse Model of Allergic Asthma

Jisu Park [1], Bo-Young Kim [1], Eun Jung Park [1], Yong-Il Shin [1,2,*] and Ji Hyeon Ryu [1,*]

[1] Research Institute for Convergence of Biomedical Science and Technology, Pusan National University Yangsan Hospital, Yangsan 50612, Gyeongnam, Republic of Korea; jiss5022@naver.com (J.P.); kimboyoung@pusan.ac.kr (B.-Y.K.); foreverpak1@nate.com (E.J.P.)

[2] Department of Rehabilitation Medicine, School of Medicine, Pusan National University, Yangsan 50612, Gyeongnam, Republic of Korea

* Correspondence: rmshin@pusan.ac.kr (Y.-I.S.); wlgus9217@naver.com or jihyeon@pnuyh.co.kr (J.H.R.); Tel.: +82-55-360-2872 (Y.-I.S.); +82-55-360-4763 (J.H.R.)

Abstract: Exposure to particulate matter (PM), especially $PM_{2.5}$, is known to exacerbate asthma, posing a significant public health risk. This study investigated the asthma-reducing effects of photobiomodulation (PBM) in a mice model mimicking allergic airway inflammation exacerbated by $PM_{2.5}$ exposure. The mice received sensitization with ovalbumin (OVA) and were subsequently treated with $PM_{2.5}$ at a dose of 0.1 mg/kg every 3 days, for 9 times over 3 weeks during the challenge. PBM, using a 610 nm wavelength LED, was applied at 1.7 mW/cm^2 to the respiratory tract via direct skin contact for 20 min daily for 19 days. Results showed that PBM significantly reduced airway hyperresponsiveness, plasma immunoglobulin E (IgE) and OVA-specific IgE, airway inflammation, T-helper type 2 cytokine, histamine and tryptase in bronchoalveolar lavage fluid (BALF), and goblet cell hyperplasia in $PM_{2.5}$-exposed asthmatic mice. Moreover, PBM alleviated subepithelial fibrosis by reducing collagen deposition, airway smooth muscle mass, and expression of fibrosis-related genes. It mitigated reactive oxygen species generation, oxidative stress, endoplasmic reticulum stress, apoptotic cell death, ferroptosis, and modulated autophagic signals in the asthmatic mice exposed to $PM_{2.5}$. These findings suggest that PBM could be a promising intervention for $PM_{2.5}$-induced respiratory complications in patients with allergic asthma.

Keywords: asthma; ferroptosis; oxidative stress; particulate matter ($PM_{2.5}$); photobiomodulation

1. Introduction

Asthma is a chronic respiratory disease characterized by airway inflammation, variable airflow obstruction, airway hyperresponsiveness (AHR), and structural remodeling of the lungs. It affects millions of individuals worldwide, posing a significant health concern [1]. The pathogenesis of asthma is complex, involving a combination of genetic predispositions and environmental factors that contribute to the development and exacerbation of this respiratory disorder.

Exposure to particulate matter (PM), one of the prominent airborne pollutants, is associated with an elevated risk of incidence and exacerbations of the severity of pulmonary diseases like asthma. Its health effects are more aggravated in children being more vulnerable than adults [2]. Fine PM, with a diameter smaller than 2.5 μm (referred to as $PM_{2.5}$), can penetrate the bronchioles and alveoli, trigger inflammation and oxidative stress, and impair respiratory functions [3]. Additionally, maternal exposure to elevated concentrations of $PM_{2.5}$ during pregnancy increases the likelihood of asthma incidence in infants [4]. $PM_{2.5}$ exposure can also cause chronic non-specific inflammatory respiratory diseases [5,6], leading to reversible airflow limitation, airway inflammation, airway remodeling, and increased AHR, thus complicating asthma management [7]. Therefore, understanding the relationship between PM exposure and asthma exacerbation, particularly emphasizing the

importance of elucidating the underlying mechanisms involved and developing targeted therapeutic interventions, has gained increased research interest.

Photobiomodulation (PBM) is a form of light therapy that uses non-ionizing light sources, such as lasers, light emitting diodes (LEDs), or broadband light, in the visible and near-infrared spectrum. It is a non-invasive treatment approach that reduces pain and inflammation, promotes tissue repair, and improves overall cellular function [8,9]. The mechanism action of PBM involves the absorption of light energy by cellular components, such as mitochondria, which leads to increased ATP production, modulation of reactive oxygen species (ROS), and activation of intracellular signaling pathways [10]. These cellular responses result in anti-inflammatory, analgesic, and regenerative effects, making PBM a promising therapeutic approach for a wide range of medical conditions. This therapy is cost-effective, easy to use, and, most importantly, free from long-term side effects [11]. Therefore, PBM therapy has garnered wide recognition for its potential therapeutic benefits across various medical fields.

Drug therapy remains the primary approach for managing chronic respiratory diseases, such as asthma. Therefore, the key focus of the reported studies has been novel drugs to treat such conditions; nevertheless, the efficacy of PBM as an adjunctive therapy for respiratory disease treatment has also been recognized. Numerous studies have shown the effectiveness of PBM therapy in experimental models of respiratory conditions. Researchers have been actively investigating the potential therapeutic effects of PBM on asthma both in clinical settings and in experimental models. Using orange LED light at a wavelength of 610 nm, PBM therapy has been shown to exhibit anti-asthmatic effects by suppressing Th2 responses and bronchoconstriction-promoting substances through inhibition in the MAPK/NF-κB cascade [12]. Moreover, PBM therapy has been demonstrated to reduce inflammation by promoting an increase in regulatory T cell population [13] and regulating mast cell degranulation and IL-10 levels [14]. Furthermore, PBM has a beneficial effect on corticosteroid-resistant asthma mice [15]. Low-intensity laser PBM has proven to be both highly effective and safe in a study involving 220 patients with bronchial asthma [16]. In another study involving low-level laser acupuncture in 48 asthmatic children, 91.7% of patients experienced improved asthma control through a notable reduction in the breath condensate fractional exhaled nitric oxide level and a significant increase in spirometry parameters [17]. This concerted effort underscores a growing interest in exploring how PBM may offer novel treatment options for individuals with asthma, highlighting the need for further exploration and validation of its efficacy in respiratory conditions. Therefore, in the context of allergic asthma exacerbated by $PM_{2.5}$ exposure, the use of PBM as a therapeutic intervention shows promise in modulating immune responses, reducing airway inflammation, and ameliorating oxidative stress-induced damage in the lungs.

The present study aimed to explore the effects of PBM on $PM_{2.5}$ exposure-exacerbated allergic asthma in a mouse model. By assessing a range of parameters, including AHR, airway inflammation, T-helper type 2 (Th2) cytokines, bronchoconstrictor mediators, subepithelial fibrosis, endoplasmic reticulum (ER) stress induced by reactive oxygen species (ROS), apoptosis, ferroptosis and autophagic signals, the study sought to elucidate the potential anti-asthmatic mechanisms of PBM treatment. The study significantly advances the knowledge in this research field by demonstrating the effectiveness of PBM in alleviating and attenuating a broad range of adverse effects caused by $PM_{2.5}$ exposure in allergic asthma. It not only highlights the potential of PBM as a promising therapeutic intervention for individuals with allergic asthma exposed to environmental pollutants like $PM_{2.5}$ but also underscores the importance of considering multiple cellular and molecular pathways in the evaluation of treatment outcomes. Overall, the study provides valuable insights into the holistic effects of PBM on various pathological mechanisms associated with allergic asthma exacerbations induced by environmental factors like $PM_{2.5}$.

2. Materials and Methods

2.1. $PM_{2.5}$ Preparation

The $PM_{2.5}$ ($PM_{2.5}$-like; ERM-CZ110) used in the study was purchased from European Reference Materials (B-2400, European Commission, Geel, Belgium) and was obtained from the walls and sidewalks of a road tunnel in Poland. The specific manufacturing processes of $PM_{2.5}$ samples are detailed in their corresponding certification reports [18]. This $PM_{2.5}$ was certified for its water-soluble ions content, which includes Na^+ (20.4 g/kg), K^+ (3.3 g/kg), Ca^{2+} (44 g/kg), Mg^{2+} (1.8 g/kg), Cl^- (26.2 g/kg), NO_3^- (7.8 g/kg), and SO_4^{2-} (75 g/kg) [18]. The $PM_{2.5}$ was diluted in phosphate-buffered saline (PBS) and sonicated before use.

2.2. Mouse Model of Asthma and $PM_{2.5}$ Exposure

All animal studies were sanctioned by the Institutional Animal Care and Use Committee of Pusan National University Yangsan Hospital and conducted in compliance with the National Institute of Health Guidelines (IACUC No.: 2021-030-A1C0(0)). The mice were assigned to six groups with 7−8 mice in each group, labeled as control, PM + OVA, PM + OVA + PBM, PM + OVA + DEX, PM, and OVA. The asthma model was established following a method outlined in a prior investigation [19]. Briefly, on days 0, 7, and 14, each mouse was sensitized by intraperitoneal injection of 75 µg OVA (BioVender, Asheville, NC, USA) in 200 µL PBS containing 2 mg aluminum hydroxide (Imject Alum; Thermo Scientific, Rockford, IL, USA). The mice were subjected to an intranasal challenge of 50 µg OVA in PBS three times a week for 3 weeks following isoflurane anesthesia induction (Hana Pharm Co., Ltd., Hwaseong, Republic of Korea; 2% induction and 1.5% maintenance, in 80% N_2O and 20% O_2). Control mice were sensitized and challenged with PBS at the corresponding times. Dexamethasone (3 mg/kg every 3 days; DEX; Sigma-Aldrich, St. Louis, MO, USA) was intraperitoneally administered 2 h before each OVA challenge. For PM-induced aggravation of asthma, mice were anesthetized with isoflurane and intranasally instilled with $PM_{2.5}$ (0.1 mg/kg/day) in 50 µL of PBS three times a week for 3 weeks before challenge (Figure 1A). The concentration of $PM_{2.5}$ used in the study was determined based on previous studies [20,21]. On the day of the procedure, measurements were taken for the spleen and thymus weights.

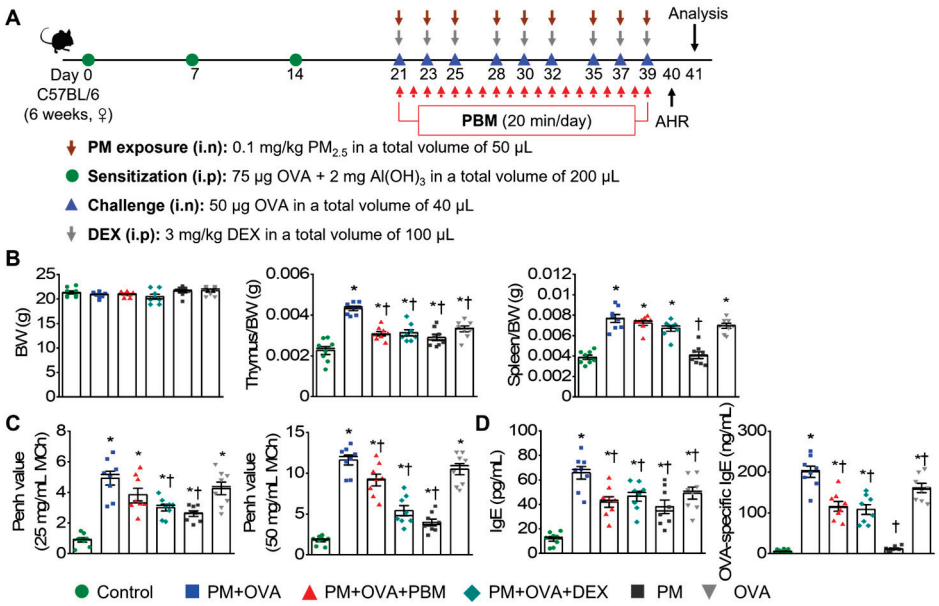

Figure 1. Inhibitory effects of PBM on the induction of airway hyperresponsiveness (AHR) and plasma IgE in a $PM_{2.5}$-exposed asthma exacerbation model. (**A**) Establishment of an allergic asthma exacerbation mouse model induced by $PM_{2.5}$ exposure. A timeline describing the asthma exacerbation

model induction and PBM treatment. (**B**) Measurement of body weight, thymus-to-body-weight ratio, and spleen-to-body-weight ratio on the final day of the experiment. (**C**) Assessment of AHR to methacholine (MCh) at concentrations of 25 and 50 mg/mL. (**D**) Measurement of total immunoglobulin E (IgE) and ovalbumin (OVA)-specific IgE in plasma. Data are shown as the mean ± SEM (n = 8). * $p < 0.05$ compared with control. † $p < 0.05$ compared with PM + OVA. i.n., intranasal injection; i.p., intraperitoneal injection; BW, body weight; PM, particulate matter; OVA, ovalbumin; PBM, photobiomodulation; DEX, dexamethasone.

2.3. Photobiomodulation Using Light-Emitting Diode (LED)

An LED device (dimensions: 4.9 × 4.9 × 1.3 cm, Color Seven Co., Seoul, Republic of Korea) was used for PBM with the following specifications: peak wavelength, 610 nm (full width at half maximum, 24 nm); power intensity, 1.7 mW/cm^2; energy density, 2.0 J/cm^2; electrode surface area, 1.6 cm; electrode spot size, 4 mm in diameter. The PBM protocol was based on a previous study [12]. Briefly, light stimulation was administered by placing probes onto the respiratory tract via direct skin contact once daily for 20 min after each OVA or PBS challenge under isoflurane anesthesia. The control group underwent the same anesthesia duration without PBM (Figure 1A).

2.4. Measurement of AHR

AHR to inhaled methacholine (MCh; Sigma) was assessed 24 h after the last challenge using whole-body plethysmography (OCP 3000, Allmedicus, Gyeonggi, Republic of Korea), following the established protocol [19]. The mice were subjected to 25 and 50 mg/mL concentrations of MCh for 10 min through a nebulizer (HARVARD73-1963; Harvard Apparatus, Holliston, MA, USA), and they were promptly placed back into their enclosures, with measurements being taken 150 s later. Enhanced pause (Penh), an indicator of airway resistance, was calculated using the average pressure recorded in the plethysmography chamber.

2.5. Bronchoalveolar Lavage Fluid (BALF) and Inflammatory Cells

The collection of BALF and subsequent differential cell counts were conducted following established procedures [19]. Mice were euthanized with a lethal dose of avertin tribromoethanol (Sigma-Aldrich Chemical Co., St. Louis, MO, USA).

A tracheostomy tube was used to flush the lung specimen with 1 mL of sterile cold PBS. BALF samples were centrifuged at 300× g for 10 min at 4 °C, and total bronchoalveolar lavage cells were enumerated using a hemocytometer. Cytospin (Thermo Shandon, Pittsburgh, PA, USA) was employed to attach differential cells to slides, which were subsequently stained with Diff-Quick (Sysmex International Reagents, Kobe, Japan). A total of 300 cells were counted under microscopy to determine the differential cell counts. BALF supernatants were stored at −80 °C until cytokine analysis.

2.6. Enzyme-Linked Immunoassay (ELISA)

Determination of total and OVA-specific IgE concentrations in plasma was assessed by sandwich ELISA (Mouse IgE ELISA kit, Bethyl Laboratories, Montgomery, TX, USA; anti-ovalbumin IgE ELISA kit, Cayman Chemical, Ann Arbor, MI, USA), as described previously [22]. Determination of IL-4, IL-5, IL-13, and histamine concentration in BALF was determined by sandwich ELISA (Th2 cytokines, R&D System, Minneapolis, MN, USA; histamine, Enzo Life Sciences, Ann Arbor, MI, USA) following the guidelines provided by the manufacturer [22]. Additionally, the levels of mast cell tryptase in BALF were also analyzed using an ELISA kit (Cusabio Biotech, Wuhan, China), as described in a previous study [23]. The optical density at 450 nm was measured with a microplate reader (SpectraMax iD5; Molecular Devices, San Jose, CA, USA).

2.7. Lung Histology and Immunohistochemistry

The lung tissues were fixed, embedded in paraffin, and 5 μm sections were prepared from the blocks. Lung inflammation was assessed via hematoxylin and eosin (H&E)

staining, mucus production was analyzed using the periodic acid–Schiff (PAS) staining kit (Millipore, Billerica, MA, USA), and collagen accumulation was evaluated by Masson's trichrome (MT) staining kit (Polysciences, Warrington, PA, USA) and Picro Sirius Red staining (Abcam, Cambridge, UK). Lung inflammation severity, mucin-positive goblet cells, and collagen deposition were scored using established grading systems [24–26]. Imaging was performed under a digital microscope (Axio Scan.Z1; Carl Zeiss, Jena, Germany), tissue analysis was conducted by three separate evaluators, and the outcomes were averaged. To determine airway smooth muscle volume, lung tissue samples were deparaffinized and kept overnight at 4 °C with monoclonal anti-actin and anti-smooth muscle actin (α-SMA)-FITC antibody (1:500; Sigma). The α-SMA immunostaining area was visualized using a confocal laser scanning microscope (LSM 900; Carl Zeiss, Germany) and quantified to assess airway smooth muscle layer thickness [27]. Immunohistochemical detection of 8-hydroxy-2′-deoxyguanosine (8-OHdG) in tissue slides was performed by antigen retrieval, and endogenous peroxidase was inactivated by treatment with 3% hydrogen peroxide. The slides were washed thrice in PBS and incubated with blocking buffer (10% normal goat serum in PBS) for 60 min at room temperature. The slides were incubated with 8-OHdG (Abcam) antibody overnight at 4 °C. Subsequently, the slides were incubated with horseradish peroxidase-conjugated goat anti-rabbit IgG antibody (DAKO, Carpinteria, CA, USA) for 60 min to detect immunoactivity, followed by detection using a DAB solution kit (DAKO). Hematoxylin was used as a counterstain. The stained specimens were examined using a digital microscope (Axio Scan.Z1; Carl Zeiss). Five randomly selected sections were quantified using ImageJ software (version 1.8.0; National Institute of Health, Bethesda, MD, USA).

2.8. Terminal Deoxynucleotidyl Transferase dUTP Nick-End Labeling (TUNEL)

TUNEL staining was performed to evaluate the degree of apoptosis using the Dead-EndTM Fluorometric TUNEL System kit (Promega, Madison, WI, USA) following the manufacturer's instructions and the procedure described in a previous study [28].

The lung sections were treated with 4′,6-diamidino-2-phenylindole (DAPI, 5 μg/mL), and cells positive for TUNEL staining were observed under a fluorescent microscope (K1-Fluo; Nanoscope Systems, Daejeon, Republic of Korea).

2.9. Perl's Prussian Blue (PPB) Staining for Iron Accumulation in Lung Tissues

Iron deposition in lung tissue was detected using PPB staining, following previously established methods [29]. Briefly, lung tissue embedded in paraffin was subjected to deparaffinization followed by hydration with distilled water. A staining solution was prepared by mixing potassium ferrocyanide (10%; Sigma-Aldrich) and hydrochloric acid (20%; Bio Basic Inc., Toronto, ON, Canada) in equal amounts. The lung tissue slides were immersed in the prepared solution for 30 min on a shaker, followed by three washes with distilled water. Subsequently, the slides were counterstained with a nuclear fast red solution (Sigma-Aldrich) for 5 min and rinsed twice with distilled water. Subsequently, the slides were affixed using a resin-based mounting material following dehydration. PPB-stained samples were evaluated using a semiquantitative scoring system as per the following criteria: 0 = absence of staining, 1 = minimal staining, 2 = mild staining, 3 = moderate staining, and 4 = intense staining [30].

2.10. Measurement of Total Free Radical Activity in Lung Tissue

Lung tissue samples were used to measure the total levels of ROS/reactive nitrogen species (RNS) by employing the OxiSelect™ ROS/RNS assay kit from Cell Biolabs (San Diego, CA, USA), following the provided instructions. Briefly, the lung samples were homogenized using radioimmunoprecipitation assay (RIPA) buffer (Thermo Fisher Scientific, Rockford, IL, USA) to obtain tissue lysates, which were then centrifuged at 12,000× *g* for 15 min at 4 °C after being sonicated on ice for 1 min. Fluorescence was evaluated under a microplate reader (SpectraMax iD5).

2.11. Measurement of Malondialdehyde (MDA) Levels in Lung Tissue

MDA concentrations in lung samples were determined using OxiSelect™ TBARS assay kit (Cell Biolabs, San Diego, CA, USA) following a previously described method [23]. Lung tissue samples were homogenized to a concentration of 50 mg/mL in PBS and then supplemented with Butylated Hydroxytoluene (BHT; 1×) to prevent further oxidation during the process.

After centrifuging the lung tissues at 10,000× *g* for 10 min at 4 °C, supernatant containing the soluble components was carefully collected for the assay. MDA standards ranging from 0 to 125 μM were prepared by serially diluting in distilled water. Subsequently, 100 μL of samples or MDA standards were transferred to microcentrifuge tubes, to which 100 μL of sodium dodecyl sulfate (SDS) lysis solution was added, thoroughly mixed, and then incubated at 20–25 °C for 5 min. Next, 250 μL of thiobarbituric acid (TBA) was added, followed by thorough mixing and incubation at 95 °C for 45 min. After cooling to 20–25 °C for 5 min, the samples were centrifuged at 800× *g* at 20–25 °C for 15 min, and the resulting supernatants were transferred into clean tubes. Subsequently, standards and samples, each at a volume of 200 μL, were added to individual wells of a 96-well plate. The optical density at 532 nm was measured with a microplate reader (SpectraMax iD5).

2.12. Measurement of Glutathione (GSH) Content in Lung Tissue

The glutathione concentration in lung tissue was measured using the OxiSelect™ Total glutathione (GSSG/GSH) assay kit (Cell Biolabs) following the manufacturer's instructions. Briefly, lung tissue lysates were prepared by treating the samples with metaphosphoric acid (MPA) for deproteination. Then 100 μL of lung samples or GSH standards were transferred to a 96-well plate, and 25 μL 1× GSH reductase solution and 25 μL 1× NADPH solution were added. Subsequently, 50 μL of 1× chromogen was added to the reaction mixture, and the absorbance was measured at 405 nm using a microplate reader (SpectraMax iD5).

2.13. Quantification of Total Calcium Content in Lung Tissue

The calcium content in lung tissue was measured using the Calcium Detection Assay kit (Abcam) following a previously described method [31]. Initially, 50 mg lung tissues were homogenized in 200 μL calcium assay buffer and sonicated for 10 s in an ice bath. The homogenate was then centrifuged at 12,000× *g* for 5 min, and the supernatant was transferred to a clean tube and used as the tissue lysate. Calcium standards were prepared in serial dilutions ranging from 0 to 1 mM in distilled water. To initiate the reaction, 50 μL calcium standard or samples were mixed with 90 μL chromogenic reagent and 60 μL calcium assay buffer in a 96-well plate. The plate was then incubated for 10 min at 20–25 °C in the dark. The absorbance was read at 575 nm using a microplate reader (SpectraMax iD5).

2.14. RNA Isolation and Real-Time Quantitative Polymerase Chain Reaction (RT-qPCR)

RT-qPCR was performed using the protocol detailed in a prior investigation [9]. Total RNA was extracted from the left lung of mice using TRIzol reagent (Invitrogen, Waltham, MA, USA). Subsequently, 2 μg total RNA was utilized for the synthesis of the first cDNA using the amfiRivert Platinum cDNA synthesis master mix (GenDEPOT, Barker, TX, USA) according to the manufacturer's instructions. Quantitative polymerase chain reaction was performed using FastStart Essential DNA Green Master (Roche Diagnostics, Mannheim, Germany). The quantification of target genes expression was determined using the $2-\Delta\Delta Ct$ comparative method with normalization against glyceraldehyde 3-phosphate dehydrogenase (*Gapdh*). Primer sequences are listed in Supplementary Table S1.

2.15. Western Blot Analyses

Western blotting was performed following established methods [19]. Briefly, lung tissues were homogenized in ice-cold RIPA buffer containing a protease inhibitor cocktail (GenDEPOT). The homogenates were sonicated and then incubated for 30 min on ice. After centrifugation (15,000× *g* for 15 min) the supernatant containing the protein samples

were moved to a microcentrifuge tube, and the protein concentration was assessed using a PierceTM BCA Protein Assay Kit (Thermo Fisher Scientific).

The lung lysates were subjected to SDS-polyacrylamide gel electrophoresis and transferred onto polyvinylidene difluoride membranes (Millipore, Darmstadt, Germany), and blocked with 5% nonfat dry milk overnight at 4 °C with the specified primary antibodies: anti-superoxide dismutase 1 (SOD1; Abcam), anti-peroxiredoxin 4 (Prdx4; Abcam), anti-protein kinase R-like ER kinase (PERK; Bioworld Technology, Minneapolis, MN, USA), anti-p-PERK (Bioworld Technology), anti-eukaryotic initiation factor 2α (eIf2-α; Bethyl Lab, Montgomery, TX, USA), p-eIF2-α (Bioworld Technology), anti-activating transcription factor (ATF4; Bioworld Technology), anti-C/EBP homologous protein (CHOP; Bioworld Technology), anti-poly ADP-ribose polymerase (PARP; Cell Signaling, Danvers, MA, USA), anti-Bcl2-associated X (Bax; Cell Signaling), anti-B-cell lymphoma protein 2 (Bcl2; Cell Signaling), anti-cleaved caspase-3 (Cell Signaling), anti-4-hydroxynoneal (4-HNE; R&D system), anti-glutathione peroxidase 4 (GPX4; Bioworld Technology), anti-solute carrier family 7 member 11 (SLC7A11; LSBio, Seattle, WA, USA), anti-heme oxygenase-1 (HO-1; Enzo life sciences, Farmingdale, NY, USA), anti-microtubule-associated protein 1A/1B-light chain 3B (LC3B; Cell Signaling), anti-autophagy related 3 (ATG3; Cell Signaling), ATG5 (Cell Signaling), ATG7 (Cell Signaling), anti-beclin-1 (Cell Signaling), and β-actin (Sigma-Aldrich). The membranes were then washed three times with Tris-buffered saline containing Tween-20 and incubated with the appropriate horseradish peroxidase-conjugated secondary antibodies (ENZO Life Sciences, Farmingdale, NY, USA) at 20–25 °C for 1 h. The HRP reaction was performed using an enhanced chemiluminescence kit (Amersham Pharmacia, Piscataway, NJ, USA), and the resulting chemiluminescence signal was captured with Amersham ImageQuant 800 (Cytiva, Marlborough, MA, USA). Each band was quantitatively determined using the ImageJ software (U. S. National Institutes of Health, Bethesda, MD, USA). The levels of relative proteins were confirmed with β-Actin acting as the loading control.

2.16. Statistics

Data are presented as the mean ± standard error of the mean (SE). Differences among groups were analyzed using either the one-way ANOVA/Bonferroni test or the Kruskal–Wallis/Mann–Whitney test, selected based on the results of the normality test (OriginPro 2020b software, OriginLab Corp., Northampton, MA, USA). A p-value of <0.05 was considered statistically significant.

3. Results

3.1. PBM Alleviated the Exacerbation of AHR and IgE Production Caused by $PM_{2.5}$ Exposure in Allergic Asthma

In an asthma exacerbation mouse model induced by exposure to $PM_{2.5}$, the anti-asthmatic effects of PBM were evaluated. The experimental groups had no significant difference in total body weight (BW) on day 41. In contrast, the thymus weight increased significantly in the PM + OVA group compared to that in the control group, which was notably reduced by treatment with PBM and DEX (Figure 1B). The spleen weight increased in all experimental groups except the PM group compared to the control group. However, the PBM did not reduce the increased weight of the spleen (Figure 1B). After the MCh challenge, the PM + OVA group demonstrated a progressive increase in Penh enhancement, which was dose-dependent. Treatment with PBM and DEX notably reduced the elevated Penh values observed in the PM + OVA group (at an MCh concentration of 50 mg/mL). Furthermore, Penh values in the asthma exacerbation group induced by PM did not show a significant difference compared to those in the OVA-alone treatment group (Figure 1C). In the PM + OVA group, plasma concentrations of total IgE and OVA-specific IgE were notably elevated. However, treatment with DEX and PBM significantly reduced these levels, with no significant difference observed between DEX and PBM treatments (Figure 1D). The IgE concentrations in the OVA group were notably lower compared to those in the OVA + PM group.

3.2. PBM Reduced the Exacerbation of Airway Inflammation and Th2 Responses Caused by $PM_{2.5}$ Exposure in Allergic Asthma

Next, we assessed the potential effect of PBM treatment on allergic airway inflammation in asthma exacerbation induced by $PM_{2.5}$ in BALF and lung tissue samples. BALF analysis revealed a significant increase in total cell count, macrophages, neutrophils, lymphocytes, and eosinophils in the PM + OVA group. Treatment with DEX and PBM attenuated these elevations with no significant differences between the two treatment groups (Figure 2A). Th2 cytokines in BALF, including IL-4, IL-5, and IL-13 were markedly increased in the OVA + PM group; however, they were significantly reduced in the DEX and PBM groups (Figure 2B). The concentrations of histamine and tryptase were significantly elevated in the PM + OVA group (Figure 2C). In contrast, these increases were significantly reduced in the PBM and DEX treatment groups, with a more pronounced effect seen in the DEX group than in the PBM group. Histological analyses of lung tissues showed increased inflammatory cell infiltration around the bronchioles in the PM + OVA group compared to the control group. The $PM_{2.5}$-induced increased lung tissue inflammation in asthmatic mice was markedly reduced in those treated with PBM and DEX (Figure 2D). Goblet cell hyperplasia was elevated in the PM + OVA mice compared to the control mice. Treatment with PBM and DEX markedly decreased the in the proportion PAS-reactive airway epithelial cells triggered by exposure to $PM_{2.5}$ (Figure 2E). Overall, PBM demonstrated comparable efficacy to DEX in reducing inflammation and mucus production in the lung tissues of mice exposed to $PM_{2.5}$ during asthma exacerbation.

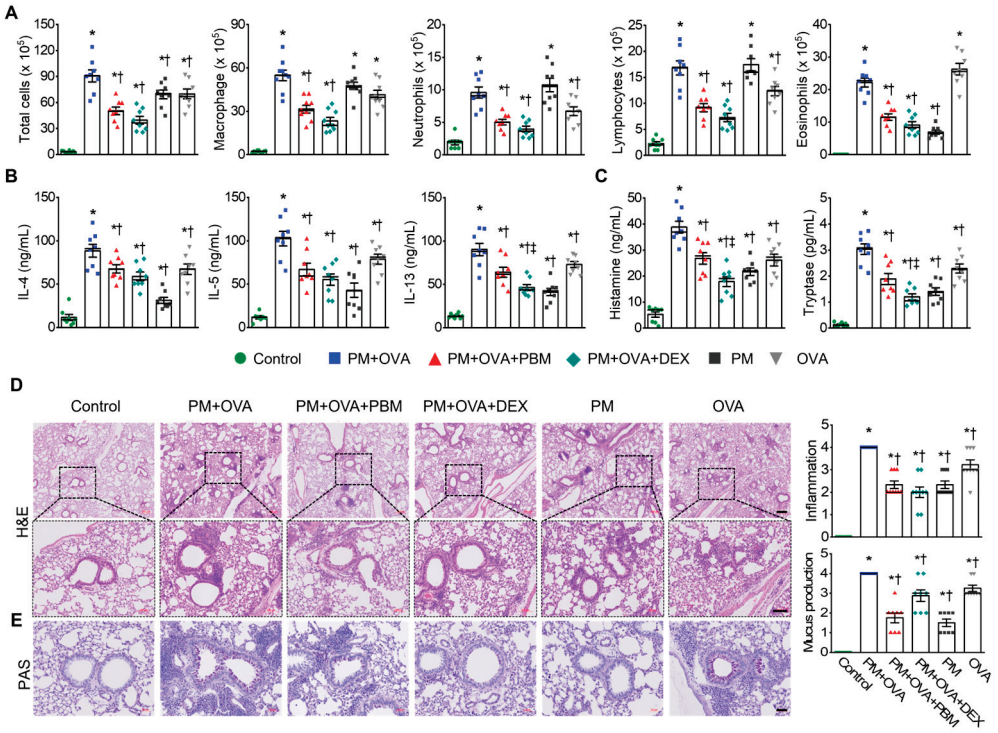

Figure 2. Inhibitory effects of PBM on the elevation of allergic airway inflammation and goblet cell metaplasia in a $PM_{2.5}$-exposed asthma exacerbation model. (**A**) Measurement of total and differential inflammatory cell counts (macrophage, neutrophils, lymphocytes, and eosinophils) in bronchoalveolar lavage fluid (BALF). (**B**) Evaluation of Th2 cytokines including interleukin (IL)-4, IL-5, and IL-13 in BALF. (**C**) Assessment of histamine and mast cell tryptase in BALF. (**D**) Representative images of H&E staining revealed the infiltration of inflammatory cells in lung tissues. Scale bar represents 200 μm (up) and 100 μm (down). The bar graphs represent the summarized score of inflammation. (**E**) Goblet cells secreting mucus in lung tissues were identified using PAS staining.

The bar graphs represent the number of PAS-reactive airway epithelial cells. Scale bar represents 50 μm. The bar graphs represent the summarized scores of PAS-positive mucus-producing cells. Data are shown as the mean ± SEM (n = 8). * $p < 0.05$ compared with control. † $p < 0.05$ compared with PM + OVA. ‡ $p < 0.05$ compared with PM + OVA + PBM.

3.3. PBM Attenuated the Exacerbation of Subepithelial Fibrosis Caused by $PM_{2.5}$ Exposure in Allergic Asthma

Subepithelial fibrosis is linked to the severity of asthma, with higher levels of collagen exhibited in the airway walls of individuals with moderate to severe asthma compared to those with a milder form of the condition [32]. Consequently, we assessed different parameters related to subepithelial fibrosis in lung tissues to examine the effect of PM exposure on subepithelial fibrosis during asthma exacerbation. Analysis of collagen accumulation using MT and Sirius red staining revealed a significant increase in collagen fiber deposition in the PM + OVA group. Remarkably, both the PM + OVA + PBM and PM + OVA + DEX groups exhibited substantial reductions in collagen deposition, showing effects similar to those of DEX or PBM treatment (Figure 3A,B). Assessment of airway smooth muscle mass using alpha-smooth muscle actin (α-SMA) immunostaining showed a significant reduction in the increased airway smooth muscle mass in PM + OVA mice treated with PBM (Figure 3C). In contrast, DEX did not affect the increased airway smooth muscle thickness.

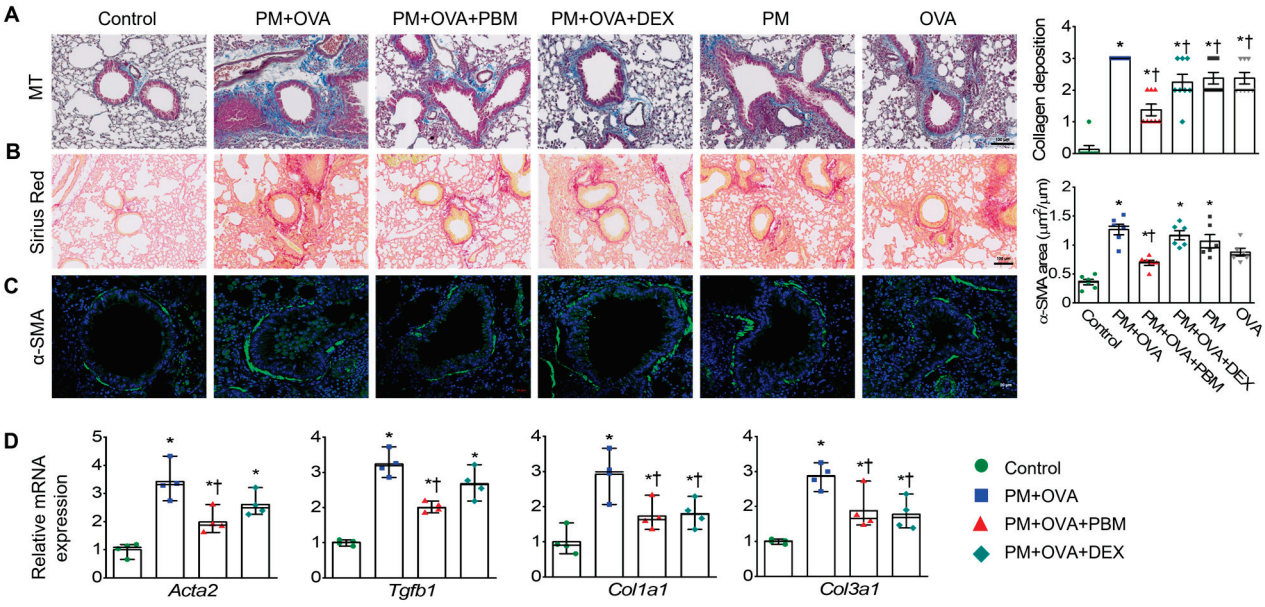

Figure 3. Inhibitory effects of PBM on the elevation of subepithelial fibrosis in a $PM_{2.5}$-exposed asthma exacerbation model. Representative histological images showing (**A**) lung collagen fiber (Masson's trichrome staining) and (**B**) collagen deposition (Sirius Red staining) in the lung tissues. Scale bar represents 100 μm. The bar graphs represent the summarized scores of collagen fiber deposition (n = 8). (**C**) Representative images of α-smooth muscle actin (α-SMA) and FITC expression, as determined by immunohistochemistry, in bronchioles of similar size. Scale bar represents 20 μm. The bar graphs represent the area of α-SMA staining per micrometer length of the bronchiolar basement membrane ($\mu m^2/\mu m$; n = 6). (**D**) Detection of the mRNA levels of *Acta2*, *Tgfb1*, *Col1a1*, and *Col3a1* in lung tissues using qRT-PCR (n = 4). Data are shown as the mean ± SEM. * $p < 0.05$ compared with control. † $p < 0.05$ compared with PM + OVA.

Subsequently, the expression of fibrosis-associated genes was measured in lung tissues. The PM + OVA group exhibited elevated mRNA levels of *Acta2* and *Tgfb1*, which were significantly reduced by PBM treatment but not by DEX. Additionally, the increased mRNA levels of *Col1a1* and *Col3a1* in the PM + OVA group were significantly decreased in both PM + OVA + PBM and PM + OVA + DEX groups (Figure 3D).

3.4. PBM Mitigated the Exacerbation of ROS-Mediated ER Stress Caused by $PM_{2.5}$ Exposure in Allergic Asthma

To investigate the effect of PBM on oxidative stress induced by PM in allergic asthma, oxidative DNA damage was evaluated in lung tissue. The expression of 8-OHdG was significantly higher in the bronchiolar and alveolar epithelia of the PM + OVA group than in the control group. Moreover, both the PM + OVA + PBM and PM + OVA + DEX groups showed significant reductions in 8-OHdG expression, demonstrating similar effects with DEX or PBM treatment (Figure 4A). ROS plays a crucial role in allergic asthma by triggering airway inflammation and oxidative stress [33,34], which can worsen symptoms and exacerbate the condition. ROS activates inflammatory pathways, leading to increased mucus production, airway constriction, and airway remodeling in allergic asthma [34]. Thus, to evaluate the effects of PBM on ROS levels during asthma exacerbation induced by $PM_{2.5}$ exposure, we measured ROS levels in the lung tissues of each experimental group. ROS levels in lung tissue were higher in the PM + OVA group than those in the control (Figure 4B). The PM + OVA + PBM group showed approximately a 45% decrease in ROS levels, while the PM + OVA + DEX group exhibited a 26% reduction compared to that in the PM + OVA group.

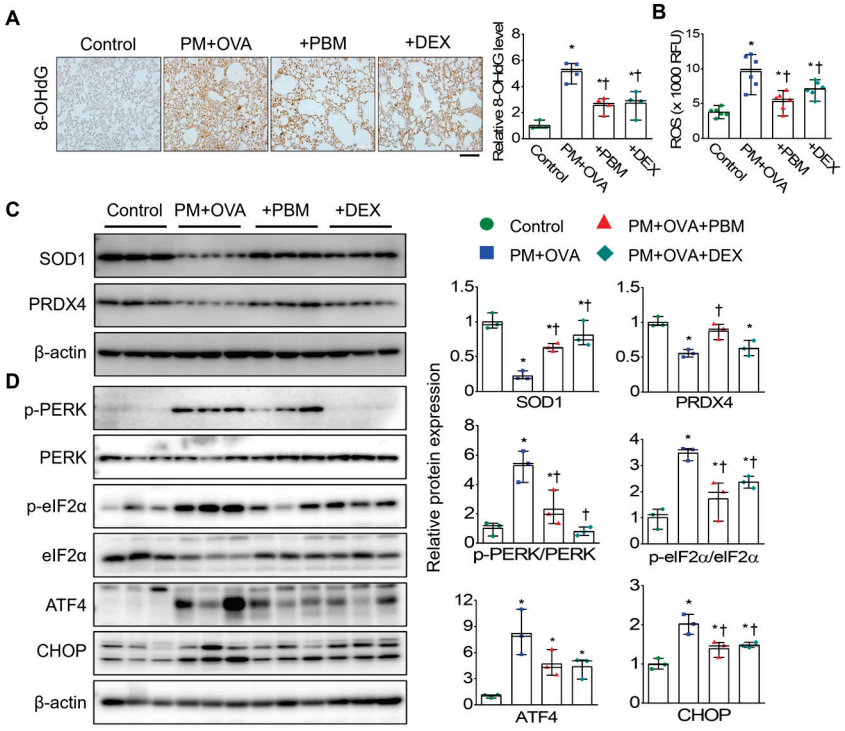

Figure 4. Inhibitory effects of PBM on the ROS-mediated ER stress in a $PM_{2.5}$-exposed asthma exacerbation model. (**A**) Representative lung sections were stained with antibody specific for 8-hydroxy-2′-deoxyguanosine (8-OHdG). Bar graphs represent the quantification of positive areas of 8-OHdG in each experimental group ($n = 4$). Scale bar represents 100 μm. (**B**) ROS levels in lung tissue were measured in relative fluorescence units (RFU). (**C**) Protein expression of superoxide dismutase 1 (SOD1) and peroxiredoxin 4 (PRDX4). (**D**) ER stress markers (PERK, eIF2α, ATF4, and CHOP) in lung tissues by Western blotting. β-actin was used as a loading control. Bar graphs represent the quantification protein expression ($n = 3$). Data are shown as the mean ± SEM. * $p < 0.05$ compared with control. † $p < 0.05$ compared with PM + OVA.

The expression levels of oxidative stress markers, such as SOD1 and PRDX4, were significantly decreased in the PM + OVA group compared to those in the control group. However, the decreased expression of these oxidative stress markers was notably increased in the PM + OVA + PBM group (Figure 4C). Furthermore, PBM as well as DEX alleviated

the increased expression of ER stress-associated proteins (PERK, eIF2α, ATF4, and CHOP) (Figure 4D).

3.5. PBM Inhibited the Exacerbation of Apoptosis, Ferroptosis, and Autophagic Signals Caused $PM_{2.5}$ Exposure in Allergic Asthma

Excessive inflammation and oxidative stress can trigger cell death [35]. To investigate the effect of PBM on cell death signaling in asthma exacerbation induced by $PM_{2.5}$ exposure, we assessed the expression levels of apoptosis, ferroptosis, and autophagic signals. TUNEL staining on lung sections performed to assess the influence of PBM on pulmonary cell death by PM and OVA challenge revealed a significant increase in apoptotic cell numbers in the PM + OVA group compared to those in the control group (Figure 5A). However, the increased apoptotic cell numbers were significantly reduced in the PBM-treated group. Moreover, analysis of the expression of apoptotic markers in lung tissues revealed that cleavage PARP (Cl-PARP), BAX/BCL-2 ratio, and cleavage of caspase 3 (Cl-Cas 3) were upregulated in the PM + OVA mice (Figure 5B). In contrast, the expression of these apoptotic proteins was significantly decreased in the PBM and DEX-treated mice.

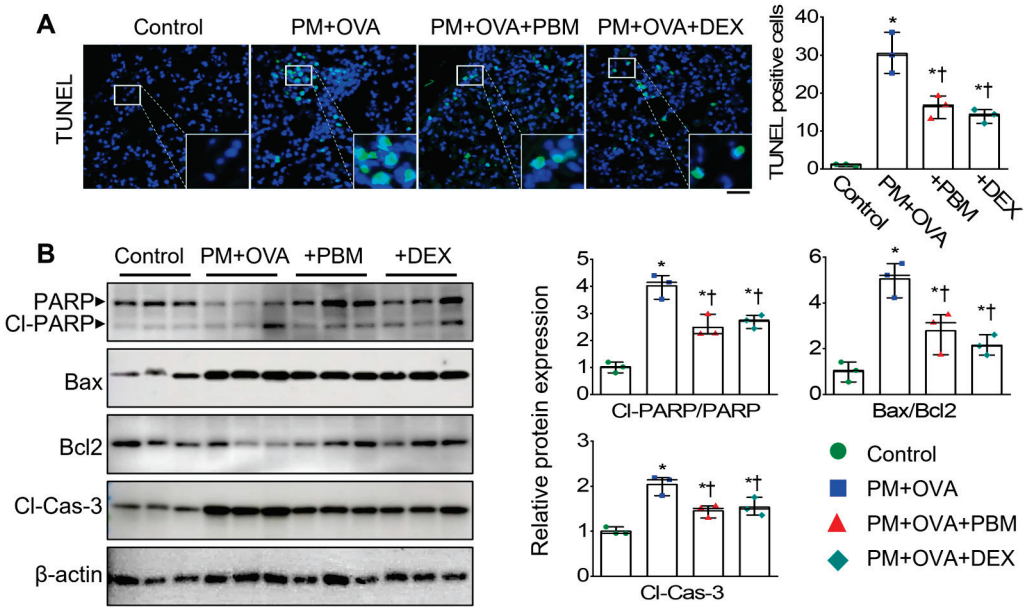

Figure 5. Inhibitory effects of PBM on the cell death in a $PM_{2.5}$-exposed asthma exacerbation model. (**A**) Representative immunofluorescence for TUNEL (green) and DAPI (blue) staining. Scale bar represents 50 μm. Bar graphs represent TUNEL (+)/DAPI (+) cells in the lung tissues (n = 3). (**B**) Apoptotic markers in lung tissues. Bar graphs represent the quantification protein expression (n = 3). Bar graphs represent the quantification protein expression (n = 3). Data are shown as the mean ± SEM. * $p < 0.05$ compared with control. † $p < 0.05$ compared with PM + OVA.

The iron-dependent accumulation of lipid-ROS, lipid peroxidation, and depletion of GSH are pivotal events in ferroptosis [36]. Additionally, iron and Ca^{2+} interact through ROS signaling [37]. Therefore, we evaluated the levels of malondialdehyde (MDA), GSH, and Ca^{2+} in lung tissues. Iron accumulation and MDA levels showed a significant increase in the PM + OVA group compared to the control group. However, the treatment of PBM and DEX significantly mitigated these elevations (Figure 6A,B). Furthermore, the decreased GSH levels in the PM + OVA group were significantly restored by treatment with PBM and DEX (Figure 6C). The increased calcium levels in the PM + OVA group were significantly reduced by treatment with PBM and DEX (Figure 6D). The levels of 4-hydroxynonenal (4-HNE), a marker of ferroptosis protein, also increased in the PM + OVA group, but were notably reduced by treatment with PBM and DEX, with both treatments showing similar effects (Figure 6E). To confirm this observation, we further analyzed the expression of

ferroptosis markers, including 4-HNE, GPX4, SLC7A11, and HO-1 in lung tissue. The expression levels 4-HNE and HO-1 were increased in the PM + OVA mice, while GPX4 and SLC7A11 expression was decreased; however, these alterations in protein expression were restored by treatment with PBM and DEX (Figure 6F).

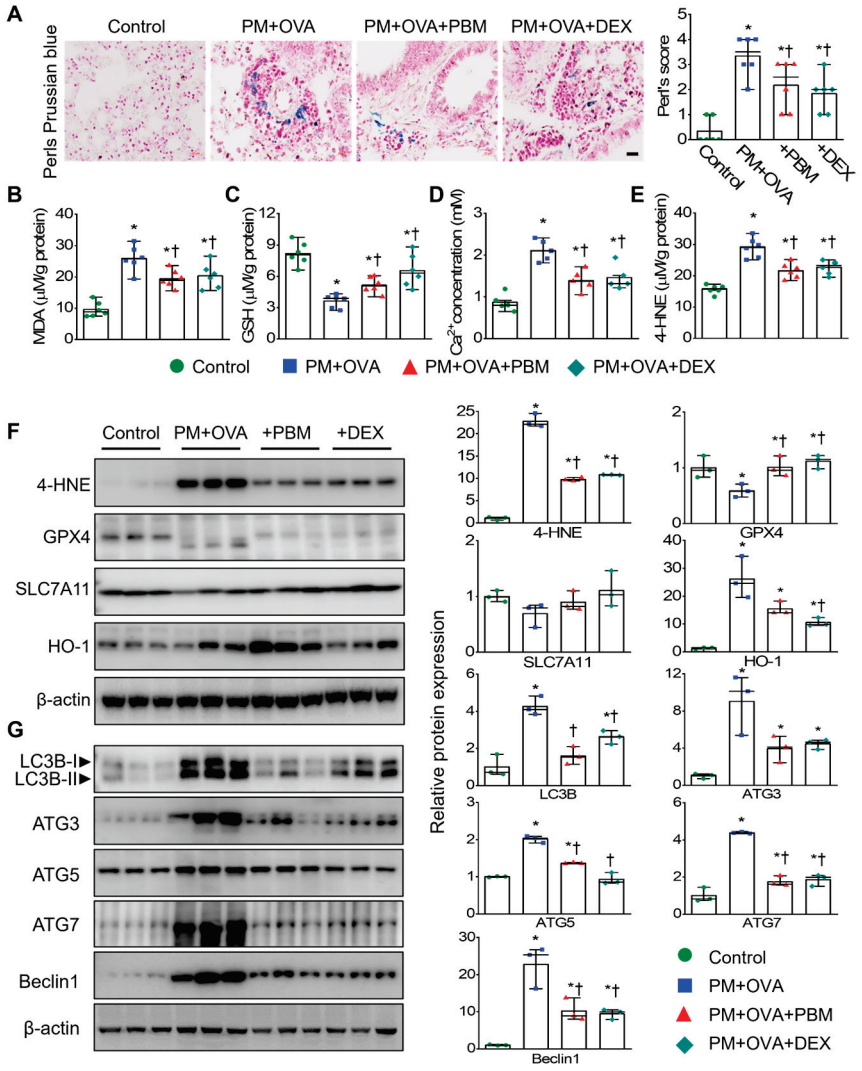

Figure 6. Inhibitory effects of PBM on the ferroptosis and autophagic signals in a $PM_{2.5}$-exposed asthma exacerbation model. (**A**) Deposition of iron in lung tissue using Perls Prussian blue staining in lung tissues (n = 6). Scale bar represents 20 μm. (**B**) Malondialdehyde (MDA) concentration in lung tissue (n = 6). (**C**) Glutathione (GSH) concentration in lung tissue (n = 6). (**D**) Ca^{2+} levels in lung tissue (n = 5). (**E**) 4-Hydroxynonenal (4-HNE) levels in lung tissue (n = 6). (**F**) Ferroptosis markers in lung tissue (n = 3). (**G**) Autophagy markers in lung tissues. Bar graphs represent the quantification protein expression (n = 3). Data are shown as the mean ± SEM. * $p < 0.05$ compared to control. † $p < 0.05$ compared to PM + OVA.

In asthma, both the initiation and progression of ferroptosis involve autophagy [38]. The assessment of autophagy marker protein expression (LC3B, ATG3, ATG5, ATG7, and Beclin-1) in lung tissue showed increased levels of LC3B, ATG3, ATG5, ATG7, and Beclin-1 in PM + OVA mice. However, in mice treated with PBM, these alterations were reversed, which were similar to those treated with DEX (Figure 6G).

4. Discussion

This study demonstrates the promising potential of PBM therapy using a 610 nm wavelength LED as a novel and effective approach for managing allergic asthma exacerbated by $PM_{2.5}$ exposure. By evaluating the key indicators of allergic asthma, the findings of this study revealed that $PM_{2.5}$ exposure heightened asthma characteristics, which were significantly alleviated by PBM treatment, suggesting that PBM therapy may serve as a valuable adjunct therapy for asthma, particularly in cases worsened by environmental pollutants like $PM_{2.5}$.

One of the key findings of this study was the significant reduction in AHR following PBM treatment. AHR is a critical characteristic of asthma, leading to bronchoconstriction and airflow limitation [39]. Dysfunctional airway smooth muscle contributes to AHR, increasing sensitivity to bronchoconstrictor stimuli [40]. Moreover, a disrupted airway epithelium drives inflammation in asthma, promoting AHR through the secretion of alarmin cytokines such as thymic stromal lymphopoietin (TSLP), IL-25, and IL-33 [41,42]. These cytokines increase the expression of Th2 cytokines, which enhance airway eosinophilia and trigger mast cells to release bronchoconstrictive mediators such as histamine, prostaglandin D2, and cysteinyl leukotrienes [42]. In our study, the significant reduction in AHR after PBM treatment indicates the potential of this therapy to address a critical characteristic of asthma that contributes to respiratory symptoms and airflow limitation. By attenuating AHR, PBM demonstrates promise in improving lung function and enhancing symptom management in patients with asthma exposed to $PM_{2.5}$. Moreover, the decreases in eosinophilic airway inflammation, levels of Th2 cytokines, and secretion of histamine and tryptase in the BALF of $PM_{2.5}$-exposed mice highlight the potent anti-inflammatory properties of PBM. These findings suggest that PBM can modulate immune responses and suppress inflammatory mediators, indicating its potential to alleviate airway inflammation associated with asthma exacerbations triggered by environmental factors (Figure 7).

Excessive ER stress can lead to cell death, including apoptosis, autophagy, paraptosis, and ferroptosis [43]. Extensive evidence suggests that ER stress and ROS production interact and disrupt each other, with the PERK/eIF2α signaling pathway regulating ROS production during ferroptosis [43,44]. Recent studies have highlighted the potential role of ferroptosis in asthma, a regulated cell death characterized by iron-dependent lipid peroxide accumulation and GSH depletion that leads to oxidative cell death [23,45]. In asthma, the autophagy of ferritin leads to elevated iron levels, triggered by the accumulation of ROS, contributing to airway inflammation and a hyper-oxidative state, ultimately leading to the ferroptosis of airway epithelial cells [36,46]. Oxidative stress, specifically lipid peroxidation, has been associated with asthma pathogenesis, sharing key characteristics with ferroptosis [47]. MDA levels have been shown to be elevated in the plasma [48,49] and breath condensate of individuals with asthma [50]. Furthermore, suppression of ferroptosis contributes to decreased airway inflammation [51,52] with elevated lipid peroxidation and ROS levels observed in asthma, suggesting the potential activation of ferroptosis during the progression of asthma [53].

Ferroptosis has been recognized as a type of autophagic cell death, with autophagy playing a pivotal role in triggering ferroptosis by regulating cellular iron balance and ROS generation [46,54]. In asthma, upregulated autophagy contributes to the development of Th2 immune responses and eosinophilic inflammation, while downregulated autophagy may be significant in neutrophilic asthma [55]. Consistent with previous findings, elevated levels of oxidative stress-mediated ER stress, ferroptosis, autophagy, and apoptosis-related markers were notably observed in the PM + OVA group. However, following PBM treatment, significant alterations in these processes were observed, suggesting a potential therapeutic effect of PBM in modulating these cellular mechanisms. Additionally, our investigation into the association between ferroptosis and autophagy revealed that PBM treatment reversed the alterations in expression of the autophagy markers observed in the PM + OVA group, suggesting a potential role of PBM in regulating autophagic cell death associated with ferroptosis. A schematic diagram of the anti-asthmatic effects of

PBM therapy on $PM_{2.5}$ exposure-induced allergic asthma in a mouse model is displayed in Figure 7.

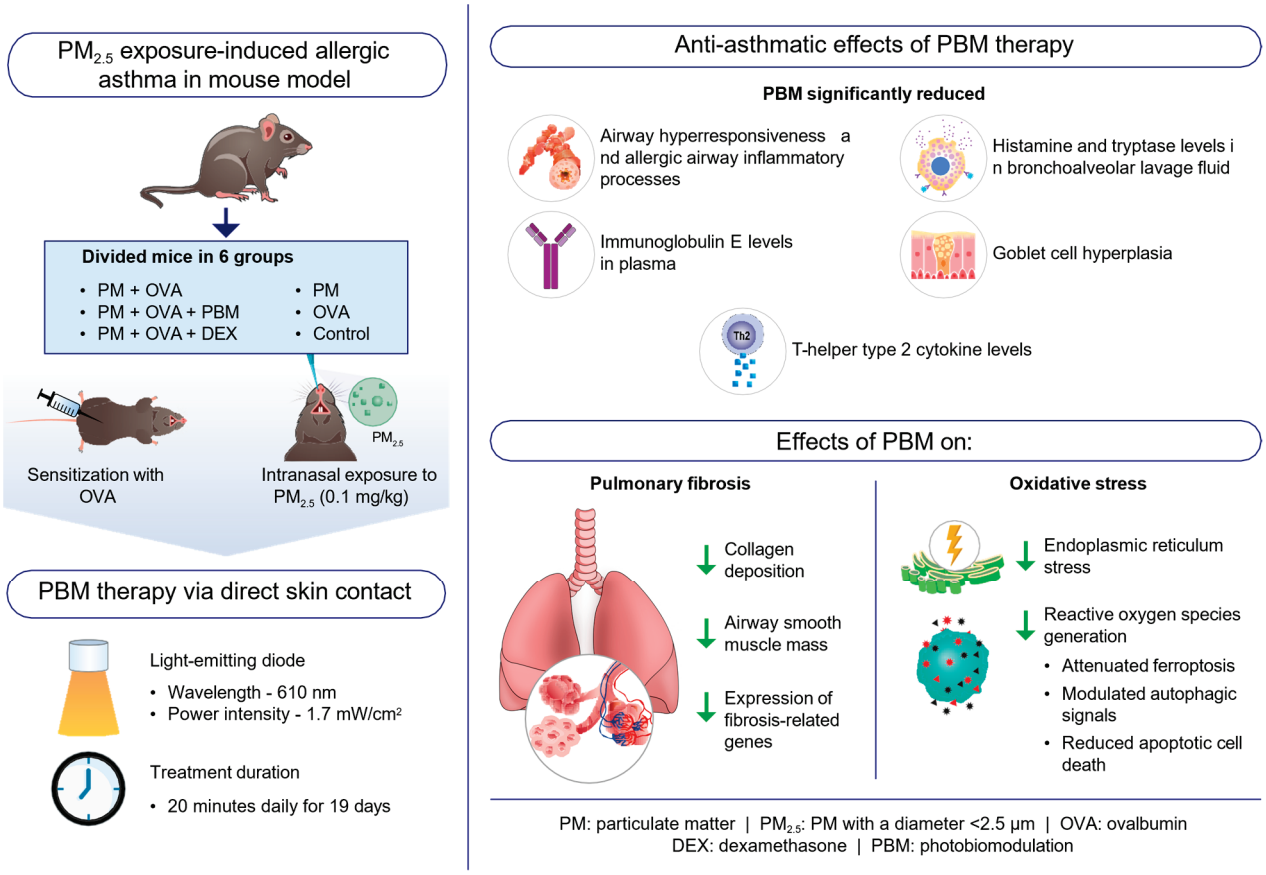

Figure 7. Schematic representation of the anti-asthmatic effects of photobiomodulation (PBM) therapy on $PM_{2.5}$ exposure-induced allergic asthma in a mouse model. PBM therapy reduces AHR, inflammation, Th2 cytokines, goblet cell hyperplasia, and subepithelial fibrosis in a $PM_{2.5}$-exacerbated allergic asthma mouse model. PBM therapy also decreases oxidative and ER stress, apoptosis, and ferroptosis, while modulating autophagy in asthmatic mice exposed to $PM_{2.5}$. These findings suggest PBM's potential as an adjunct to asthma treatment in patients exposed to environmental pollutants. Abbreviations: DEX, dexamethasone; OVA, ovalbumin; PBM, photobiomodulation; PM, particulate matter, $PM_{2.5}$, PM with a diameter < 2.5 µm.

While our study showed promising results, it is important to acknowledge several limitations that warrant further consideration. Our study focused on the short-term effects of PBM therapy, underscoring the need for extensive research to evaluate its long-term efficacy and safety profile in managing allergic asthma. Additionally, the precise molecular mechanisms through which PBM exerts its anti-asthmatic effects were not conclusively elucidated in our study, indicating a critical need for in-depth investigation in this area. Our study did not explore potential variations in treatment response stemming from diverse doses or durations of PBM therapy. Selecting suboptimal parameters of PBM could lead to decreased effectiveness or potentially negative treatment outcomes [56]. To better understand the precise therapeutic pathways targeting specific conditions, quantifying and standardizing light specifications, including wavelength, duration of exposure, power intensity, pulse pattern, and application time, is crucial. These limitations highlight the need for the validation of efficacy through rigorous scientific clinical trials [9]. Lastly, the generalizability of our findings to diverse patient populations or asthma phenotypes needs to be established through additional research.

5. Conclusions

In conclusion, PBM therapy using a 610 nm wavelength LED demonstrated significant efficacy in alleviating asthma symptoms in a mouse model of allergic airway inflammation exacerbated by $PM_{2.5}$ exposure. The therapy effectively reduced AHR, inflammation, mucus hyperplasia, subepithelial fibrosis, and ROS-mediated ER stress as well as apoptosis, ferroptosis, and autophagy. These findings suggest that PBM therapy holds promise as an adjunct treatment for managing asthma exacerbations and shed light on the possible mechanisms underlying asthma exacerbation due to environmental pollutants. Future research should focus on validating these results in clinical trials, exploring the precise mechanisms and long-term effects, and optimizing PBM treatment parameters to facilitate its integration into clinical practice for the benefit of patients with asthma.

Supplementary Materials: The following supporting information can be downloaded at: https://www.mdpi.com/article/10.3390/antiox13081003/s1, Figure S1: The raw images of the Western blot in Figure 4; Figure S2. The raw images of the Western blot in Figures 5 and 6; Table S1: Primer sequences used for qRT-PCR analysis in this study.

Author Contributions: Conceptualization, J.H.R. and Y.-I.S.; methodology, J.P., B.-Y.K., E.J.P., and J.H.R.; software, J.P. and B.-Y.K.; validation, J.P. and B.-Y.K.; formal analysis, J.P., B.-Y.K., and E.J.P.; investigation, J.P.; data curation, E.J.P.; writing—original draft preparation, J.H.R.; writing—review and editing, J.H.R.; visualization, J.P. and B.-Y.K.; supervision, J.H.R. and Y.-I.S.; project administration, B.-Y.K.; funding acquisition, J.H.R. and Y.-I.S. All authors have read and agreed to the published version of the manuscript.

Funding: This research was funded by a National Research Foundation of Korean (NRF) grant supported by the Korean government (MSIT) (Grant No. NRF-2021R1F1A1053630 and 2021M3A9E4081652).

Institutional Review Board Statement: This study was conducted in accordance with the Declaration of Helsinki and approved by the Animal Care and Use Committee of Pusan National University Yangsan Hospital (IACUC No.: 2021-030-A1C0(0)).

Informed Consent Statement: Not applicable.

Data Availability Statement: Data are contained within the article and Supplementary Materials.

Acknowledgments: We appreciate Color Seven Co., Ltd. for providing the LED device.

Conflicts of Interest: The authors declare no conflicts of interest.

References

1. Brusselle, G.G.; Koppelman, G.H. Biologic therapies for severe asthma. *N. Engl. J. Med.* **2022**, *386*, 157–171. [CrossRef]
2. Delfino, R.J.; Wu, J.; Tjoa, T.; Gullesserian, S.K.; Nickerson, B.; Gillen, D.L. Asthma morbidity and ambient air pollution: Effect modification by residential traffic-related air pollution. *Epidemiology* **2014**, *25*, 48–57. [CrossRef]
3. Garcia, A.; Santa-Helena, E.; De Falco, A.; de Paula Ribeiro, J.; Gioda, A.; Gioda, C.R. Toxicological effects of fine particulate matter (PM2. 5): Health risks and associated systemic injuries—Systematic review. *Water Air Soil Pollut.* **2023**, *234*, 346. [CrossRef]
4. Hazlehurst, M.F.; Carroll, K.N.; Loftus, C.T.; Szpiro, A.A.; Moore, P.E.; Kaufman, J.D.; Kirwa, K.; LeWinn, K.Z.; Bush, N.R.; Sathyanarayana, S. Maternal exposure to PM2. 5 during pregnancy and asthma risk in early childhood: Consideration of phases of fetal lung development. *Environ. Epidemiol.* **2021**, *5*, e130. [CrossRef]
5. Lommatzsch, M. Immune modulation in asthma: Current concepts and future strategies. *Respiration* **2020**, *99*, 566–576. [CrossRef] [PubMed]
6. Li, T.; Hu, R.; Chen, Z.; Li, Q.; Huang, S.; Zhu, Z.; Zhou, L.-F. Fine particulate matter (PM2.5): The culprit for chronic lung diseases in China. *Chronic. Dis. Transl. Med.* **2018**, *4*, 176–186. [CrossRef] [PubMed]
7. To, T.; Zhu, J.; Larsen, K.; Simatovic, J.; Feldman, L.; Ryckman, K.; Gershon, A.; Lougheed, M.D.; Licskai, C.; Chen, H. Progression from asthma to chronic obstructive pulmonary disease. Is air pollution a risk factor? *Am. J. Respir. Crit. Care Med.* **2016**, *194*, 429–438. [CrossRef]
8. Zhang, R.; Qu, J. The mechanisms and efficacy of photobiomodulation therapy for arthritis: A comprehensive review. *Int. J. Mol. Sci.* **2023**, *24*, 14293. [CrossRef]
9. Ryu, J.H.; Park, J.; Kim, B.-Y.; Kim, Y.; Kim, N.G.; Shin, Y.-I. Photobiomodulation ameliorates inflammatory parameters in fibroblast-like synoviocytes and experimental animal models of rheumatoid arthritis. *Front. Immunol.* **2023**, *14*, 1122581. [CrossRef] [PubMed]

10. De Freitas, L.F.; Hamblin, M.R. Proposed mechanisms of photobiomodulation or low-level light therapy. *IEEE J. Sel. Top. Quantum Electron.* **2016**, *22*, 348–364. [CrossRef]
11. Abijo, A.; Lee, C.-Y.; Huang, C.-Y.; Ho, P.-C.; Tsai, K.-J. The beneficial role of photobiomodulation in neurodegenerative diseases. *Biomedicines* **2023**, *11*, 1828. [CrossRef]
12. Ryu, J.H.; Kim, Y.; Kim, T.; Kim, Y.M.; Jung, J.; Lee, S.Y.; Lee, S.E.; Kim, N.G.; Shin, Y.I. Light-emitting diode–based photobiomodulation reduces features of allergic asthma in mice. *Allergy* **2020**, *75*, 230. [CrossRef]
13. De Brito, A.A.; Gonçalves Santos, T.; Herculano, K.Z.; Estefano-Alves, C.; de Alvarenga Nascimento, C.R.; Rigonato-Oliveira, N.C.; Chavantes, M.C.; Aimbire, F.; Da Palma, R.K.; Ligeiro de Oliveira, A.P. Photobiomodulation therapy restores IL-10 secretion in a murine model of chronic asthma: Relevance to the population of CD4+ CD25+ Foxp3+ cells in lung. *Front. Immunol.* **2022**, *12*, 789426. [CrossRef]
14. Alonso, P.T.; Schapochnik, A.; Klein, S.; Brochetti, R.; Damazo, A.S.; de Souza Setubal Destro, M.F.; Lino-dos-Santos-Franco, A. Transcutaneous systemic photobiomodulation reduced lung inflammation in experimental model of asthma by altering the mast cell degranulation and interleukin 10 level. *Lasers Med. Sci.* **2022**, *37*, 1101–1109. [CrossRef]
15. Brochetti, R.A.; Klein, S.; Alonso, P.T.; Schapochnik, A.; Damazo, A.S.; Hamblin, M.R.; de Souza Setubal Destro, M.F.; Lino-dos-Santos-Franco, A. Beneficial effects of infrared light-emitting diode in corticosteroid-resistant asthma. *Lasers Med. Sci.* **2021**, *37*, 1963–1971. [CrossRef]
16. Landyshev, I.S.; Avdeeva, N.; Goborov, N.; Krasavina, N.; Tikhonova, G.; Tkacheva, S. Efficacy of low intensity laser irradiation and sodium nedocromil in the complex treatment of patients with bronchial asthma. *Ter. Arkh.* **2002**, *74*, 25–28. [PubMed]
17. Dabbous, O.A.; Soliman, M.M.; Mohamed, N.H.; Elseify, M.Y.; Elsheikh, M.S.; Alsharkawy, A.A.; Abd al Aziz, M.M. Evaluation of the improvement effect of laser acupuncture biostimulation in asthmatic children by exhaled inflammatory biomarker level of nitric oxide. *Lasers Med. Sci.* **2017**, *32*, 53–59. [CrossRef]
18. Emma, G.; Santoro, A.; Snell, J.; Charoud-Got, J.; Held, A. *Certification Report: The Certification of Water-Soluble Ions in a Fine Dust (PM2, 5-Like) Material: ERM-CZ110*; Publications Office of the European Union: Luxembourg, 2020.
19. Lee, B.; Kim, Y.; Kim, Y.M.; Jung, J.; Kim, T.; Lee, S.-Y.; Shin, Y.-I.; Ryu, J.H. Anti-oxidant and anti-inflammatory effects of aquatic exercise in allergic airway inflammation in mice. *Front. Physiol.* **2019**, *10*, 1227. [CrossRef]
20. Dai, S.; Wang, Z.; Cai, M.; Guo, T.; Mao, S.; Yang, Y. A multi-omics investigation of the lung injury induced by PM2. 5 at environmental levels via the lung-gut axis. *Sci. Total Environ.* **2024**, *926*, 172027. [CrossRef]
21. Chen, X.; Guo, J.; Huang, Y.; Liu, S.; Huang, Y.; Zhang, Z.; Zhang, F.; Lu, Z.; Li, F.; Zheng, J.C. Urban airborne PM2. 5-activated microglia mediate neurotoxicity through glutaminase-containing extracellular vesicles in olfactory bulb. *Environ. Pollut.* **2020**, *264*, 114716. [CrossRef]
22. Ryu, J.H.; Xie, C.; Kim, E.-J.; Park, S.-H.; Choi, Y.J.; Kang, S.S.; Shin, M.-K.; Kang, D. Reduction of asthmatic parameters by sea hare hydrolysates in a mouse model of allergic asthma. *Nutrients* **2017**, *9*, 699. [CrossRef] [PubMed]
23. Ryu, J.H.; Woo, M.S.; Cao, D.L.; Kim, E.-J.; Jeong, Y.Y.; Koh, E.-H.; Cho, K.M.; Kang, S.S.; Kang, D. Fermented and aged ginseng sprouts (Panax ginseng) and their main component, compound k, alleviate asthma parameters in a mouse model of allergic asthma through suppression of inflammation, apoptosis, ER stress, and ferroptosis. *Antioxidants* **2022**, *11*, 2052. [CrossRef]
24. Myou, S.; Leff, A.R.; Myo, S.; Boetticher, E.; Tong, J.; Meliton, A.Y.; Liu, J.; Munoz, N.M.; Zhu, X. Blockade of inflammation and airway hyperresponsiveness in immune-sensitized mice by dominant-negative phosphoinositide 3-kinase–TAT. *J. Exp. Med.* **2003**, *198*, 1573–1582. [CrossRef]
25. Ford, J.G.; Rennick, D.; Donaldson, D.D.; Venkayya, R.; McArthur, C.; Hansell, E.; Kurup, V.P.; Warnock, M.; Grunig, G. IL-13 and IFN-γ: Interactions in lung inflammation. *J. Immunol.* **2001**, *167*, 1769–1777. [CrossRef]
26. Di Valentin, E.; Crahay, C.; Garbacki, N.; Hennuy, B.; Guéders, M.; Noël, A.; Foidart, J.-M.; Grooten, J.; Colige, A.; Piette, J. New asthma biomarkers: Lessons from murine models of acute and chronic asthma. *Am. J. Physiol.-Lung Cell. Mol. Physiol.* **2009**, *296*, L185–L197. [CrossRef]
27. Cho, J.Y.; Miller, M.; Baek, K.J.; Han, J.W.; Nayar, J.; Rodriguez, M.; Lee, S.Y.; McElwain, K.; McElwain, S.; Raz, E. Immunostimulatory DNA inhibits transforming growth factor-β expression and airway remodeling. *Am. J. Respir. Cell Mol. Biol.* **2004**, *30*, 651–661. [CrossRef]
28. Siregar, A.S.; Nyiramana, M.M.; Kim, E.-J.; Cho, S.B.; Woo, M.S.; Lee, D.K.; Hong, S.-G.; Han, J.; Kang, S.S.; Kim, D.R. Oyster-derived Tyr-Ala (YA) peptide prevents lipopolysaccharide/D-galactosamine-induced acute liver failure by suppressing inflammatory, apoptotic, ferroptotic, and pyroptotic signals. *Mar. Drugs* **2021**, *19*, 614. [CrossRef]
29. Ghio, A.J.; Roggli, V.L. Perls' Prussian blue stains of lung tissue, bronchoalveolar lavage, and sputum. *J. Environ. Pathol. Toxicol. Oncol.* **2021**, *40*, 1–15. [CrossRef]
30. Hall, A.P.; Davies, W.; Stamp, K.; Clamp, I.; Bigley, A. Comparison of computerized image analysis with traditional semiquantitative scoring of Perls' Prussian Blue stained hepatic iron deposition. *Toxicol. Pathol.* **2013**, *41*, 992–1000. [CrossRef]
31. Siregar, A.S.; Nyiramana, M.M.; Kim, E.J.; Shin, E.J.; Woo, M.S.; Kim, J.M.; Park, S.H.; Hahm, J.R.; Choi, Y.J.; Kang, D. Oyster broth concentrate and its major component taurine alleviate acute alcohol-induced liver damage. *Food Sci. Nutr.* **2022**, *10*, 2390–2399. [CrossRef]
32. Chakir, J.; Shannon, J.; Molet, S.; Fukakusa, M.; Elias, J.; Laviolette, M.; Boulet, L.-P.; Hamid, Q. Airway remodeling-associated mediators in moderate to severe asthma: Effect of steroids on TGF-β, IL-11, IL-17, and type I and type III collagen expression. *J. Allergy Clin. Immunol.* **2003**, *111*, 1293–1298. [CrossRef] [PubMed]

33. Jiang, L.; Diaz, P.T.; Best, T.M.; Stimpfl, J.N.; He, F.; Zuo, L. Molecular characterization of redox mechanisms in allergic asthma. *Ann. Allergy Asthma Immunol.* **2014**, *113*, 137–142. [CrossRef] [PubMed]
34. Qu, J.; Li, Y.; Zhong, W.; Gao, P.; Hu, C. Recent developments in the role of reactive oxygen species in allergic asthma. *J. Thorac. Dis.* **2017**, *9*, E32. [CrossRef] [PubMed]
35. Jian, Z.; Guo, H.; Liu, H.; Cui, H.; Fang, J.; Zuo, Z.; Deng, J.; Li, Y.; Wang, X.; Zhao, L. Oxidative stress, apoptosis and inflammatory responses involved in copper-induced pulmonary toxicity in mice. *Aging* **2020**, *12*, 16867. [CrossRef] [PubMed]
36. Chen, X.; Kang, R.; Kroemer, G.; Tang, D. Ferroptosis in infection, inflammation, and immunity. *J. Exp. Med.* **2021**, *218*, e20210518. [CrossRef]
37. Gleitze, S.; Paula-Lima, A.; Núñez, M.T.; Hidalgo, C. The calcium–iron connection in ferroptosis-mediated neuronal death. *Free Radic. Biol. Med.* **2021**, *175*, 28–41. [CrossRef] [PubMed]
38. Lv, X.; Tang, W.; Qin, J.; Wang, W.; Dong, J.; Wei, Y. The crosslinks between ferroptosis and autophagy in asthma. *Front. Immunol.* **2023**, *14*, 1140791. [CrossRef] [PubMed]
39. ten BRINKE, A.; Zwinderman, A.H.; Sterk, P.J.; Rabe, K.F.; Bel, E.H. Factors associated with persistent airflow limitation in severe asthma. *Am. J. Respir. Crit. Care Med.* **2001**, *164*, 744–748. [CrossRef]
40. Lauzon, A.-M.; Martin, J.G. Airway hyperresponsiveness; smooth muscle as the principal actor. *F1000Research* **2016**, *5*, 306. [CrossRef]
41. Bradding, P.; Porsbjerg, C.; Côté, A.; Dahlén, S.-E.; Hallstrand, T.S.; Brightling, C.E. Airway hyperresponsiveness in asthma: The role of the epithelium. *J. Allergy Clin. Immunol.* **2024**, *153*, 1181–1193. [CrossRef]
42. Whetstone, C.E.; Ranjbar, M.; Omer, H.; Cusack, R.P.; Gauvreau, G.M. The role of airway epithelial cell alarmins in asthma. *Cells* **2022**, *11*, 1105. [CrossRef]
43. Gagliardi, M.; Cotella, D.; Santoro, C.; Corà, D.; Barlev, N.A.; Piacentini, M.; Corazzari, M. Aldo-keto reductases protect metastatic melanoma from ER stress-independent ferroptosis. *Cell Death Dis.* **2019**, *10*, 902. [CrossRef] [PubMed]
44. Dixon, S.J.; Patel, D.N.; Welsch, M.; Skouta, R.; Lee, E.D.; Hayano, M.; Thomas, A.G.; Gleason, C.E.; Tatonetti, N.P.; Slusher, B.S. Pharmacological inhibition of cystine–glutamate exchange induces endoplasmic reticulum stress and ferroptosis. *eLife* **2014**, *3*, e02523. [CrossRef] [PubMed]
45. Yu, S.; Jia, J.; Zheng, J.; Zhou, Y.; Jia, D.; Wang, J. Recent progress of ferroptosis in lung diseases. *Front. Cell Dev. Biol.* **2021**, *9*, 789517. [CrossRef]
46. Hou, W.; Xie, Y.; Song, X.; Sun, X.; Lotze, M.T.; Zeh III, H.J.; Kang, R.; Tang, D. Autophagy promotes ferroptosis by degradation of ferritin. *Autophagy* **2016**, *12*, 1425–1428. [CrossRef]
47. Wood, L.; Gibson, P.; Garg, M. Biomarkers of lipid peroxidation, airway inflammation and asthma. *Eur. Respir. J.* **2003**, *21*, 177–186. [CrossRef]
48. Ozaras, R.; Tahan, V.; Turkmen, S.; Talay, F.; Besirli, K.; Aydin, S.; Uzun, H.; Cetinkaya, A. Changes in malondialdehyde levels in bronchoalveolar fluid and serum by the treatment of asthma with inhaled steroid and beta2-agonist. *Respirology* **2000**, *5*, 289–292. [CrossRef] [PubMed]
49. Shanmugasundaram, K.R.; Kumar, S.S.; Rajajee, S. Excessive free radical generation in the blood of children suffering from asthma. *Clin. Chim. Acta* **2001**, *305*, 107–114. [CrossRef] [PubMed]
50. Antczak, A.; Nowak, D.; Shariati, B.; Krol, M.; Piasecka, G.; Kurmanowska, Z. Increased hydrogen peroxide and thiobarbituric acid-reactive products in expired breath condensate of asthmatic patients. *Eur. Respir. J.* **1997**, *10*, 1235–1241. [CrossRef]
51. Tang, W.; Dong, M.; Teng, F.; Cui, J.; Zhu, X.; Wang, W.; Wuniqiemu, T.; Qin, J.; Yi, L.; Wang, S. Environmental allergens house dust mite-induced asthma is associated with ferroptosis in the lungs. *Exp. Ther. Med.* **2021**, *22*, 1483. [CrossRef]
52. Han, F.; Li, S.; Yang, Y.; Bai, Z. Interleukin-6 promotes ferroptosis in bronchial epithelial cells by inducing reactive oxygen species-dependent lipid peroxidation and disrupting iron homeostasis. *Bioengineered* **2021**, *12*, 5279–5288. [CrossRef] [PubMed]
53. Yang, N.; Shang, Y. Ferrostatin-1 and 3-methyladenine ameliorate ferroptosis in OVA-induced asthma model and in IL-13-challenged BEAS-2B cells. *Oxid. Med. Cell. Longev.* **2022**, *2022*, 9657933. [CrossRef] [PubMed]
54. Gao, M.; Monian, P.; Pan, Q.; Zhang, W.; Xiang, J.; Jiang, X. Ferroptosis is an autophagic cell death process. *Cell Res.* **2016**, *26*, 1021–1032. [CrossRef] [PubMed]
55. Barnes, P.J.; Baker, J.; Donnelly, L.E. Autophagy in asthma and chronic obstructive pulmonary disease. *Clin. Sci.* **2022**, *136*, 733–746. [CrossRef]
56. Chung, H.; Dai, T.; Sharma, S.K.; Huang, Y.-Y.; Carroll, J.D.; Hamblin, M.R. The nuts and bolts of low-level laser (light) therapy. *Ann. Biomed. Eng.* **2012**, *40*, 516–533. [CrossRef]

MDPI AG
Grosspeteranlage 5
4052 Basel
Switzerland
Tel.: +41 61 683 77 34

Antioxidants Editorial Office
E-mail: antioxidants@mdpi.com
www.mdpi.com/journal/antioxidants

Academic Open
Access Publishing

mdpi.com

ISBN 978-3-7258-7151-3